FINAL THESIS REPORT

A STUDY INTO THE FEASIBILITY OF TSUNAMI PROTECTION STRUCTURES FOR BANDA ACEH

&

A PRELIMINARY DESIGN OF AN OFFSHORE RUBBLE-MOUND TSUNAMI BARRIER

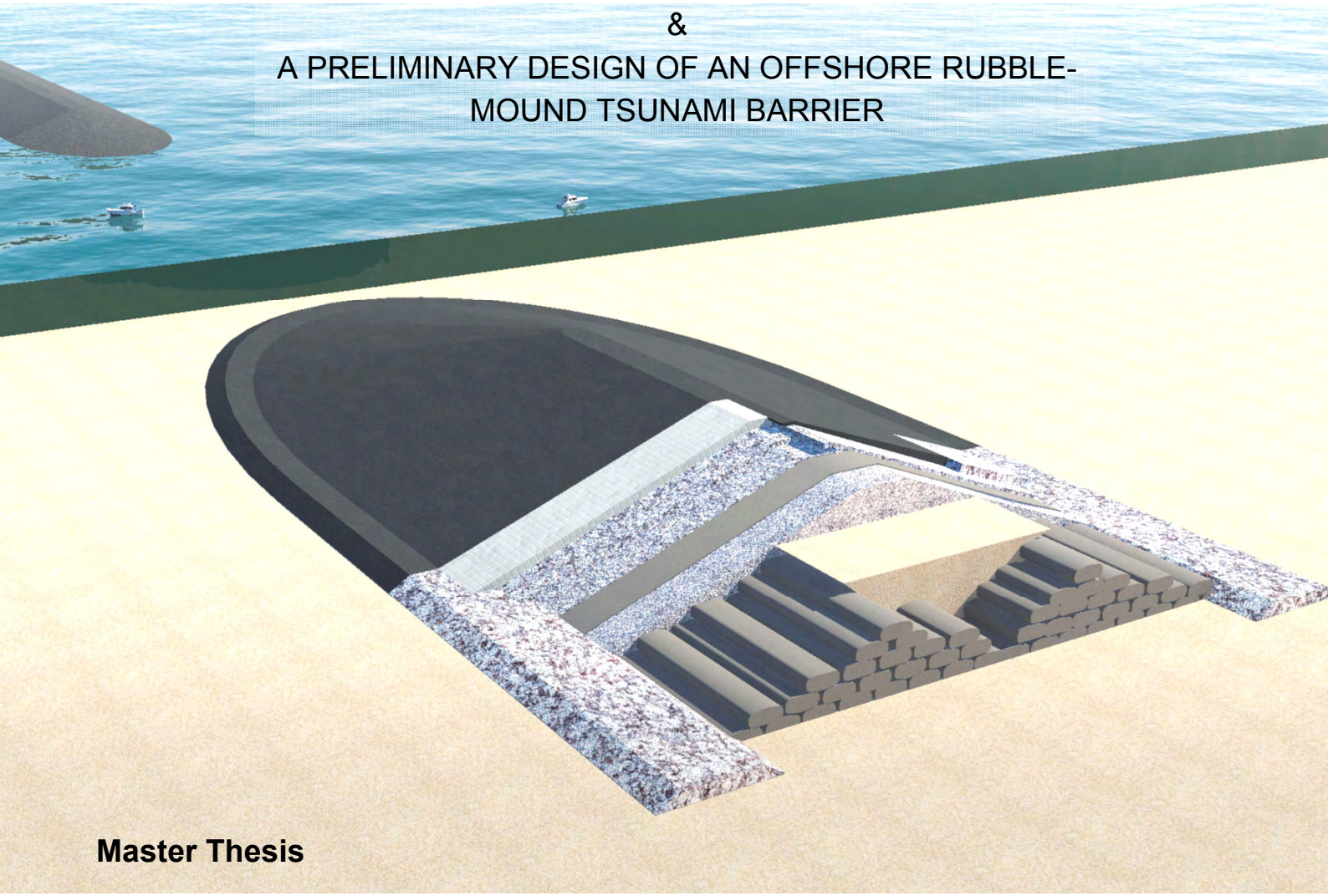

Master Thesis

Master	Hydraulic Engineering
Study	Civil Engineering and Geosciences

Company	**DHV**
Supervisors	Ir. B. van der Boon
	Ir. O. Nieuwenhuis
Author	Ton van der Plas, BSc.
Date	November 15, 2007

University	**Delft University of Technology**
Supervisors	Prof. Dr. Ir. G.S. Stelling
	Ir. H.J. Verhagen
	Prof. Drs. Ir. J.K. Vrijling (Chairman)

PREFACE

"Natural disasters may invade again when the people have forgotten the past one."

Japanese proverb

It is a pleasure to me to write this very last personal page of my thesis. I have been looking forward to this moment to be able to thank all that helped me to succeed this thesis.

This report is the final thesis for the master degree in Civil Engineering at the Delft University of Technology. The study was conducted in cooperation with the DHV.

I would like to thank the following people who attributed to the realization of this thesis. First of all, I would like to thank my graduation committee at TU Delft: Prof. Drs. Ir. J.K. Vrijling, who as chairman gave many practical suggestions, Ir. H.J. Verhagen for his thorough technical advice about many subjects related to hydraulic engineering and Dr. Ir. G.S. Stelling for providing his numerical model and unlimited enthusiasm for everything to do with tsunami modeling.

At DHV, I like to express my heartfelt thanks to Ir. Odelinde Nieuwenhuis who supported me throughout the entire study in writing this final thesis report. Ir. Bram van der Boon: many thanks for providing advice during the study period in Banda Aceh.

Colleagues at the Sea Defence Consultants Project in Banda Aceh: thanks for your support and advice! Special thanks for Alam Syah (alias Chezto) for your assistance with the numerical modeling!

I like to thank the colleagues at DHV who showed interest in this topic and were always available for detailed advice regarding specific topics. In general would like to thank DHV in general for the opportunity they gave me to do this study (partly) abroad. I have had a wonderful time in Indonesia!

Last but not least I want to thanks all friends, relatives and most of all my family for their support during all these years. Your comments and ideas inspired me always.

It is hoped that this study will attribute to a greater awareness of tsunami risk and insight in possible protection alternatives.

Ton van der Plas
Amersfoort, 15 November 2007

GLOSSARY

Amplitude	The rise above or drop below the ambient water level as read on a tide gage.
Arrival time	Time of arrival, usually of the first wave of the tsunami, at a particular location.
Bore	Travelling wave with an abrupt vertical front or wall of water. Under certain conditions, the leading edge of a tsunami wave may form a bore as it approaches and runs onshore. A bore may also be formed when a tsunami wave enters a river channel, and may travel upstream penetrating to a greater distance inland than the general inundation.
CBA	Cost Benefit Analysis; A type of economic evaluation in which both the costs and consequences (benefits) of different alternatives are expressed in monetary units.
Hinterland	The land or district behind the borders of a coast or structure.
Resonance	The continued reflection and interference of waves from the edge of a harbour or narrow bay which can cause amplification of the wave heights, and extend the duration of wave activity from a tsunami.
Inundation	The depth to which a particular location is covered by water
Inundation distance or **Penetration Length**	The distance that a tsunami wave penetrates onto the shore, measured horizontally from the mean sea level position of the water's edge. Usually measured as the maximum distance for a particular segment of the coast.
Negative tsunami wave	Initial tsunami wave is a trough, causing a draw down of water level. Also called a leading-depression wave.
Positive tsunami wave	Initial tsunami wave is a crest, causing a rise in water level. Also called a leading-elevation or leading-positive wave.
MCA	Multi Criteria Analysis; A tool that has been developed for complex multi criteria problems to support decision making. The method enables to quantify qualitative aspects of various alternatives.
M_w: Moment Magnitude	Magnitude based on the size and characteristics of the fault rupture, and determined from long-period seismic waves

Period	The length of time between two successive peaks or troughs.
Probability of Occurrence	The expectation of the occurrence of a particular event, often expressed in a certain *Return Period*
Retaining Height	For offshore structures this is the freeboard. For dry structures, the total structure height. This can also be seen as the height of the visible part of a structure.
Return Period	The average length of time, separating events of a similar magnitude
Risk	In engineering, risk is defined as: (the probability of an event) X (the consequences of this event)
Run-up	Maximum height of the water onshore observed above a reference sea level. Usually measured at the horizontal inundation limit.
SDC	Sea Defence Consultants. Consortium of Dutch companies under the lead of DHV
Tsunamigenic earthquake	Any earthquake which produces a tsunami
Tsunami magnitude	A number which characterizes the strength of a tsunami based on the tsunami wave amplitudes. Several different tsunami magnitude determination methods have been proposed.
TWS	Tsunami Warning System, organization of 26 Pacific Member States which coordinates international monitoring and warning dissemination. TEWS; Tsunami Early Warning Systems from a part of the *SDC*-project.
Wave celerity or **Wave speed**	The speed of the wave shape. This is not the same as the velocity of the particles in the wave.

EXECUTIVE SUMMARY

Tsunamis are a series of long waves, caused by rapid perturbations of the water level. For Banda Aceh, only submarine earthquakes are a likely cause of tsunami-generation and only negative waves (with an initial decrease of the water level) will arrive at the shore line. The probability of *tsunamigenic* earthquakes in Banda Aceh was investigated, based on existing models;

Estimated Return Periods for tsunamigenic earthquakes along the Sunda Trench

Earthquake Magnitude M_w	Return Period at one specific spot (Banda Aceh)	Wave Height at the Shoreline (2D Model runs)
7,5	100 YEARS	1-2 M
8	150 YEARS	2-3 M
8,5	200 YEARS	3-5 M
9	500 YEARS	5-8 M
9,5	1000 YEARS	8-9 M

The propagation of a tsunami wave can be described with equations that are valid for normal shallow water waves. Difficulties arise in determining the initial signal (excitation) in relation with earthquake magnitude. Furthermore, simple shoaling laws are not accurate close to the shore. Therefore a depth-averaged 2D-model is used to determine the wave heights at the Banda Aceh shoreline for different earthquakes magnitudes (see Table above).

The reference case is the Dec2004 Tsunami that caused almost 300.000 missing or dead people in the countries around the Indian Ocean. In Banda Aceh alone, more than 70.000 people were reported dead or missing and the damage was estimated to 1,12 billion USD.

It is concluded that for higher tsunamis, low-crested structures and protection by mangrove trees or other vegetation is not effective. Protection should aim at reflection of the tsunami wave. Therefore, three main tsunami protection alternatives are developed; 1) a tsunami barrier located offshore at 10m water depth, 2) a coastal barrier and 3) an inland barrier. These structures are designed and modelled in such a way that overtopping could occur. Many sub-alternatives are modelled, both in numerical (depth-averaged) 2D and 1D-models.

The *effectiveness* of each alternative is expressed in the amount of inundation volume that still entered the area of Banda Aceh compared to the Dec2004 Tsunami event.
It was found that offshore structures show the highest reduction of the tsunami wave in relation to their retaining height (i.e. the visible height of the structure).

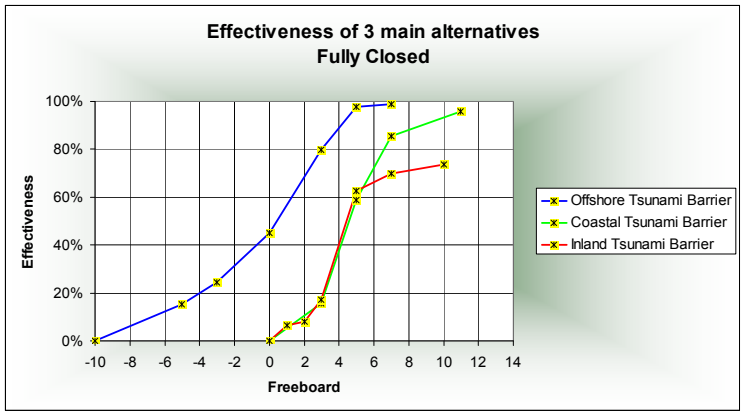

The height of a tsunami wave at the shore that is stopped by a certain protection is called *protection level.* To provide a protection level of 10m height, an offshore barrier would require 6,3m retaining height, a coastal barrier 14m and an inland barrier 8,8m.

A procedure is set up to relate tsunami inundation volume with damage. With decreasing protection level the *residual* damage increases. By relating this *residual* damage with the probability of tsunami-events, the *residual risk* for each protection level is defined.

Based on typical designs for the three alternatives, construction costs are estimated. By adding up the (Net Present Value) of the *residual risk* and the construction costs, the optimal design level for the three alternatives is derived. The lowest costs were found for the offshore barrier at 6,3m retaining height (16,3m structure height), for the coastal barrier at 12,6m, and for the inland barrier at 9,7m structure height.

For these optimal levels, the costs of tsunami protection are compared with the benefits (i.e. the *prevented risk)*. From this *Cost Benefit Analysis* it is concluded that none of the alternatives is *economically feasible,* except under very favourable conditions. In this case only the inland and coastal alternatives show a positive cost-benefit ratio. For the offshore barrier, the costs consequently outweighed the benefits.

Nonetheless, considerations about the 1) little escape time between a tsunami warning and the actual arrival, 2) the value of life, and 3) other non-quantifiable advantages of a tsunami protection structure, could still support a decision in favour of an extensive tsunami protection. In that case, a *Multi Criteria Analysis* showed that offshore solutions are most preferable. High structures on land will unacceptably affect the socio-economic development of Banda Aceh. Thereby, tsunami height, run-up, velocities and impact are smaller in offshore conditions. Therefore it was decided to elaborate further on the design of an offshore tsunami barrier, despite the negative cost-benefit ratio.

The design aims at reflecting the energy of the tsunami waves. The optimal design level of 6,3m is rounded at 7m. Considering the extreme nature of high tsunamis, damage is allowed as long as the primary retaining function was kept. Tsunami overtopping is allowed, so that the rear side had to be protected against high velocities (≈10m/s). Asphalt is proposed. To ensure stability against an earthquake prior to a tsunami, GeoContainers are applied in the core. The permeability is high, to prevent pressure built-up. The front side is designed to withstand 1/100 year storm waves with minor damage. One layer of 4,6-ton elements is applied.

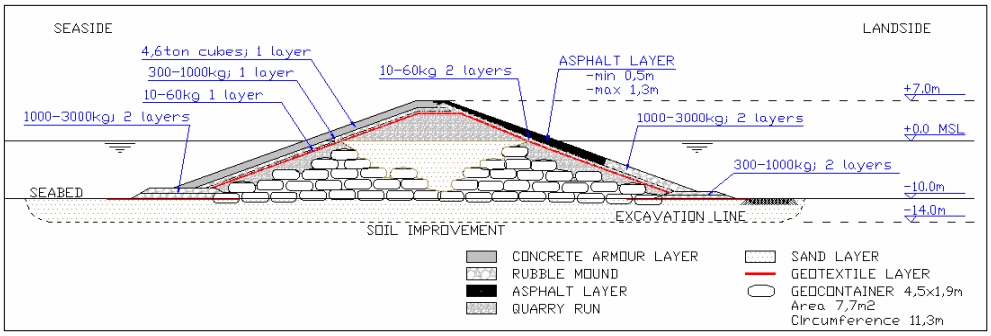

The breakwater heads (slope 1:6) are completely covered with asphalt. The bottom of the gaps are protected with geotextile and cabled mattresses of concrete elements to prevent severe scouring due to the high velocities (≈12m/s).

TABLE OF CONTENTS

PREFACE I

GLOSSARY II

EXECUTIVE SUMMARY IV

CHAPTER 1. INTRODUCTION 1

1.1 PROBLEM DESCRIPTION 1
1.2 PROBLEM STATEMENT 2
1.3 OBJECTIVE 2
1.4 GENERAL APPROACH 2
1.5 COMMENTS 3

CHAPTER 2. INTRODUCTION TO TSUNAMIS 5

2.1 INTRODUCTION 5
2.2 NATURE AND ORIGIN OF TSUNAMIS 5
2.3 MECHANICS OF GENERATION 6
2.3.1 Earthquake generated tsunamis 6
2.3.2 Landslides 7
2.3.3 Volcanic eruptions 8
2.3.4 Meteor impacts 8
2.3.5 Overview and application 8
2.4 TSUNAMI PROPAGATION 9
2.4.1 Shoaling 9
2.4.2 Wave reflection 10
2.4.3 Wave refraction, diffraction and spreading 12
2.4.4 Wave dispersion 13
2.4.5 Friction 13
2.4.6 Overview and application 14
2.5 SHORELINE INTERACTION 14
2.5.1 Wave breaking 15
2.5.2 Run-up 16
2.5.3 Velocities 18
2.5.4 Penetration 18
2.5.5 Overview and application 19
2.6 INTERACTION WITH STRUCTURES 19
2.6.1 Forces of non-broken waves on high-crested structures 19
2.6.2 Forces of broken waves on high-crested structures 21
2.6.3 Overview tsunami force on high-crested structures 21
2.6.4 Low-crested, submerged and 'soft' structures. 23
2.6.5 Overview and application 24
2.7 EXISTING TSUNAMI BARRIERS 25
2.7.1 Seawalls along the Sanriku Coast, Japan 25
2.7.2 The Ohfunato Tsunami Protection Breakwater 26

2.7.3 *Kamaishi port, Japan* 27
2.7.4 *Kawaragi breakwater* 27
2.7.5 *Lhok'Nga Breakwater* 28
2.8 SUMMARY **30**

CHAPTER 3. INDONESIA IN THE RING OF FIRE **33**
3.1 INTRODUCTION **33**
3.2 FACTS AND FIGURES **33**
3.3 RING OF FIRE **35**
3.3.1 *Geology* 35
3.3.2 *Earthquakes* 37
3.3.3 *Other possible causes for tsunamis* 38
3.4 TSUNAMI OCCURRENCE **38**
3.5 THE DEC 2004 TSUNAMI **41**
3.5.1 *What happened* 42
3.5.2 *Facts and figures* 44
3.5.3 *Damage and casualties figures* 46
3.6 SUMMARY **48**

CHAPTER 4. NUMERICAL MODELLING **49**
4.1 INTRODUCTION **49**
4.2 1D MODEL **50**
4.2.1 *Description* 50
4.2.2 *Model runs* 50
4.2.3 *Results* 51
4.3 SEMI-1D MODEL **52**
4.3.1 *Description* 52
4.3.2 *Model runs* 53
4.3.3 *Results* 54
4.4 2D-TSUNAMI MODEL **56**
4.4.1 *Description* 56
4.4.2 *Model runs* 58
4.4.3 *Results* 58
4.5 DAMAGE MODEL **60**
4.5.1 *Description* 60
4.5.2 *Model runs* 62
4.5.3 *Results* 62
4.6 SUMMARY **62**

CHAPTER 5. TSUNAMI PROTECTION ALTERNATIVES FOR BANDA ACEH **65**
5.1 INTRODUCTION **65**
5.2 TSUNAMI PROTECTION ALTERNATIVES (IN PLAN POSITION) **65**
5.2.1 *Offshore Tsunami Protection* 65
5.2.2 *Coastal Tsunami Protection* 67
5.2.3 *Inland Tsunami Protection* 68
5.2.4 *Overview of developed alternatives* 70
5.3 MODELLING OF ALTERNATIVES **71**

5.3.1 Modelling 71
5.3.2 Output parameters 71
5.4 ALTERNATIVE 0: CURRENT SITUATION 72
5.4.1 Effectiveness under tsunami conditions 73
5.5 ALTERNATIVE 1: OFFSHORE TSUNAMI BARRIER 74
5.5.1 Model runs and effectiveness under tsunami conditions 74
5.5.2 (Dis)advantages 76
5.6 ALTERNATIVE 2: COASTAL TSUNAMI BARRIER 77
5.6.1 Model runs and effectiveness under tsunami conditions 77
5.6.2 (Dis)advantages 78
5.7 ALTERNATIVE 3: INLAND TSUNAMI BARRIER 79
5.7.1 Model runs and effectiveness under tsunami conditions 79
5.7.2 (Dis)advantages 80
5.8 SUMMARY OF MODELLING RESULTS 81
5.9 POSSIBLE CROSS SECTIONS FOR TSUNAMI PROTECTION ALTERNATIVES 82
5.9.1 Innovative solutions 82
5.9.2 Traditional solutions 85
5.10 SUMMARY 87

CHAPTER 6. ASSESSMENT OF ALTERNATIVES 89
6.1 INTRODUCTION 89
6.2 ALTERNATIVES 89
6.3 COST BENEFIT ANALYSIS 90
6.3.1 Introduction 90
6.3.2 Relation Tsunami Height and Probability 92
6.3.3 Relation Tsunami Height and Damage 92
6.3.4 Relation Probability and Damage 93
6.3.5 Residual Risk of Tsunami Protection Alternatives 94
6.3.6 Investment Costs of Tsunami Protection Alternatives 97
6.3.7 Total costs of Tsunami Protection Alternatives 98
6.3.8 Conclusion CBA 103
6.4 MULTI CRITERIA ANALYSIS 104
6.4.1 Criteria 104
6.4.2 Scores 105
6.4.3 Weighting factors 106
6.4.4 Alternatives 106
6.4.5 Results 106
6.4.6 Conclusion MCA 110
6.5 SUMMARY AND CHOICE 110

CHAPTER 7. DESIGN TSUNAMI BARRIER 112
7.1 INTRODUCTION 112
7.2 DESIGN CONSIDERATIONS 112
7.2.1 Plan view 112
7.2.2 Cross-section 114
7.3 DESIGN LOADS 115
7.3.1 Normal wave attack 115

7.3.2 *Tsunami attack* 115
7.3.3 *Earthquakes* 119
7.4 FAILURE MECHANISMS 119
7.5 DESIGN OFFSHORE TSUNAMI BARRIER 120
7.5.1 *Overtopping* 120
7.5.2 *Normal wave attack* 122
7.5.3 *Sliding* 122
7.5.4 *Excess water pressures / micro stability* 123
7.5.5 *Liquefaction* 124
7.5.6 *Gaps* 124
7.6 SUMMARY AND DRAWINGS 124

CHAPTER 8. CONCLUSIONS AND RECOMMENDATIONS 128
8.1 CONCLUSIONS 128
8.2 RECOMMENDATIONS 130

LIST OF REFERENCES 133

LIST OF FIGURES

Figure 2-1 Terminology for tsunami waves [61] 5
Figure 2-2 Impression of a (thrust) dip-slip fault and associated water levels. [62] 6
Figure 2-3 Comparison of sub-aerial and submarine landslides as tsunami wave sources [45] 7
Figure 2-4 Typical parameters for tsunamis [32] 10
Figure 2-5 Shoaling, reflection and a combination of these processes 11
Figure 2-6 Spreading and refraction of the 2004 Tsunami, [55] 12
Figure 2-7 Breaking limit for various slopes 15
Figure 2-8 Variety of Dec 2004 Tsunami appearance at various locations. Source [52] 16
Figure 2-9 Maximum run-up factor for bores running on a dry bed as a function of velocity 17
Figure 2-10 Horizontal tsunami forces according to Cross, Yamamoto, Tanimoto, Ikeno and Kato. 22
Figure 2-11 Definition sketch of submerged breakwater [27] 24
Figure 2-14 Plan view of breakwater at Lhok'Nga and direction of primary waves 28
Figure 2-15 Helicopter view of breakwater Lhok'Nga, source [47] 29
Figure 2-16 Left: The partly restored seaside protection. Right: The new and displaced Tetrapods at the head. 29
Figure 3-1 Indonesia and its islands. The red box indicates the location of Aceh. [58] 33
Figure 3-2 The Ring of Fire. Indonesia lies north of the Java or Sunda trench [64]. 35
Figure 3-3 Overview major and minor plates [66] 36
Figure 3-4 Impression of the subduction zone along the Java (Sunda) trench [65] 36
Figure 3-5 Historic record of earthquakes that triggered tsunamis along the Sunda Trench [50]. 37
Figure 3-6 Tsunami height hazard curves at four locations in the Indian Ocean region [41]. 39
Figure 3-7 Sumatra, the islands of Simeulue and Nias and the epicentre of the Dec 2004 earthquake 41
Figure 3-8 Left: modelling of excitation signal along entire fault line. Right: timeframe of the Indian Ocean 2D-model where the refraction of the tsunami waves around the northern islands is shown. Scale in meters. 42
Figure 3-9 Aerial photographs of Banda Aceh and Lhok'Nga before and after the tsunami. The water penetrated from the southwest (Lhok'Nga) and from the north (Banda Aceh) met in the middle [67] 44
Figure 3-10 Banda Aceh port area. Mosque in Ulee Lheue, directly on the coastline. Close to this location the 12m inundation depth was measured. Almost all (simple) buildings were destroyed [67]. 45
Figure 3-11 Banda Aceh. Downtown, approx. 3km inland, close to the Great Mosque. The boat was most probably moored in the river next to this site. A lot of debris is in the streets but the (concrete) buildings do not show structural damage [67]. 46
Figure 4-1 Maximum velocities and water levels for offshore breakwater 51
Figure 4-2 Maximum shoaling at the coast for various foreshore bathymetries 52
Figure 4-3 Tsunami shape signal that has been applied at the open boundary of the model (vertical scale in meters) [32]. 52
Figure 4-4 1D model: Maximum water levels for varying bathymetry. $H_{boundary}$=6m. 55
Figure 4-5 Comparison between effectiveness of seawall +4m, inland wall +4m and combined measure. 56
Figure 4-6 Five detailed model domains. The Northern Aceh model is 200x200m^2 and 50x50m^2 grid [32]. 57
Figure 4-7 Tsunami Flood Map for 9,2 Magnitude (Dec2004 Tsunami) [32]. 59
Figure 4-8 Timeframe of a 2D-model run with offshore barrier +5m MSL. Scale in m. 60
Figure 4-9 Input and output (Damage map) for DamageModule [32]. 61
Figure 5-1 Length of offshore protection vs. length of protected coastline; Ofunato Bay, Japan. The red circle indicates the location of the breakwater 66
Figure 5-2 Offshore Tsunami Protection Alternative, following the 10m bathymetry line. 67
Figure 5-3 Coastal Tsunami Protection Alternative, following the original coastline. 68
Figure 5-4 Proposed ring road (red line). Source: RTRW Kota Banda Aceh. 69
Figure 5-5 Inland Tsunami Protection Alternative, following the trajectory of the proposed ring road. 69
Figure 5-6 Overview of the main alternatives 70
Figure 5-7 Correlation between Inundation Volume and Damage 72
Figure 5-8 Cross section of existing revetment (left) and floodwall (right) [SDC] 73

Figure 5-9 Maximum inundation of Banda Aceh, with floodwall +2,6m (left, red line), and without any protection (right). 73
Figure 5-10 Inundation map for Offshore Barrier, retaining height 3m, no gaps 74
Figure 5-11 Effectiveness Offshore Barrier -10m; Fully Closed for Dec2004 Tsunami Signal 76
Figure 5-12 Impression of an offshore tsunami barrier +7m MSL 77
Figure 5-13 Effectiveness Coastal Barrier; Fully Closed for Dec2004 Tsunami Signal 78
Figure 5-14 Impression of a coastal tsunami barrier of 10m height 79
Figure 5-15 Effectiveness Inland Barrier; Fully Closed for Dec2004 Tsunami Signal 80
Figure 5-16 An impression of an inland wall, height +8.0m 81
Figure 5-17 Comparison of effectiveness of the three main alternatives 82
Figure 5-18 Working principle of Blow Pipe and 3D-impression. Right the description as presented by the designers. 83
Figure 5-19 Working principle of the movable wall. Right the description as presented by the designers [68]. 84
Figure 5-20 Comparison of wave growth for situation with (red line) and without structure (blue line). 85
Figure 5-21 Basic cross section of an offshore tsunami protection at -10m bathymetry line. 86
Figure 5-22 Comparison of effectiveness of the three main alternatives 88
Figure 6-1 Working principle of Cost Benefit Analysis 91
Figure 6-2 Relation Tsunami Height and Probability 92
Figure 6-3 Relation between Tsunami Height and Damage 93
Figure 6-4 Relation between Probability and Damage. The total area under the graph is the total risk. 94
Figure 6-5 The residual risk and benefits (on annual basis) for each protection level 95
Figure 6-6 The Net Present Value of the residual risk for varying lifetime and discount/growth rates. 96
Figure 6-7 Overview investment (construction- and additional) costs for the main alternatives 97
Figure 6-8 Net Present Value of Investment Costs (3 Alternatives), d=5% 99
Figure 6-9 Total costs of Tsunami Protection; Offshore 100
Figure 6-10 Total costs of Tsunami Protection; Coastal 101
Figure 6-11 Total costs of Tsunami Protection; Inland. Note that the scale is different from the previous 'total costs' figures. 102
Figure 6-12 MCA results: the appreciation of various structures 107
Figure 6-13 VC-ratio based on 1 Dec2004 Tsunami event 109
Figure 6-14 VC-ratio based on 2 Dec2004 Tsunami events 109
Figure 7-1 Plan view of Banda Aceh with Offshore Tsunami Barrier 113
Figure 7-2 Initial cross section as used in cost calculation (left) and changed design as starting point for the detailed design in this chapter. 114
Figure 7-3 Two situations when sliding could occur. Left figure: increased water level at landside and dropdown at seaside; seaward sliding. Right figure: increased water level at seaside and lowering water level at landside; landward sliding. Scale in meters. 116
Figure 7-4 Maximum depth averaged velocities with offshore barrier at -10m bathymetry. Label in m/s 116
Figure 7-5 Definition sketch flow acceleration through gaps 117
Figure 7-6 Maximum velocities and water levels for offshore breakwater 118
Figure 7-7 Failure mechanisms Offshore Tsunami Barrier Banda Aceh 120
Figure 7-8 Left: a cabled concrete block revetment. Right: Wedge-shaped block system [6] 121
Figure 7-9 Sliding; Loads according to Tanimoto, Kato and 1D-model and resistance 123
Figure 7-10 Cross section Offshore Tsunami Barrier; composition 125
Figure 7-11 Cross section Offshore Tsunami Barrier; dimensions and quantities 125
Figure 7-12 Plan view and cross section of gap and general layout of gap protection 126
Figure 7-13 3-D impression of offshore tsunami barrier; gap 127
Figure 7-14 3-D impression of offshore tsunami barrier; composition 127

LIST OF TABLES

Table 2-1: Causes of tsunami for all listed events [50] 8
Table 2-2: Typical values of n for different terrain types [53] . 13
Table 2-3: Dimensions of the Ohfunato Tsunami Protection Breakwater (source: Ida, 1981) 26
Table 3-1: General facts and figures, 2006 [59]. 34
Table 3-2: Historic tsunamis in Indonesia caused by other events then earthquakes. Source: [50]. 38
Table 3-3: Estimated recurrence interval for tsunamigenic earthquakes along the Sumatra-Andaman fault line. 40
Table 3-4: Wave heights and effects of the 26Dec 2004 Tsunami in various countries 43
Table 3-5: Investigated tsunami parameters in the Banda Aceh Region [25] 45
Table 3-6: Damage and loss assessment for whole Aceh and Nias, various sources. January 2005. 47
Table 4-1: Calculated damage with DamageModule for various tsunami-heights 62
Table 5-1: Overview model run without structural measures 71
Table 5-2: Overview model runs and effectiveness for offshore alternatives. M_w = 9.2 75
Table 5-3: Overview model runs and effectiveness for the coastal alternatives. M_w=9.2 77
Table 5-4: Overview model runs and effectiveness for inland alternatives. M_w= 9.2 79
Table 6-1: Estimated return periods along the Sumatra-Andaman fault line. 92
Table 6-2: Cost figures for offshore, coastal and inland tsunami barrier 97

Chapter 1. INTRODUCTION

1.1 PROBLEM DESCRIPTION

The Sumatra–Andaman Islands earthquake of magnitude 9.2 that occurred on December 26, 2004 at 00:58 UTC at a point 250 km south of Banda Aceh was the largest earthquake since the magnitude 9.2 Alaskan earthquake of 1964, and was among the five largest earthquakes in the past century. The earthquake triggered a large number of after shocks extending to the Andaman Islands and generated a large tsunami that caused extreme inundation and destruction in the northern Indian Ocean[1]. It resulted in massive loss of life and damage to the west and north coast of Aceh Province in the Republic of Indonesia. In total, almost 300.000 people were reported dead or missing and more than 500,000 people lost their livelihoods.

The Government of Indonesia has formulated a priority program, the Aceh Nias Tsunami and Earthquake Response Program (ANTERP), consisting of a number of initiatives. One of them is the Sea defence, flood protection, refuge and early warnings systems initiative.

The Aceh and Nias Sea Defence Project follows from this initiative, and is executed by a Dutch/Indonesian consortium under the lead of DHV. The project focuses on the following subjects in the coastal area of Aceh and Nias:

1. Immediate measures to restore physical and social environment to at least the original pre-tsunami levels
2. Long term measures to reduce the impact of possible future tsunamis
3. Capacity building to support the management of the protection system developed under this project.

The challenge faced by this project is to create a safe habitable environment that enables economic recovery and sustainable development in Aceh and Nias Island. This safe environment is obtained through the development and implementation of a robust sea defence system, which will reduce risks of future floods.

A possible long term measure to reduce the impact of future tsunami events is to create a tsunami reducing (or retaining) barrier. Several activities on this subject have already been executed or are under execution within the Aceh & Nias Sea Defence Project. For example:

- Semi-1D modelling has been executed to assess effectiveness of different coastal measures in tsunami impact reduction
- A preliminary assessment of different aspects of importance and general assumptions for design of structures in tsunami conditions has been set up.

From these activities, in combination with results from hazard mapping, damage modelling and a risk assessment, it was concluded that for the main capital of Aceh, Banda Aceh, where the highest loss of human life and economic value was counted after the December 2004 tsunami, a further study into the feasibility of a tsunami protection structure is required.

[1] *Hereinafter referred to as the "Dec2004 Tsunami"*

This is the starting point for this final thesis work. Based on these initial findings, the focus has been set to Banda Aceh. However, many questions remain. Tsunami-protection by means of a structure is unknown in this area, probably because tsunamis were rather infrequent last centuries. This yields questions concerning the frequency and heights of future tsunamis. Is it necessary to have tsunami protection? What is the relation between costs and benefits?

Related with these questions are matters concerning the actual load on a structure. Is it anyhow possible to protect against extreme tsunami events and preceding earthquakes? To what extend is tsunami impact influenced by structure type, structure location, bathymetry, etc.

These questions have to be answered to assess the feasibility of a tsunami protection structure for Banda Aceh.

1.2 PROBLEM STATEMENT

At this moment limited knowlegde is available about the feasibility of tsunami-protection structures for the Banda Aceh region. To conclude about feasibility, more should be known about the characteristics and consequences of tsunamis and about the location, required dimensions and associated costs of tsunami protection structures for Banda Aceh.

1.3 OBJECTIVE

The objective of this final thesis work is to:

Provide insight into the feasibility of tsunami protection measures for Banda Aceh and set up a preliminary design for a tsunami protection structure.

The general feasibility is subdivided in *technical* feasibility and *financial* feasibility. Financial feasibility refers to the question if the costs of such a structure outweigh the benefits. Technical feasibility refers to the question if the structure can withstand the design tsunami.

1.4 GENERAL APPROACH

This thesis aims to cover the following subjects:

a) Literature study
b) Numerical modelling of tsunamis and structures
c) Development of tsunami protection alternatives
d) Evaluation of tsunami protection alternatives
e) A technical design of a tsunami protection structure

These activities are partly executed during the stay in Aceh from mid February till May 2007 and partly in Amersfoort at the headquarters of DHV. This work forms part of the Sea Defence Consultants Project (SDC-project) under the lead of DHV.

As stated before, feasibility can be divided into the technical feasibility and the financial feasibility. Is it possible to defend against tsunamis and if so, do the benefits outweigh the costs?

To answer this question a good understanding of tsunami physics and statistics in common and knowledge about existing tsunami protection is required. (Chapter 2).

To define the actual risk of tsunamis, it is important to know what tsunamis can be expected in Banda Aceh, and how often they occur. The result of this investigation is a relation between tsunami height and associated probability for Banda Aceh. To evaluate the benefits of tsunami protection it is necessary to know what damage is related with a certain tsunami height. If the structure is not built, what is the resulting damage? The answer on this question requires a lot of information, which is at this time available for one well-reported event: the Dec2004 Tsunami. (Chapter 3).

Various numerical models have been used in this thesis study. To study the general behaviour of tsunamis for varying bathymetry, shape and height, simple 1D-models are used. These models are also used to get a general idea about the effectiveness of several structural measures (and combinations). A description of a 2D-model is also presented. (Chapter 4).

For tsunami protection measures, various alternatives are possible. Not all alternatives are equally effective and some have more (negative) socio-economic side-effects then others. The effectiveness is computed with the 2D-model. The computed inundation can be expressed in damage which is a direct measure for the benefit of the structure (Chapter 5)..

Together with the probability of occurrence these benefits can be compared with the costs of the structure. This analysis enables to define an optimal protection level and gives an idea about the *financial feasibility* (CBA). However, this method does not provide a full picture of reality. Is it possible to build high structures without severely affecting society and economic development of the region? How are coastal structures evaluated compared with offshore solutions? (MCA). The combined result of this evaluation results in the selection of one alternative to be worked out in more detail (Chapter 6).

The proposed structure has to withstand tsunamis to a certain extent, but also the standard loads which normally attack a hydraulic structure. How should the structure be built with regard to the high loads induced by tsunamis? And how to deal with loads by (wind) waves and earthquakes? The final result is a (preliminary) *technical feasible* design of the proposed barrier, supported by calculations (Chapter 7).

1.5 COMMENTS

The described ‘design route’ seems straightforward and uncomplicated. Protection alternatives are assessed with by well-known and widely-accepted methods. The Cost-Benefit-Analysis enables to draw conclusions about the *financial feasibility*. However, not all aspects can be expressed in monetary units. Consequently, certain (dis)advantages are not taken into account in this evaluation method.

The Multi-Criteria-Analysis accounts for these *non-quantifiable* benefits and costs, by attributing a value to each alternative, based on certain criteria. However, it remains difficult to compare an (arbitrary) value with a cost-figure. Therefore, this evaluation method neither provides a clear answer, although it does provide insight into the *social feasibility* of various protection alternatives.

The question is: what is the value of a human life? Or, how to translate the number of body bags into a damage figure? How to deal with the physical and emotional suffering of survivors, the disruption of families? Or the uncertainty about living near a sea which can so easily destroy everything you have, but on the other hand provides food and income? And even though the loss of live can be minimized with a proper Early Warning System and a network of solid refuge buildings and roads, shouldn't one aim to create a less vulnerable area that enables sustainable and long-term economical development? The absence of constant fear for another devastating tsunami could probably level the entire city out of poverty.

Although these questions do not form part of this thesis study, they clearly emphasize that the decision about tsunami protection can not be made purely on basis of the outcome of technical evaluation methods.

This report aims to increase awareness about tsunami protection possibilities and the involved costs and consequences. For Banda Aceh the *financial, social* and *technical* feasibility of tsunami protection alternatives are evaluated. Although this study is aimed at Banda Aceh, it can also be used in a broader sense. It is hoped that it will attribute to a conscientious decision process.

Note: the use of trademarks in any publication of Delft University of Technology does not imply any endorsement or disapproval of this product by the University.

In this report the following trademarks are mentioned:

- *Geocontainer* is a registered trademark of Ten Cate Nicolon, The Netherlands
- *Xbloc* is a registered trademark of Delta Marine Consultants, The Netherlands
- *Armorflex* is a registered trademark of Armourtec, USA
- *GreenFlex betonblokkenmatten* is a registered trademark of Greenbanks erosion control, Appeltern, The Netherlands
- *The Movable Tsunami Flood Barrier* is a registered trademark of Van den Noort-Innovations, Kampen, The Netherlands

Chapter 2. INTRODUCTION TO TSUNAMIS

2.1 INTRODUCTION

The term tsunami is derived from two Japanese words: 'tsu', meaning *harbor*, and 'nami', meaning *wave*. That is because these waves may create large surges or oscillations in bays or harbours, which are not responsive to the action of normal sea waves. In deep water, a tsunami is hardly noticeable, but near the coast various mechanisms cause the wave to grow with sometimes devastating effects. The term 'tsunami' was created by fishermen who returned to their ports to find the surrounding area devastated, although they had not been aware of any wave in the open water.
The theory describing this phenomenon is summarized in this Chapter, together with an introduction to existing tsunami barriers. Some background information is presented in Appendix I. This Chapter summarizes the main aspects about the generation, propagation, and shoreline interaction of these intriguing waves.

2.2 NATURE AND ORIGIN OF TSUNAMIS

Tsunamis are caused by rapid perturbations of the seabed or of the water column above it, which either lift the sea surface up above its normal level (the usual case) or depress it. This perturbation produces a series of waves, or wave train, which then propagates outwards from the source area until it either dissipates or collides with a coastline. The physics of this propagation process are considered later. The used terminology is presented in Figure 2-1.

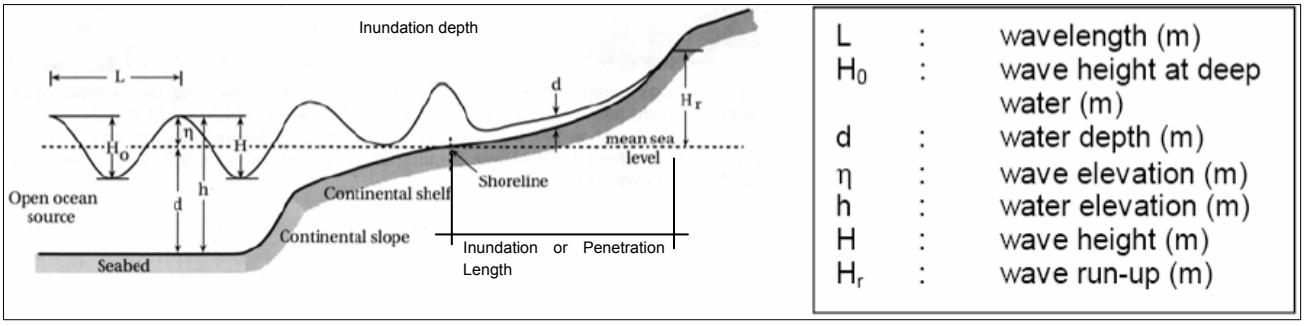

Figure 2-1 Terminology for tsunami waves [61]

Tsunamis can be triggered by:

1. Earthquakes
2. Landslides
3. Volcanic eruptions
4. Meteor impact

Combinations of these generation mechanisms do often occur. As earthquakes are the most common cause of tsunamis, they will be elaborated in more detail.

2.3 MECHANICS OF GENERATION

2.3.1 Earthquake generated tsunamis

The most common cause of tsunamis is seismic activity. The earth's crust can generally be divided into fifteen major rigid plates. These plates move relative to each other causing them to collide at certain locations and drift apart elsewhere. These boundaries are called *fault lines.* The contact between these massive plates does not run smooth, resulting in a build up of stresses along the fault. When the stress exceeds the resistance of the rocks, an earthquake occurs that (partially) releases the built-up stresses in a certain time span. This process can result in displacements of the earth's surface up to several meters and subsequent displacement of the overlying water mass. This will sometimes result in a series of waves, called tsunamis. When this happens, this earthquake is called *tsunamigenic*.

The energy involved with these tsunamis can be expressed in a magnitude scale and an intensity scale (see Appendix I.1.1) and depends on either the earthquake magnitude M_w or the resulting run-up of the tsunami-waves. The probability of tsunami-generation depends also on the depth of the epicentre (*focal depth*). With a focal depth of 30km, one needs at least an 8.0 magnitude earthquake for trigger a significant tsunami with run-up heights of 4-6m.

Two main fault types can be distinguished: a dip-slip and a strike slip fault. A dip-slip earthquake can be on a vertical or a dipping plane, where the latter is called a thrust-dip. These fault types can be in normal and reverse direction. An impression of a dip-slip fault is presented in Figure 2-2**.** A more detailed description of various fault-types is presented in Appendix I.1.2.

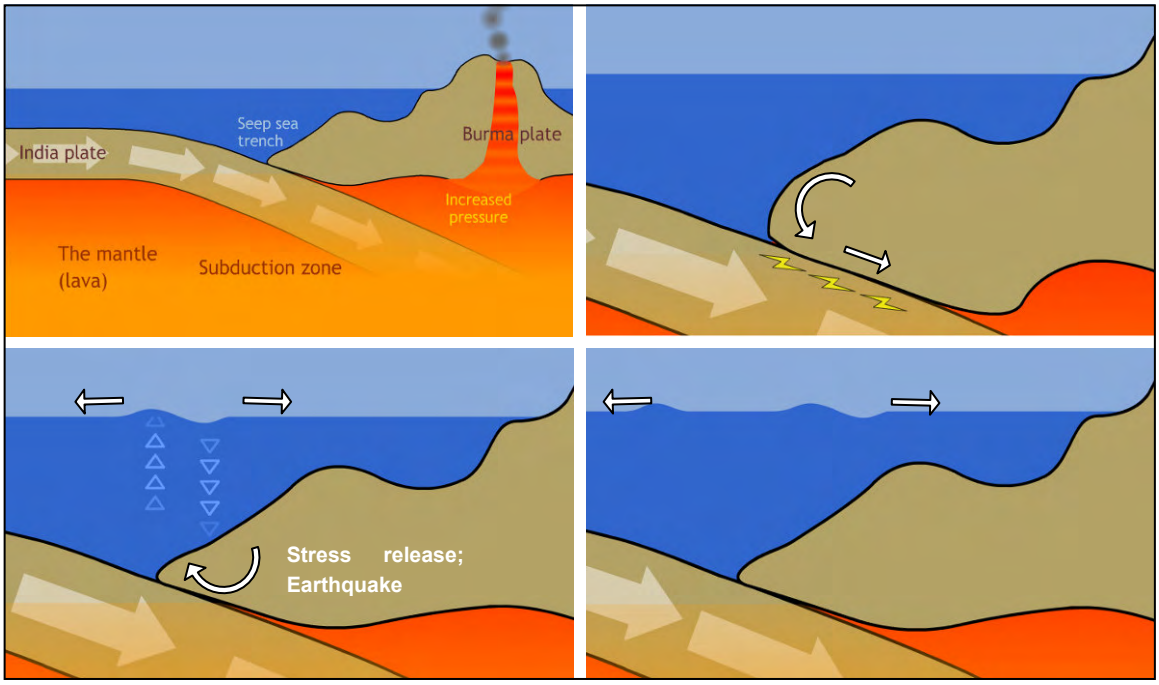

Figure 2-2 Impression of a (thrust) dip-slip fault and associated water levels. [62]

As can be seen in above figure, the fault-type determines the characteristics of the wave. If a coast-line is located on the sub-ducted plate (at the right of Figure 2-2) a *negative wave* is

expected, meaning an initial drop-down of the water level. The coastline located on the sub-ducting plate (at the left) will receive a *positive tsunami.* Negative tsunamis are generally more powerful then *positive tsunamis* (see Appendix II-5).

Tsunami wave heights are highly variable. Many parameters determine the final wave height at the coast. Also the earthquake signal plays an important role. This means that (general) relations between earthquake and resulting tsunami magnitude, intensity or run-up are not suited for design purposes.

Besides that, earthquakes can go together with landslides. This type of generation is treated in the next paragraph.

2.3.2 Landslides

The characteristics of tsunamis generated by landslides are different from those generated by earthquakes. One of the more important differences is the fact that the direction of propagation of tsunamis generated by landslides is more focused. The slide moves in a down-slope direction and the wave propagates both upslope and parallel to the slide.
Two mechanisms can be distinguished, submarine and sub-aerial landslides. See
Figure 2-3. As explained in the figure, sub-aerial landslides are more effective in generating waves, since it yields a net addition of volume to the sea floor.

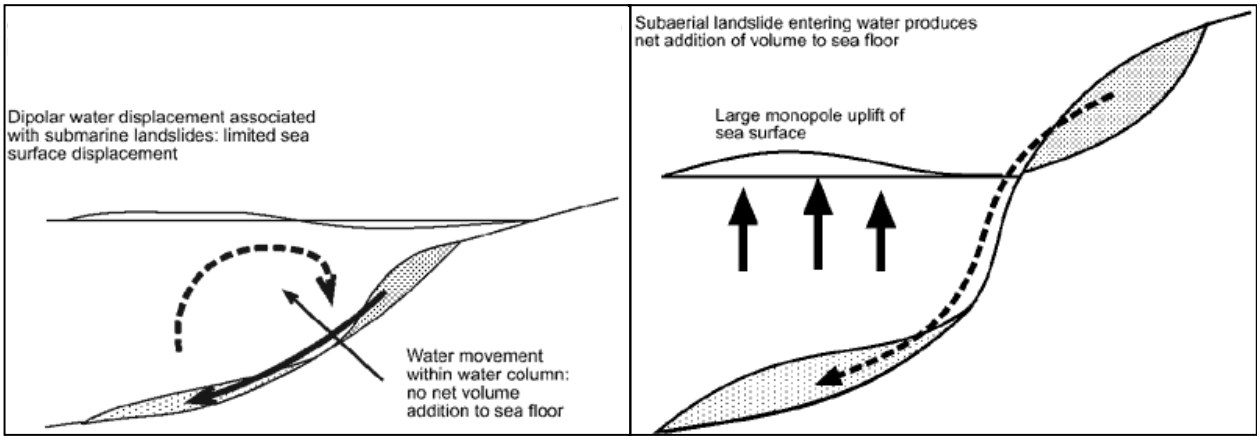

Figure 2-3 Comparison of sub-aerial and submarine landslides as tsunami wave sources [45]

Wave generation by landslides depends primarily upon the volume of the material moved and submerged, the speed of the landslide and the mechanism of movement. The effect of landslide speed on tsunami generation is treated in more detail in Appendix I.1.3

Generally, the wavelengths and periods of landslide-generated tsunami range between 1 and 10km and 1 and 5 minutes respectively. These values are much shorter than those produced by earthquakes [3].

2.3.3 Volcanic eruptions

Volcanic eruptions can generate tsunami in many different ways. The majority of eruptions are accompanied by seismic tremors, which can trigger tsunami if they are big enough and lie in or near the ocean. Volcanic activity can also induce submarine landslides (as discussed in the previous paragraph) and submarine eruptions/explosions. The latter can cause violent tsunami, when ocean water comes in contact with the magma chamber. This water is converted instantly into steam, causing an explosion, which can generate large ocean waves. It is believed that the August 1883 Krakatau eruption produced a 40m tsunami by this mechanism.

Other volcano-linked mechanisms that may induce tsunami are: pyro-clastic flows, caldera formations, basal surges, lahars, atmospheric pressure waves and lava. These mechanisms will not be described here.

2.3.4 Meteor impacts

Unlike earthquakes, which cause most tsunami but have a well-defined upper limit, the potential tsunami height caused by meteor-impact is almost unlimited. However, most objects smaller than 100 - 200 m in diameter explode in the atmosphere and will not produce significant waves.

2.3.5 Overview and application

Although a distinction has been made among different causes for tsunami, it is most likely that a lot of tsunamis are caused by a combination of these mechanisms.

In Table 2-1 the percentage distribution of events and deaths are presented for tsunami-events over the past 2000 year. Also joint occurrences are listed.

Table 2-1: Causes of tsunami for all listed events [50]

Cause	Number of Events	Percentage of Events	Death toll	Percentage of Deaths
Unknown Cause	42	3,9%	0	0,0%
Earthquake	883	81,6%	463.997	87,7%
Questionable Earthquake	1	0,1%	0	0,0%
Earthquake and Landslide	54	5,0%	20.346	3,8%
Volcano and Earthquake	9	0,8%	35	0,0%
Volcano, Earthquake, and Landslide	4	0,4%	5775	1,1%
Volcano	53	4,9%	37.215	7,0%
Volcano and Landslide	5	0,5%	128	0,0%
Landslide	30	2,8%	1.647	0,3%
Meteor impact	0	0,0%	0	0,0%
Explosion	1	0,1%	0	0,0%
Astronomical Tide	0	0,0%	0	0,0%
Total	**1082**	**100%**	**529143**	**100%**

Comment 1: The listed events are only most-probable and definite tsunami events

Comment 2: *The high death toll for tsunami is mainly because the 2004 Indian Tsunami, as it caused 297.548 deaths. Without this event, the percentage of deaths due to earthquakes becomes 71,9%.*

From this table it becomes clear that earthquake-induced tsunami form the biggest threat as they are responsible for over 80% of all tsunami events and deaths.

The question arises: *Can this information be used for design purposes?*

Answer: For design purposes it is important to have knowledge about the possible causes of tsunamis to determine the likelihood for a certain location. However, relations between a generation mechanism and the actual tsunami wave height are too general to use. These relations are more useable in large-scale tsunami hazard mapping.

2.4 TSUNAMI PROPAGATION

Much of the terminology used for ordinary wind waves can be used to describe tsunami waves. Tsunamis have a wavelength (L), a period (T) and a height (H). They undergo shoaling, refraction and diffraction. Most tsunami travel in wave trains containing several large waves. In deep water, the height is generally in the order of decimetres.
Although tsunami wave characteristics are highly variable (especially at the coast) it is possible to present a simple approach, which enables one to generally describe the propagation of tsunami waves in deep oceans. Because of their long periods and corresponding wavelengths, the train of waves forming a tsunami can be understood as shallow-water waves at their origin and propagation across the ocean. This approach is presented in following section.

2.4.1 Shoaling

The most important property of tsunamis is the incredible speed they travel with in deep water. For small ratios of (H/d) and for L>>d, the wave propagation speed *c* is equal to:

$$c = \sqrt{gd}$$

For the derivation, see Appendix I.2.1.

In deep oceans, the wave travels with a speed comparable of that of jet planes. In Figure 2-4 this is quantified for a typical tsunami wave. Typical values for tsunami wave lengths are also shown. The increase in wave height is called *shoaling.*

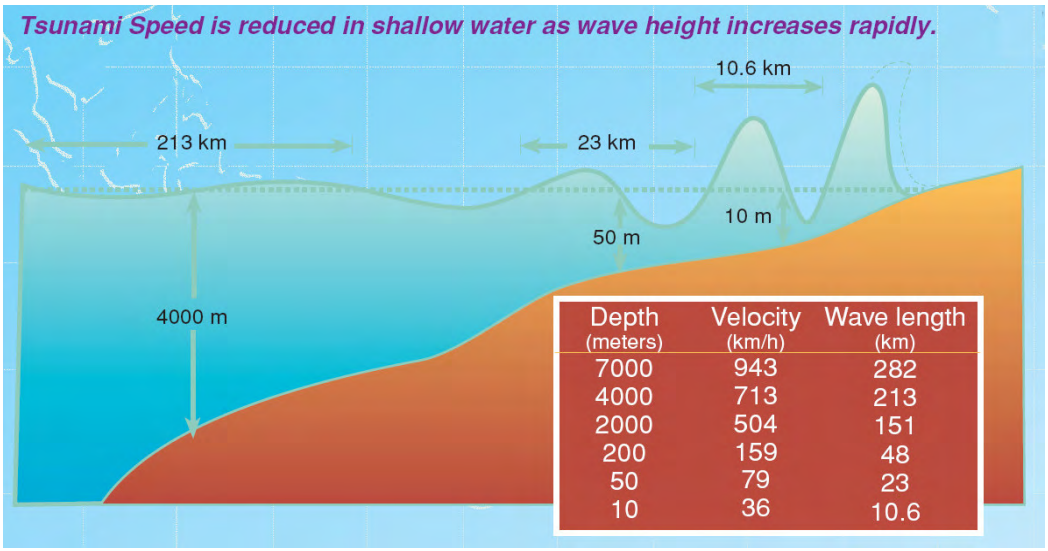

Figure 2-4 Typical parameters for tsunamis [32]

Because the wave propagation speed is independent of the wave period, all waves travel at the same speed. This means that no dispersion occurs. Some remarks on this assumption will be given later.

Appendix I.2.1 shows that energy conservation finally gives the following expression for wave shoaling: (see also Figure 2-5)

$$\frac{H_2}{H_1} = \left(\frac{d_1}{d_2}\right)^{\frac{1}{4}}$$

This equation is the well-known Green's Law and describes the shoaling process of waves propagating in decreasing water depth. Above derived equations do not account for refraction, diffraction and dispersion. Also, this law does not account for wave reflection from bottom slopes and results in calculated wave amplitudes that are too high. Especially in case of abrupt depth transitions, the differences are considerable, due to wave reflection.

2.4.2 Wave reflection

Abrupt depth transitions in oceans, like continental shelf, cause waves to become higher and shorter. Also dispersion may occur. Lamb (1932) derived equations for single waves, passing over an abrupt change in depth. The difference between shoaling (Green's Law), reflection and the combination (Lamb's law) is explained in Figure 2-5.

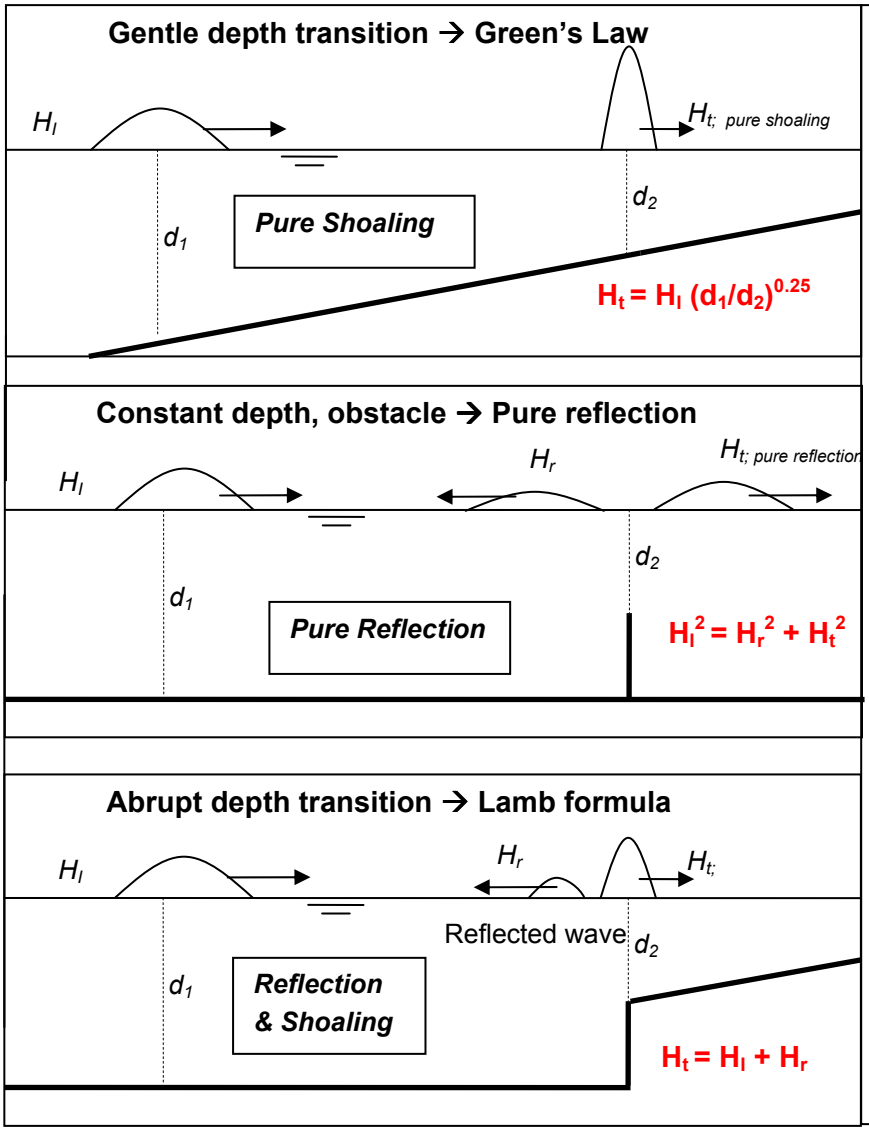

Left figures show the difference between pure shoaling (Green's Law), pure reflection and the combination (Lamb's Formula). In this overview, the influence of friction is not included.
For pure shoaling, the wave grows due to decreasing wave celerity and wave length.

In situations with pure reflection, the transmitted wave H_t is smaller then the incoming wave H_I.

With an abrupt depth transition, the transmitted wave is higher than the incoming wave, due to shoaling. However, because a part of the wave is reflected, H_t is lower than in case of a gentle depth transition (for similar H_1,d_1 and d_2).

However, for low ratios of H/d the actual shoaling of the wave is well predicted by Green's Law. For higher ratios of H/d, this law generally overestimates the wave height.

Figure 2-5 Shoaling, reflection and a combination of these processes

So, in general, a gentle bathymetry will cause higher wave heights then an abrupt transition in depth. However, this conclusion is only valid for low ratios of H/d. When the ratio H/d increases, non-linear processes play a significant role and the wave growth can not be described by these simple theories.

In wave trains, reflected waves interfere with incoming waves, generating a wave field which cannot be calculated with above presented laws. Depending on the signal (shape of the wave train), wave heights can even become higher than indicated by Green's Law.

Reflected waves are normally of secondary, but not negligible, magnitude according to this theory. At certain locations, convergence may cause reflected waves to be of primary magnitude. There is proof that the highest and most damaging tsunami waves at locations on Hawaii from the 1 April 1946 tsunami, were reflected waves from the continental slopes of Japan [4].

2.4.3 Wave refraction, diffraction and spreading

Because tsunami waves are shallow water waves, they *feel* the ocean bottom at any depth and their crests undergo refraction or bending around higher topography (diffraction). A simulation of the Dec2004 Tsunami clearly shows spreading and refraction, see Figure 2-6.

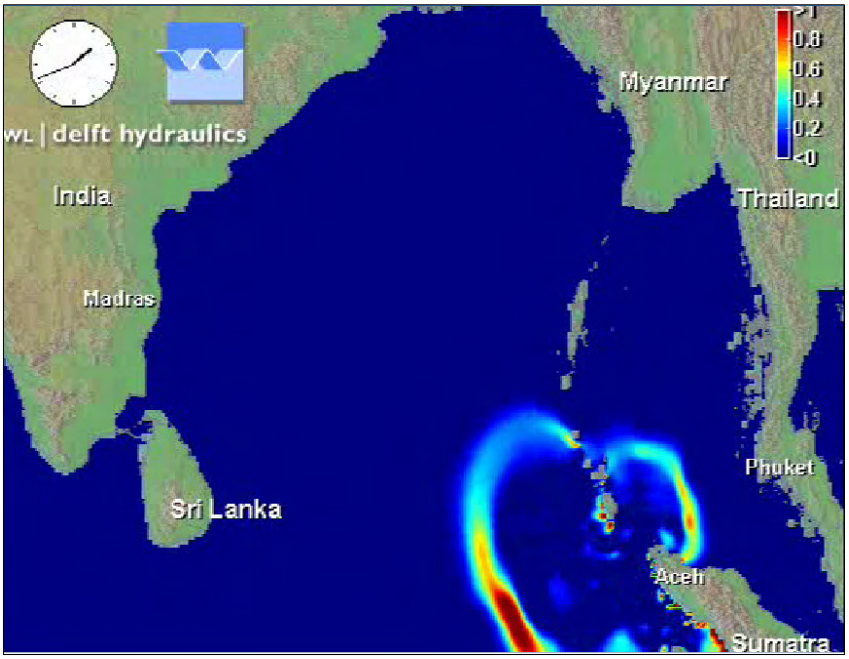

Figure 2-6 Spreading and refraction of the 2004 Tsunami, [55]

Refraction is the change in direction of a wave due to a change in its speed. This mechanism occurs especially in coastal areas, where the decreasing water depth causes a decrease in wave celerity. When waves have an oblique incidence on the coast, the depth under a wave crest varies along the crest. The part of the wave crest closer to shore is in shallower water and is moving slower than the part away from the shore in deeper water. The wave crest in deeper water catches up so that the wave crest tends to become parallel to the shore. This deflection causes an attenuation of the wave height. Some typical refraction patterns are depicted in Appendix I.2.2.

Diffraction is the process that waves bend around obstacles and spread their energy laterally to the leeside of the obstacle.

Another process causing attenuation of the wave is geometrical spreading. Initially tsunami waves diverge near the source, spreading out over the earth's sphere. These waves will converge again at a point on the opposite side of the globe [4],[53].

Generally, wave refraction, diffraction and spreading will decrease the energy and thereby reduce the wave height. However, local obstacles can refract tsunami waves in such a way that its energy is concentrated or focused upon specific locations. Especially headlands are vulnerably, because they attract a relative large portion of the wave crest to break on it.

Other local effects like resonance can sweep up the waves. Especially harbours can show resonance, where the natural period of the harbour basin (depends on the length and depth)

could be equal to (a whole portion of) wave period in the wave train. Structures in bays and harbours can change the natural period, and induce higher wave heights in case of tsunami attack. Remind that the word *tsunami* (harbour wave) has direct relation with this phenomenon.

It is important to be aware of the nature and consequences of these mechanisms. Local bathymetry and topography greatly attribute to the development of the tsunami-waves. They can cause large differences in tsunami-inundation and damage, even for cities located close to each other[2].

2.4.4 Wave dispersion

For large ratios of L/d, like tsunamis, the wave celerity becomes independent of the wavelength (and thus wave period). This means that the wave is non-dispersive. All wave components with different periods travel at the same speed and arrive at the same time. However, this assumption is not completely valid, as was shown by Kulikov [15], who observed dispersion in satellite images made from the Dec2004 Tsunami.
It was shown that non-dispersive numerical models generate reliable (conservative) results with respect to wave heights and run-up. In some cases however, significant differences were found, although mostly for offshore propagating tsunamis [44]. It is important to be aware of the limited accuracy of these models with respect to wave run-ups.

2.4.5 Friction

Tsunami waves on the open ocean loose energy mainly due to spreading. In shallow water however, the main source of energy dissipation is friction with the bed and on land (in case of inundation). The friction coefficient *f* [-] can be related with Manning roughness coefficient *n* by:

$$f = n^2 g \cdot (d + H)^{-\frac{1}{3}}$$

with *n* is Manning's roughness in [$m^{-\frac{1}{3}}s$], d is depth in [m] en H is the tsunami height above mean sea level [m]. *f* is dimensionless. Note that friction decreases with increasing depth. Typical values of *n* for both sea and dry terrain are presented in Table 2-2.

Table 2-2: Typical values of n for different terrain types [53] .

Terrain type	Roughness coefficient *n*
Sea	0,026
Mud flats, ice, open fields without crops	0,015
200m strip of coast	0,026 –0,035
Built up areas	0,035
Forest, jungle, etc.	0,05-0,07

[2] *During the Dec 2004 Tsunami, the wave heights at Banda Aceh reached a (run-up) height of approximately 10-12m. The waves in Lhok'Nga (about 11km away from Banda Aceh) ran up almost 35m ([49].[50]). Differences in near-shore bathymetry are a possible cause, although some researchers think that minor, local earthquakes caused these waves.*

2.4.6 Overview and application

In this subparagraph a short overview has been given of the governing mechanisms that describe the propagation and alteration of tsunami waves in deep oceans, over continental shelves, along islands and other varying topography. Although this theory is generally valid, the question arises:

How can this information be used for design purposes?

The answer is: Suppose one knows the tsunami wave characteristics (L, H, T) at deep water and knows the bathymetry between that point and the region of interest. In that case it is possible to calculate the behaviour of the wave towards the coast and at the point of interest. One should mainly account for shoaling and reflection (from shelves). If there are obstacles, diffraction is important. However, in the near-shore region, where the ratio H/d becomes sufficiently large, non-linear effects play a role. Also friction is coming into effect, since the depth becomes smaller. The simple shoaling law of Green is not accurate anymore. Especially for this near shore region, computer models are necessary to account for all described mechanisms and present reliable wave heights. The local geometry (bays, harbours) and bathymetry (steep, gentle) become very important.

In the next subparagraph, the interaction with the shoreline is treated. Typical features of tsunamis approaching the shore and running into land are discussed and expressions are presented to roughly estimate the resulting run-up and inundation.

2.5 SHORELINE INTERACTION

The arrival of a tsunami at a shoreline can be a threatening sight, but is often not as obvious as it is suggested. In contrast to many impressions and movies, tsunamis will not often show up as a breaking wave. Depending on the wave parameters (the initial signal), local topography and bathymetry, the wave can manifest as a rapid rising water level, a plunging breaker, or a bore running inland. Especially in wave trains, the appearance can vary greatly between the successive waves. The first wave could be a rapid increase in water level, but when the water runs down, the second waves can develop in a bore that continuously breaks over the back-flowing water and form a wall of water.

2.5.1 Wave breaking

In general waves break as a result of instability. When the particle velocity '*u*' exceeds the wave celerity c, the particles leave the wave profile. This occurs when a wave is very steep (in deep water) or because the water is very shallow or a combination of both mechanisms. It was found (Appendix I.3.1) that the tsunami breaking criterion as suggested by Bryant [1] is similar with the well-known Iribarren expression:

$$\xi = \frac{\tan\beta}{\sqrt{H/L_0}}$$

Where $L_0 = \frac{gT^2}{2\pi}$. The transition between breaking and non-breaking lies around ξ = 3-5, where a higher value indicates non-breaking conditions.

For two fore-shore slopes of 1:100 and 1:200, the breaking limit is depicted in Figure 2-7. It can be seen that for typical tsunami-periods (20 minutes or 1200 seconds and higher), almost no breaking would occur.

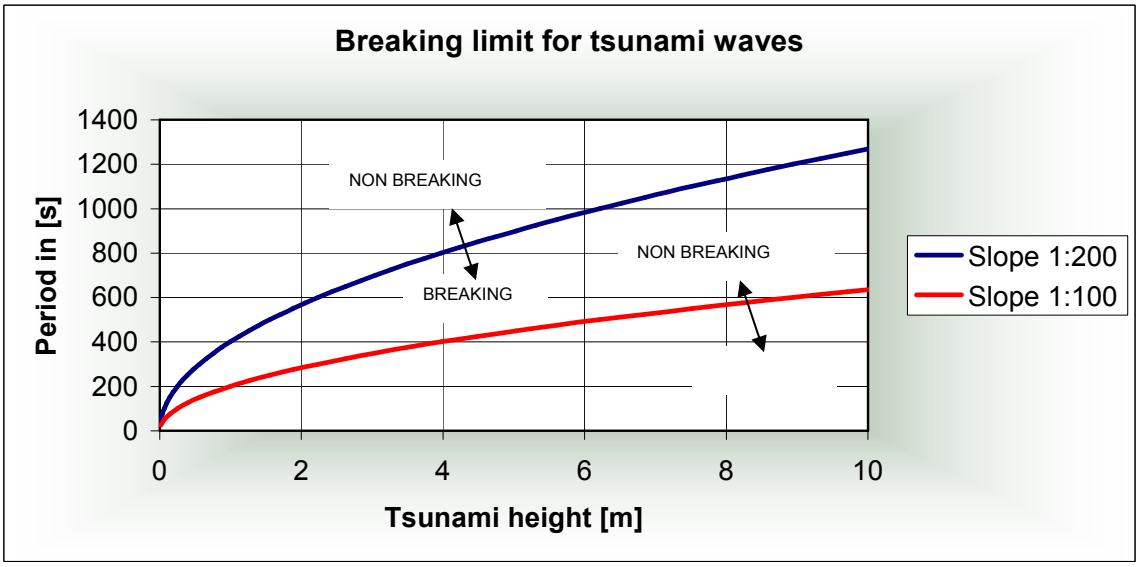

Figure 2-7 Breaking limit for various slopes

This indicates that tsunami waves show almost the same behaviour as wind or swell waves. Only, the very long wavelength and period of tsunami changes the notions 'steep' and 'gentle' completely. This is clearly illustrated by the fact that most tsunami do not break on beaches with slopes of 1:100 and steeper, but surge onto shore and are even reflected. For a tsunami of 6m-height and a period of 20min, a slope of 1:100 is just as steep as a slope of 1:1 is for a wave with a period of a few seconds.

Reality is more complicated though. Dispersion can cause the tsunami wave to split into smaller parts, which can plunge on the coast. So-called 'soliton fissions', smaller waves riding on the face of the main tsunami wave, also occur. These mechanisms attribute to the versatile nature of

tsunami appearances at the coast. A short impression of various coastline-interactions of the Dec2004 Tsunami is shown in Figure 2-8.

Koh Lanta, Thailand. Surging breaker

Banda Aceh. It is hard to see on this picture, but here the tsunami acted like a rapid rising tide

Krabi Beach, Thailand. So called 'soliton fissions', acting like a series of bores

Phuket, Thailand. Series of breaking waves

Figure 2-8 Variety of Dec 2004 Tsunami appearance at various locations. Source [52]

2.5.2 Run-up

Run-up is defined as the maximum water level on a slope during a wave period. The heights are relative to the Still Water Level (SWL).
For 'normal', breaking waves, the run-up is given by Hunt's formula:

$$\frac{H_r}{H} = \xi \quad [30]$$

The maximum lies around ξ =2,5-3 for normal waves. If the wave is a non - breaking or tranquil wave ($\xi \rightarrow \infty$) the run-up height is roughly equal to this initial height. This is called a standing wave. For higher velocities and bores an experimental maximum of ξ =4,5-5 is obtained [4].
Because the general behaviour of tsunamis is similar to normal waves, it can be expected that for non-breaking tsunamis the run-up height is equal to the wave height. $H_r = H$. The main difference is that this occurs also for more gentle slopes and not only against vertical walls. See also previous section.

It becomes clear that besides the wave height, the velocity associated with the wave is the most governing factor. For tsunamis, running up a dry bed as a bore, Freeman and Le Mehaute (1964) in [5] give:

$$H_r = \frac{u^2}{2g} \frac{(1+A)(1+2A)}{\left(1+\frac{f}{A^2 S}\right)} \qquad \text{(for bores)}$$

With $A = Fr^{-1}$, S= ground slope, and *u* is the current velocity of the surge, $Fr = \frac{u}{\sqrt{gh}}$ and h is the surge height at the shoreline. Run-up decreases with increasing roughness and decreasing slope. The value of Fr was proposed to be 2. With this value, the maximum run-up for infinite slopes (S $\rightarrow \infty$, vertical walls) becomes $H_r/H = 6$, with H is equal to h, because depth and 'wave height' is the same for bores. This value is somewhat higher than experimentally obtained values for breaking waves running up a vertical wall. Camfield and Street [4] derived values between 4,5 and 5,0 for this type of run-up. For the expression of Freeman and Le Mehaute [5], the maximum run-up is calculated for various velocities; see **Figure 2-9**.

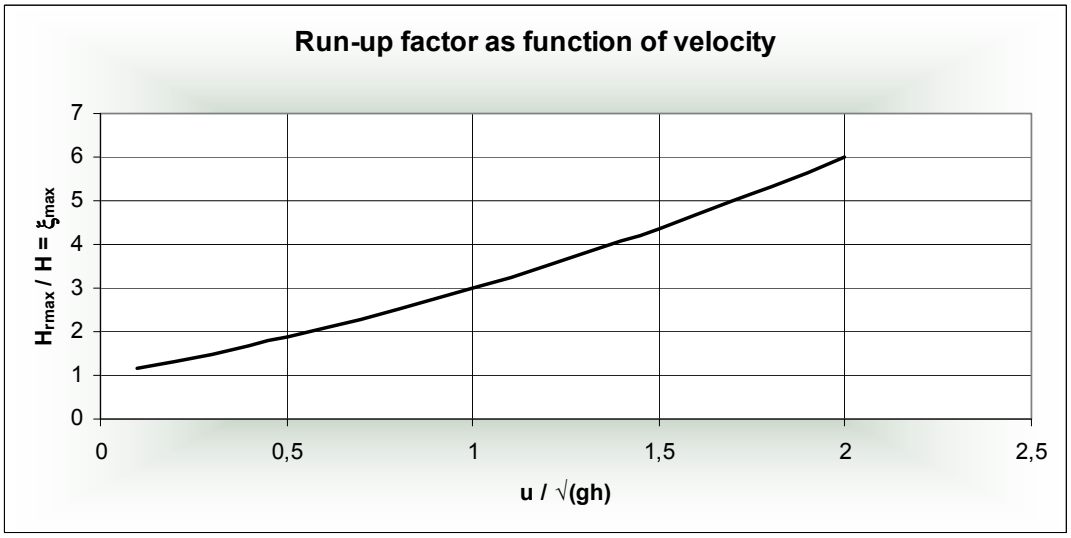

Figure 2-9 Maximum run-up factor for bores running on a dry bed as a function of velocity

The maximum run-up in Hunt's formula for normal waves (with H_r/H = 3), corresponds with a Froude number of 1 in Freeman and Le Mehaute's expression. This indicates velocities equal to $\sqrt{(gH)}$. For low velocities, the run-up factor tends to 1, indicating a standing wave.

Apparently, the current velocity of the wave is a governing factor in the run-up.

2.5.3 Velocities

The tsunami-waves travel with a speed equal to √(gd). However, this is the velocity of the wave profile (or wave propagation speed or wave celerity), and NOT the velocity of the water particles. For shallow water waves (tsunamis), the horizontal particle velocity is given by:

$$u_{particle} = a\sqrt{\frac{g}{d}}\sin\theta$$

with :

$$\theta = \varpi t - kx; \quad \varpi = \frac{2\pi}{T}; \quad k = \frac{2\pi}{L}$$

$$a = \frac{H}{2}$$

E.g., for a 3m high tsunami at 20m water depth, the wave celerity is 14m/s and the (maximum) particle velocity 1,1m/s. The difference decreases towards the shore.
When the tsunami approaches the shore and becomes higher, the particle velocity would exceed the wave celerity. Ultimately, instability in the form of breaking is induced. Eventually, a bore is formed. At this point, there is no difference between wave celerity and particle velocity.

The theoretical values for the velocity of tsunami waves, running inland, vary between:

$$u = 1{,}1\sqrt{gh} \text{ and } u = 2\sqrt{gh}$$ (see more in Appendix I.3.2)

After the Dec2004 Tsunami in Banda Aceh surveys were carried out and inundation depths were measured134 [25]. Velocities were obtained from video footages. The relation of inundation depth *d* and velocities *u* is calculated in Chapter 4, Table 3-5. The values vary between:

$$u = 0{,}8\sqrt{gh} \text{ and } u = 1{,}3\sqrt{gh}\ .$$

Little information is available on velocities nearby offshore structures. If the wave does not break in front of the structure, steady flow situations will develop, due to the long period of tsunami waves. See section 2.6 on this topic.

2.5.4 Penetration

The penetration length of tsunamis depends mainly on the wave height and the slope of the coastal zone. Friction is another important parameter. However, since tsunamis mostly consist of a series of waves, the friction is reduced during the successive penetration. The 2nd and later waves can normally penetrate much farther, because the first tsunami wave in a series typically removes most of the obstructions in its path, reducing surface roughness for the later waves in the series. Thereby, successive waves 'ride' on the water layer left behind after the first penetration. Appendix II-3 presents a clear impression of successive wave penetration.

2.5.5 Overview and application

In this paragraph, tsunami-interaction with the shoreline has been treated. Typical features of tsunamis approaching the shore and running into land were discussed and expressions were presented to roughly estimate the resulting run-up and inundation.

How can this information be used for design purposes?

It is obvious that the appearance of the tsunami wave front at the location of the structure is important. This determines the associated velocities. Relations for the run-up height present a maximum value. For design purposes this could be useful because this would result in conservative designs. For higher tsunamis however, (H =8 - 10m), the run-up factors of 2 a 3 will result in extremely high structures, which are not realistic and maybe not necessary either. Instead of using these theoretical relations it is better to use numerical models to accurately simulate the slopes of the structure, thereby making use of the actual tsunami signal.

2.6 INTERACTION WITH STRUCTURES

Breakwater, seawalls and other, 'soft', measures may provide protection against tsunamis. It may decrease the inundation on land as well as reduce the current velocities. However, structures may also have undesired effects on other areas (by reflection) or even on the area to be protected, because it may affect the resonant period of bays and harbours so that wave height increases instead of decreases.

The energy of a tsunami wave, which is either dissipated on land or reflected when there is no structure, must now be reflected by the structure. The resulting forces on the structure as well as current velocities depend highly on the wave height and waveform. When the tsunami acts like a rapid increasing water level, the resulting (impact) pressure on the structure is lower than in case of a bore-like wave.

This paragraph gives a short overview of the existing theory to describe forces and velocities on (sufficiently) high structures for both non-broken (2.6.1) and broken (2.6.2) waves. Furthermore, the effectiveness of low-crested, submerged and soft measures like trees and mangrove is discussed.

2.6.1 Forces of non-broken waves on high-crested structures

High-crested structures have a crest-level that is at least comparable with the height of the tsunami.

Vertical wall

To determine the forces on a vertical wall due to tsunami forces, Tanimoto [21] studied the wave pressure distribution for different values of h/L. Based on these results and Goda's formula for storm waves, a wave pressure distribution to calculate tsunami forces on a vertical wall is proposed. This method is only valid for relatively deep water offshore, so that no breaking tsunami occurs. The method is presented in Appendix I.4.1.

Although this method showed good agreement with laboratory results and explained the collapse of the Kawaragi caisson-breakwater during the 1968 tsunami (see also section 2.7.4), its general validity or applicability is limited by:

- The use of the tsunami shape signal. It was not mentioned in the study which type of tsunami-signal was used. Positive or negative tsunamis, as well as the number of waves, period, etc. all will have important consequences for the run-up and impact forces.
- The vertical face of the structure. Only vertical structures were investigated. For sloping structures, the tsunami will cause different impact forces.
- The definition of 'non-broken tsunami'. It is obvious that between non-broken and a breaking tsunami a transition area of increasing impact force will exist. In what region should this method be placed?
- The definition of the tsunami wave height. The 'reflected height' is proposed. But this height will vary for many parameters as mentioned above.

Rubble-mound structure

With this 'Tanimoto-method' it is possible to compute the stability of the structure as a whole. However, in case of rubble-mound structures, the stability of the armour layer is a point of bigger concern. Failure of a rubble mound structure under tsunami conditions can occur due to:

- Instability due to direct loads from the tsunami wave. Especially the crest and rear side are vulnerable due to overtopping.
- Instability due to long duration of tsunami wave, due to direct load on the structure (drag forces) or erosion of the seabed. This is especially important in the gaps, where the bottom is unprotected and extremely high velocities occur.
- Failure of the armour layer due to internal pressures
- Unequal settlements over axis of breakwater due to seismic activity, maybe resulting in liquefaction of seabed and/or structure body and unequal settlements along the axis of the breakwater leading to damage of armour layer.

The stability of the structural parts (toe, armour, crest, etc.) depends highly on the characteristic stone diameter. For normal waves, formulas exist (Van der Meer, etc.) in which a characteristic stone diameter can be calculated for given conditions. However, these formulae cannot be used for determining the stone stability under tsunami conditions. The tsunami period, height and length are out of the calibration range of these formulae.

A possible approach is to translate the tsunami impact to current velocities. Due to the long duration of the tsunami wave, the flow of the wave can be characterized by a steady flow. This means that the stability of the stones under tsunami attack can be considered and calculated as the stability of stones under flow conditions. For this load situation various formulas are available.

Tanimoto's method assumes a non-broken tsunami. This logically means that the associated velocities are also low. However, the velocities and thus the impact forces of a broken tsunami are much higher, as also indicated by the research of Ikeno, Kato *et al* [22], [23]. The forces due to tsunamis acting like bores are treated in the next paragraph.

2.6.2 Forces of broken waves on high-crested structures

The velocities within non-broken tsunami waves are relatively low. Most of the initial damage of such tsunamis will be due to buoyancy and hydrostatic forces. In case of a steep topography, the retreat of the tsunami occurs much more rapid than the run-up, causing more damage than the initial wave loading. In case of a gentle slope, the retreat is slower due to lower velocities.

When the tsunami forms a bore-like wave, the current velocities are much higher. The dynamic water pressure will increase too. Another important parameter is the inclination of the face of the bore. The steeper the face of the bore, the higher is the impact on a structure.

Following Tanimoto's study, additional research by Ikeno *et al* investigated the effect of bore-like tsunamis on offshore upright walls [22] and tsunamis running on land [23]. Respectively, a maximum increase of wave pressure with factor 1,5 and 2,0 compared to Tanimoto's method was found. Kato *et al* [19] investigated the impact on sloping dikes. They found even higher values (factor 2,3 higher) under certain circumstances. See Figure 2-10 for an overview.

For structures on land the following expression for the dynamic water pressure p_{dyn} is used by Yamamoto *et al* [48]:

$$p_{dyn} = 0{,}5C\rho u^2$$

with $u = 1{,}1\sqrt{gh}$, h is the inundation depth, ρ is the density of sea water (kg/m^3) and C is a shape coefficient (=2 for rectangle sections and 1,2 for circular sections).

Yamamoto surveyed disaster situations in the west coast of Thailand and the south coast of Sri Lanka where damage due to the Indian Ocean tsunami of December 2004 was severe and investigated the destruction mechanism of structures due to the tsunami. He found that above expression for the dynamic water pressure predicted the force on the building quite well.

For bore-like tsunamis, Cross (1967, in [4]) derived a theoretical expression based on velocities of $u = 2{,}0\sqrt{gh}$. In Appendix I.4.2, this expression is presented.

2.6.3 Overview tsunami force on high-crested structures

So far, six methods have been described. All have their limitations, but together they will provide insight in the range wherein tsunami-impact forces can be expected. The methods are:

- Cross (1967), a theoretical expression, based on velocities of $u = 2{,}0\sqrt{gh}$
- Tanimoto (1984), non-broken tsunamis on offshore and vertical structures
- Ikeno (2001), bore-like tsunamis on offshore and vertical structures
- Ikeno (2003), bore-like tsunamis on vertical structures on land
- Yamamoto (2005), investigated tsunami damage on land due to Dec2004 Tsunami
- Kato (2006), bore-like tsunamis on sloping structures on land

These methods give an indication about the impact forces due to tsunami-attack for various circumstances. However, the influence of the tsunami-shape signal and the definition of the tsunami height remain unclear. Therefore these methods should be used with care.

Under some assumptions, these methods are compared to each other for varying tsunami surge height (see Figure 2-10). To have a more complete overview, the hydrostatic force is also added.

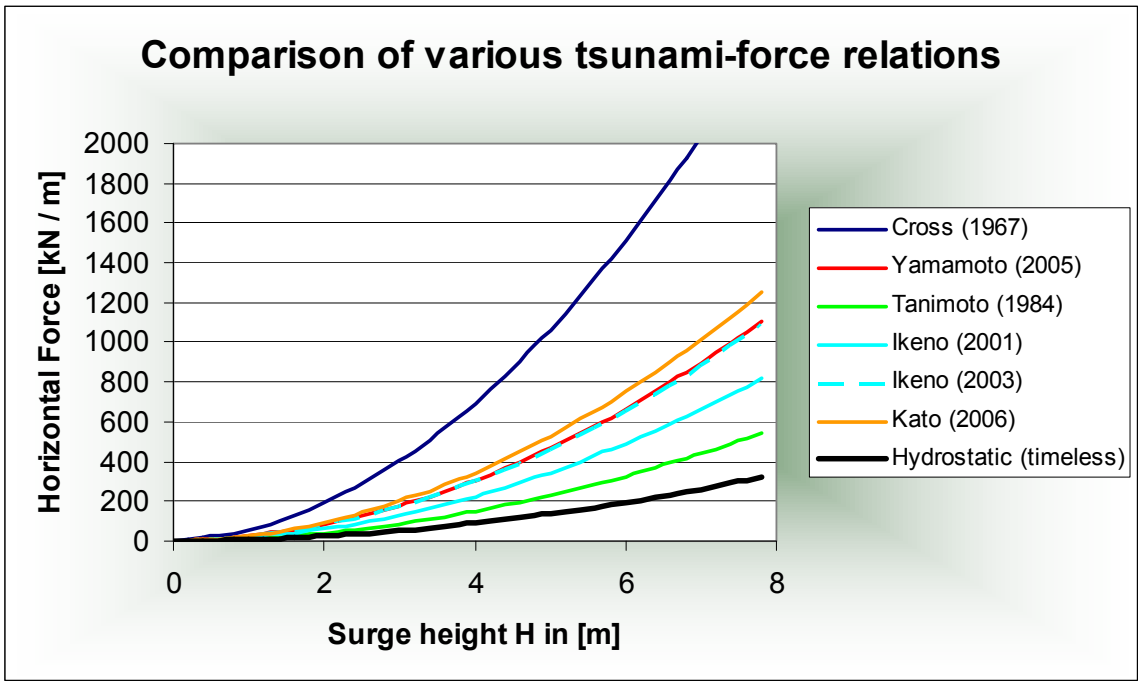

Figure 2-10 Horizontal tsunami forces according to Cross, Yamamoto, Tanimoto, Ikeno and Kato.

The results show a large variety. This is not weird in itself, since tsunamis are highly variable too. However, the theoretical expression of Cross falls completely outside the range indicated by the other methods. It is believed that the assumed velocity of $u = 2{,}0\sqrt{gh}$ is not realistic and leads to too high impact forces. Even for bore-like tsunamis running on land the model tests *and* the survey of Yamamoto indicates impact forces which are 2,3 times lower than indicated by Cross. Because this method is based on knowledge of 40years ago, it is believed that it is not realistic and will lead to too conservative designs.

Therefore, it seems that for realistic values the method of Kato forms an upper limit for the horizontal impact forces, while the Tanimoto-method can be used as a lower bound. The methods that lie in between, probably describe impact forces belonging to tsunami-shapes which are in the transition between broken and unbroken.

It can also be concluded that bores on land (Ikeno 2003, Yamamoto, Kato) induce higher loads then bore-like tsunamis offshore (Ikeno, 2001).

Conclusively, although described methods all have their limited usability, they clearly indicate the region of tsunami-impact force depending on location (offshore/onshore) and wave form (broken/unbroken). This information is quite valuable in the development of tsunami protection alternatives.

2.6.4 Low-crested, submerged and 'soft' structures.

Although standard coastal protection against storm surges and high tides are often too low in case of significant tsunami, these structures can be effective in reducing the current velocities and resulting damage. The same accounts for soft measures, like mangrove or other greenbelts.

Investigations and surveys indicate that these 'structures' can be somewhat effective in case of overtopping tsunamis. It must be noted that the term 'overtopping' is normally used for occasional wave overtopping, whereby only a small part of the wave (e.g. 1%) is allowed to overtop the structure, causing a limited discharge of water over the structure. An overtopping tsunami however can cause a flow of water during tens of minutes. This changes the standard concept of minor and occasional overtopping completely, because the long duration of the flow increases the loads on the structure and gives large flooding.

The forces on a structure that is overtopped by a tsunami can be calculated by adding hydrostatic and dynamic water pressures, but besides that buoyancy must be considered. This can significantly reduce the resistance against sliding and overturning. Another aspect of overtopping is that a return flow can develop. Especially for a steep topography, the retreating flow will induce higher loads on the structure that the initial impact. The overtopping velocities thereby are often high and could cause severe erosion around the structure.

Low-crested structures

Low-crested structures have a crest level higher than the still water level (if offshore) and a crest level that is considerably lower than the tsunami waves attacking it.
Little theory is available about the reducing effect of low-crested structures to flooding. In Appendix I.4.3, the empirical equation of Kaplan [4] is presented, which relates the structure height, tsunami height and overtopping volume. The limited validity of this expression is demonstrated in Appendix II-3. It shows that it is difficult to describe the effect of successively penetrating waves.

A survey in Thailand [57], carried out after the Dec2004 Tsunami, found that most of the low seawalls were not damaged by the tsunami, and, despite the fact that the walls were overtopped by the higher tsunami waves, structures landward of the walls were somewhat protected compared to areas without seawalls. Apparently, the structures had a small peak-cut effect on the initial impact, but the resulting flooding was still considerable.
In Aonae, Japan, a seawall nearly 4,5 meters high was built. This wall was overtopped by a tsunami in 1993, and more than 185 people were killed [57]. The wall itself was partly damaged. Since then, the wall has been rebuilt, and there is an ongoing debate about the effectiveness of the wall, which is so high nowadays that it obstructs the view on the sea and was extremely expensive to build.

In both examples, the tsunami height in relation to the crest height is not mentioned. It is obvious that the effectiveness of low-crested seawalls depends highly on the difference between wave height and structure height (as indicated by Kaplan's expression). In case of large overtopping volumes, the resulting flooding will still cause severe damage and loss of live. In case of lower tsunami-heights, the peak-cut effect will be higher.
Therefore, low seawalls can not be seen as a reliable means of tsunami-protection.

Submerged structures

Another way of reducing waves is by submerged structures. Submerged structures have a crest level lower than the Still Water Level. See Figure 2-11 for a definition sketch.

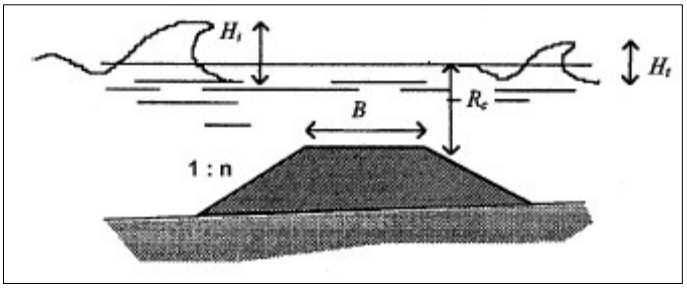

Figure 2-11 Definition sketch of submerged breakwater [27]

However, as described in Appendix I.4.4, the effectiveness of a submerged structure depends on the ratio B/L and R_c/H. Decreasing these ratios will increase the transmission and thus decrease the effectiveness of the structure.It is expected that for tsunami with wave lengths in the order of kilometres, the effectiveness of submerged structures is limited. The ratio B/L is almost zero, which corresponds with a high transmission.

'Soft measures'

Besides hard structures, trees and other dense vegetation may also offer some protection against tsunami. Groves of trees can dissipate tsunami energy and reduce surge heights, but may also be sheared off and add debris to the flow.

For limited tsunami heights (H<3m), the reduction rate of the inundation depth is studied by Harada and Kawata,[12]. It was found that coastal forest could reduce velocities and inundation with approx. 50%, but is generally collapsed by tsunamis higher than 4m (see Appendix I.4.5 for more). Surveys and analysis of field data ([16][18][20]) do not provide a clear answer about the actual effectiveness of green-belts. There is a world-wide ongoing discussion on this topic, which is also fed by environmentalists stressing general benefits of green belts.

In general it is believed that green-belts of trees are *somewhat* effective in case of smaller tsunamis. However, it is emphasized that this protection is very limited and unsure. A tsunami with a length of several kilometres, heights of 5-10m, flowing with 6-10m/s, cannot be stopped or significantly reduced by a forest of 300m width. Like submerged structures, the width of the forest should be in the same order of magnitude as the wave length.

Moreover, this protection measure could become a disadvantage as trees can be uprooted or sheared by higher tsunamis and add debris to the flow. That's why it is said that coastal forest is a double-edged sword as a tsunami countermeasure.

2.6.5 Overview and application

In this paragraph (2.6), tsunami-interaction with structures has been treated. Methods to determine forces of broken and unbroken tsunamis on high structures have been presented. The effectiveness of low-crested, submerged and 'soft' structures is discussed.

How can this information be used for design purposes?

The velocity of the attacking tsunami is a governing factor in the impact force. In case of tranquil motions, the water pressures tend to be hydrostatic. When the tsunami attacks like a bore, the velocity increases and subsequently the dynamic water pressures. The location of the structure is also important, since offshore bores induce lower loads then bores running on land. For rubble-mound structures, the (local) velocity causes scour. Various methods are presented to calculate the impact forces and give an indication about the current velocities. This can be used in the design.

Both submerged structures and mangrove belts aim at dissipating the energy of the waves. It was found that belts of trees or mangroves have limited effect on tsunami inundation. Some peak-cut effect of the current velocities can be expected. For higher tsunamis, the trees will be uprooted and add debris to the flow. Submerged structures are not effective in tsunami-reduction.

Therefore, protection against tsunamis should aim at reflecting the energy rather then dissipating it. This will become an important starting point for the design of tsunami protection measures.

2.7 EXISTING TSUNAMI BARRIERS

Especially Japan has a long history with devastating tsunamis. The high population-density in coastal areas and the many bays (which enforce wave heights and damage) together with regular tsunami attack forced the government to several tsunami countermeasures. Besides the protection of the entire coast by seawalls, a number of breakwaters have been build to reduce the tsunami impact. A selection has been made.

2.7.1 Seawalls along the Sanriku Coast, Japan

Description

After the heavy loss of life and property by the Sanriku Tsunami (1933) the Japanese Government recommended to prepare new housing sites on higher ground. Many sites were created but the lack of building space in combination with an increase in households caused many people to inhabit the dangerous low land near the shore. This situation required the construction of seawalls to protect the low-lying fishing villages against future tsunami attacks.

Figure 2-12 Seawall of 10m height in Taro, Japan [10]

Because of financial difficulties the construction of these walls slowed down and only a few villages had completed construction before the attack of the 1960 Chilean tsunami. This event brought very heavy loss along the Sanriku coast and urges the Government to enact a special law for subsidizing 80% of all construction costs and restoration.

Effectiveness
Low seawalls have very limited effectiveness in case of overtopping. Therefore walls up to 10m are built, see Figure 2-12. The reduction of flooding and will be significant under most tsunami-attacks (simply because most tsunamis will be lower), supposed no considerable overtopping or failure occurs.

2.7.2 The Ohfunato Tsunami Protection Breakwater

Description
The reasons to construct breakwater instead of seawall in this situation are:

- Seawalls may obstruct future development of the Ohfunato Port and City
- A breakwater preserves the assets of the bay (ships, nurseries, timber, etc.) where a seawall only protects the port and city
- The shape of the bay is narrow and long, which would require several kilometres of seawall to sufficiently defend the city and port. Though expensive, a relative short breakwater can protect a large area which results in relatively low costs

Table 2-3: Dimensions of the Ohfunato Tsunami Protection Breakwater (source: Ida, 1981)

Parameter	Value
Total length	737 m
Entrance depth	16,3 m
Entrance width	200 m
Range in water depth	12 – 35 m
Maximum height	40 m
Number of caissons	48
Height above LWL	+5,0 m

The breakwater consists of 2 visible parts, constructed of concrete caissons placed on top of rubble mounds (10 to 50 kg) with an entrance gap in the middle.

The breakwater was designed against wave force, seismic force and tsunami force. The latter was calculated as an elliptic trochoidal wave. For seismic design a modified seismic coefficient method was adopted because of the height of this structure (40m). For 'normal' wave attack a design wave height of 3,5m was applied.

The dimensions of the caissons as well as the gradient of the mound slope were determined by the tsunami force. The breakwater was completed in 1967 after 4 years of construction work.

Effectiveness
In Dec. 1968 the Tokachi tsunami attacked this region. Tide gauge stations at the inside of the breakwater observed a deviation in water lever of 1,2m. Calculations showed an expected deviation of 2,2m without breakwater. The peak-cut effect was recognized to be about 1m.

The maximum settlement of the breakwater has amounted to about 45cm (10% of maximum retaining height) and is mainly due to heavy earthquakes

2.7.3 Kamaishi port, Japan

Description

The deepest breakwater in Japan is constructed at the mouth of Kamaishi Bay, to protect the port area from tsunamis. The Kamaishi Tsunami Protection Breakwater reduces the bay-mouth opening to lessen tsunami run-up height as well as wind waves and swell. The deepest point in the bay-mouth is 63m. The retaining height is approximately 5,0m +MSL

After the construction of the breakwater, the opening sectional area of the bay will become 5% of the original one. As a consequence, strong currents will be generated when tsunamis attack. Detailed information on the tsunami flow around the opening section is difficult to predict, therefore, experimental studies have been conducted to support the breakwater design and to develop a method to protect the rubble-mound from scouring. This lead to the conclusion that block movement could be accurately described by the "CERC-formula" [13], [7]. See more in Appendix VIII on this matter.

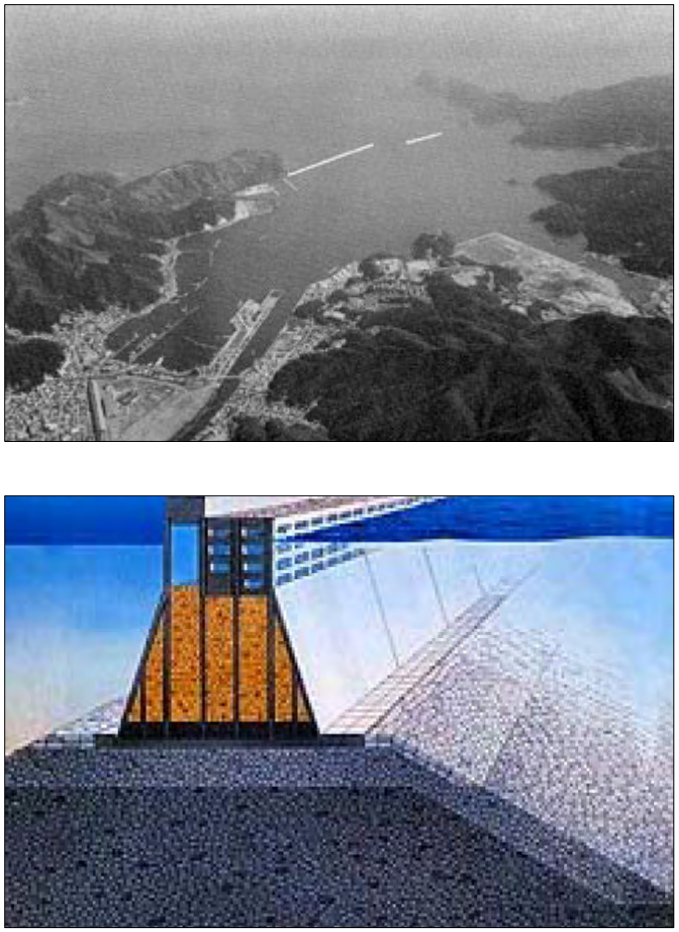

Figure 2-13 Plan view and impression of Kamaishi Breakwater in Japan [63]

Effectiveness

The effectiveness is studied in numerical simulations and physical model tests. No information is found in literature about the effectiveness under real tsunami attack, probably because no tsunami has occurred till now.

2.7.4 Kawaragi breakwater

Description

The Kawaragi breakwater was a caisson-type structure. The maximum water depth it was built in was -6,5m compared to mean sea level. The freeboard was +2,85m MSL.

Effectiveness

This breakwater collapsed due to the 1968 tsunami. The incoming tsunami wave height was estimated 3m. Failure occurred due to sliding of the breakwater. Because of this event, research was carried out by Tanimoto to investigate the forces on caisson-type offshore breakwaters. This method is presented in section 2.6.1.

2.7.5 Lhok'Nga Breakwater

Description

Lhok'Nga is a small village nearby Banda Aceh. All buildings were wept away by the tsunami, except for the mosque. South of the village a giant cement factory, Lafarge SA, is located. The company has its own harbour, where ships up to 10.000 DWT can be moored. The harbour is protected by breakwater. This breakwater was not designed as a tsunami protection, but only to provide shelter against 'normal' waves.

Although the breakwater head was damaged by the Dec2004 Tsunami (Tetrapods at the head, above and below water were displaced and crest elements were damaged), the breakwater in Lhok'Nga kept its function and was still capable of providing shelter for mooring facilities. However, the jetty was not accessible due to a ship that sunk. See Figure 2-14 and Figure 2-15.

Figure 2-14 Plan view of breakwater at Lhok'Nga and direction of primary waves

Figure 2-15 Helicopter view of breakwater Lhok'Nga, source [47]

Cross section

The height of the breakwater is 9,3m +MSL. The crest elements are reinforced, and based on gravel. The foundation is coral rock. The sea side slope is protected with 32-ton Tetrapods, placed on 300-1000kg rubble mound, with a slope of 1:1,5. The core consists of gravel and is covered with geotextile to prevent wash out of material.

Figure 2-16 Left: The partly restored seaside protection. Right: The new and displaced Tetrapods at the head.

Based on interviews with the port authorities and evaluation of the damage, it was concluded that the wave overtopped the breakwater. This caused local scour at the harbour side but did not lead to instability. Only at the head the crest elements were turned over and broken. Most likely, the first wave displaced the Tetrapods at the seaside to such an extent that the base material (gravel) was exposed to the successive waves. This led to scour and finally to instability and turn-over of

the crest elements. However, the crest element at the harbour side of the head was still in place indicating that the severest loads were at the sea side.

2.8 SUMMARY

General

Tsunamis are long waves, caused by rapid perturbations of the water level. These perturbations can be caused by earthquakes, landslides, volcanic eruptions and meteor impact. Combinations of these mechanisms occur, but earthquakes alone cause 82% of all tsunamis. Because of the long wavelength (order of hundreds of kilometres), tsunami-waves are shallow water waves. The Shallow Water Equations therefore also account for tsunamis.

- An important property is the wave propagation speed, which is $c = \sqrt{gd}$.
- The wave height increases according to Green's Law (shoaling). Tsunamis show diffraction, refraction, reflection, (limited) dispersion and resonance.

Limitations

Close to the shore where the wave height becomes a significant part of the water depth, non-linear processes play a role. The final wave height at the coast depends on many variables and is highly variable. The initial signal (magnitude, intensity), bathymetry (slopes or shelves) and geometry (bays, islands, etc.) all influence the wave characteristics. Therefore:

- Close to the shore, Green's shoaling law is not valid anymore.
- General relations between earthquake magnitude and wave height are indicative and cannot be used for design purposes
- General relations between wave height and run-up are indicative and can hardly be used for design purposes

Engineering

Both for run-up and tsunami-impact force, the wave height, wave shape and wave velocity is important. The behaviour of unbroken tsunamis is comparable with fast rising tides.

- Unbroken tsunamis induce relatively low velocities and the associated forces and run-ups are also low.
- The method of Tanimoto can be used to calculate the pressure distribution on vertical walls.

Broken or breaking tsunami waves do occur and are much more devastating for structures. Maximum run-up factors up to 3 times the incident wave height are expectable. The dynamic load depends strongly on the velocities.

- Broken waves induce high loads on structures and run up significantly more.
- Measurements for the velocity under broken tsunamis vary between $u = 0{,}8\sqrt{gh}$ and $u = 1{,}3\sqrt{gh}$.
- The methods of Ikeno, Kato and Yamamoto all describe bore-like tsunami impact on both sea and land. Kato's expression forms an upper limit.

Tsunami protection measures

Existing tsunami-barriers are mostly concentrated in Japan, in the entrance of bays, and constructed of caissons or in composition with a rubble-mound base. High seawalls have also been constructed. The effectiveness depends on the height of the structure and the width of the gaps in relation to the tsunami height. In one case a caisson-breakwater collapsed due to sliding.

- Rubble-mound structures can be stable under high flow velocities (Kamaishi-breakwater)
- In case of significant overtopping, the effectiveness of a seawall is very limited
- Submerged breakwaters have very limited effectiveness.

'Soft' measures as mangroves and other vegetation are some-what effective up to tsunami-heights of 3 a 4m, provided that they are placed in high density. For high tsunamis, no reduction should be expected.

- For tsunamis above 3 á 4m, mangroves and other vegetation are not effective in tsunami reduction and even increase damage.

An interesting case study was the breakwater in Lhok'Nga. During the attack of the Dec2004 Tsunami, this (composite) rubble mound structure generally remained intact, except for the head. It should be noted that the blocks were 32-ton! High flow velocities around the head caused erosion, leading to partial collapse of the structure. However, this case shows that:

- It is possible to construct a (partly) rubble-mound structure that does not entirely fail under tsunami conditions.

Chapter 3. INDONESIA IN THE RING OF FIRE

3.1 INTRODUCTION

From the previous Chapter it was concluded that the tsunami characteristics are highly variable. General relations between, for instance, earthquake magnitude and tsunami height cannot be used for design purposes. In order to derive the design values for the area of interest it is necessary to have a closer look into the study area. What tsunamis can be expected there? And how often they occur?

This Chapter treats some general facts about Indonesia and Aceh in particular, and then focuses on earthquakes and tsunamis in this region, finishing with an extensive description about the Dec2004 Tsunami.

3.2 FACTS AND FIGURES

Indonesia is an archipelago in Southeast Asia consisting of 17,000 islands (6,000 inhabited) and straddling the equator. The largest islands are Sumatra, Java (the most populous), Bali, Kalimantan (Indonesia's part of Borneo), Sulawesi (Celebes), the Nusa Tenggara islands (Tenggara means South-East and these islands include Lombok, Sumba, Sumbawa, Flores, etc), the Moluccas Islands, and Irian Jaya (also called West Papua), the western part of New Guinea. Its neighbour to the north is Malaysia and to the east is Papua New Guinea. See also Figure 3-1.

Figure 3-1 Indonesia and its islands. The red box indicates the location of Aceh. [58]

Table 3-1: General facts and figures, 2006 [59].

General	
National Name	Republik Indonesia
Total Land Area	1.826.440 km^2
Population	245.452.739
Population Density	135 / km^2
Growth Rate	1,4%
Languages	Bahasa Indonesia, English, Dutch and Javanese
Main Religion	Islam (88%)
Capital	Jakarta

Indonesia, part of the "ring of fire," has the largest number of active volcanoes in the world. Earthquakes and tsunamis are frequent. More about this in paragraph 3.3. Besides these natural hazard, other hazards, (partly) related with human activities, are flooding caused by torrential rainfall (recently, in February 2007, Jakarta was flooded). Landslides also occur, often caused by deforestation. Since May 2006, there is an uncontrollable mud volcano in Sidoardjo, East Java. The mud volcano erupted after an incident during an oil drilling project. The mud had covered more than 300 ha of land. More than 10,000 people are displaced and more than 1,000 people lost their job.

Aceh

Aceh is the northernmost province of Sumatra, and has a population of about 3 million people and a land area of 55.400 km^2 (about 1,5 times the Netherlands). The capital and largest city is Banda Aceh. Aceh has rich petroleum and natural gas deposits as well as valuable rubber, oil palm, and timber resources. The Acehnese, like most Indonesians, are Muslim, but are generally more conservative. Since 1 January 2002, the Shari'a Law is in effect.

Aceh reached the height of its power in the early 17th cent. The Dutch gained control of the coast in 1873 and engaged in a partly successful effort to subdue the interior until 1910.
Aceh also resisted Indonesian control and in 1959 was designated a special region with autonomy in religion, culture, and education. Late in 1976 the Movement for a Free Aceh (GAM) declared the province independent but was suppressed; guerrilla warfare resumed in the late 1980s and continued through the rest of the century. A peace agreement providing for greater Acehnese autonomy was signed in 2002, but with neither side willing to compromise, Indonesia ended the subsequent talks in 2003, imposed martial law (reduced to a state of emergency in 2004 and ended in 2005), and launched new attacks against the rebels.

In the aftermath of the Dec2004 Tsunami, the GAM and government held a series of talks aimed at ending the fighting. A new peace accord was signed in Helsinki in August 2005. An autonomy law for Aceh was passed by the Indonesian parliament in 2006, but some Acehnese criticized it for provisions that left the central government with more powers in Aceh than had been envisioned by the peace agreement. In December 2006, Irawandi Yusuf, a former GAM rebel, was elected governor.

3.3 RING OF FIRE

3.3.1 Geology

As said before, Indonesia is located in the Ring of Fire. The Pacific Ring of Fire is an area of frequent earthquakes and volcanic eruptions encircling the basin of the Pacific Ocean. In a 40,000 km horseshoe shape, it is associated with a nearly continuous series of oceanic trenches, island arcs, and volcanic mountain ranges and/or plate movements. See also Figure 3-2.

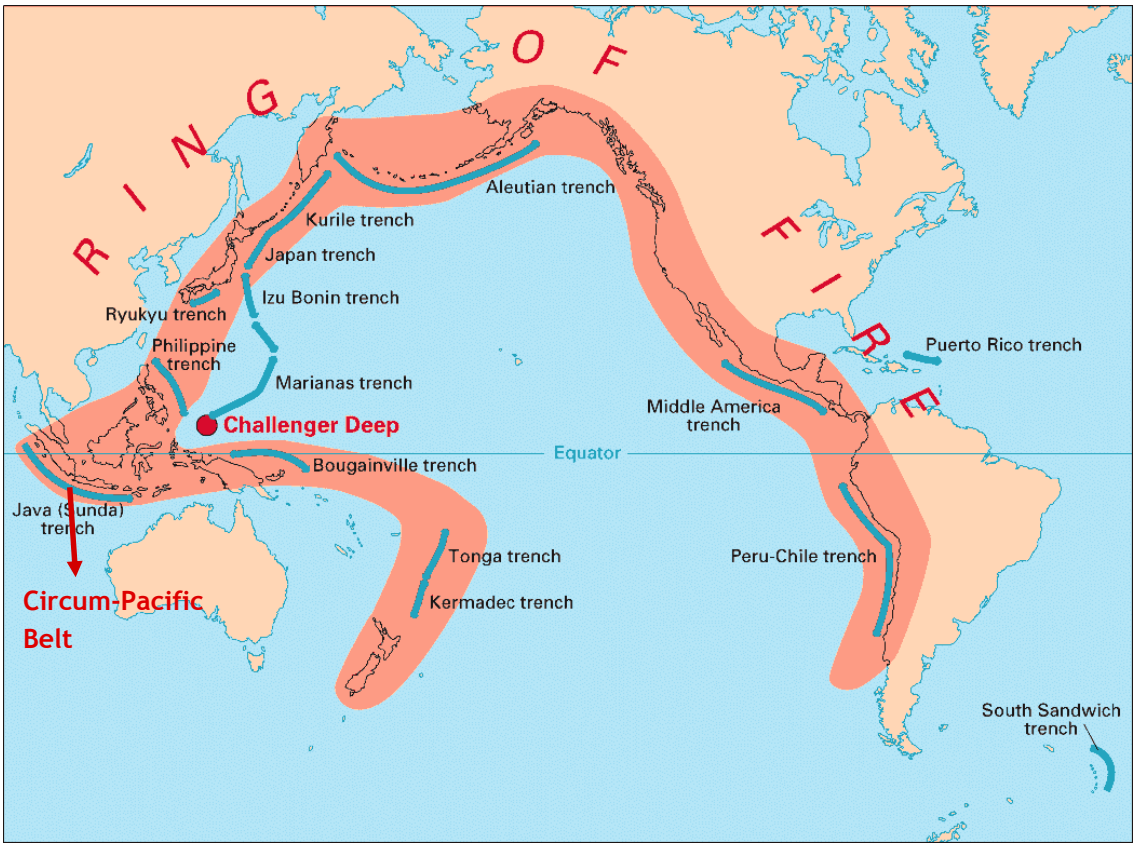

Figure 3-2 The Ring of Fire. Indonesia lies north of the Java or Sunda trench [64].

In this figure the trenches are shown in blue. The volcanic island arcs, although not labelled, are parallel to, and always landward of the trenches.

Almost 90% of the world's earthquakes occur along the Ring of Fire. The most active zone is called the circum-Pacific belt, a 3500km long line, extending from Sumatra to Flores in Indonesia. Along this line, the Indian Plate moves under the Burma Plate with a velocity of approximately 6 cm/year, causing many volcanic activity and earthquakes. See Figure 3-3 and Figure 3-4.

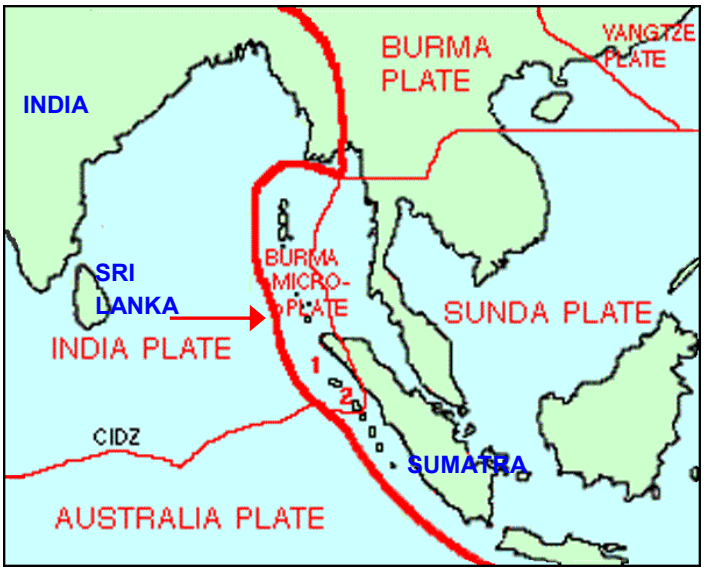

Figure 3-3 Overview major and minor plates [66]

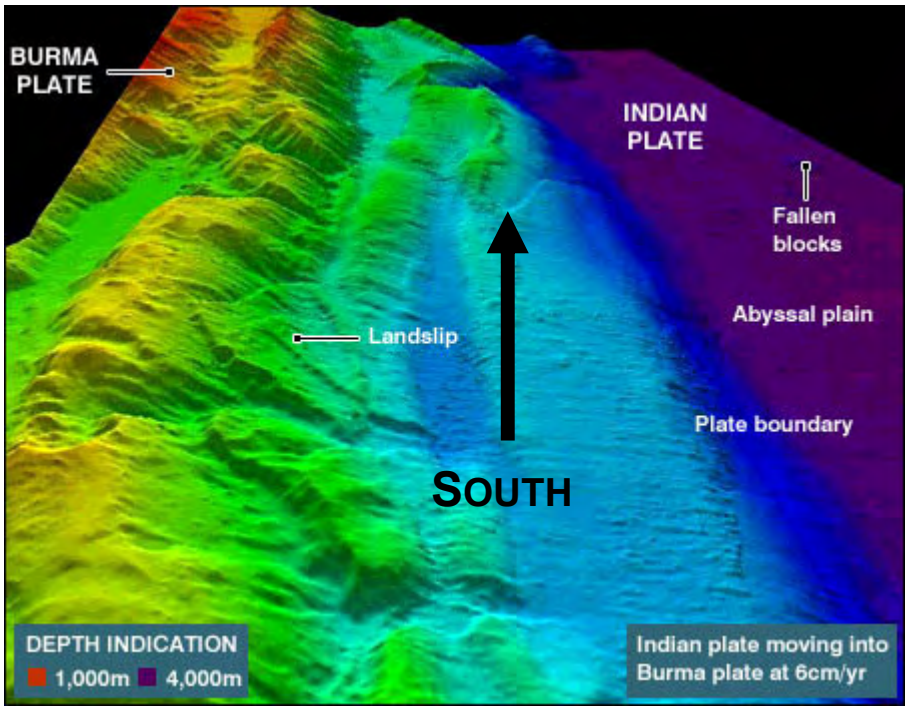

Figure 3-4 Impression of the subduction zone along the Java (Sunda) trench [65]

The movement of the plates is not a smooth process. During time stresses are built up between the plate boundaries and pressures increase in the magma under the plates. If the stress exceeds the friction, stress is released and the plates shift relative to each other. This goes along with displacements and tremors. The magnitude of these tremors (earthquakes) depends on the magnitude of the stress release. The longer stress is being built up, without being released by minor earthquakes, the more a major earthquake can be expected. See also Figure 2-2.The probability of future earthquakes is therefore directly related with past events.

Wave shape

The fact that Sumatra is located on the Burma (micro) Plate, which is being sub-ducted by the Indian Plate, means that it will receive negative tsunami waves. Every tsunami, initiated by tectonic activity in the Sunda trench, will send a wave towards the Sumatran coastline with a leading trough. As a consequence, the water will draw back before the (positive) tsunami wave arrives.

3.3.2 Earthquakes

The historical record shows considerable earthquake activity in both the Great Sumatran Fault and the Sunda Trench. Over the past millennium there were giant earthquakes about every 230 years. Analysis of (the few) historic earthquakes, and geomorphic evidence derived from offsets of valleys and other landforms, indicate that seismic hazard is greater in the north of Sumatra than in the south.

Average recurrence intervals for the mega thrust earthquakes along the Sunda Trench are more difficult to determine. Examination of secondary sources such as the growth rings on Porites corals suggests an average recurrence interval for great thrust earthquakes (which are likely to cause tsunamis) of about 230 years for Tanabalah Island – the northernmost of the Mentawi Islands (south of Nias) off the western coast of Sumatra [26]. However, it is not clear whether this average rate also applies to the more northerly and more southerly sections of the Sunda Trench.

Only under certain circumstances these earthquakes are able to cause tsunamis. See Chapter 2.3.1. But at least ten triggered significant tsunamis (M_w>7,5) along the west Sumatra fault zone in the last 235 years (see Figure 3-5). The December 2004 tsunami seems to have been the largest and most destructive for at least the last two centuries.

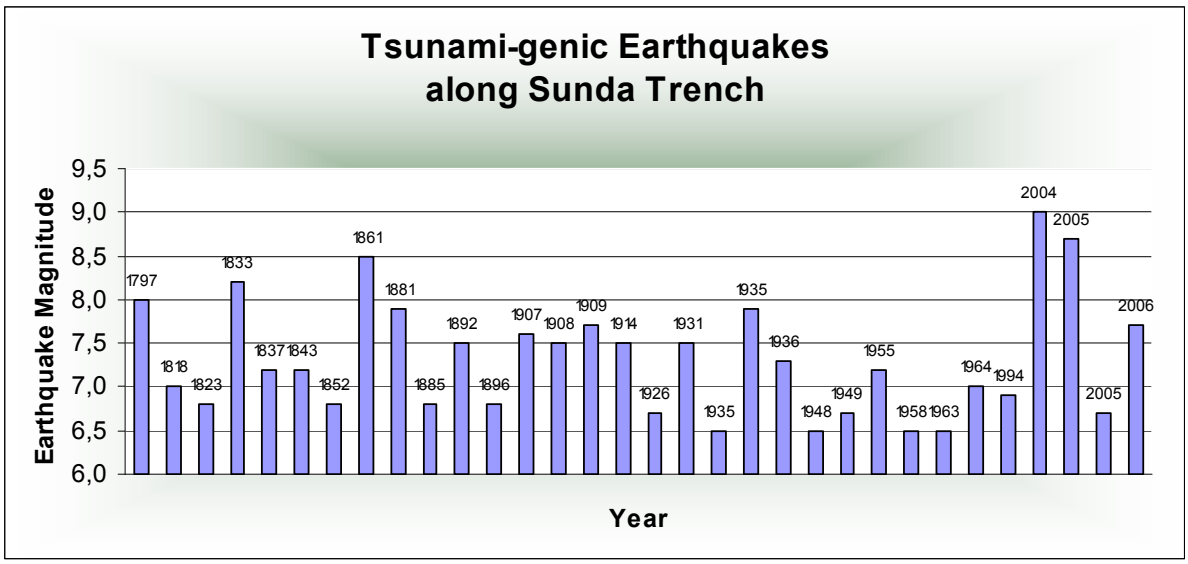

Figure 3-5 Historic record of earthquakes that triggered tsunamis along the Sunda Trench [50].

It was noted that for segments of the fault directly southeast of the segments that broke in 2004, strain was not fully relieved by the 26Dec 2004 earthquake [35],[60]. The remaining stresses and

pressure were still high, especially in the southern part of the fault line. As a consequence, the probability of an earthquake in the next 100 years may have actually increased, as illustrated by the March 2005 earthquake with magnitude 8.7. However, this earthquake did not cause an ocean wide tsunami, because rupture did not extend to the seafloor and because the presence of islands, whose uplift does not excite a tsunami.

3.3.3 Other possible causes for tsunamis

Earthquakes are not the only cause of tsunamis. Volcanic eruptions, landslides (or combinations) and even meteor impact can trigger tsunamis. Volcanoes and landslides have been recorded as cause for a number of tsunamis in Indonesia. Table 3-2 gives an overview of significant tsunamis (intensity > 1) caused by these events.

Table 3-2: Historic tsunamis in Indonesia caused by other events then earthquakes. Source: [50].

Cause	Year	Location	Tsunami Intensity
Volcano	1673	N. MOLUCCAS ISLANDS	1.00
Volcano	1815	JAVA-FLORES SEA	1.50
Volcano	1856	SULAWESI	1.00
Volcano and Earthquake	1857	BISMARCK SEA	1.50
Volcano, Earthquake and Landslide	1871	SULAWESI	3.50
Volcano, Earthquake and Landslide	1878	BISMARCK SEA	2.00
Volcano	1883	KRAKATAU	5.00
Volcano and Landslide	1888	BISMARCK SEA	3.50
Volcano and Earthquake	1889	N. MOLUCCAS ISLANDS, INDONESIA	2.50
Volcano	1892	AURI, HALMAHERA,INDONESIA	1.00
Volcano	1892	SULAWESI	1.00
Volcano and Landslide	1928	FLORES SEA	3.00
Volcano	1937	BISMARCK SEA	1.50

All the listed events caused local tsunamis, except for the 1883 Krakatau volcanic eruption. However, it is clear that all volcanic activity is located in the central and eastern part of Indonesia and generated tsunamis did not affect north-west Sumatra.
For tsunamis generated west of Indonesia (for instance by the volcanoes located on the Andaman and Nicobar Islands) no historical evidence is available. The same accounts for meteor impacts and ‘stand-alone’ landslides.

Based on this historic data, it is expected that North-west Sumatra (including Aceh) is not prone to tsunamis caused by landslides or volcanic activity. It is therefore concluded that tsunami-occurrence is only related to earthquakes in this region.

3.4 TSUNAMI OCCURRENCE

There is no single up-to-date authoritative database on tsunami occurrence in the Indian Ocean region. The amount of (tsunami data) for a particular location is limited and not sufficient for a statistical analysis.

Therefore it is very difficult to estimate with high precision the likelihood of a tsunami at a specific coastline. Preliminary work by Professors Seth Stein and Emil Okal of North-western University indicate that the expected recurrence interval for the particular segment of the fault causing the 2004 tsunami is about 500 – 1,000 years. This estimate is based on the rate of convergence of the Indian-Burma Plates, and the assumption that future events will have similar slip during the tsunami-generating earthquake [60].

One way of indicating the tsunami hazard is to use a combination of fault model and wave propagation modelling. Preliminary probabilistic tsunami hazard calculations for the Sumatra-Andaman subduction zone ([41]) are based on a set of 2,000 scenario earthquakes to provide a probabilistic description of earthquake occurrence in the region. Then, the complete tsunami wave field for each scenario earthquake is computed.

This is a logical method and generally valid for the Banda Aceh region, since it was concluded that tsunamis for this region are only due to earthquakes.

The results of this modelling are presented in Figure 3-6 which shows tsunami wave height hazard curves at four locations in the northeast Indian Ocean region. Note that these wave heights are at the 15m depth contour. The height of tsunami waves increase before reaching the shoreline. 1D-modelling indicates that this increase could be considerable (see Figure 4-4), depending on the bathymetry. This means that a tsunami wave of 5m at an original depth of -15m could have a height of 7m or more on the shore. Therefore, the determination of the actual tsunami hazard should be based on tsunami heights at the coast instead of the 15m-depth heights.

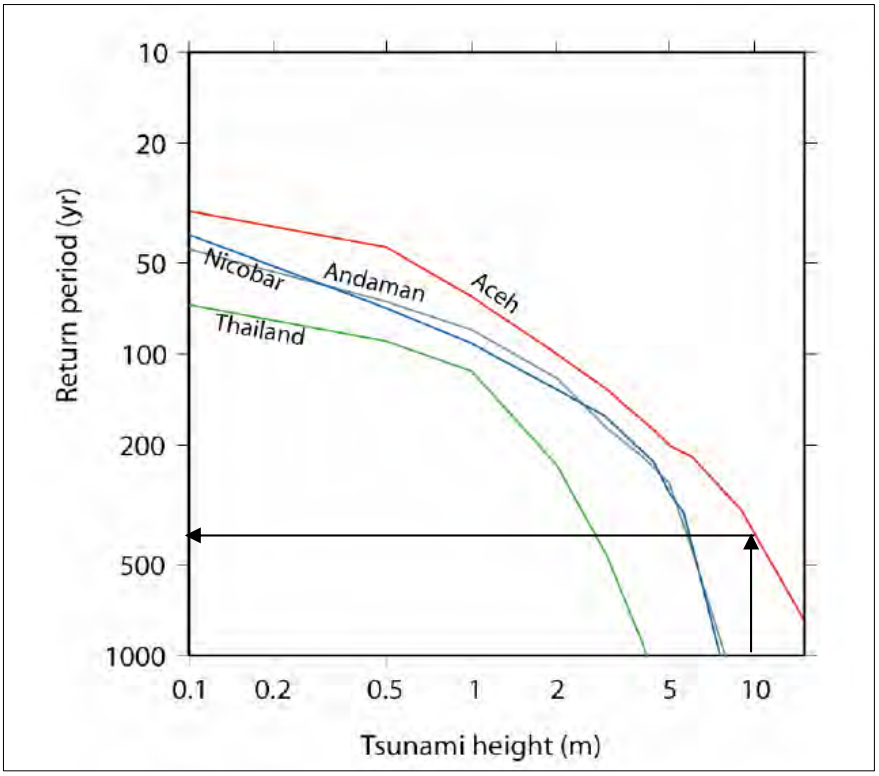

Figure 3-6 Tsunami height hazard curves at four locations in the Indian Ocean region [41].

However, although this curve provides a good insight in the general hazard for Aceh, it can not be used for one location. As described in Chapter 2, the actual wave height arriving at the coast depends on many variables. Most of all, the local bathymetry is of crucial influence. It was mentioned that for the same tsunami-event, the wave heights (on the shore) differed widely between Banda Aceh and Lhok'Nga (within 11km distance).

It is therefore not possible to use the general curve for Aceh in Figure 3-6, to derive specific information for one particular spot, (Banda Aceh).

However, within the SDC-project, efforts have been made to reproduce the findings of Thio et al. With the 2D Tsunami-model (which will be described in Chapter 4.4), wave fields were computed for different magnitudes (in total 107 scenarios). Comparison of these two data sources showed that both results are consistent for the wave heights at the -15m bathymetry line. So, the 2D-model gives a relation between earthquake parameters and wave heights at -15m and also simulates the resulting flooding accurately.

This fact is used in this study to find the relation between tsunami heights at the shoreline (as a measure for the flooding/damage) and return periods for Banda Aceh. The results are presented in Table 3-3.

Table 3-3: Estimated recurrence interval for tsunamigenic earthquakes along the Sumatra-Andaman fault line.

Magnitude	Recurrence interval at one specific spot	Wave Height at the Shoreline (2D Model runs)
7,5	100 YEARS	1-2 M
8	150 YEARS	2-3 M
8,5	200 YEARS	3-5 M
9	500 YEARS	5-8 M
9,5	1000 YEARS	8-9 M

Compared to the 'Thio-curve' for the west-coasts of Aceh in Figure 3-6, it must be concluded that the relation between return period and wave height (at the shore) for Banda Aceh differs from the values indicated in above table.

This significant difference can (partly) be explained by the favourable location of Banda Aceh region. Where the west coast is almost completely exposed to the open sea, Banda Aceh is located in a more sheltered area. The main tsunami waves, coming from south-west, have to curve around the islands, loosing energy due to refraction.
Another possible explanation is the favourable near-shore bathymetry of Banda Aceh. The bathymetric profile of Banda Aceh is more or less convex. As indicated by 1D-modelling of various profiles, the wave heights and run-ups are less then for instance at Lhok'Nga. See, Figure 4-4 in Chapter 4.3 and Appendix II on this matter.

3.5 THE DEC 2004 TSUNAMI

At 07:59 (local time at epicentre), December 26, 2004, a major earthquake with a moment magnitude of Mw = 9,3[3] occurred off the west coast of Northern Sumatra (3.307°N, 95.847°W), This earthquake generated a devastating tsunami. An earthquake of M_w > 9,0 had not occurred in this region for the last 200 years. The tsunami struck Banda Aceh, the most devastated city, and heavily damaged lives, properties, buildings and infrastructure. The dead and missing people has amounted to a value of 297.248 [50]. The fact that many people lived in low-lying coastal areas without refuge places and building, and (most of all) the lack of tsunami knowledge and early warning system, are partly responsible for this major human loss.

Figure 3-7 Sumatra, the islands of Simeulue and Nias and the epicentre of the Dec 2004 earthquake

In this section a description is presented about the effects of this disaster. The focus is on the study area: Banda Aceh.

[3] *The published values of the earthquake magnitude on Richter scale vary between 9,0 and 9,3. However, recent analysis of long-period earthquake waves [60] shows that the energy involved with this earthquake indicates a magnitude M_w of 9,3.*

3.5.1 What happened

From the epicentre, the rupture propagated northward along the Sunda Trench, all the way to the Andaman Islands. Approximately 1300km section of the fault line shifted 10-20m, with the greatest slip concentrated in the southern 400km, near the epicentre (see also Figure 3-8**)**. The hypocenter was at 10km depth and the dip angle approximately 10°. The released energy was estimated at $2 \cdot 10^{18}$ J, equivalent to 23.000 Hiroshima atomic bombs[4].

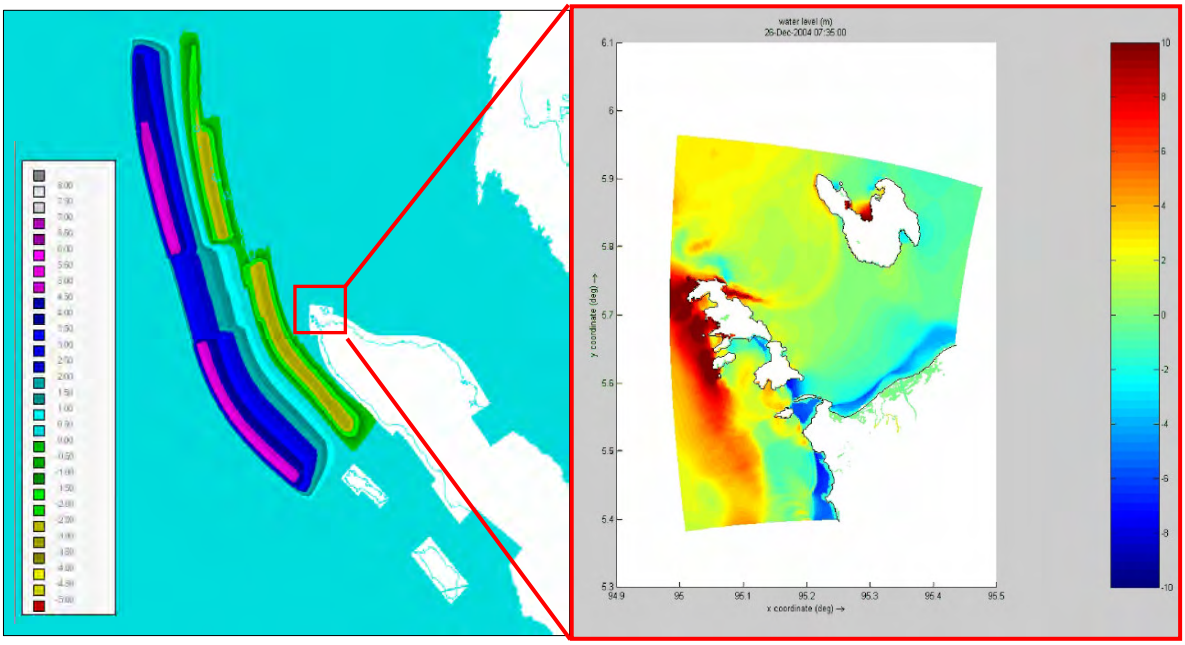

Figure 3-8 Left: modelling of excitation signal along entire fault line. Right: timeframe of the Indian Ocean 2D-model where the refraction of the tsunami waves around the northern islands is shown. Scale in meters.

Along this entire fault waves were generated. The waves heading west, towards Sri-Lanka and India, had an initial crest, while waves heading east, towards Sumatra and Thailand, began with a trough (see 3.3.2).

Within 20 minutes the tsunami waves hit the coast of Northern Sumatra. In 1,5-2 hours, Thailand and Burma were hit and within 2,5 hours, the waves reached the coasts of Sri Lanka and India. After 8-10 hours the tsunami reached East Africa. In Table 3-4 a short overview is presented.

[4] *This calculation is based on M_w 9.0 magnitude. Recent analysis of the low-frequency wave spectrum indicates a magnitude of 9.3. The energy involved would then be 3 times higher! Note that the Richter scale is logarithmic.*

Table 3-4: Wave heights and effects of the 26Dec 2004 Tsunami in various countries

Country	Run-up height	Death toll	Missing people	Displaced people
INDONESIA	UP TO 35M 10-20M GENERAL	108.100	127.700	426.800
SRI LANKA	5-10M	30.900	5.400	552.600
INDIA	UP TO 10M	10.700	5.600	112.500
THAILAND	3-5M	5.300	3.100	-
SOMALIA	UP TO 3M	150	-	5.000
MYANMAR	UP TO 3M	90	10	3.200
MALDIVES	UP TO 3M	82	26	21.600
MALAYSIA	UP TO 3M	68	6	4.200
SEYCHELLES, BANGLADESH, KENYA	UP TO 3M	5	-	-
TOTAL		**155.395**	**141.842**	**1.125.900**

Note: The killed and missing people add up to 297.237, which is the figure presented in [50]. One third of dead were children.

The question arises why this was such a tremendous disaster. Several reasons can be given:

- High population density on low-lying coastal areas around the Indian Ocean. The world population has doubled since 1960 (the great Chile quake).
- Short distance from tsunamis source to populated areas, leaving little time for warning and refuge.
- No tsunami warning system in Indian Ocean. Almost 85% of the world's tsunamis do occur in the Pacific Ocean, where an effective warning system is in effect.
- Poor and developing countries with vulnerable infrastructure (hardly any coastal defence) and minimal disaster preparedness
- Little public awareness of tsunami hazard. The last major tsunami in Indonesia was caused by the 1883 Krakatau eruption that killed 35.000 people.

Besides the high death toll, the tsunami devastated houses, infrastructure, etc. The economic damage and losses were estimated over $10 billion.

The extent of the impact of this disaster shocked the world. One of the greatest disaster relief efforts in history was initiated. From all over the world funding was promised and hundreds of NGO's moved to the affected areas.

Although this tsunami had almost worldwide effects (even in the USA seiches were recorded), the focus in this thesis report will be on Banda Aceh. In the next paragraph, damage figures are presented. Within the Sea Defence Consultants Project, models were developed to simulate the tsunami propagation and the resulting flooding and damage of Aceh. These models will be presented shortly, because they will be used in this thesis work to simulate the effect of measures to prevent against disasters like the Dec 2004 Tsunami.

3.5.2 Facts and figures

Within 20 minutes the waves reached the coast of Banda Aceh. Although this city is relatively protected against waves from the east, the initial wave curved around the islands north of Banda Aceh (see Figure 3-8) and was followed by the waves generated in the northern part of the fault line. In Figure 3-9 the effects of the flooding are shown, both for Banda Aceh and Lhok'Nga.

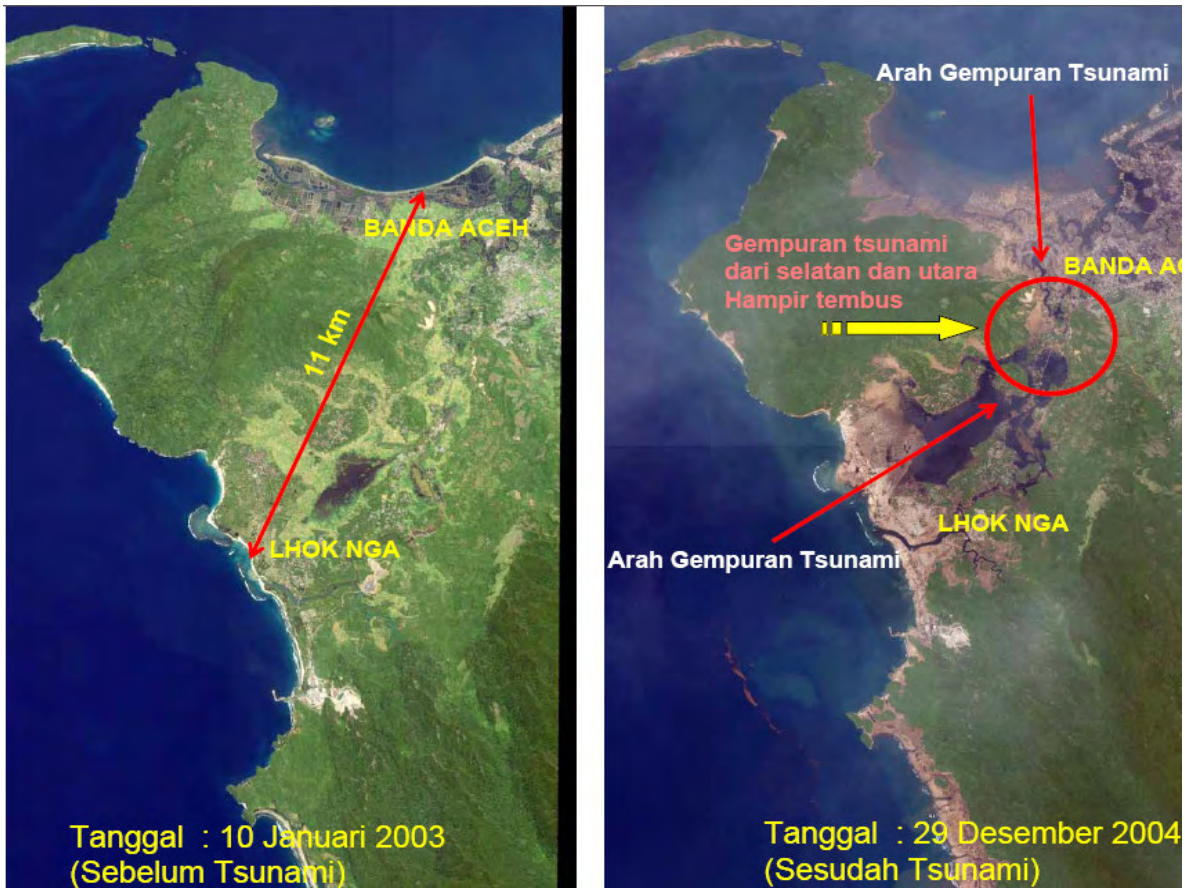

Figure 3-9 Aerial photographs of Banda Aceh and Lhok'Nga before and after the tsunami. The water penetrated from the southwest (Lhok'Nga) and from the north (Banda Aceh) met in the middle [67]

In Banda Aceh the waves penetrated up to 5km inland, completely destroying the first 2km of coastal area, except for some massive buildings (like the Ulee Lheue mosque, Figure 3-10). The initial dropdown of the water level caused a drawback of the water line up to 500m offshore. The total wave train consisted of 3 big waves, and several smaller waves. Each consecutive wave could penetrate further, since the previous waves smoothed the landscape by destroying buildings and other obstacles and, moreover, because they ran over a layer of water left behind by the previous wave, also decreasing friction.

The resulting (maximum) inundation was studied by various teams. Matsutomi et al. [25] investigated the aspects of inundated flow (among others: current velocity, fluid force, relation between inundation depth and damage, etc.) of the 2004 Tsunami in Southern Thailand and Northern Sumatra. The resulting figures for Banda Aceh and Lhok'Nga are presented in Table 3-5.

Table 3-5: Investigated tsunami parameters in the Banda Aceh Region [25]

Location name		Distance inland	Inundation depth *h*	Velocity *v*	Relation *v* and *h*.	Drag force ($\rho \cdot u^2$)
Banda	Ulee Lheue 1*	0 km	12 m			
Aceh city	Ulee Lheue 2	0,9 km	4,7 m	7,7 m/s	1,13 √gh	61 kN/m^2
"	Ulee Lheue 3	1,3 km	4,0 m	5,2 m/s	0,83 √gh	28 kN/m^2
"	Ulee Lheue 4	2,3 km	3,9 m	5,8 m/s	0,94 √gh	34 kN/m^2
"	Great Mosque**	3,5km	1,6 m	5,2 m/s	1,31 √gh	
"	Power plant	3 km	3,0 m			
Lhok'Nga	Lhok'Nga, cement-factory	50 m	15,8 m	16 m/s	1,29 √gh	264 kN/m^2

** See Figure 3-10* *** See Figure 3-11*

Figure 3-10 Banda Aceh port area. Mosque in Ulee Lheue, directly on the coastline. Close to this location the 12m inundation depth was measured. Almost all (simple) buildings were destroyed [67].

Figure 3-11 Banda Aceh. Downtown, approx. 3km inland, close to the Great Mosque. The boat was most probably moored in the river next to this site. A lot of debris is in the streets but the (concrete) buildings do not show structural damage [67].

The depths were measured, using marks on buildings. The velocities are mainly obtained from video footages [51] where floating objects were used as a measure for the current velocities.

In this table, the measured inundation depths and velocities are compared with each other, based on the relation presented in Chapter 2.5. In literature the relation varies between $v = 1{,}1\sqrt{gh}$ and $v = 2\sqrt{gh}$ for waves running on land. In the measurements this relation varies between $v = 0{,}83\sqrt{gh}$ and $v = 1{,}31\sqrt{gh}$, where the lower value belongs to open areas (Ulee Lheue is the relatively flat port-area of Banda Aceh). The highest value is measured in the city centre, where the water was pushed through the streets.

The drag force ($\rho \cdot v2$, with $v = 1{,}0\sqrt{gh}$) on objects is also shown in Table 3-5. It was shown that the damage to buildings could be explained by using this load [25][48].

3.5.3 Damage and casualties figures

The effect of the tsunami has been analyzed by various institutes. Table 3-6 presents the damage for Aceh and Nias, for various sectors.

Table 3-6: Damage and loss assessment for whole Aceh and Nias, various sources. January 2005.

Sector parts	Damage and Losses [M USD]	
	BRR&Worldbank [24]	**Bappenas 2005 [1]**
Social Sector	372	310
Education	*170*	*131*
Health	*104*	*94*
Community, culture and religion	*98*	*85*
Infrastructure and Housing	2.492	2.365
Housing	*1.533*	*1.469*
Transport	*537*	*548*
Communications	*39*	*22*
Energy	*90*	*70*
Water & Sanitation	*40*	*30*
Flood control, irrigation works	*221*	*226*
Other Infrastructure	*34*	-
Productive Sectors	1.183	1.168
Agriculture & Livestock	*225*	*189*
Fisheries	*511*	*522*
Enterprise	*447*	*456*
Cross Sectoral	685	666
Environment	*562*	*561*
Governance & Administration (incl. Land)	*109*	*91*
Bank & Finance	*14*	*14*
Total	**4.733**	**4.509***

** The original values were in Indonesian Rupiah. A currency rate of 9155 IDR = 1USD is used.*

Both sources show similar results in their damage assessment. The highest value will be used here. The total damage in the province Aceh (and Nias) amounts to 4,7 Billion USD. The damage for Banda Aceh alone is 1,13 Billion USD, which is almost 25% of the total damage in Aceh and Nias.

It is very difficult to separate the additional damage due to the tsunami from the direct damage due to the earthquake. In the assessment of prevented damage in case a structure is built, only the additional damage should be used. Because these figures are not available, the above-presented figures will be used.

The total number of deaths in Banda Aceh, as reported by the JICA (Japan International Cooperation Agency) study team is 54.868. With 16.569 people missing (which were presumed death later), the total number of victims is 71.436 [16].

Women and children were worst hit, though accurate numbers are not available.

3.6 SUMMARY

Indonesia is prone to many hazards, directly related with tectonic activity. Direct consequences are earthquakes and volcanic eruptions, which can, in their turn, trigger tsunamis. Analysis of historical data shows that most tsunamis are caused by earthquakes, although volcanic eruptions cause a significant part of all tsunamis. For tsunamis caused by (single) landslides and meteor impact, no historical evidence is available. This data regards the whole Indonesian archipelago.

For the area of interest, Banda Aceh, it was concluded that the only likely cause of tsunamis is (submarine) earthquakes. They originate in the Sunda trench, where the Indian Plate is subducting the Burma Plate. As a consequence, Sumatra will always receive a negative wave, causing an initial drawback of the water line at the coast, before the (positive) wave arrives.

Volcanoes are more located in the middle and east of Indonesia and although they could generate tsunamis, these will not affect Banda Aceh. Based on this finding, and with the help of various previous studies, a relation between tsunami heights (at the coastline) and return period is derived for the area of Banda Aceh.

The 26Dec 2004 Tsunami was a disaster of enormous extent. In the countries around the Indian Ocean, the total number of missing and dead people amounted to almost 297.237. Only for Banda Aceh this figure was 71.436 with a total damage of 1,12 billion USD.

Although Banda Aceh is relatively protected against waves from the east, the tsunami waves from the east curved around the northern islands followed by waves generated in the northern part of the 1300km long fault line. The main wave train consisted of three waves and caused a maximum (measured) inundation of 12m directly at the coast. Approximately 3km inland, this height was reduced to 3m.

The maximum measured velocity was 7,7m/s. The derived relation between velocity and inundation depth varied between $v = 0{,}83\sqrt{gh}$ and $v = 1{,}31\ \sqrt{gh}$, were the latter value was observed in streets in the town centre. In the relatively flat coastal area, velocities related to inundation depth with approximately $v=1{,}0\sqrt{gh}$. In a study of Matsutomi et al. it was shown that with an assumed velocity $v=1{,}0\sqrt{gh}$, the failure of typical buildings was well described. These 'moderate' velocities indicate that for Banda Aceh no bores occurred.

Chapter 4. NUMERICAL MODELLING

4.1 INTRODUCTION

Within the Sea Defence Consultants Consortium, several models were developed to simulate the effect of the tsunami. Various simulations were already carried out and evaluated and this thesis partly elaborates on this work. In the overview below, this work is referred to as '*existing*' work.
Also, a large number of additional simulations have been carried out in this study. This modelling is called '*additional modelling*'. An overview of the 'existing' modelling efforts and the 'additional' modelling is given below:

Existing modelling efforts with respect to tsunami-protection:

- Development of the 2-dimensional Indian Ocean Tsunami Model in Delft3D and refined (sub) models for various regions (a.o. Banda Aceh). This model is calibrated on the Dec2004 Tsunami event and simulates other tsunamis by variations in excitation signal.
- The refined (sub) model also simulates the flooding and drying of Banda Aceh[5].
- Development of semi-1D-model [6] to simulate the effectiveness of various tsunami protection alternatives (offshore structure, coastal structure and mangrove), with various tsunami and structure heights. Based on an assumed bathymetry. With this model 33 runs were made.
- Calibration of the 2D Tsunami model, based on the 1D-model results, in order to simulate the effect of low-crested structures on the flooding of Banda Aceh. The actual simulations with this model are part of this final thesis work (see Chapter 5).
- Development of Damage Module which relates inundation with damage.

Additional modelling activities, carried out in this thesis work:

- Modelling with an 1D-model, programmed in Fortran[7]. Modelling of structures to obtain velocities and water levels over the structure and calculate impact forces. Also modelling of the near-shore bathymetric influence on wave shoaling.
- Additional modelling with the existing semi-1D-model to study the influence of bathymetry on wave height and run-up, the influence of positive/negative tsunamis and additional structure modelling.
- Additional modelling with the available 2D Tsunami model. In total 31 alternatives are schematized and their effectiveness in tsunami reduction is computed. No existing modelling of low-crested structured was available.
- 5 additional model runs with the DamageModule to simulate the damage related to various tsunami events without structural measures. Based on inundation volume this is translated to the situation with structural measures.

---

[5] *This model will be referred to as the '2D Tsunami model'*
[6] *This one will be referred to as 'semi-1D-model'*
[7] *This model was provided by Prof. G.S Stelling, member of the thesis-committee. This one will be referred to as '1D-model'.*

The results of these modelling efforts are presented in this Chapter. For each model, the existing modelling and additional modelling is treated.

Note: the reason to treat the numerical modelling of tsunamis and tsunami protection measures before the actual development of protection alternatives (Chapter 5), is to reduce the number of model runs with the 2D-model. 1D models require much less CPU-time and provide a good insight in the effectiveness of various protection measures. Based on the 1D-modelling a number of non-effective protection measures can be excluded.

4.2 1D MODEL

4.2.1 Description

The model is based on the 1D-nonlinerar shallow water equations which are divided in an equation of momentum and continuity:

Momentum:
$$\frac{\partial V}{\partial t} + V\frac{\partial V}{\partial x} = -g\frac{\partial \eta}{\partial x} - C_f \frac{V|V|}{d+\eta}$$

Continuity:
$$\frac{\partial (d+\eta)}{\partial t} = -\frac{\partial [(d+\eta)V]}{\partial x}$$

V	=	depth averaged horizontal velocity vector [m/s]
η	=	water elevation [m]
d	=	water depth [m]
C_f	=	non-dimensional friction coefficient [-]
g	=	gravitational acceleration [m/s$_2$]
t	=	time [s]
x	=	distance [m]

The model is based upon a numerical scheme, which solves these equations but also adds conservation properties. A description of the numerical technique used in this model can be found in reference [36].

The model had to be rebuilt to simulate the velocities of tsunamis over structures for a bathymetry typical for Banda Aceh. The way in which the bathymetry of Banda Aceh, the tsunami signal and structures are modelled is described in Appendix IX.

4.2.2 Model runs

No existing model runs could be used for this thesis study. Several (offshore) structures are schematized in the model, simply by adjusting the depth. The local grid size is refined to 1m.

The influence of near-shore bathymetry was studied by performing various runs with convex and concave profiles. See Appendix IX for an elaborate presentation of all modelling and output.

4.2.3 Results

Some results are presented here. The resulting water levels and velocities for a Dec2004 Tsunami signal are depicted in Figure 4-1.

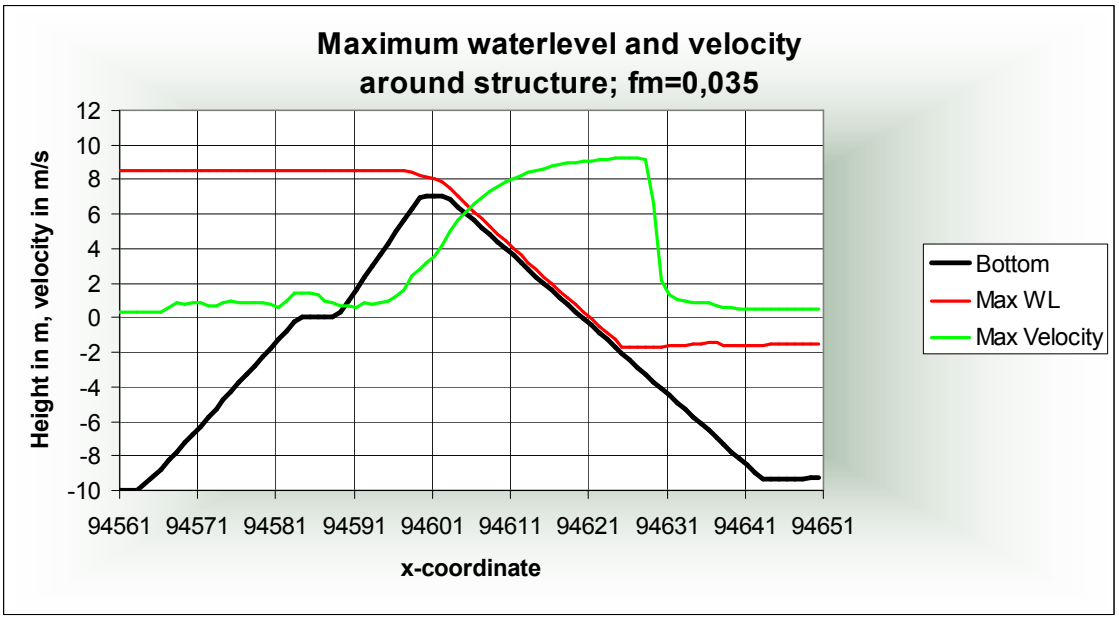

Figure 4-1 Maximum velocities and water levels for offshore breakwater

The maximum occurring velocity is 9,3 m/s in horizontal direction.

The near-shore bathymetry has influence on the wave shoaling. The differences between convex and concave profiles are however lower than indicated by the other 1D-model (Delft3d), see section 4.3.3.

More structure-modelling and calibration of the results is presented in Appendix IX.

The influence of the near-shore bathymetry on the wave shoaling is studied. For the Dec2004 tsunami signal, the maximum wave heights are depicted in Figure 4-2.

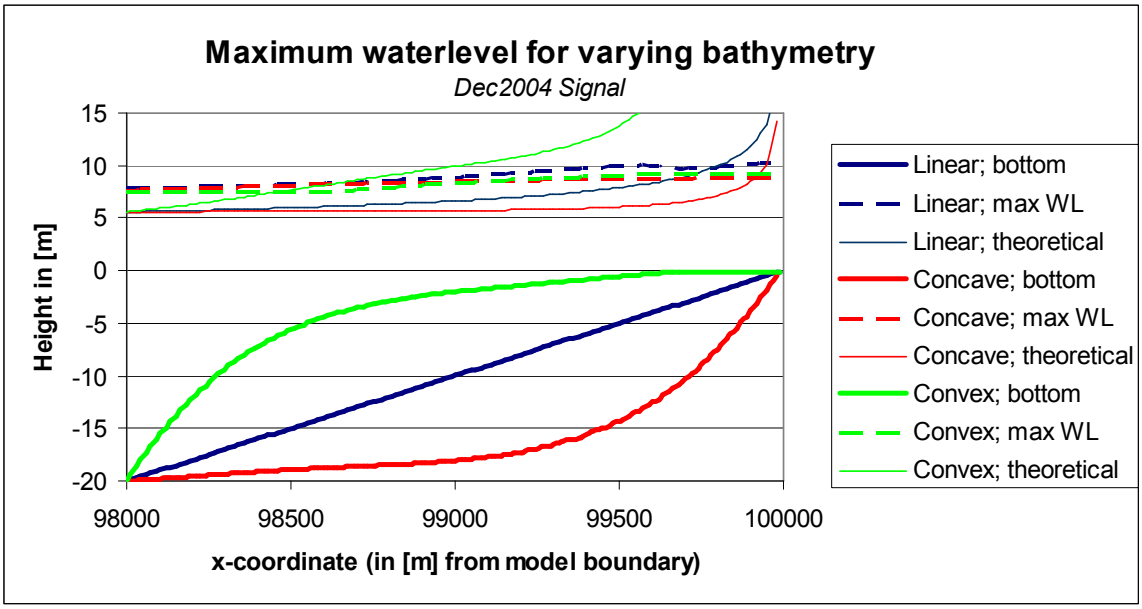

Figure 4-2 Maximum shoaling at the coast for various foreshore bathymetries

The results of this modelling indicate that the tsunami wave heights do differ for various profiles. The linear profile provides the highest waves, followed by the convex profile. The concave profile is the lowest. The differences however are small.

4.3 SEMI-1D MODEL

4.3.1 Description

An extensive description of this 1D model can be found in SDC (2007) [32]. The conditions (the tsunami signal) at the open boundary of the model are obtained from the 2D model, which is described in paragraph 4.4. This signal has the temporal characteristics of the Dec2004 Tsunami and is rescaled in order to simulate different tsunami heights. The signal is depicted in Figure 4-3.

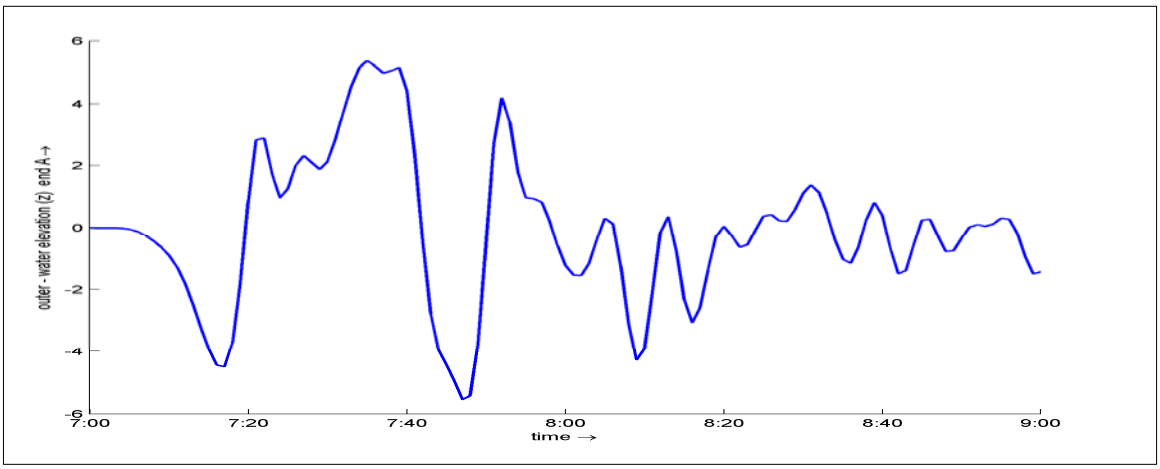

Figure 4-3 Tsunami shape signal that has been applied at the open boundary of the model (vertical scale in meters) [32].

For the bathymetric profile, a near-shore profile (1:100 gradually decreasing to 1:300) and a coastal topographical profile of 1:1000 was assumed.

For each model run, the following 5 output parameters have been selected:

1. Run up height
2. Horizontal inundation length from the shoreline
3. Maximum inundation water depth on the land during entire simulation period
4. Max. flow velocity computed on the land during entire simulation period
5. Energy head ratio at 240 m after the shore line, with and without structural coastal protection measures (to get an indication of the effect of the measures). The relation for the energy head that is applied is given by: $E = \text{Max}(\zeta(t) + U(t)^2/2g)$.

The grid resolution varies with the bathymetry and the location of structures. At the anticipated breakwater and seawall sites the grid has a resolution of approximately 3 meters. At the open boundary where the depth equals 20 meter, the grid size equals 40 meters. Along the coastal strip the grid size equals approximately 10 m.

4.3.2 Model runs

Existing runs (made within SDC-project)
Several model runs were available already. These runs use an assumed bathymetry and vary in:

- Tsunami height (1,5 / 3,0 / 4,5 / 6 / 7m at the left boundary) → 5 base cases
- Structural measures
  - Offshore breakwater at 15m water depth with varying height → 10 runs
  - Seawall with varying height → 4 runs
  - Mangrove with varying height and width → 8 runs
- Combinations of measures → 6 runs

A description of all model runs can be found in [32]. With these runs, an effort has been made to harmonise the model results (penetration/overtopping) with the overtopping theory presented in Appendix 1.4.3. The results are summarized in 4.3.3.

Additional model runs (in this thesis work)
In addition to these runs, more 1D-model runs are carried out. The following subjects are studied:

- The influence of the near-shore bathymetry (shape) on the wave development (without structures)
- The influence of bathymetry (shape) on the run-up against structures
- The influence of tsunami shape signal on structures
- Combined measures versus separate measures

The results from the additional model runs are presented in Appendix II.

4.3.3 Results

A description of the model and used parameters can be found in Appendix II. The results are summarized here.

Results existing runs

It was concluded that protection against high tsunami events is difficult to achieve with any type of measure. Offshore breakwaters and seawalls both require a freeboard about equal to the tsunami height on the shoreline. The effectiveness of an offshore breakwater at this height is better than of a seawall. Mangroves have shown hardly any effectiveness for tsunami heights > 3m.

Again, these results were already available. It was tried to match this simulation results with theory regarding overtopping volumes (see Appendix II-2 and II-3). It turned out that this theory consequently underestimates the overtopping volume as calculated by the 1D-model. See Appendix II-3. The reason is that a tsunami consists of several waves, 'riding' on each other. The total penetration of 3 or more successive waves is much higher than is indicated by the theoretical expression of Kaplan.

Results additional model runs

See Appendix II-4 for an extensive presentation of the modelling results and conclusions. The main findings are repeated below.

Influence near-shore bathymetry

The modelling results indicate that the near-shore bathymetry has a major influence on the development (or shoaling) of the wave. In case of a concave profile the run-up is approximately 1,5 times as high as in case of a convex profile, where the wave hardly shoals towards the coast. See Figure 4-4.

In this figure, the so-called '2D-profile', is obtained from the 2D-model, where the actual bathymetry is used. The profile called 'original 1D-profile' is the profile as used in the existing 1D-model runs.

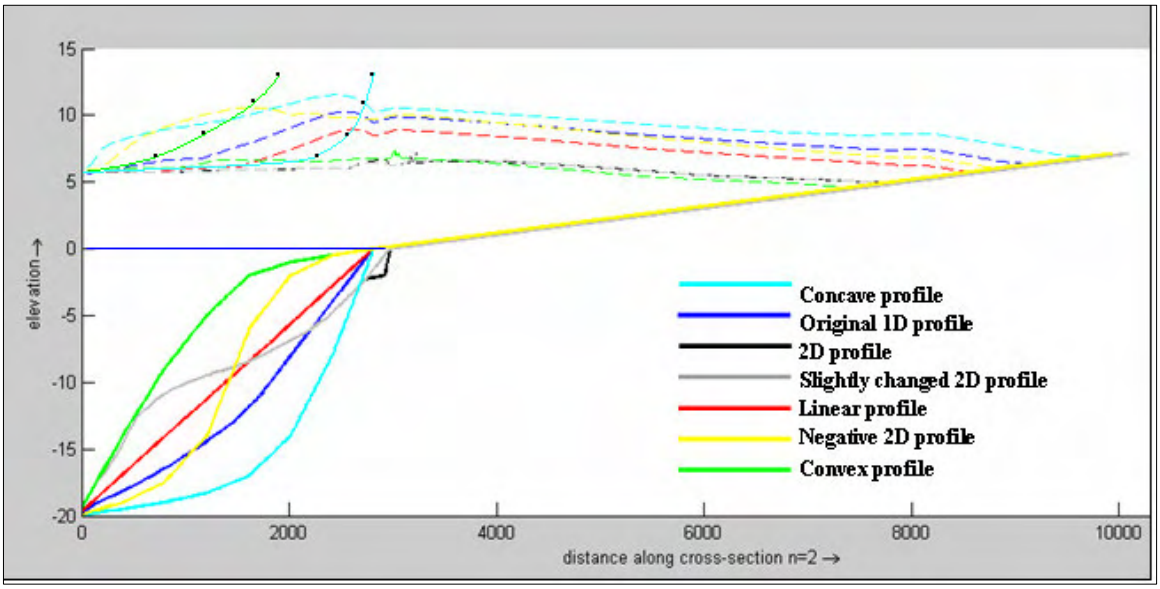

Figure 4-4 1D model: Maximum water levels for varying bathymetry. $H_{boundary}$=6m.

The dashed lines in Figure 4-4 indicate the maximum water level during the entire run. The black-dotted green line indicates the theoretical shoaling[8] for the convex profile and the black-dotted blue line represents the theoretical shoaling for the concave profile. It is clear that the wave development close to the shore cannot be described by this simple law. Non-linear effects play an important role.

The results indicate that whatever tsunami signal is applied, the maximum water levels are higher for the 1D-(concave)-profile then for the 2D-(convex)-profile.
The run-up against structures with the same tsunami signal is more than 1,7 times higher in case of the 1D-profile (concave) then with the 2D-profile (more convex). See Appendix II-4 for output.

However, the findings of this semi-1D modelling are not consistent with the 1D-model (Fortran) results (Figure 4-2 and Appendix IX). The maximum wave heights do differ for various profiles, but the differences are much smaller. And where the 1D-modelling (Fortran) suggests the highest shoaling for linear profiles, the semi-1D model finds that concave profiles induce the highest waves.

This major difference is probably caused by the schematization of both the open boundary in the semi-1D model and the closed boundary in the 1D-model (FORTRAN). Unfortunately, a more detailed study into this matter falls beyond the scope of this thesis work. It is strongly recommended however that the influence of the bottom profile on the wave development (shoaling vs reflection) is studied in more detail. Because Green's shoaling law is obviously not accurate in the last hundreds of meters before the coast, tsunami risk assessments (often based on simple shoaling laws) can not be trusted either.

[8] *Theoretical shoaling means the wave growth according to Green's Law, following* $(d_1/d_2)^{0.25}$. *See Chapter 2 on this matter.*

Influence tsunami shape signal (positive vs. negative)

Model runs with linear profiles and positive and negative sine-signals indicate that negative tsunamis (with preceding trough) have higher impact (run-ups etc.) than positive tsunamis. The higher run-up seems not associated with higher wave heights, but with higher steepness.

Effectiveness of combined measures

The effect of combined measures is very limited in case of tsunami wave trains. The first wave(s) overtops the first barrier and fills up the area to the 2nd barrier. The successive wave(s) will simply 'ride over' the stored water and overtop the 2nd barrier. See Figure 4-5. It seems much more effective to invest in making one (high!) structure instead of two structures with limited heights.

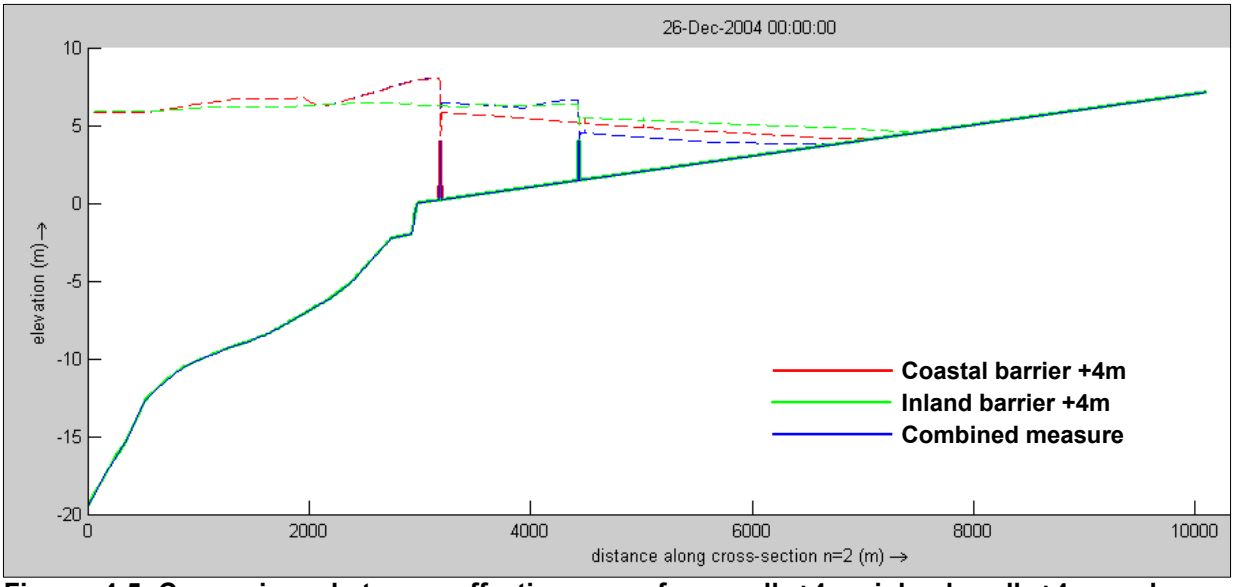

Figure 4-5 Comparison between effectiveness of seawall +4m, inland wall +4m and combined measure.

4.4 2D-TSUNAMI MODEL

4.4.1 Description

In 2005 numerical models were set-up with Delft3d-software, to compute the propagation and simulate the flooding caused by the 26-12-2004 Indian Ocean tsunami. The tsunami wave heights simulated by the propagation model were compared with relative sea level heights measured by the four radar altimeter satellite that recorded the running tsunami wave in the Indian Ocean on December the 26th 2004. Though the tsunami heights in the deep ocean were overall very well reproduced, near the coast line the wave heights were underestimated by a factor of approximately 2.

To overcome this problem, the 300 m resolution flooding model of North Aceh was developed, which showed a more accurate reproduction of the observed flooding pattern in Northern Aceh.

Nevertheless, partly due to lack of data and partly due to lack of resolution, the inundation pattern in detail showed some important differences when compared to the actual flooding.

This was a reason to update the model. Finally, the combined tsunami propagation and flooding models has been divided into 6 coupled sub-models (see also Figure 4-6)

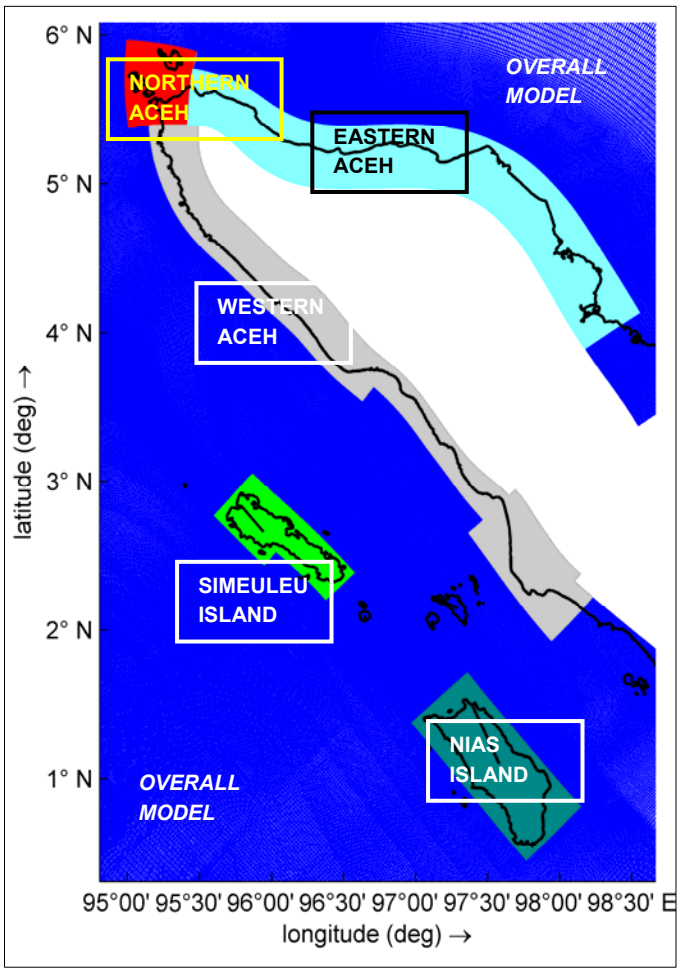

Figure 4-6 Five detailed model domains. The Northern Aceh model is 200x200m^2 and 50x50m^2 grid [32].

- a 200m grid Eastern Aceh model
- a 200m grid Western Aceh model
- a 200m grid Northern Aceh model
- a 50m grid Northern Aceh model to simulate the effect of structural measures
- a 200m grid Simeuleu Island model
- a 200m grid Nias Island model

With this refined grid, the flooding as calculated by the model corresponded well with the observed flooding by the 2004 Tsunami. The use of the model was further extended by also simulating the resulting flooding which would have been caused by other earthquake events (M_w 7,5/8,0/8,5/9,0 and 9,5 were modelled).

To simulate the effect of structures, the Northern Aceh 200m-model was further refined to 50x50m^2.

A more elaborated description of the 2D-Tsunami Model, including the modelling of the excitation signal and the applied difference scheme to solve the shallow water equations can be found in SDC-R-60014 [32].

4.4.2 Model runs

Existing modelling
The resulting flooding due to the Dec2004 Tsunami (with M_w = 9,2) and the flooding pattern caused by other earthquake events (M_w 7,5/8,0/8,5/9,0 and 9,5) were modelled.

Additional modelling
A large number of model runs are made, with fully-retaining structures[9] and 'low-crested' structures[10], to allow (minor) overtopping of the tsunami.
All model runs with structures (offshore, coastal and inland), which have been executed within this thesis project are listed in Appendix III.

4.4.3 Results

The model generates water levels and velocities in every grid for each time-step. From this data, the maximum water level and inundation depth (=water level minus ground level) during the entire run can be obtained. The maximum water level can be presented as a flood map of Banda Aceh.

Existing modelling
For the 26Dec2004 Tsunami, the flood map is presented in Figure 4-7.

[9] *In the first model runs, the structures were modelled as dry points in Delft3D, and do not allow wave transmission. It means that the tsunami wave is blocked completely and are therefore called full-retaining structures.*
[10] *A study was carried out ([32]) to investigate the applicability and accuracy of the 'local weir' or '2D weir' features as implemented in Delft3D-FLOW. The 'weirs' were primarily calibrated by comparing water levels with 1D-model runs. Finally, it was decided to simulate low-crested structures using a 2D weir with a calibration coefficient of 0.85. Although the model was development by SDC, all runs are made within this thesis study.*

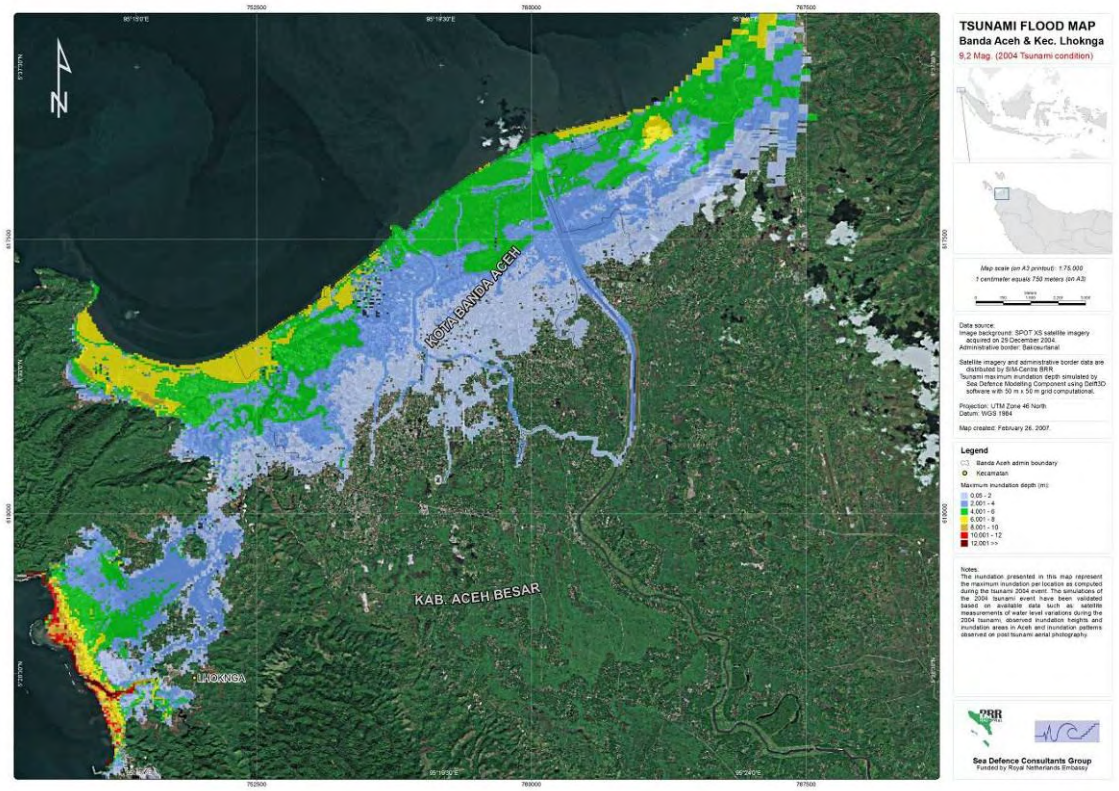

Figure 4-7 Tsunami Flood Map for 9,2 Magnitude (Dec2004 Tsunami) [32].

Inundation depths amount to 10-12m in Banda Aceh, while in Lhok'Nga depths over 12m are obtained. The penetration length is approximately 5km.

Additional modelling

A time-frame of a model run for an offshore barrier with a freeboard of 5m is shown in Figure 4-8. The Dec2004 Tsunami signal is used in this model run.

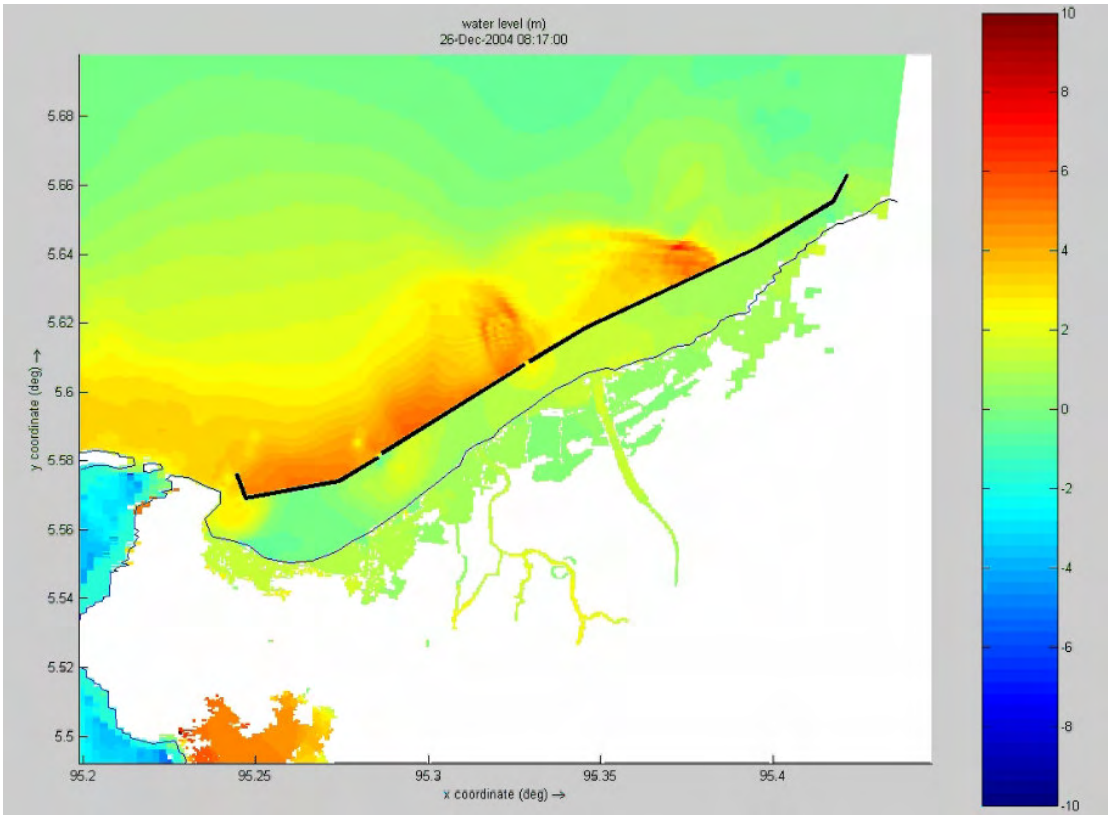

Figure 4-8 Timeframe of a 2D-model run with offshore barrier +5m MSL. Scale in m.

The results and interpretation form part of Chapter 5, and will therefore not be presented here.

Some inundation maps with structural measures are presented in Appendix III.

4.5 DAMAGE MODEL

4.5.1 Description

Within the Sea Defence Consultants Consortium, a damage model is developed as part of the flood risk modelling. It contains damage and casualties functions that describe the relation between characteristics of the tsunami (inundation volume) and respectively damage costs and the number of expected casualties.

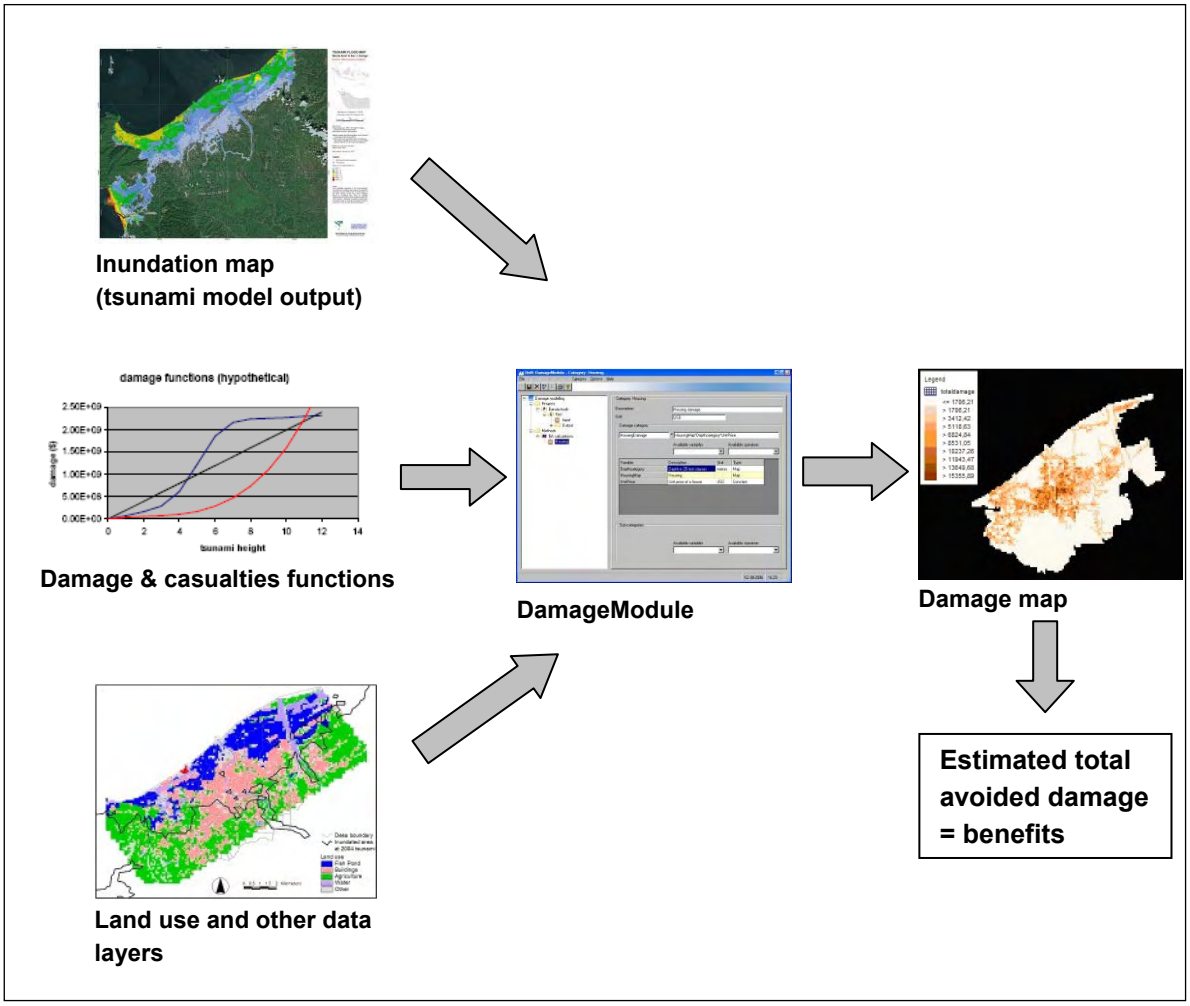

Figure 4-9 Input and output (Damage map) for DamageModule [32].

The relations are based on an analysis of data from the December 2004 tsunami and inundation depths from the 2D-model (see previous section). The areas studied are Banda Aceh, Calang & Samatiga and Lhokseumaweh.

The DamageModule software calculates flood risk maps by combining an inundation map (like Figure 4-7) and land use maps using the damage and casualties functions. Flood damage is calculated for the land use categories housing, infrastructure (roads and bridges), agriculture, fisheries (aquaculture), industry & trade and the environment (mangroves and forests).

The model generates maps as an indication of the damage sustained if a similar tsunami would happen with the present land use. The total damage for a certain tsunami event can be calculated by integrating the damage over all the categories and grids. The Damage Model is used in this thesis study to assess the damage for various flood-situations, which finally generates the input for a cost benefit analysis for flood protection measures. The methodology is presented in Figure 4-9. An elaborate description of the DamageModule can be found in [32].

4.5.2 Model runs

Existing runs
The reference case, the Dec2004 Tsunami, was available.

Additional runs
For the tsunamis caused by earthquakes magnitudes 7,5/8/8,5/9 and 9,5, the damage was calculated.

4.5.3 Results

Existing runs
The total damage of the Dec2004 Tsunami, calculated with the DamageModule amounted to 1,1 Billion USD.

Additional runs
The results are shown in Table 4-1.

Table 4-1: Calculated damage with DamageModule for various tsunami-heights

Magnitude	Max. wave height at the shoreline Calculated with 2D-Tsunami model	Damage [Billion USD] Calculated with DamageModule
7,5	1,05M	0,010
8	2,36M	0,149
8,5	4,43M	0,485
9	7,95M	1,090
9,5	8,51M	1,273

These results are used in the assessment of the alternatives. The methodology is described in 5.3.2.

4.6 SUMMARY

In total 4 models have been used to investigate the effectiveness of tsunami protection measures. Partly, existing model runs have been used, but also a large number of additional modelling is carried out.

It was concluded that protection against high tsunami events is difficult to achieve with any type of measure. Offshore breakwaters and seawalls both require a freeboard about equal to the tsunami height on the shoreline. The effectiveness of an offshore breakwater at this height is better than of a seawall. Mangroves have shown hardly any effectiveness for tsunami heights > 3m.
Comparison of the wave heights with the 2D-model showed significant difference. Therefore, additional runs were carried out.

Additional semi-1D model runs showed a big influence of the near shore bathymetry. The assumed linear profile in the existing 1D-model runs generates higher waves at the coast then the actual bathymetry as is used in the 2D-model. Shoaling of the wave from -20m bathymetry to

the coast was 1,5times higher for a concave profile then a convex profile. This explained the difference between the original 1D-runs and 2D runs.

As the near-shore profile in Banda Aceh is slightly convex, the actual shoaling is limited. Several structures were modelled in this profile. The run-up against these structures is also lower as a consequence of the favourable fore-shore bathymetry.

However, the results from the 1D-model (Fortran) are not consistent with these findings and gave much lower differences between convex and concave bathymetric profiles. Additional modelling is recommended to gain more insight in this matter.

In general, negative tsunamis (with leading trough) have higher impact and run-up.

An attempt has been made to reproduce the model results with Kaplan's empirical expression for overtopping volumes. A big difference was found in overtopping volumes. The facts that several waves overtopped the structure and ride on top of each other are an explanation for this difference.

Combined measures result in very limited reduction of the flooding. It seems better to invest in one high structure then in two lower structures.

The 2D-Tsunami Model has been described and will be used to simulate the flooding of Banda Aceh with and without structural measures for various tsunami events (presented as earthquake magnitude).

The 2D-Tsunami Model produces inundation depths in every grid. This is used in the DamageModule, which calculates the associated damage based on (pre-dec2004) land-use data.

Chapter 5. TSUNAMI PROTECTION ALTERNATIVES FOR BANDA ACEH

5.1 INTRODUCTION

The high loss of human life and economical damage in Banda Aceh raises the question: can Banda Aceh be protected against future tsunami-events? This question not only implies a technical part, whether a certain structure can withstand the forces of a tsunami, but also questions concerning social and environmental issues.

In this Chapter various alternatives are developed and their effectiveness in tsunami reduction is simulated. The structures are schematized with the 2D-model as described in Chapter 4.4.

Initially, the focus is on the position of the alternatives in plan view. The main alternatives therefore vary in location (offshore, at the coast or inland). Within these alternatives, various heights and configurations are modelled.
However, except for the retaining height, no remarks are made about the actual shape of the cross section. This topic will be shortly discussed in section 5.9.

The result of this modelling is information about the effectiveness. To what extent do the various alternatives reduce the flooding due to the tsunami? All model runs use the Dec2004 Tsunami as input signal. This is to reduce the number of model runs. When the most effective structure is selected, more runs are done with various tsunami signals.

5.2 TSUNAMI PROTECTION ALTERNATIVES (IN PLAN POSITION)

5.2.1 Offshore Tsunami Protection

Typically, protection against the sea is located either offshore or on the shore. Offshore solutions can have the advantage of a strong reduction in structure costs. In Japan for instance, many fisher villages are located in a bay, with a narrow entrance to the sea.

In this case, building offshore could significantly reduce the costs of an offshore structure, because the required length is much less that a solution on the shore. In Ofunato Bay in Japan, for instance, a (tsunami) breakwater was built at the entrance of the bay, see Figure 5-1. The total length of the breakwater is 737m. Defending the city on the shoreline would require a seawall with a length of at least 8km. See also Figure 5-1 and section 2.7.2.

Ofunato Bay Japan
Length coastline: 8.000 m
Length tsunami barrier: 737 m

1 m barrier protects 10,9 m coast.

Banda Aceh (see Figure 5-2)
Length coastline: 22.500 m
Length tsunami barrier: ±22.000 m

1 m barrier protects ±1 m coast.

Figure 5-1 Length of offshore protection vs. length of protected coastline; Ofunato Bay, Japan. The red circle indicates the location of the breakwater

In Banda Aceh, the situation is different. Banda Aceh is not located in a bay. This means that even an offshore solution requires a structure which stretches from the hills in the southeast to the hills in the northwest. An offshore structure would approximately have the same length as a structure on the shoreline. See Figure 5-2.

Although this fact decreases the attractiveness of an offshore barrier, there are sufficient reasons to take an offshore alternative into consideration. These reasons are:

- An offshore solution has much less impact on the society.
- The wave will be steeper and higher (shoaling) closer to the shore. Thus the required retaining height (run-up) and strength are higher for a structure onshore that offshore. This also accounts for the current velocities under the wave. Consequently, the loads on an offshore structure are less.
- Land acquisition issues are much less delicate for offshore solutions

Therefore, offshore protection alternatives for Banda Aceh are proposed. In this study, two offshore alternatives will be considered:

1. An offshore barrier at -15m bathymetry line
2. An offshore barrier at -10m bathymetry line (see Figure 5-2)

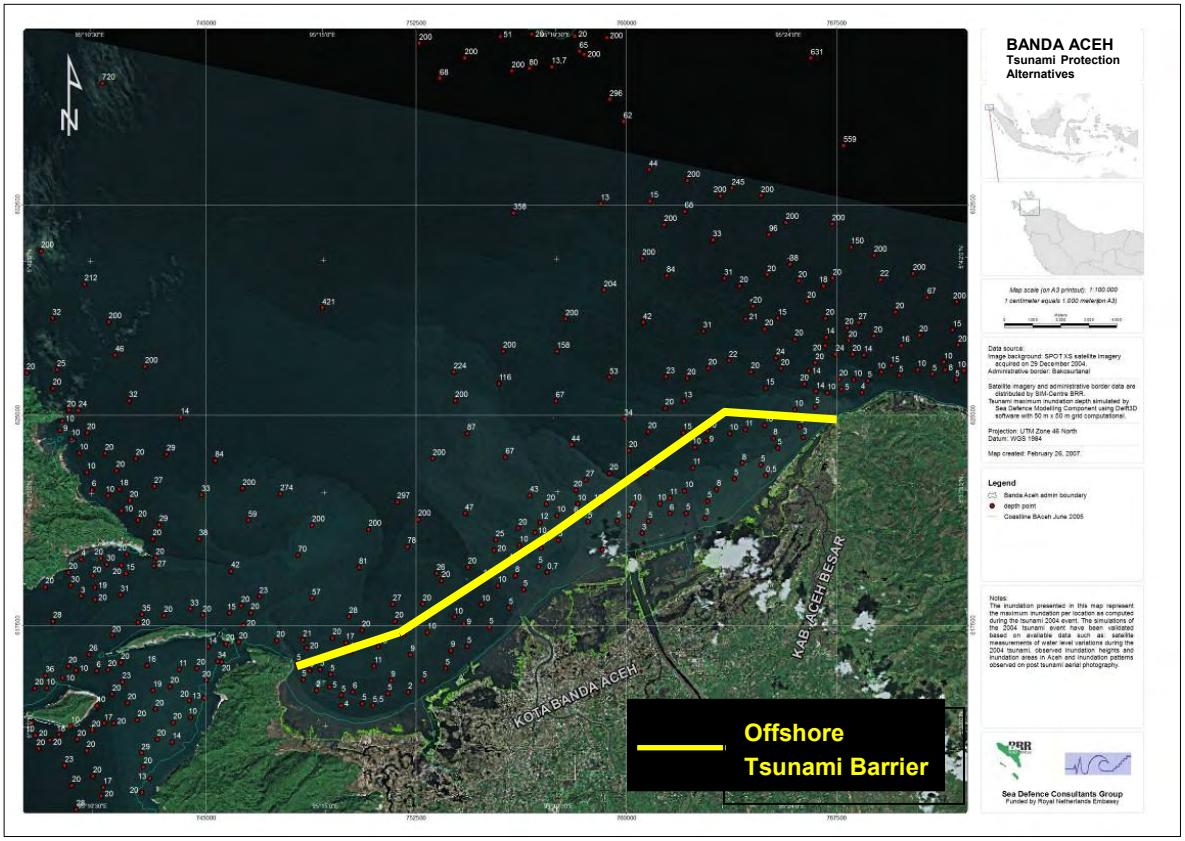

Figure 5-2 Offshore Tsunami Protection Alternative, following the 10m bathymetry line.

Within these alternatives, many sub-alternatives are modelled with various retaining heights and configurations.

5.2.2 Coastal Tsunami Protection

Besides these offshore alternatives, a solution on the shore can also be attractive. The reasons are:

- Although the wave height at the shore is higher than offshore, the total structure height will be less. The costs for a solution on the shore will be significantly lower than for an offshore solution.
- Offshore solutions can block or change important long-shore and cross-shore currents, causing changes in sediment transport (sedimentation/erosion). It can also reduce the tidal motions, which are important for the fish ponds in Banda Aceh.
- Operation and maintenance of 'dry structures' is less complicated and costly then for offshore solutions

For these reasons a coastal tsunami protection alternative is proposed, following the trajectory of the original (before Dec2004) coastline. See Figure 5-3.

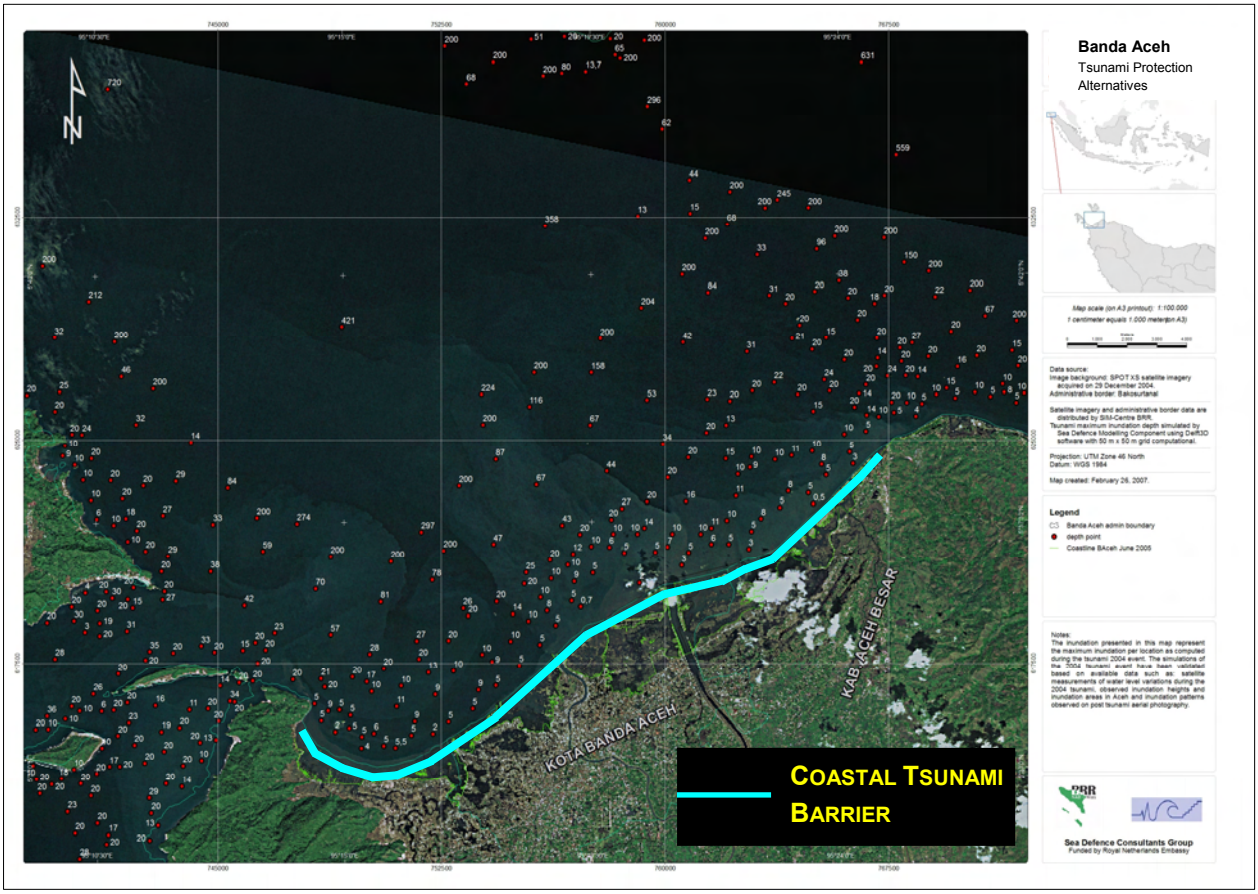

Figure 5-3 Coastal Tsunami Protection Alternative, following the original coastline.

5.2.3 Inland Tsunami Protection

The third possible alternative is an inland barrier. Considerations in favour of this alternative are:

- The wave height decreases inland, partly by reflection, partly by dissipation due to friction. The required retaining height will then also be less.
- Several studies (JICA Study Team and Department for Spatial Planning of Banda Aceh; RTRW Kota Banda Aceh) propose a ring road to improve accessibility of the city centre and to provide good access to the escape roads. See Figure 5-4. Because land acquisition issues are highly delicate, a combination of this road with an inland barrier gives a big advantage.
- On the seaside of the wall are many fishponds and there is only little urban development.. The unprotected area therefore represents only minor economical value.

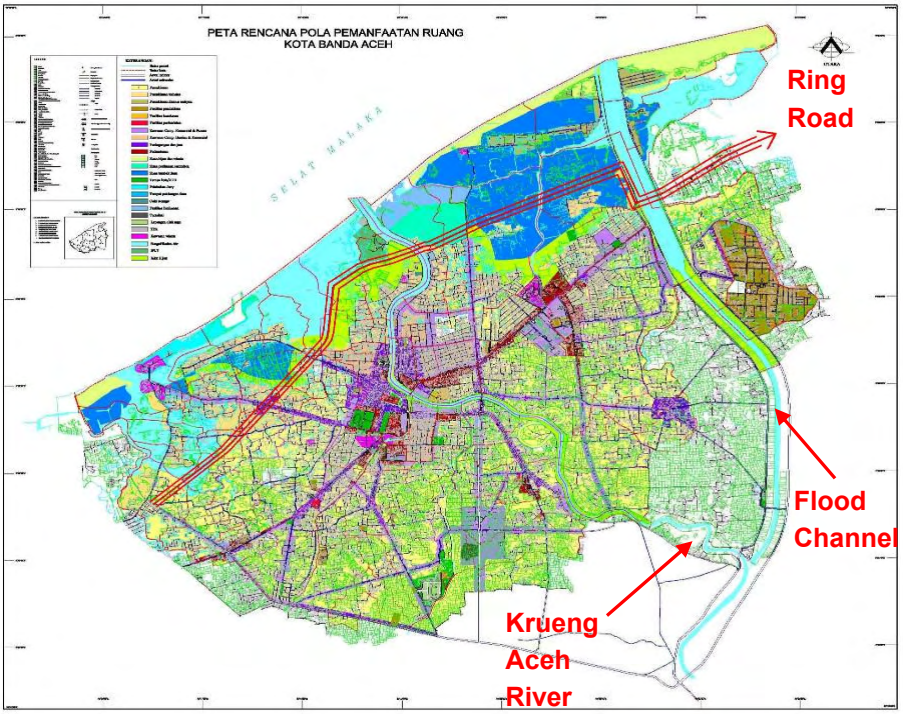

Figure 5-4 Proposed ring road (red line). Source: RTRW Kota Banda Aceh.

Although inland protection is not common, above considerations indicate that this alternative is worth a more thorough study. The plan view of the inland wall (and proposed ring road) is depicted in Figure 5-5.

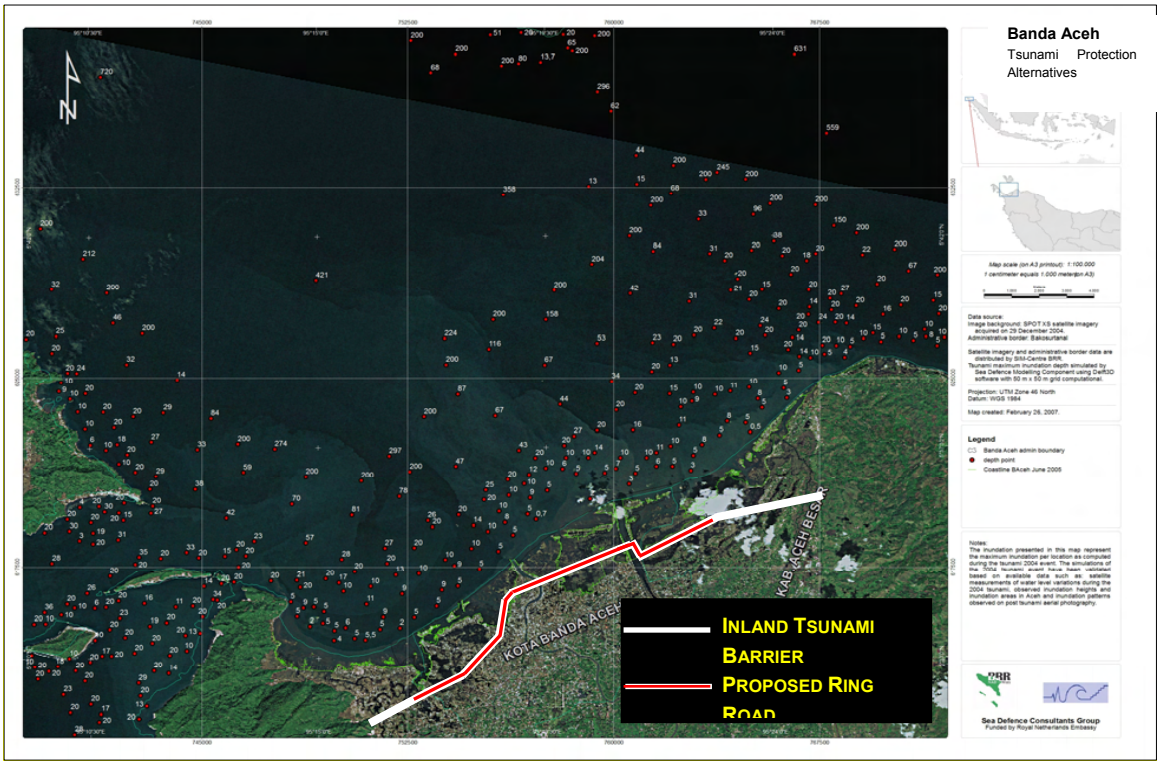

Figure 5-5 Inland Tsunami Protection Alternative, following the trajectory of the proposed ring road.

5.2.4 Overview of developed alternatives

Three main alternatives are developed as tsunami protection measure. A 4th alternative can be added, which is the current situation. The alternatives are:

Alternative 0: No Tsunami Protection; current situation
Alternative 1: Offshore Tsunami Barrier
Alternative 2: Coastal Tsunami Barrier
Alternative 3: Inland Tsunami Barrier

The plan view of alternatives 1 to 3 is depicted in Figure 5-6.

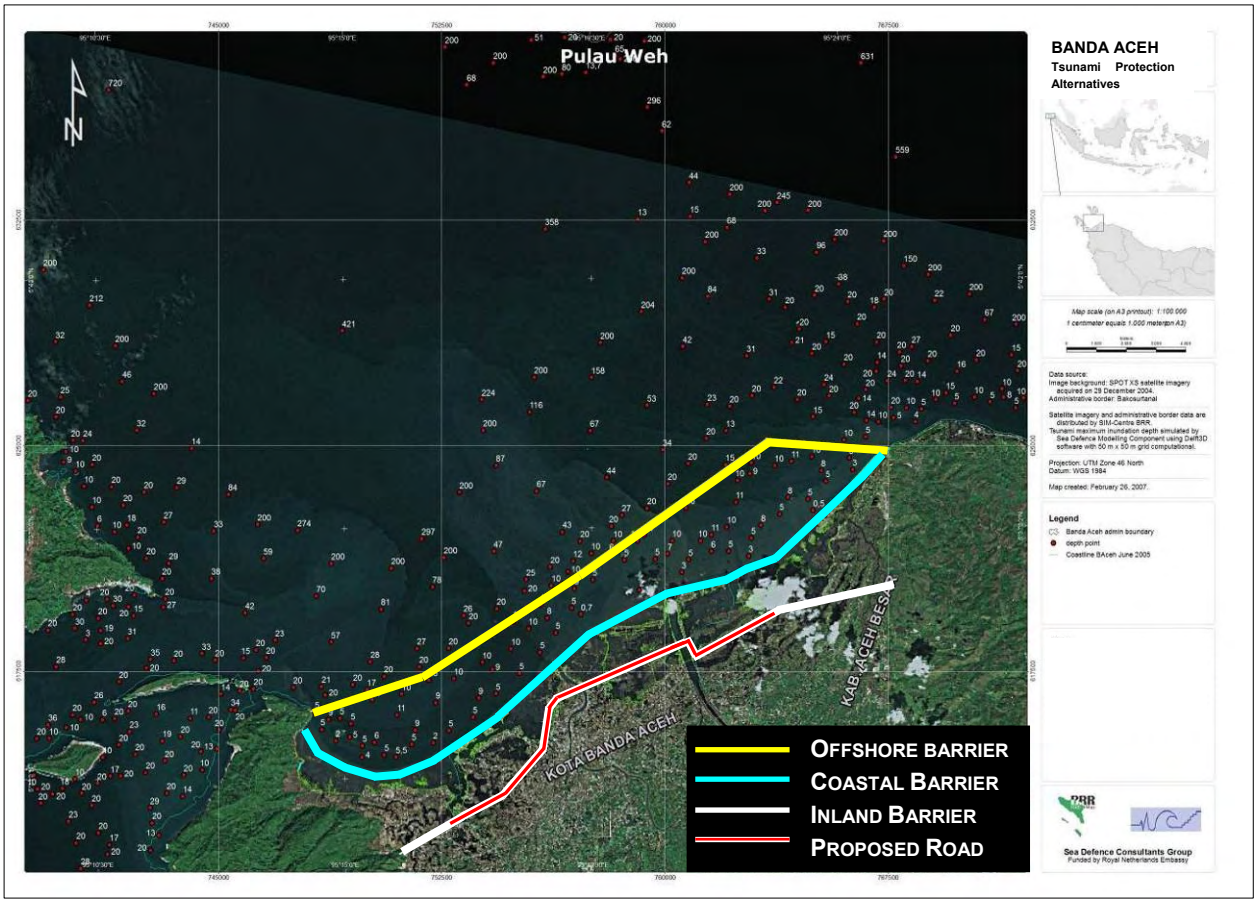

Figure 5-6 Overview of the main alternatives

These alternatives will be schematized in the 2D-model, and their effectiveness in tsunami reduction is computed. Based on the results, sub-alternatives are developed, with varying height, configuration, gaps, etc.

Although the development of alternatives was mainly focussed on the location (in plan view), it is necessary to say something about possible cross-sections. In this context, some 'innovative' solutions have been developed in the past years. These solutions will be discussed later on, in section 5.9. For the modelling of the proposed alternatives, detailed information about the actual shape of the cross section is not necessary.

5.3 MODELLING OF ALTERNATIVES

5.3.1 Modelling

The 2D-Tsunami Model, as described in Chapter 4.4 is used. The structures are modelled as 2D-weirs. For the structure modelling the Dec2004 Tsunami signal is used. To gain insight in the relation between inundation and damage, other tsunami scenarios are applied. The resulting flooding can be presented in flood maps, but as this requires a lot of work, some specific output is selected.

5.3.2 Output parameters

A lot of output is generated by the 2D model. The main output however, is the maximum inundation depth. The effectiveness of the structure depends on the reduction of damage it provides for the hinterland. This damage could be calculated by loading the maximum inundation file into the Damage-Module (see Chapter 4.5). Because a lot of alternatives are modelled this would involve a lot of operations. To reduce the workload, a linear relation between damage and maximum inundation is assumed.

For every model run, the maximum inundation volume during an entire run is calculated by (grid 1 to *i*):

$$\sum_{1}^{i} Max\_Inundation\_Depth \cdot Gridarea$$

This total volume for the entire model area is higher than the actual volume which enters the land as computed by the 2D-model. This is because the *maximum* inundation in each grid for the entire runtime is added up instead of the instantaneous volume. However, this figure gives better results since damage is more related with the highest wave rolling over land, than with the final inundation depth after several waves.

A linear relation between inundation volume and damage is assumed. The inundation patterns of the Dec2004 Tsunami are used to calibrate the model. This inundation pattern is related with the the damage caused by the Dec2004 Tsunami. Assuming that this relation also exists for other cases, the damage can easily be calculated for each inundation volume.

The reason to use this procedure is that it requires a lot of operations to calculate the damage with the Damage Module.

To check this assumption, a couple of model runs are executed (with the 2D-model and the DamageModule) for various Tsunami signals. See Table 5-1.

Table 5-1: Overview model run without structural measures

Magnitude Richter Scale	Max Inundation Volume [10^6 m^3]	Damage (determined with Damage Module) [Billion USD]	Wave Height at the Shore line [m]
7,5	1	0,069	1,05
8	3,89	0,149	2,36
8,5	22,8	0,485	4,43

Magnitude Richter Scale	Max Inundation Volume [10^6 m^3]	Damage (determined with Damage Module) [Billion USD]	Wave Height at the Shore line [m]
9	77,9	1,090	7,95
9,5	126	1,273	8,51

The correlation between inundation depth and the maximum inundation is obtained, based on the damage calculated with the Damage Module.

The relation is depicted in Figure 5-7. The data-points show a decreasing rise in damage for increasing inundation volume. Although this trend is neglected by the linear assumption, the correlation is good. The R^2-value of 0,91 indicates that the actual damage can be fairly well estimated by using a linear relation between damage and inundation volume. For preliminary assessments this relation can be used. For the cost-benefit analysis (Chapter 6), the damage as computed by the Damage Module is used.

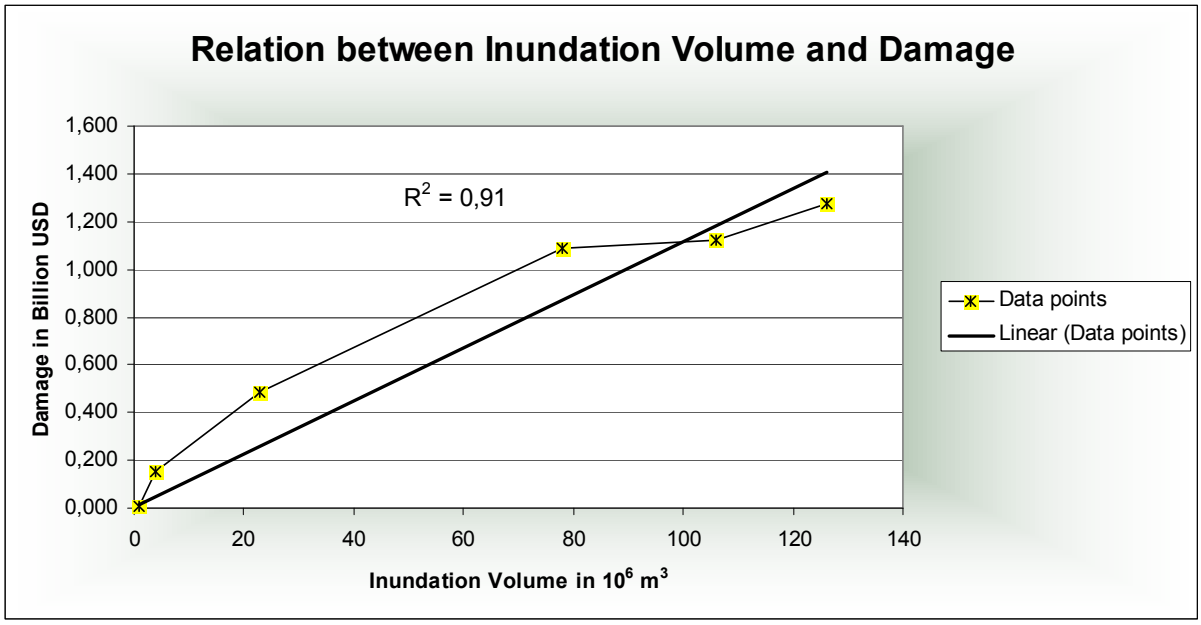

Figure 5-7 Correlation between Inundation Volume and Damage

In the sections 5.5 to 5.7, the effectiveness under tsunami attack of the developed alternatives is calculated and presented. The resulting flooding is compared to the flooding during the Dec2004 Tsunami. However, at this moment, a simple coastal defence system is constructed to protect against further coastal erosion and against tidal flooding. The effectiveness of these structures under tsunami attack is discussed first.

5.4 ALTERNATIVE 0: CURRENT SITUATION

At this moment reconstruction of 'normal' coastal protection is finished for the Banda Aceh region. 'Normal' means: standard protection against wave attack, high water and erosion, so regular non-tsunami events. Two types of protection are present in Banda Aceh:

1. A revetment, built on the coastline, aimed to prevent wave overtopping
2. The second type is a tidal dike, built 300-500m inland. This structure has to protect the hinterland against flooding in case of spring tide.

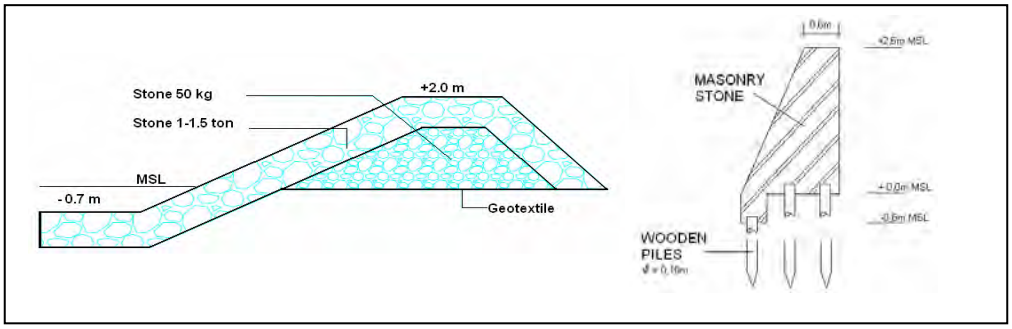

Figure 5-8 Cross section of existing revetment (left) and floodwall (right) [SDC]

The height of the revetment is +2,0m MSL. The rubble mound protection (slope and toe) is 1-1,5ton stones. The seaward slope is 1:2 and the rear slope 1:1. This structure is very porous.

The retaining height of the flood wall, build somewhat inland is +2,6m MSL. The wall is founded on wooden piles Ø10cm and constructed of masonry stones.

5.4.1 Effectiveness under tsunami conditions

A model run is carried out with a barrier of +2,6m with 5 gates along the coastline. This structure represents the floodwall. The Dec2004 Tsunami signal is used. The results are depicted in Figure 5-9.

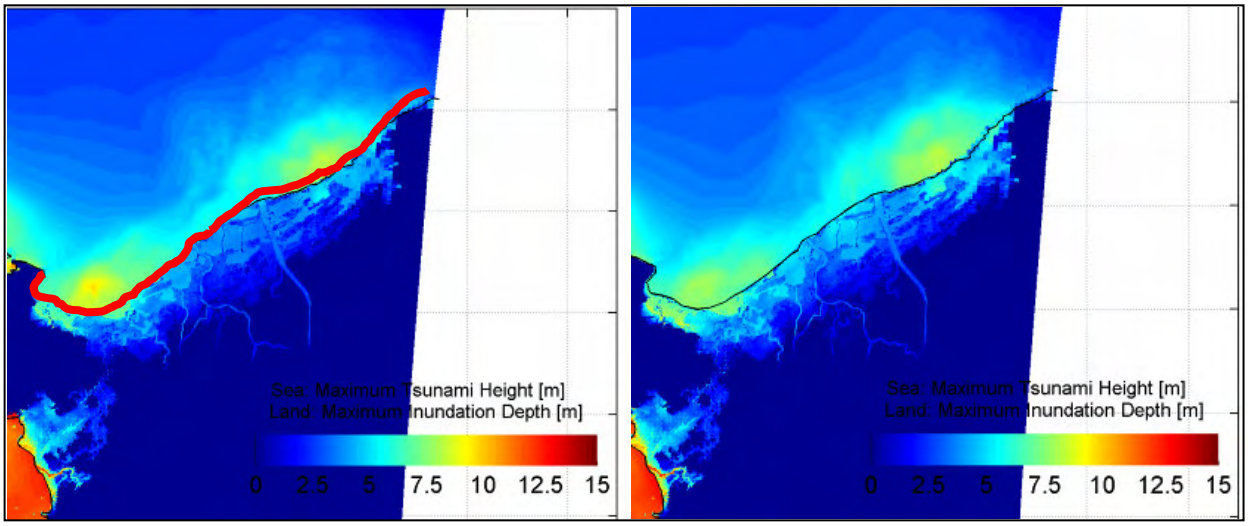

Figure 5-9 Maximum inundation of Banda Aceh, with floodwall +2,6m (left, red line), and without any protection (right).

The results show a slight reduction in inundation depth and penetration. However, for this tsunami event the wave heights at the coast are in the order of 8 to 10m. Both structures (revetment and floodwall) will be completely overtopped and it is expected that the structure will be severely

damaged after the first wave. As a consequence, the successive waves will penetrate further inland than indicated by the model simulation.

As mentioned in Chapter 2, low seawalls can be somewhat effective in protecting the hinterland against the initial impact of the wave. Significant overtopping however will result in flooding and damage which is comparable with the situation without any protection (see 2.7.1).

Conclusion: the existing coastal protection is not effective under tsunami conditions. Even if the structures (revetment & floodwall) remain intact, only minor reduction of inundation is expected.

5.5 ALTERNATIVE 1: OFFSHORE TSUNAMI BARRIER

5.5.1 Model runs and effectiveness under tsunami conditions

In total 17 model runs are carried out with offshore structures. The inundation map and calculation of the effectiveness for 1 computation is shown, see Figure 5-10.

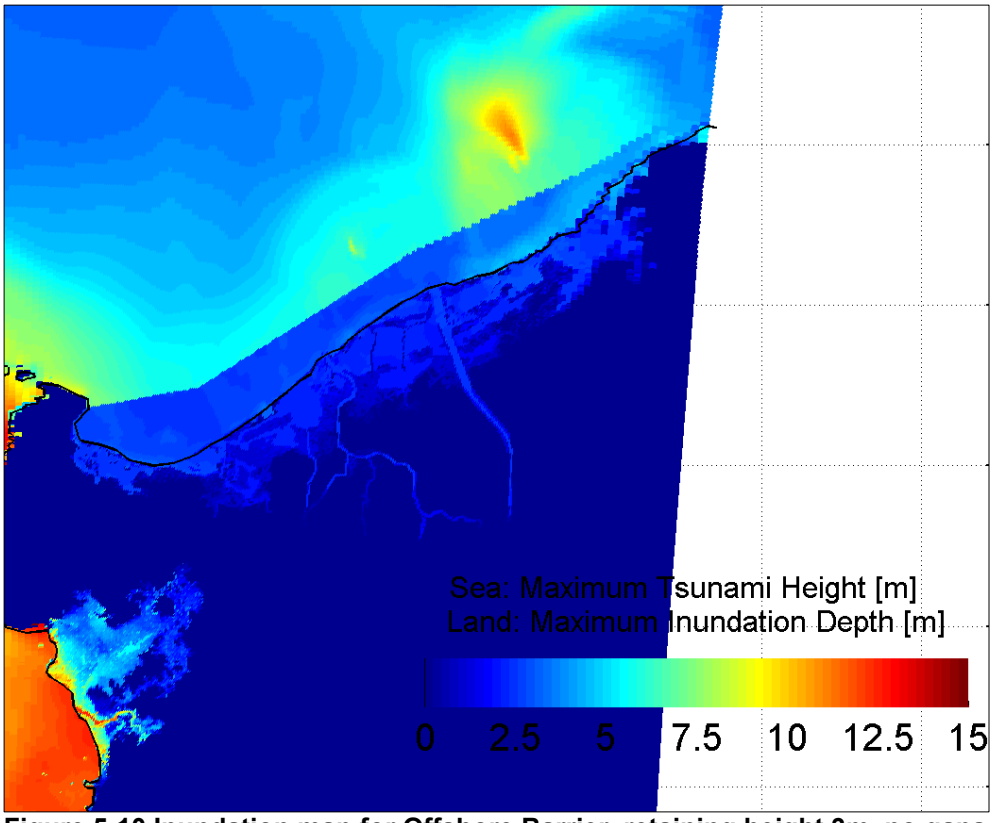

Figure 5-10 Inundation map for Offshore Barrier, retaining height 3m, no gaps

The maximum inundation volume (on land) for an offshore barrier with retaining height 3m and no gaps, after the attack of a Dec2004 Tsunami, amounts to 21,5 million m^3. Without tsunami protection, the inundation volume is 106 million m^3.

The effectiveness of this sub-alternative is therefore: (1 – 21,5/106) * 100% = 79,7%

The same calculations are made for all 17 sub-alternatives. An overview and the resulting effectiveness of all model runs is presented in Table 5-2.

Table 5-2: Overview model runs and effectiveness for offshore alternatives. M_w = 9.2

Depth	Retaining height	Specification	Inundation Volume [10^6 m^3]	Effectiveness
-	-	BASE CASE (DEC2004 TSUNAMI)	106	0%
-15M	3M	NO GAPS	13,1	87,7%
-15M	5M	NO GAPS	1,73	98,4%
-10M	-3M	NO GAPS	80,1	24,4%
-10M	0M	NO GAPS	58,1	45,2%
-10M	3M	NO GAPS	21,5	79,7%
-10M	5M	NO GAPS	2,34	97,8%
-10M	7M	NO GAPS	1,06	99,0%
-10M	7M	GAP 1X200M	1,75	98,4%
-10M	7M	GAP 2X200M	3,10	97,1%
-10M	3M	OPEN NORTH	20,5	80,7%
-10M	5M	OPEN NORTH	2,47	97,7%
-10M	7M	OPEN NORTH	1,12	98,9%
-10M	5M	OPEN NORTH + GAP 1X100M	2,94	97,2%
-10M	5M	OPEN NORTH + GAP 2X200M	3,92	96,3%
-10M	5M	OPEN NORTH/SOUTH	7,23	93,2%
-10M	5M	OPEN NORTH/SOUTH + GAP 2X200M	8,79	91,7%
-10M	5M	OPEN NORTH/SOUTH_ISLAND + GAP 2X200M	10,64	90,0%

The variant with no gaps are modelled to gain insight in the general behaviour of the alternative. The absence of gaps means either a fully closed structure either a structure with gates that can be closed in case of a tsunami warning. Both options are regarded as non-feasible. The construction, maintenance and operation of offshore gates for extreme events will be extremely difficult and costly.

Open north and south means that the breakwater is not connected to the coast. These openings are approximately 800m.

The resulting effectiveness for the alternatives without gaps is depicted in Figure 5-11.

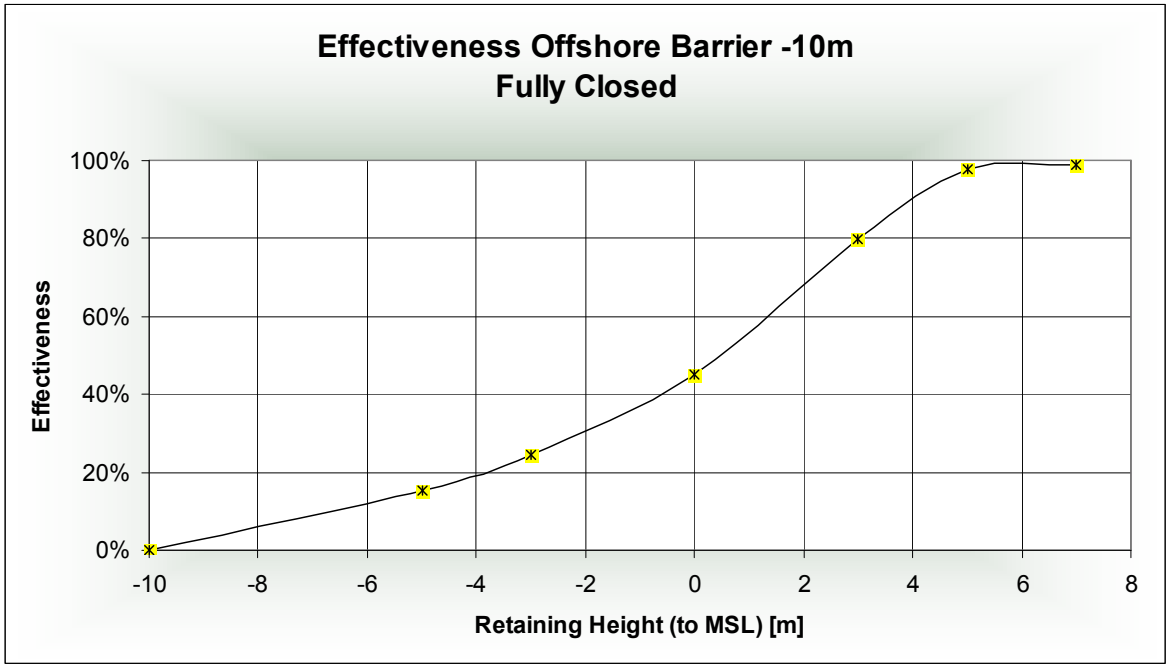

Figure 5-11 Effectiveness Offshore Barrier -10m; Fully Closed for Dec2004 Tsunami Signal

It can be observed that the overtopping of the tsunami is minimal. The wave height at -10m bathymetry line is approximately 5m. For a barrier height of 7m, almost the complete wave is blocked. Furthermore, retaining to MSL (0m in graph) still reduces inundation with 45%, indicating that the velocity is indeed equally distributed along the entire water column.

5.5.2 (Dis)advantages

Advantages

- The main reason to build offshore is to reduce the impact on the coastal area. Coastal structures will directly affect the (mostly) highly populated coastal area, by disturbing free access to the sea and/or beach and views. See Figure 5-12 for an impression.
- No land acquisition
- An offshore structure requires less high freeboard (i.e. the visible part of the structure), because the tsunami wave height is smaller in deeper water. The height at the shore can increase significantly, depending on the actual bathymetric profile (see Chapter 4.3)
- Except for the wave height, the impact on the structure will be less (see Chapter 2). The run-up and impact forces depend directly on the wave steepness, which will be less in deeper water.
- The active zone, in which sediment transport takes place, extends up to 4m water depth. In front of the barrier, no sedimentation or erosion is expected under normal wave conditions.
- Besides tsunamis, the offshore breakwater will also reduce normal waves.

Disadvantages

- Because a major part of the structure is under water, the total volume is much higher than for structures on land. As costs are related with structure volume and offshore

execution is more complicated than on land, the costs of this alternative will be significantly higher.

- Because the offshore breakwater will also reduce normal waves, the wave-induced long-shore and cross-shore currents will also be reduced. Reduction of these currents could affect the quality of the sea-water in between the structure and the coast. The actual retention time of waste-water, discharged by the river, could increase. Moreover, sedimentation and erosion can occur. Increasing the number of gaps, especially close to the coast, will increase water circulation and decrease retention time.

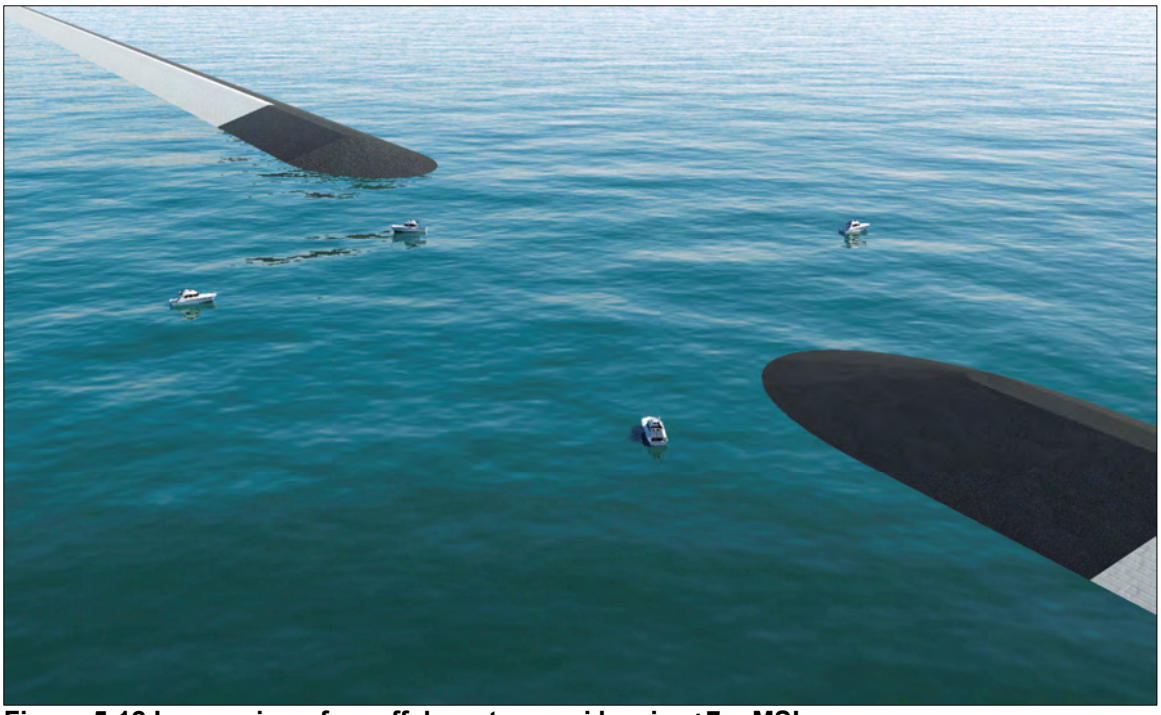

Figure 5-12 Impression of an offshore tsunami barrier +7m MSL

5.6 ALTERNATIVE 2: COASTAL TSUNAMI BARRIER

5.6.1 Model runs and effectiveness under tsunami conditions

The following model runs are carried out, see
Table 5-3.

Table 5-3: Overview model runs and effectiveness for the coastal alternatives. M_w=9.2

Retaining height	*Specification*	*Inundation Volume [10^6 m^3]*	*Effectiveness*
-	*BASE CASE (DEC2004 TSUNAMI)*	*106*	*0%*
3M	*NO GAPS*	*89,5*	*15,5%*
5M	*NO GAPS*	*43,8*	*58,7%*
7M	*NO GAPS*	*15,4*	*85,5%*
11M	*NO GAPS*	*1,45*	*95,8%*

Retaining height	*Specification*	*Inundation Volume [10^6 m^3]*	*Effectiveness*
7M	*GAPS 3X100M*	*19,2*	*81,9%*

The variant with no gaps are modelled to gain insight in the general behaviour of the alternative. The absence of gaps means either a fully closed structure or a structure with gates that can be closed (fast) in case of a tsunami warning. For coastal structures it is possible to have gates in the entrances (rivers and channels). However, since the operation and maintenance of such gates is difficult, one run is made with gaps. The gap width of 100m is possible, considering the absence of large vessels. The influence of the constriction of the discharge-channels in case of a torrential rainfall is simulated with an available SOBEK-model. For 1/100-year conditions, no flooding was caused by the decreased discharge openings.

The resulting effectiveness for the alternatives without gaps is depicted in Figure 5-13.

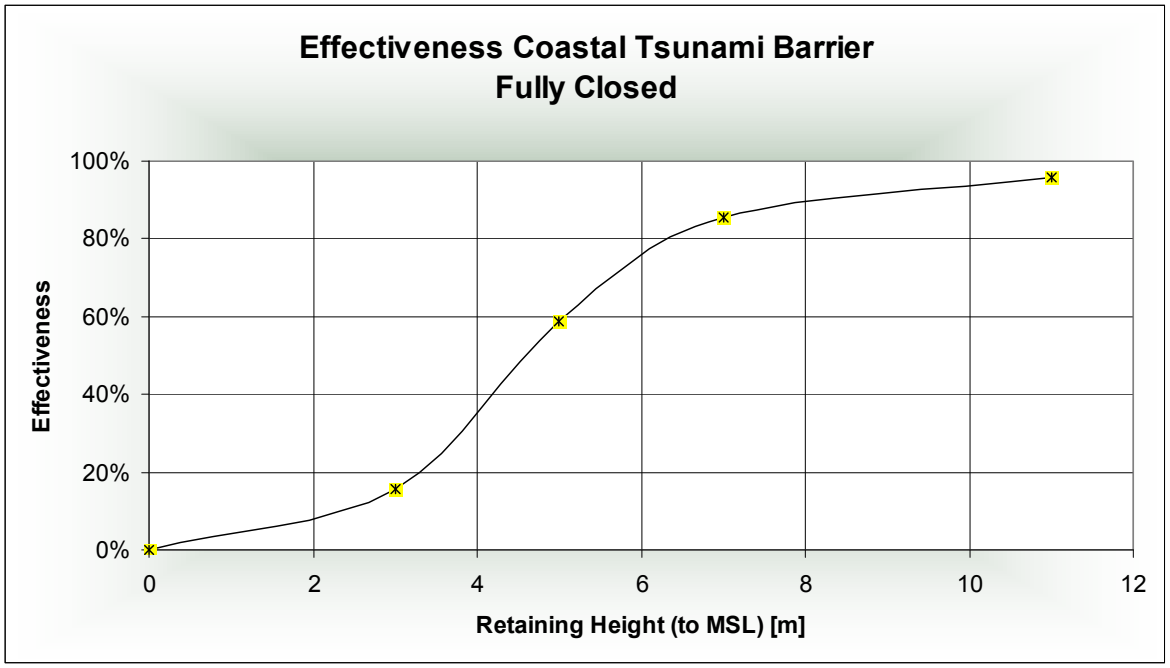

Figure 5-13 Effectiveness Coastal Barrier; Fully Closed for Dec2004 Tsunami Signal

It can be concluded that significant reduction requires high structures. To obtain an effective reduction of 95%, an 11m high structure is necessary. Lower structures will be overtopped considerably.

5.6.2 (Dis)advantages

Advantages

- The total height of the structure is smaller then for offshore alternatives, leading to lower construction costs
- Conditions on the sea are not influenced by construction on land. No change in sediment transport due to this structure has to be expected.

Disadvantages

- The tsunami will be more powerful close to the coast. This is due to shoaling and steepening of the wave. Velocities and wave run-up are higher compared to offshore structures.
- The coastline barrier forms literally a barrier along the coast, affecting the interaction between land and sea activities. Accessing the sea will mean crossing high obstacle, which only has openings near river and canal mouths.
- The barrier will affect the sea view, hence affecting the aesthetical value of the coastal area in Banda Aceh. The barrier will also affect light and wind conditions of the land along the barrier. In Japan, people complained about poor air quality in the area behind a seawall of 4,5m.
- The coastal barrier may affect land use and land use values in its direct vicinity.
- The barrier may affect future coastal development.

In Figure 5-14 an impression is shown of a 10m high coastal barrier. The size of the structure relation to the size of people cars and houses is clearly visible.

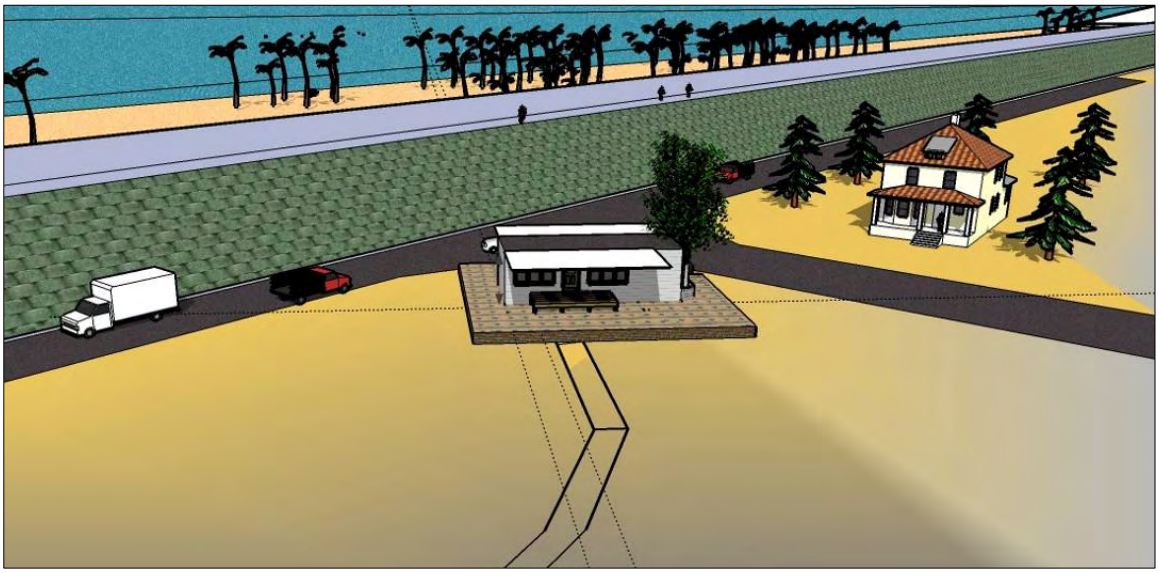

Figure 5-14 Impression of a coastal tsunami barrier of 10m height

5.7 ALTERNATIVE 3: INLAND TSUNAMI BARRIER

5.7.1 Model runs and effectiveness under tsunami conditions

Table 5-4 lists the model runs and resulting effectiveness.

Table 5-4: Overview model runs and effectiveness for inland alternatives. M_w= 9.2

Retaining height	Specification	Inundation Volume [10^6 m^3]	Effectiveness

Retaining height	Specification	Inundation Volume [10^6 m^3]	Effectiveness
-	BASE CASE (DEC2004 TSUNAMI)	106	0%
2M	NO GAPS	67,0	36,8%
3M	NO GAPS	61,7	41,8%
5M	NO GAPS	35,1	66,8%
7M	NO GAPS	30,9	70,8%
FR	FULL REFLECTION	28,7	73,0%
7M	NO GAPS, OTHER DIRECTION	29,5	72,2%
7M	GAPS 4X100M	35,9	66,1%

The resulting effectiveness for the alternatives without gaps is depicted in Figure 5-15.

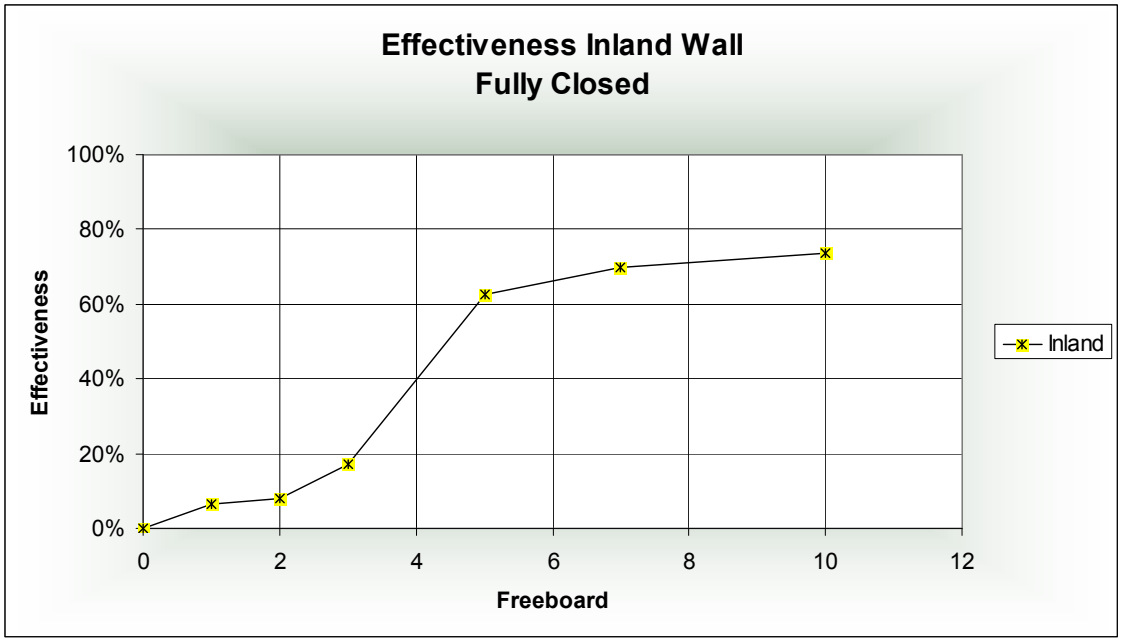

Figure 5-15 Effectiveness Inland Barrier; Fully Closed for Dec2004 Tsunami Signal

5.7.2 (Dis)advantages

Advantages

- The total height of the structure is smaller than for offshore alternatives and coastal structures. The wave height decreases while going inland. This leads to lower construction costs compared to offshore and coastal solutions.
- Conditions on the sea are not influences by construction on land. No change in sediment transport due to this structure has to be expected.

Disadvantages

- The tsunami will be more powerful on land than offshore, although the wave height decreases while the wave is going inland. Velocities and wave run-up are higher compared to offshore structures. See also Chapter 2.
- The area in front of the inland wall is not protected. It will even be inundated more than without structure and consequently suffer more damage.
- The fact that a protected and unprotected zone is created has social consequences. In the unprotected zone still tsunami impact mitigation measures need to be carried out. In general, the barrier affects the socio-economic structure of the city.
- The inland barrier forms a physical barrier between the protected and unprotected side. It reduces the number of connections between two parts of the city. Also, views are blocked and fresh air can become a problem for people who live behind the wall. The structure can become a hindrance for the economical development of the city. An impression of an 8m high wall is shown in Figure 5-16.
- Land use and land values near the barrier may be affected.

In Figure 5-16 an impression is shown where the integration with the road is also shown.

Figure 5-16 An impression of an inland wall, height +8.0m

5.8 SUMMARY OF MODELLING RESULTS

The effectiveness in tsunami reduction of three separate alternatives is calculated. By only looking at the freeboard (i.e. the visible part of the structure) the offshore barrier is more effective then the 'dry' barriers. The effectiveness of the three alternatives is depicted in one graph, see Figure 5-22.

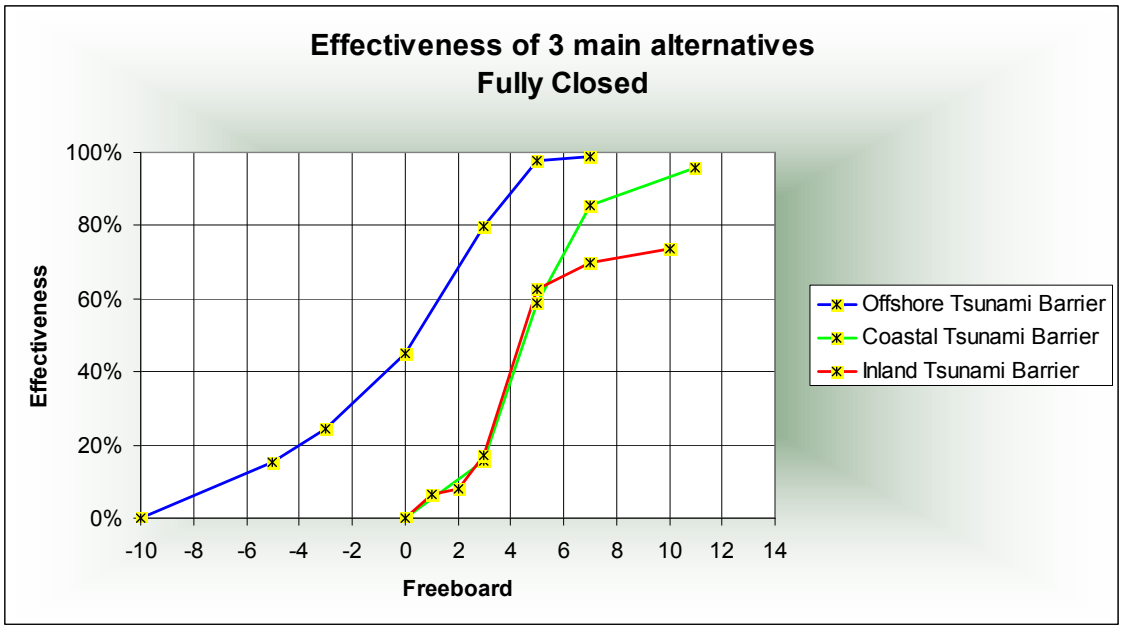

Figure 5-17 Comparison of effectiveness of the three main alternatives

The maximum effectiveness of the inland wall is 73%, because 27% of the entire Banda Aceh region is not protected by this alternative.

The main objective of these model runs was to determine the effectiveness of tsunami protection alternatives for varying location and height. The actual shape of the cross section was not discussed.

The following chapter (Chapter 6) deals with the assessment of these alternatives. This assessment requires more detailed information about the cross sectional properties, especially for the calculation of the costs. Therefore it is necessary to make some comments about the basic shape of the cross section. This is the subject of the following section.

5.9 POSSIBLE CROSS SECTIONS FOR TSUNAMI PROTECTION ALTERNATIVES

5.9.1 Innovative solutions

After the Dec2004 Tsunami several state-of-the-art 'tsunami-stoppers' were developed. Some of these innovative solutions, the 'blowpipe' and a 'movable wall' are shortly mentioned and discussed here.

5.9.1.1 Blow pipe

As part of an Innovative-Tsunami-Mitigation-Project an innovative tsunami decelerator was designed. The working principle is shown in Figure 5-18.

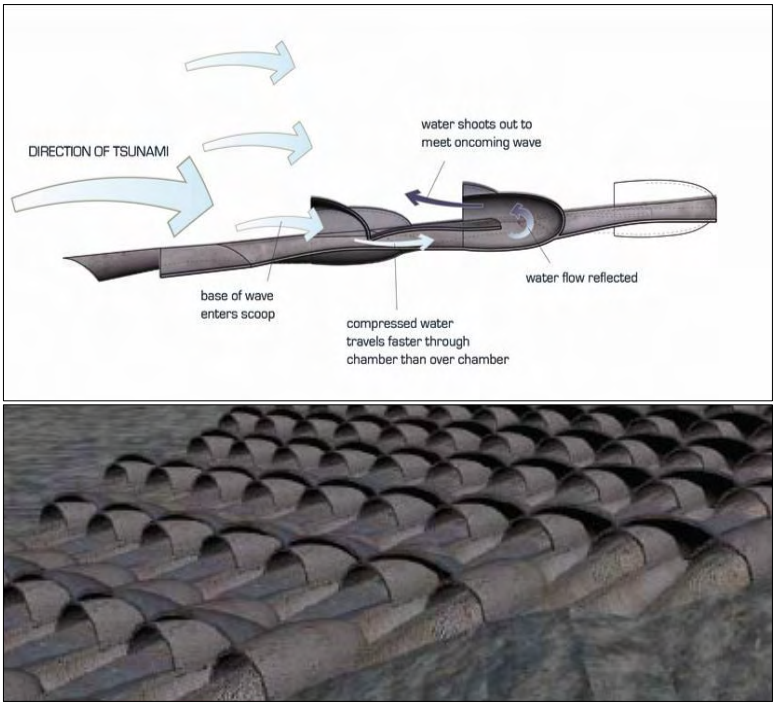

Shell-like scoops are deployed as the tsunami approaches the shore. These shells are designed to gather the energy of the incoming wave and reflect it back upon itself. The initial thrust of the wave is deflected down by the first shell, into a standing energy transfer pool. The water in the pool is rapidly forced backwards through the second shell, contacting the base of the wave and canceling out its forward-thrusting kinetic energy. In this way, the vast energy of the wave is used against itself.

An array of these shells would continue to impede the progress of the wave, negating the majority of its destructive energy before it reaches the shore. A conical deployment of these objects would protect a greater length of coast, effectively creating a tsunami 'shadow' of protected shoreline. This impact-energy reduction device could act as an element in a greater system of coastal defense.

Figure 5-18 Working principle of Blow Pipe and 3D-impression. Right the description as presented by the designers.

Discussion

The working principle is based on the idea that the energy under a tsunami wave is distributed over the complete water column. This agrees with the Shallow Water theory and is also supported by the modelling results (see Figure 5-11). Although this agrees with the shallow-water wave theory, several questions arise concerning the effect of this innovation:

- According to the impression, a complete array of shells is placed on the seafloor. Because the water-inlets are almost on a horizontal level, it is highly questionable if the shells behind the first row will give any additional reduction. As a consequence only the first or first two rows will be effective.
- The velocities at the bottom of the water column are lower than velocities in the upper part. This water with lower velocity is taken in and experiences friction and energy losses before it is used against the upper part of the wave. To be effective, the inlet height should be at least half the water depth, and even in this case it is very doubtful if the upper-part of the water column experiences any additional friction due to the reversed currents. Most likely, the inlet just acts like a submerged breakwater with a height equal or slightly less that the height of the shells.
- Execution of this structure would be extremely difficult, causing the costs to rise above standard (and proven) solutions like breakwaters.

Conclusively, this solution will act like an area of locally increased friction, which is considered as non-effective as tsunami-countermeasure (see section 2.6.4)

5.9.1.2 Movable wall

Van den Noort-Innovations (source www.noort-innovations.nl) developed a movable tsunami barrier, which is based on the idea that a tsunami is preceded by an initial draw back of the water. The working principle is depicted and explained in more detail in Figure 5-19.

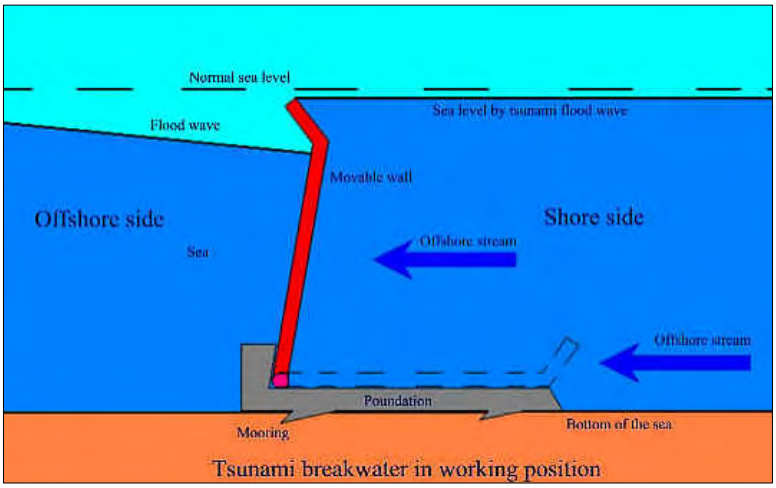

When a tsunami or flood wave runs to the coast there shall be first a water stream from the coast to offshore. In shallow water the wave is built up in height by pulling all the water from the shore. By blocking this stream the wave cannot build itself up.
The tsunami breakwater is so constructed that it blocks the offshore water stream and the water will not run offshore. So the tsunami gets no more water and will be reduced before it reaches the coast.

Figure 5-19 Working principle of the movable wall. Right the description as presented by the designers [68].

Discussion

As mentioned in the description, the basic idea is that the wall moves up by the offshore stream induced by the approaching tsunami. As a consequence, the blocking of the water prevents build-up of the positive wave. Questions arising with this innovation are:

- The initial arrival of a tsunami at the coast as a positive either negative wave, depends on the fault-type and location of the coastline with respect to the subduction zone. Coasts located ón the sub-ducting place will have an initial positive wave. In this case, the movable wall will not function. For Banda Aceh however, the initial signal for an earthquake-induced tsunami will be negative, causing an initial drawback of the water.
- The balance of forces seems quite precarious. The density of the ‘door’ is bounded within strict limits. Besides this, the horizontal equilibrium for the moment of arrival of the positive tsunami-wave is questionable. From correspondence with Van den Noort BV it turned out that the wall is locked in lifted positions.
- The theoretical assumption that the wave-build-up is reduced by blocking the offshore stream was tested in a 1D-model run. For an offshore breakwater at -10m, the wave development was compared with the situation without structure. See Figure 5-20. As visible, the wave growth is identical for the case with and without structure. Moreover, the inundation is even more, because the wave experiences less friction on the water stored between the structure and the coast. This finding was also mentioned in the correspondence with Van den Noort, but it was stressed that laboratory results show a strong reduction in wave growth.

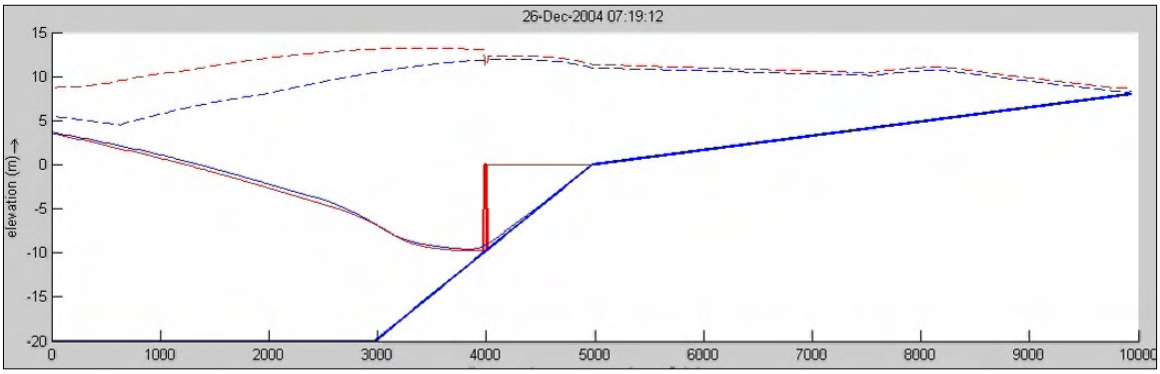

Figure 5-20 Comparison of wave growth for situation with (red line) and without structure (blue line).

- The most difficult point is however the working of this structure after several years. Since tsunami events are extreme events, the structure is probably not functioning for tens or even hundreds of years. Minor sedimentation or marine growth on the 'doors' will prohibit the uplift in case of a tsunami. Construction and maintenance will be difficult. The presence of hinges also makes the structure complicated.

It turns out that the working principle of these 'innovative solutions' is questionable. Besides that it is very doubtful if it is possible to realize and maintain these structures in an offshore and under-water environment.

Therefore, as a starting point, the emphasis will be on 'traditional cross sections' which are usually applied in hydraulic engineering.

5.9.2 Traditional solutions

Tsunami protection structures are scarce around the world and. The design and execution of these structures differs from standard coastal defence structures. However, because the composition and shape are often comparable with traditional structures, these solutions are called 'traditional' in this study.

In Chapter 2.7 some tsunami breakwaters (caisson and composite) are mentioned as well as an extensive seawall construction. The effectiveness of some of these structures was confirmed during past tsunami events. Therefore, these cross sections are basically a potentially realistic solution in tsunami protection.

A short list of possible cross sections:

<u>Offshore</u>

- Caisson breakwater
- Composite breakwater (caisson placed on rubble-mound)
  - (see section 2.7.2, 2.7.3)
    * Note that the Kawaragi breakwater collapsed (see 2.7.4)
  - Concrete wall protected by Tetrapods (see 2.7.5)
- Rubble mound breakwater

Onshore

- Sloping wall / embankment (see 2.7.1)
- Upright wall (not described in this report, but in Japan some nearly vertical concrete walls act as tsunami protection.)

A detailed discussion about the actual shape is for each of the three alternatives is not required right now. However, to enable a reliable cost calculation some basic cross sections for both offshore and onshore alternatives are presented here

5.9.2.1 Basic cross section for offshore tsunami protection

In general three types of offshore structures can be distinguished:

- rubble-mound structures
- caisson-type structures
- composite structures

The main advantage of a caisson-type structure in tsunami-conditions is that no instability of individual structure parts can occur. For a rubble-mound structure, replacement of the armour layer and core material can lead to collapse of the structure (see 2.7.5, Lhok'Nga breakwater). On the other hand, instability of the caisson as a whole could lead to collapse (see 2.7.4; the Kawaragi breakwater). The high flow velocities in case of tsunami overtopping are a point of concern when the armour layer consists of stones.

The main advantage of rubble-mound structures is that the execution is easier. Especially in this case, with retaining heights up to 7m in a water depth of 10m. The total structure height would amount to approximately 17m. Because this is impossible to realize with one single caisson, a part of the structure has to be executed in rubble-mound; a *composite* breakwater. Even if only the dry part of the structure would be constructed as caisson, the dimensions are extensive. Sinking of the caissons is impossible in that case since the large freeboard requires a large draught. In-situ construction is required and the expectation is that this will induce high construction costs.

Therefore the choice is made to propose a rubble-mound structure as offshore tsunami protection alternative. A very basic cross-section for an offshore barrier at -10m bathymetry line is presented in Figure 5-21.

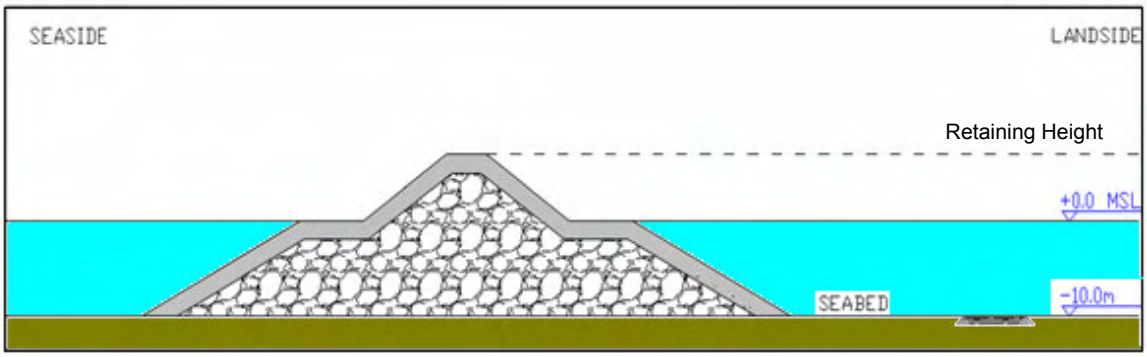

Figure 5-21 Basic cross section of an offshore tsunami protection at -10m bathymetry line.

The cost calculation in Appendix V is based on above cross section, with assumptions for the core material, dimensions, slope steepness, etc.

In Chapter 7 a more detailed cross section is presented, where these assumptions are checked with design calculations.

5.9.2.2 Basic cross section for onshore tsunami protection

Without further justification a basic cross section of an onshore structure is presented.

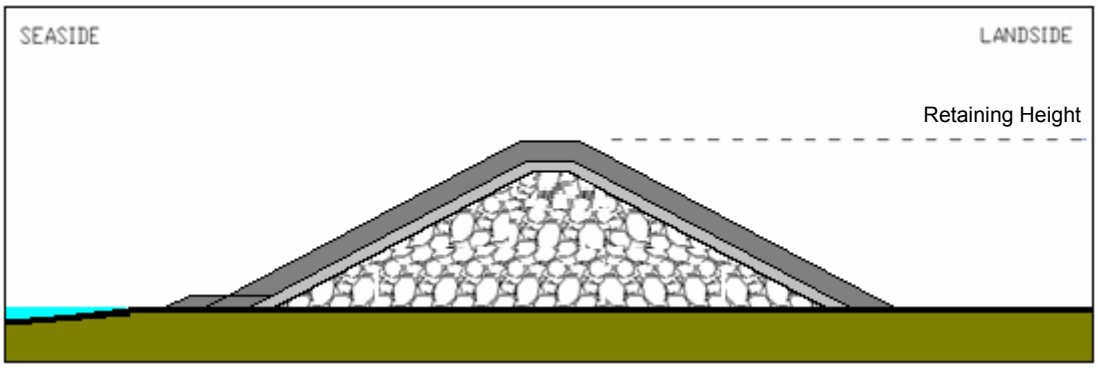

It consists of a sandy core covered by a geotextile. The upper layer is (not reinforced) concrete, founded on several layers of rubble mound.

This basic cross section forms the basis of the cost calculation in Appendix V.

5.10 SUMMARY

Three alternatives are developed, an offshore, coastal and inland tsunami barrier. The main alternatives and many sub-alternatives are modelled in a 2D-model. The results are expressed in an effectiveness-percentage, which represents the reduction of flooding compared to a situation without protection. By only looking at the freeboard (i.e. the visible part of the structure) the offshore barrier is more effective then the 'dry' barriers. The effectiveness of the three alternatives is depicted in one graph, see Figure 5-22.

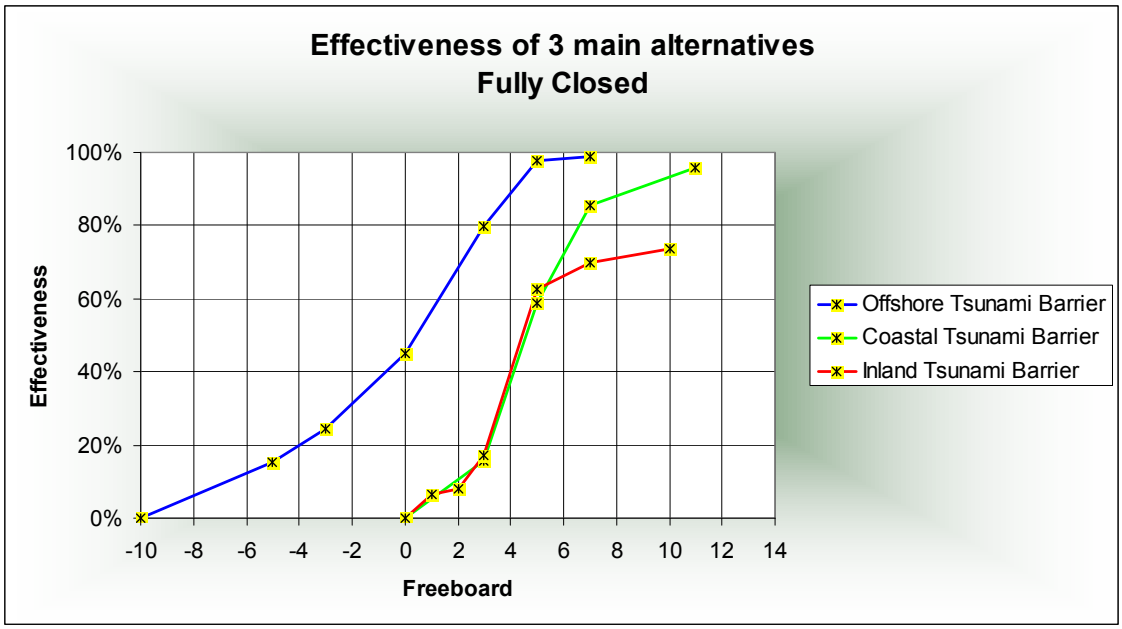

Figure 5-22 Comparison of effectiveness of the three main alternatives

Other aspects of the three alternatives were mentioned. The social impact, structure volume/costs, land acquisition, etc. are important input for the final assessment of the alternatives. This assessment is worked out in the next Chapter by means of a Cost Benefit Analysis (CBA) and a Multi Criteria Analysis (MCA).

'Innovative solutions' were assessed as not realistic and even the theoretical assumptions behind these ideas are found questionable. Two basic cross sections, based on 'traditional' hydraulic structures are proposed.

These cross sections form the basis for the cost calculation and assessment of the developed alternatives.

Chapter 6. ASSESSMENT OF ALTERNATIVES

6.1 INTRODUCTION

In the previous Chapter a wide range of possible structural measures is simulated. The results were presented as a relation between retaining height and effectiveness.

The effectiveness, expressed as a percentage of inundation-reduction, is a measure for the actual benefits of the structure. The more effective, the less damage is expected and the higher the benefits. This benefit can be compared with the costs to get an idea of the financial feasibility of the various alternatives. This chapter presents the Cost Benefit Analyses (CBA's) for all three alternatives and for various retaining heights. The question is:

Should one always build that structure with the highest benefits compared to the costs?

It is obvious that this question can not be answered by assessing financial aspects only. In the CBA, only (easily) quantifiable aspects are taken into account. But other, non-financial aspects are also at stake, or even of major importance. Extensive structures affect daily live and possibly disrupt social and economical development. These non-quantifiable or qualitative aspects are assessed with the help of a Multi Criteria Analysis (MCA). This results in a certain value for each alternative.

These two methods however, do not present the final answer. The final decision is a political and societal process rather then the outcome of technical evaluation methods. Besides facts and figures, people are at stake. Due to the Dec 2004 Tsunami hundreds of thousands people died. These deaths in itself can never be expressed in money. And neither can the emotional and social damage due to these deaths. The consequences of the disruption of society and the diminishing of a specific population group[11] induce long-term and indirect damage which is rather under-estimated then over-estimated.
Therefore, in case that costs are higher than the calculated benefits, it can still be a good choice to build a sound protection. A strong and visible structure can give an increased feeling of safety, increase liveability and consequently increase the value of the protected area.

6.2 ALTERNATIVES

The main alternatives that will be assessed are:

- An offshore tsunami protection at -10m water depth
- A coastal tsunami protection
- An inland tsunami protection

For each of these alternatives the assessments includes the entire range of modelled sub-alternatives and structure heights. The actual shape of the cross section is not part of this assessment.

[11] E.g. women and children were more severely hit than mature men

6.3 COST BENEFIT ANALYSIS

6.3.1 Introduction

In the model runs the Dec 2004 Tsunami was chosen as design tsunami. For this single event, the effectiveness of the structures was expressed in a percentage of inundation-reduction.
However, in a risk analysis, all possible events should be taken into account. By combining the frequency of all possible tsunami-events with the associated damage, the total risk for Banda Aceh can be derived. The total risk is defined as:

Total Risk = Probability x Consequences (i.e. damage)

Both the probability and the consequence depend on the tsunami height. A small tsunami will have a higher probability then a high tsunami, but the associated damage will be lower. Determining the total risk therefore requires an integration of all possible events multiplied with their associated damage.

A tsunami protection structure reduces the damage and consequently the risk. This yields a benefit, which is equal to all avoided damage; the damage associated with the design level, but also all smaller tsunamis.

On the other hand there is a remaining damage. A structure of 10m height will not protect against a 20m high tsunami. This remaining damage can be translated into a 'remaining risk' or 'residual risk', by taking the associated return periods into account.

Various alternatives are developed in the previous section. These alternatives have different effectiveness. A 5m high offshore barrier is not as effective as a 5m high coastal barrier. The construction costs of these alternatives are different.

The 'residual risk' for each protection alternative can be added by the costs. The result is a graph that depicts the total costs (damage + construction costs) for each alternative. The point of lowest costs is the optimal design level, from an economical point of view. All values are expressed in the Net Present Value.

Ultimately, the construction costs are compared with the benefits for this optimal design level (CBA). This results in a conclusion about the (financial) feasibility for each alternative.

It is stressed again that defining a safety standard is a political decision which should take into account other aspects and considerations as well. Nevertheless, a CBA provides valuable insight into the financial feasibility of tsunami protection.

For this analysis the following data is required (for Banda Aceh):

- probability of occurrence for tsunamis of different magnitude and the corresponding wave height (section 6.3.2 and 6.3.3)
- a relation between damage occurring for tsunamis with different wave height (6.3.4)
- cost analysis of the various structure-types for varying structure height (6.3.6)
- the effectiveness of measures in reducing the damage of a tsunami (Chapter 5)

The working principle of this analysis is depicted in Figure 6-2.

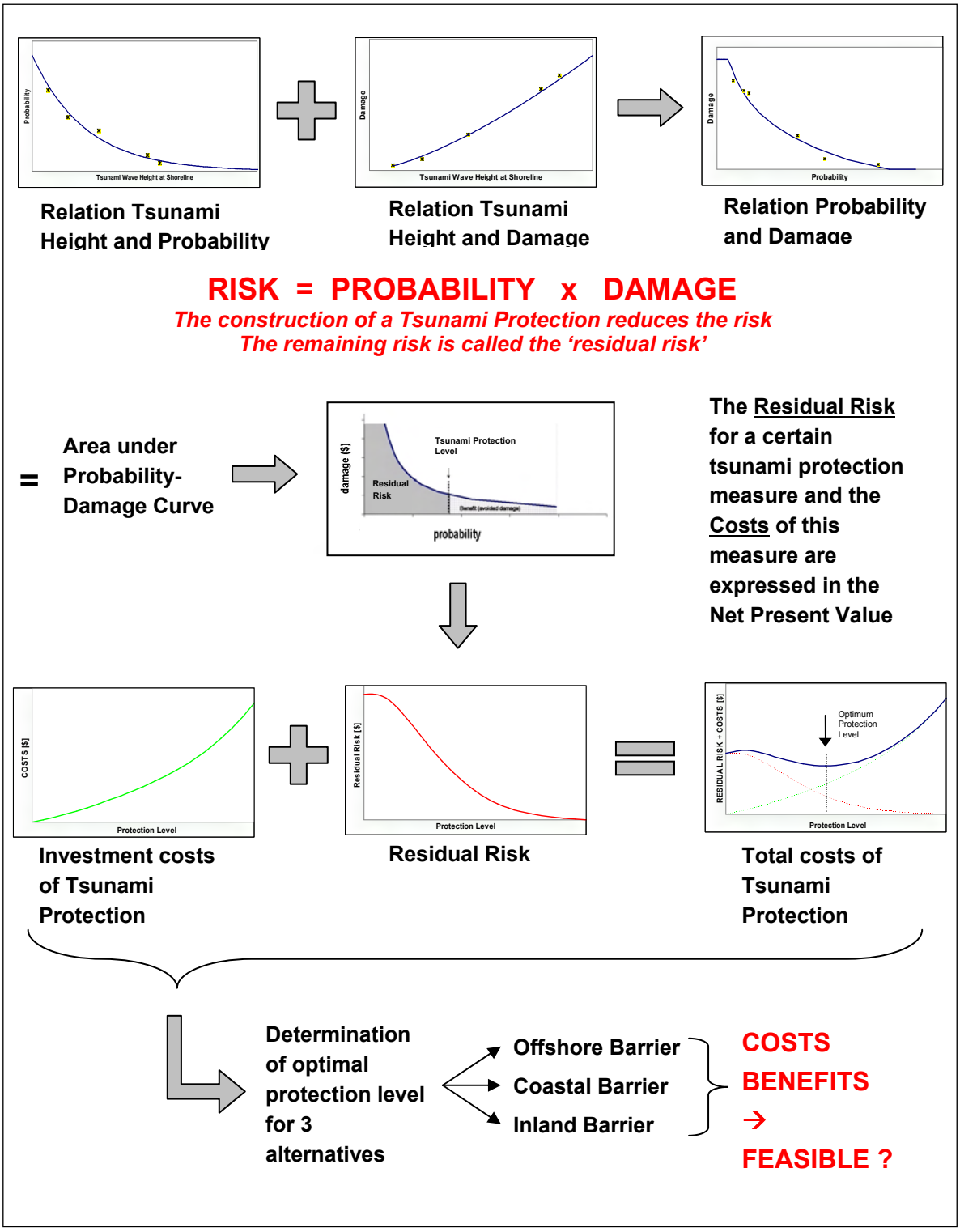

Figure 6-1 Working principle of Cost Benefit Analysis

6.3.2 Relation Tsunami Height and Probability

In Chapter 3, the probability of occurrence of tsunamis is treated. In Table 6-1 the estimates for the return periods for different tsunami events are listed. The magnitude is expressed in Richter scale.

Table 6-1: Estimated return periods along the Sumatra-Andaman fault line.

Magnitude	Return Period for one specific spot	Wave Height at the Shoreline (Model runs)	Damage [Billion USD]
7,5	100 YEARS	1,05	0,010
8	150 YEARS	2,36	0,149
8,5	200 YEARS	4,43	0,485
9	500 YEARS	7,95	1,090
9,5	1000 YEARS	8,51	1,273

The data is plotted in Figure 6-2 , together with a fitted power-function.

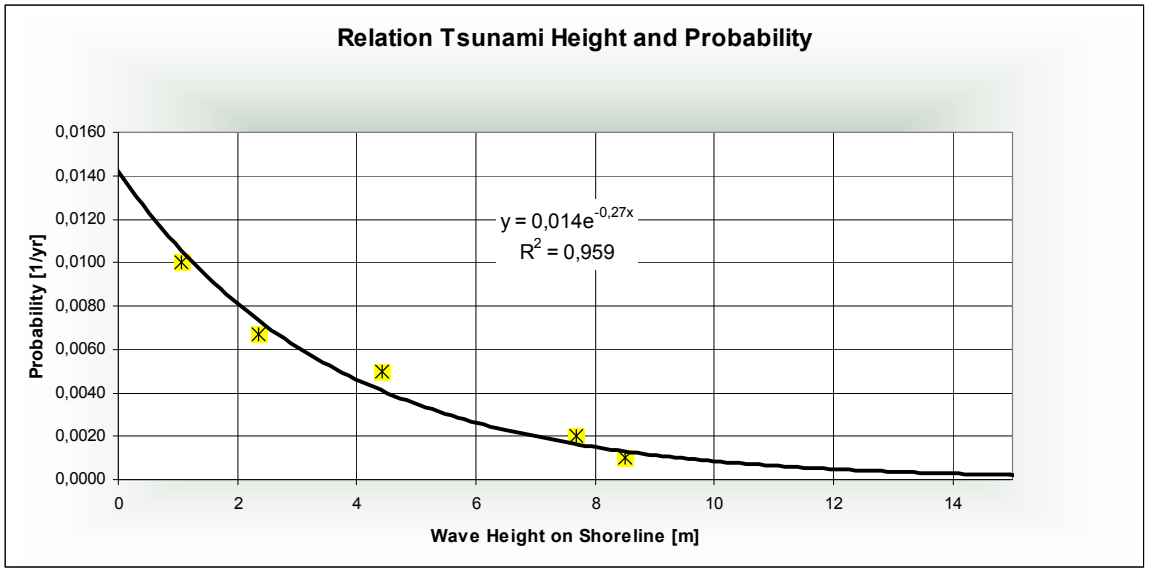

Figure 6-2 Relation Tsunami Height and Probability

The relation between probability of occurrence (P) and wave height (H) is approximated by:

$$P = 0{,}014 \cdot e^{-0{,}27H} \quad \text{or} \quad H = -3{,}7 \cdot \ln(71P)$$

6.3.3 Relation Tsunami Height and Damage

For all magnitudes the damage is calculated, based on the maximum inundation depth. The relation between damage and wave height is almost linear, as shown in Figure 6-3.

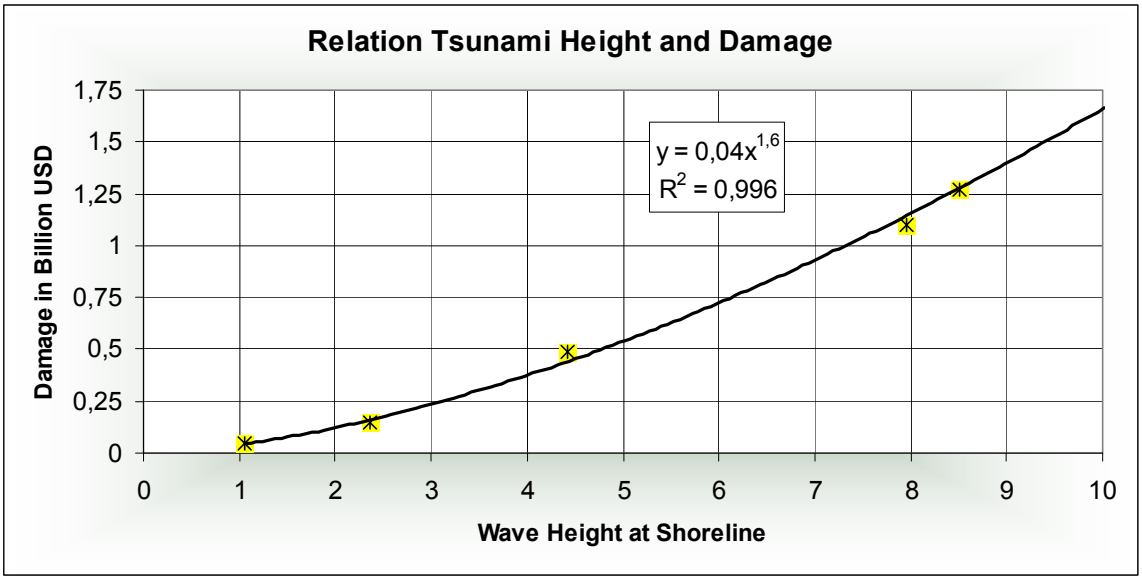

Figure 6-3 Relation between Tsunami Height and Damage

The relation between tsunami wave height (H) and damage (D) is approximated by:

$$D = 0{,}04 \cdot H^{1,6}$$

6.3.4 Relation Probability and Damage

The afore-derived equations can be combined to obtain the relation between damage and probability:

$$D = 0{,}32 \cdot Ln^{1,6}(71P)$$

See also Figure 6-4.

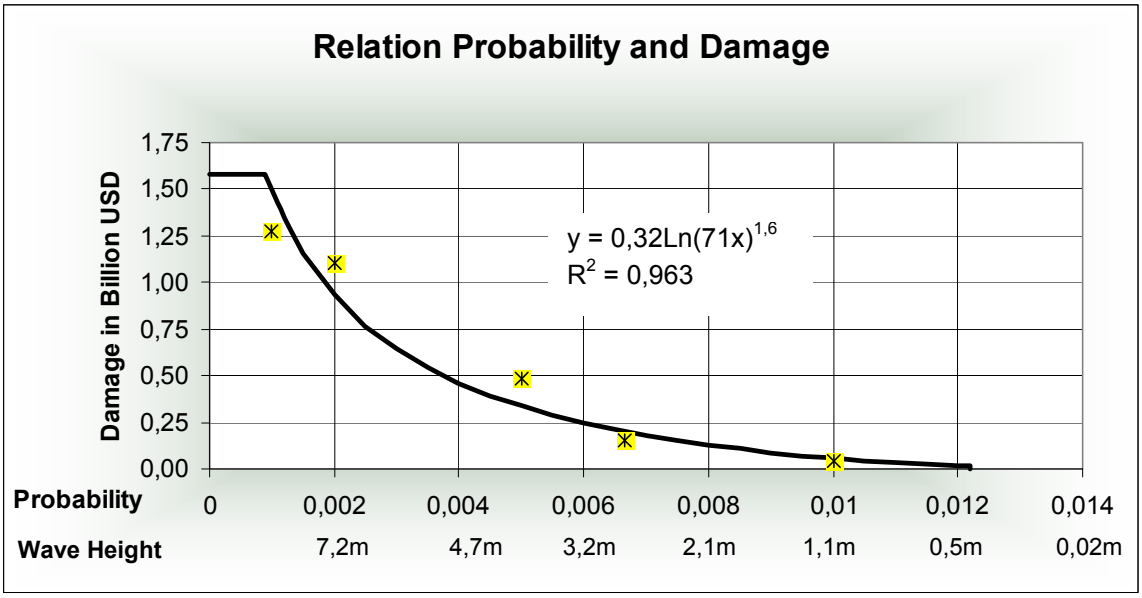

Figure 6-4 Relation between Probability and Damage. The total area under the graph is the total risk.

This 'Risk-area' is on the left hand-side limited to $1,557 Billion, as this is the maximum damage for Banda Aceh (see Chapter 4.4.3). On the right hand-side it is limited at 0,0123, as this probability is related to a tsunami wave height at the coast of 0,5m. It is assumed that the damage for a wave lower than 0,5m is negligible.

The total area under this graph is the total (annual) risk: $ 5.700.000 / year.

A protection measure will reduce this risk, depending on the provided protection.

6.3.5 Residual Risk of Tsunami Protection Alternatives

For reasons of simplicity, the term 'protection level' is introduced:

Protection level = the height of the tsunami wave, expressed in meter height at the coastline, which is stopped by a certain protection measure.

'To stop' means an effective reduction of the inundation volume in the protected area of at least 98% based on the 2D-model runs.

The prevented damage for each protection level can be derived by integrating the graph in Figure 6-4). When for instance the prevented damage is calculated for a protection level of 3,2m, the graph should be integrated from P=0,006 to P=0,0123:

$$PREVENTED\_DAMAGE_{Level=3,2m} = \int_{0,006}^{0,0123} \{0,32Ln^{1,6}(71P)\}dP \approx \$\ 620.000 \text{ / year.}$$

This prevented damage, or benefit, is on annual basis, since the probability is expressed in 1/yr.

So, building a protection scheme (offshore, coastal or inland) that can stop tsunamis with a wave height at the coast of 3,2m, will generate a yearly benefit of $620.000.
The remaining risk, or *residual risk* amounts to: $ 5.700.000 – 620.000 = $ 5.080.000 / year[12].

This *residual risk* is calculated for each protection level. The results are depicted in Figure 6-5. The higher the protection level, the lower the *residual risk* and the more *benefit* is created, since all tsunamis lower than that level will be stopped and contribute to the total prevented damage. Note that the residual risk and the prevented risk (benefits) together amount to $5.700.000.

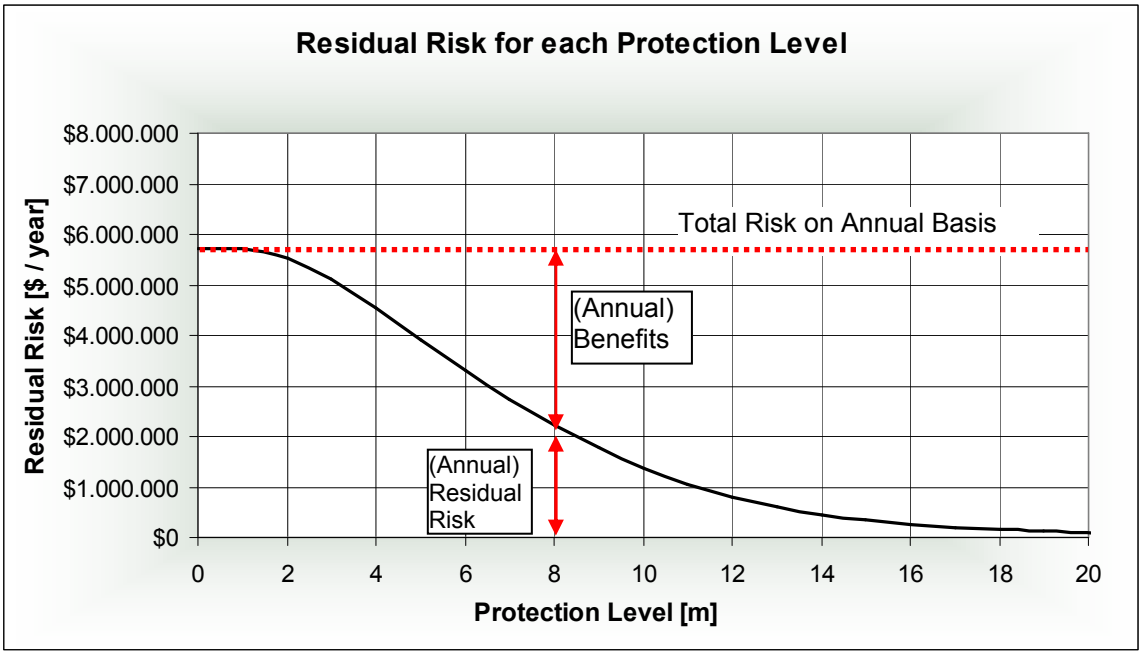

Figure 6-5 The residual risk and benefits (on annual basis) for each protection level[13]

Following the graph, the construction of a protection scheme against an 8m tsunami (and all smaller events!) will still induce a residual risk of 2,3 million USD (every year). The yearly generated benefit is 3,4 million USD.

This benefit is generated as long as the structure fulfils its function. For hydraulic structures a lifetime of at least 50years up to 100years is not uncommon. During this period, a yearly benefit of 3,4 million USD is generated. Two figures however, change the Net Present Value (NPV) of this money:

1. Discount rate δ

[12] *Note: In this calculation it is assumed that if the tsunami height exceeds the protection level, the structure will fail completely. However, depending on the design of the tsunami protection, there still can be a significant reduction of higher tsunamis. For reasons of simplicity, this favorable effect is neglected.*
[13] *Note: Because the damage for small tsunamis is very low compared to major tsunamis, the graph is almost horizontal for low values of the Protection Level. If the land-level is (far) below sea-level (e.g. The Netherlands) the damage for small events is comparable to that of major events.*

The Net Present Value of this income is decreased by the discount rate, which reflects the social view on how future benefits and costs should be valued against present ones. A value of 5-6% is chosen.

2. Growth rate g

The yearly benefit is based on the damage caused by the tsunami. However, this damage will increase with increasing economical growth. A rate of 5-6% is used.

With these rates, the Net Present Value can be calculated by:

$$NPV = \sum_{t=0}^{t=n} B \cdot \left(\frac{(1+g)}{(1+\delta)} \right)^n , \quad \text{with}$$

B = Yearly generated benefit
n = Time-span in years (50 á 100 yrs)
g = Growth rate
δ = Discount rate

Above mentioned rates have a great influence on the Net Present Value (NPV) of the total residual risk. Therefore, the NPV for varying discount rate (d), growth rate (g) and structure lifetime (L) is calculated. See Figure 6-6.

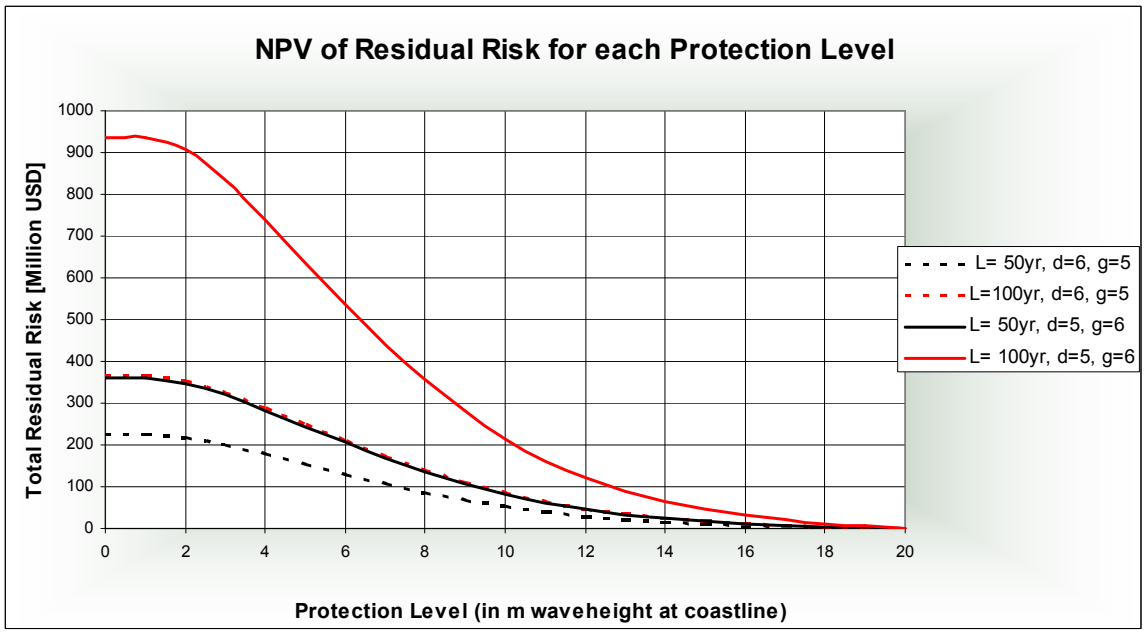

Figure 6-6 The Net Present Value of the residual risk for varying lifetime and discount/growth rates.

Changing from d=6% and g=5% into a discount rate (d) of 5% and a growth rate (g) of 6%, will decrease the residual risk with factor 1,6 for a lifetime of 50years and with factor 2,6 for a lifetime of 100years.

6.3.6 Investment Costs of Tsunami Protection Alternatives

In Appendix V an extensive cost calculation is made for three alternatives[14]. The results for the three main alternatives are presented in Table 6-2. Figure 6-7 gives an estimate for the costs for varying structure height.

Table 6-2: Cost figures for offshore, coastal and inland tsunami barrier

Structure	Total height	Costs	Amount
OFFSHORE BARRIER AT -10M, FREEBOARD 7M.	17 M	CONSTRUCTION COSTS	$ 1.200.000.000
		ADDITIONAL COSTS	$ 320.000.000
		MAINTENANCE COSTS	$ 17.000.000 / YEAR
COASTAL BARRIER	11 M	CONSTRUCTION COSTS	$ 425.000.000
		ADDITIONAL COSTS	$ 60.850.000
		MAINTENANCE COSTS	$ 4.250.000 / YEAR
INLAND BARRIER	8 M	CONSTRUCTION COSTS	$ 200.000.000
		ADDITIONAL COSTS	$ 67.500.000
		MAINTENANCE COSTS	$ 2.000.000 / YEAR

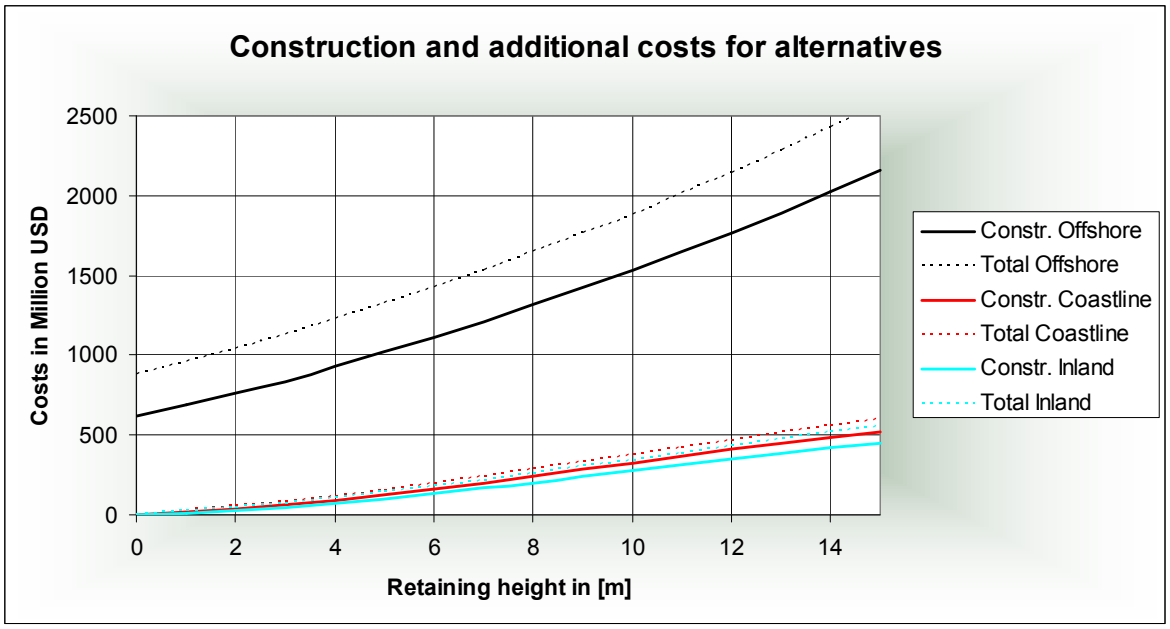

Figure 6-7 Overview investment (construction- and additional) costs for the main alternatives

The horizontal axis shows the retaining height. This can also be seen as the visible height of the structure. An offshore breakwater at -10m water depth with no retaining height, or visible height, still has construction costs around USD $600 million. These are the costs for constructing the under-water-part of the structure.

[14] This calculation is based on basic cross sections as presented in Appendix V. In Chapter 7, the design is changed with respect to slope steepness and slope protection. It was found however, that the difference in construction costs is less then 5%, which does not influence the findings of the feasibility study. (See section 7.6) The heights in Table 6-2 are chosen more or less random, as reference calculation. The optimal structure height is determined later.

6.3.7 Total costs of Tsunami Protection Alternatives

In the previous section the benefits are coupled with a certain protection level. This protection level was expressed in meters tsunami height at the shoreline.

This was done to ultimately account for the varying effectiveness of the three main alternatives. To stop a tsunami with 8m at the shoreline, an offshore barrier will have another required height then an inland wall. These differences were obtained from the model runs, see Figure 5-22. If regarding only full-reflecting structures, the following structure height are necessary to stop[15] a tsunami of 8m height at the coast line (8m protection level):

- Offshore structure: 5m → correction factor = (5 / 8) = **0,63**
- Coastal structure: 11m → correction factor = (11/ 8) = **1,4**
- Inland structure: 7m → correction factor = (7 / 8) = **0,88**

Compared with the wave height at the shoreline, the 'run-up' factors are 0.63, 1.4 and 0.88 respectively. With these factors it becomes possible to link the protection level with the associated structure height for the various alternatives. This height is related with the structure costs, see Figure 6-7. The estimation of these costs is presented in Appendix V.

Also for the investments, the Net Present Value (NPV) has to be calculated. The investments are split up in two parts:

1. Construction costs

For the NPV, the construction costs are equally distributed over three years, and the construction starts two years after the project start.

2. Maintenance (1% of construction costs)

The maintenance costs (*M*) have to be paid each year. The NPV is calculated by:

$$NPV = M \cdot \sum_{t=0}^{t=n} \left(\frac{1}{1+\delta} \right)^n \qquad \left(\approx \frac{M}{\delta} \text{ for large } n \right)$$

with the costs being paid after completion of the structure. A discount rate $\delta = 5\%$ is used. For each level of protection, the NPV's of the required investments are calculated. The values for the three variants are depicted in Figure 6-8.

[15] *'to stop' means an effective reduction of the inundation of at least 98% based on the 2D-model runs. For the inland wall this can not be achieved, since the sea-side area will be inundated independent of the structure height. A reduction of 98% for the inland structure therefore refers to the reduced inundation of the protected landward area of the structure. The effect of the unprotected area is expressed in a reduced benefit of the inland wall.*

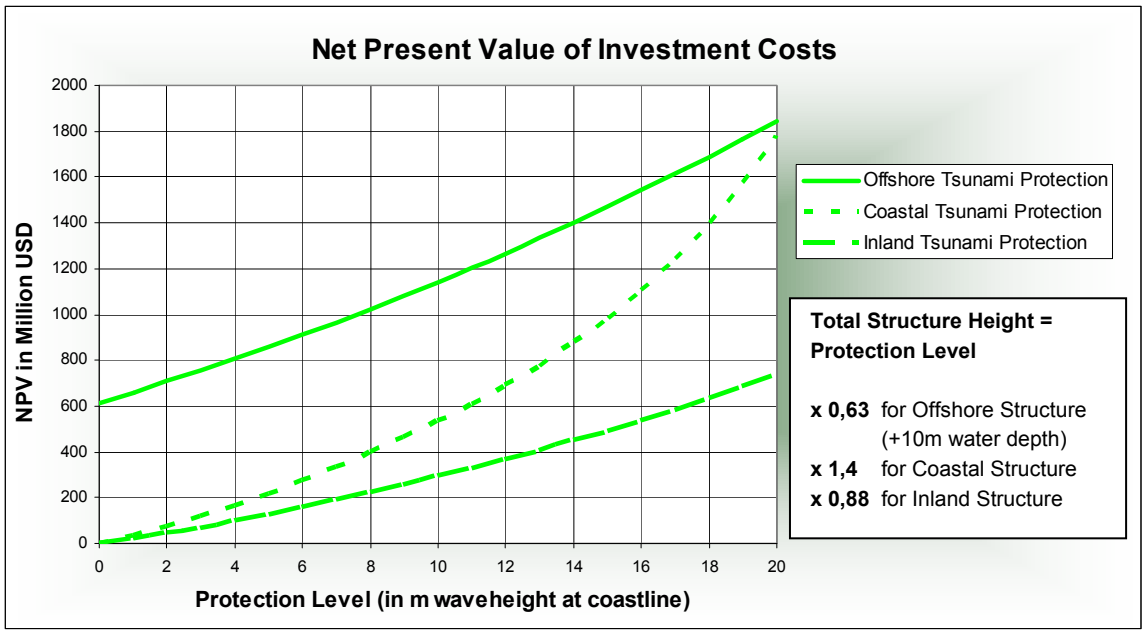

Figure 6-8 Net Present Value of Investment Costs (3 Alternatives), d=5%[16]

To obtain de total costs induced with a certain protection measure and a certain protection level, the *residual risk* is plotted together with the construction costs. The residual risk is based on a lifetime of 100years, a discount ratio of 5% and a growth ratio of 6%. Note that this is the most favourable assumption for the benefits. These two costs (both corrected for their NPV) together form the total costs of tsunami protection.

Now, the optimal protection level is defined as the point where the total costs are minimal. This optimum is an economic optimum, and only determines the point where the total costs of construction, maintenance and remaining damage due to exceeding tsunamis are minimal. The optimal level in societal or environmental sense can be different.

This economically optimal level is determined separately for the three main alternatives.

6.3.7.1 Optimal Protection Level; Offshore Tsunami Protection

For the offshore barrier, the costs and the sum are plotted in Figure 6-9.

[16] *By coincidence, the total NPV-value for the construction and maintenance costs for d=5%, approximately equals the (plain) construction costs as presented in Figure 6-7.*

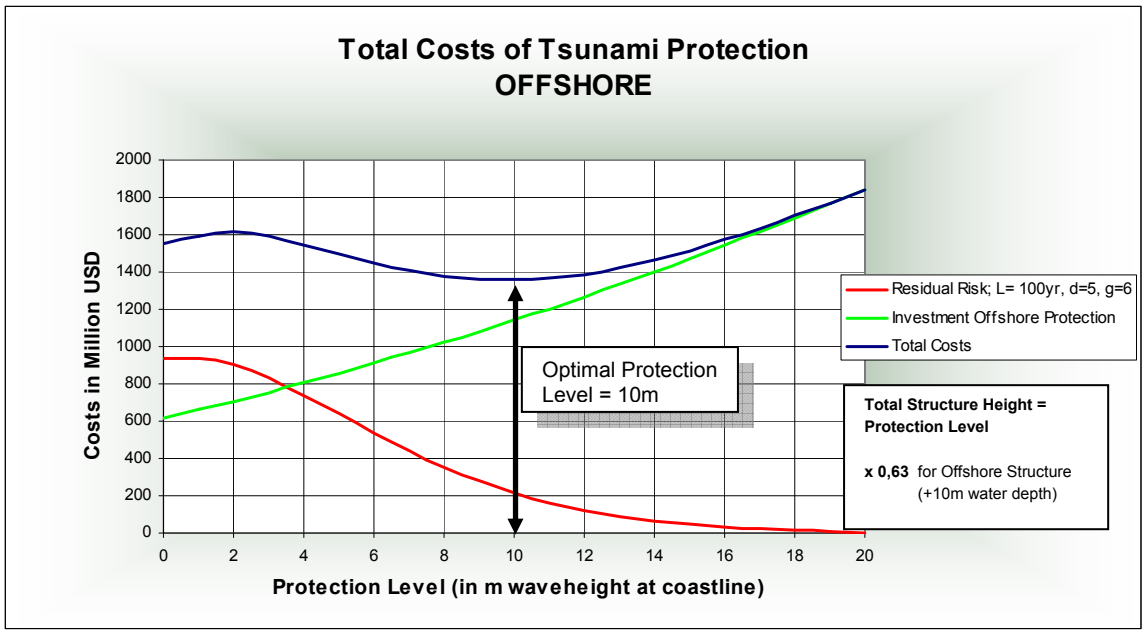

Figure 6-9 Total costs of Tsunami Protection; Offshore

The total costs show an increase for low values of the protection level. This is caused by the assumption that tsunami waves smaller then 0,5m at the coast line have zero damage, and that the damage is slowly increasing for heights up to 2m. The investment costs however increase in this region, which causes the total costs to increase slightly initially.

For offshore tsunami protection at 10m water depth, the optimal protection level is found at 10m.

This equals an optimal structure height of: 10m + 0,63*10	=	16,3m
The investment (NPV of construction and maintenance) costs are:	=	**$ 1140 Million**
The total risk during a lifetime of 100 year with d=5%, g=6%	=	$ 935 Million
The residual risk for a protection level 10m	=	$ 220 Million -
The prevented risk in this period (i.e. the benefits)	=	**$ 715 Million**
Profit = Benefits - Investment Costs = 715 - 1140	=	**- $ 425 Million**

Even at the optimal protection level, construction of an offshore tsunami protection with a lifetime of 100 years, will induce a net loss of 425 Million USD.

For less favourable growth and discount ratios and smaller lifetimes (see Figure 6-6), no minimum is found in the total costs for protection levels higher than 0m. In these cases, no protection (Protection Level = 0), generates the smallest loss. Doing nothing is the cheapest option.

6.3.7.2 Optimal Protection Level; Coastal Tsunami Protection

The same analysis is done for the coastal alternative. The results are presented in Figure 6-10.

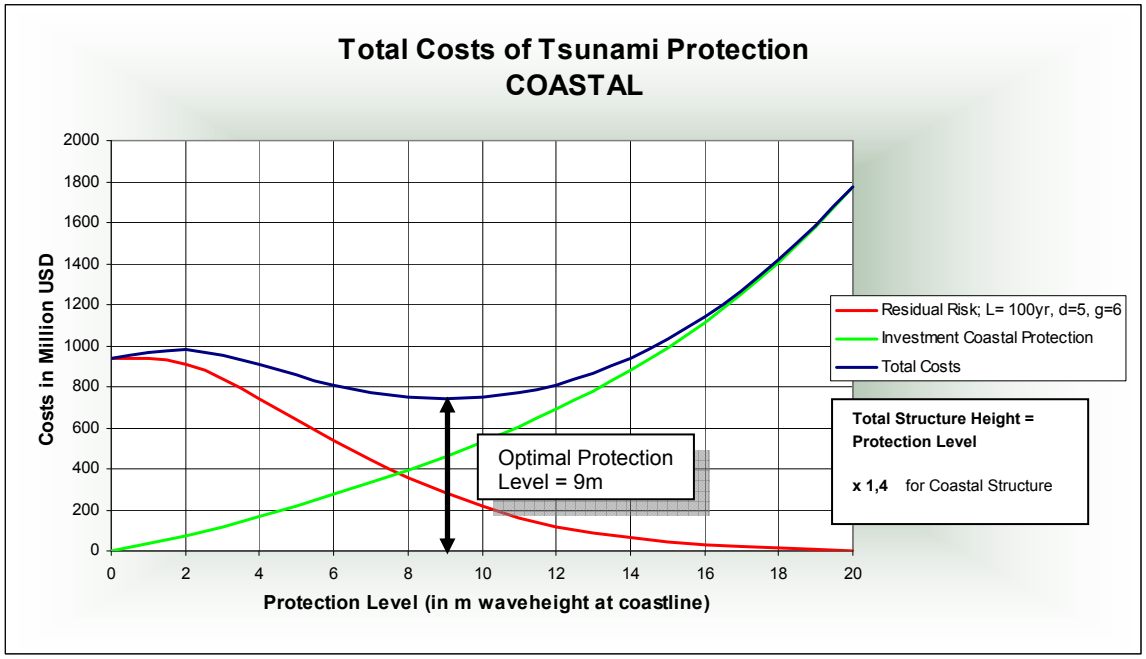

Figure 6-10 Total costs of Tsunami Protection; Coastal

.

For coastal tsunami protection, the optimal protection level is found at 9m.

This equals an optimal structure height of: 1,4 * 9	=	12,6 m
The investment (NPV of construction and maintenance) costs are:	=	**$ 461 Million**
The total risk during a lifetime of 100 year with d=5%, g=6%	=	$ 935 Million
The residual risk for a protection level 10m	=	$ 280 Million -
The prevented risk in this period (i.e. the benefits)	=	**$ 655 Million**
Profit = Benefits - Investment Costs = 655 - 461	=	**+ $ 194 Million**

At the optimal protection level, construction of a coastal tsunami protection, with a lifetime of 100years, will induce a net profit of 194 Million USD.

For less favourable growth and discount ratios and smaller lifetimes (see Figure 6-6), no minimum is found in the total costs for protection levels higher than 0m. In these cases, no protection (Protection Level = 0), generates the smallest loss. Doing nothing is the cheapest option.

6.3.7.3 Optimal Protection Level; Inland Tsunami Protection

The analysis for the inland alternative is somewhat more complicated. The analysis differs from the previous ones on the following points:

- Because the area seaward of the inland wall is not protected, the economic value of the protected area is smaller. A protection measure will therefore have a lower possible benefit. Consequently, the residual risk (the red line, Figure 6-11) is lower than for offshore and coastal alternatives, where the economic value of the entire city is at stake.
- Thereby, due to an inland structure the inundation will be higher in front of the wall. A small tsunami (let's say 1m) will be reflected by the inland structure and induce higher inundation at the seaside area (roughly 2m), then without structure. The total damage will increase for small tsunamis in case of protection and consequently, the residual risk will increase slightly for low values of protection level.

This results in another relation between the residual risk and protection level. The total costs for inland tsunami protection is depicted in Figure 6-9.

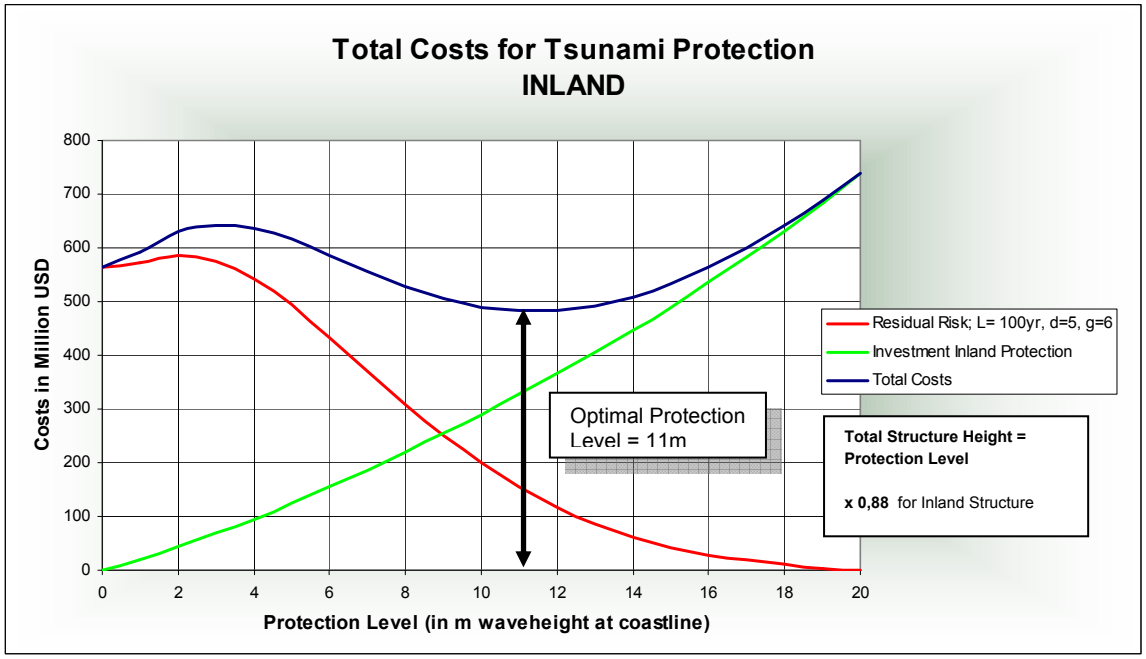

Figure 6-11 Total costs of Tsunami Protection; Inland. Note that the scale is different from the previous 'total costs' figures.

For inland tsunami protection, the optimal protection level is found at 11m.

This equals an optimal structure height of: 0,88 * 11	=	9,7 m
The investment (NPV of construction and maintenance) costs are:	=	**$ 327 Million**
The total risk during a lifetime of 100 year with d=5%, g=6%	=	$ 570 Million
The residual risk for a protection level 10m	=	$ 155 Million -
The prevented risk in this period (i.e. the benefits)	=	**$ 415 Million**

Profit = Benefits - Investment Costs = 415 - 327 = **+ $ 88 Million**
At the optimal protection level, construction of a coastal tsunami protection, with a lifetime of 100years, will induce a net profit of 88 Million USD.

For less favourable growth and discount ratios and smaller lifetimes (see Figure 6-6), no minimum is found in the total costs for protection levels higher than 0m. In these cases, no protection (Protection Level = 0), generates the smallest loss. Doing nothing is the cheapest option.

6.3.8 Conclusion CBA

The analysis carried out in this paragraph showed that only under very favourable circumstances (structure lifetime 100 years, discount ratio 5%, growth ratio 6%) an optimum protection level could be defined.

For other ratios (lifetime 50 years, d=6%, g=5% and combinations) no positive return is obtained the losses only increase for increasing protection level. Thus, the smallest loss would be obtained by a protection level of 0m, i.e. doing nothing. This accounts for all alternatives.

The parameters used in this Cost Benefit Analysis are highly sensitive and influence the benefits significantly. Even for standard life-times for hydraulic structures of 50year, it is impossible to present reliable discount and growth rates. For the 100-year analysis, the situation is even more precarious.

Despite these restrictions, it is clear that from an economical point of view the coastal and inland walls are more viable than offshore alternatives. This is due to the high construction costs involved with offshore works.

With an expected structure lifetime of 100years, a discount of 5% and a growth of 6%, the optimal protection levels for the three main alternatives, and the associated profit, become:

Offshore Tsunami Protection
- Optimal structure height 16,3 m
- Profit in entire lifetime **- $ 425 Million (Loss)**

Offshore Tsunami Protection
- Optimal structure height 12,6 m
- Profit for entire lifetime $ **194 Million**

Offshore Tsunami Protection
- Optimal structure height 9,7 m
- Profit for entire lifetime $ **88 Million**

As mentioned in the start of this paragraph, the analysis was only done for ‘full-reflecting’ structures. It was assumed that in case of significant overtopping (>2%), the damage would be related to a base-case situation. This assumption is rather conservative, as low-crested structure

surely will reduce the impact and damage of higher waves. Especially for offshore structures it was concluded from the model runs, that lower freeboards show significant reduction in inundation volume. This fact will be in favour of the economical feasibility of the alternatives (the prevented damage level will increase), but the highest advantage would be obtained for the offshore structure.

Although a net return is calculated for the coastal and inland alternatives, one should realize that the used parameters are quite favourable. Even with these parameters, an offshore structure is not feasible in economic sense. Coastal and inland alternatives perform better.

Finally, the definition of the safety level and the choice for the means of tsunami protection are a political decision, which should take into account other aspects and considerations as well. Some of these aspects are assessed with the help of a Multi Criteria Analysis which is elaborated in the following paragraph.

6.4 MULTI CRITERIA ANALYSIS

To account for non-quantifiable (or hardly-quantifiable) aspects of tsunami protection alternatives, a Multi Criteria Analysis (MCA) is used in addition to the CBA. This MCA gives insight in the value of different tsunami-protection options. The question answered by the MCA is:

Suppose that a structure is built, what solution is, independent of its efficiency in tsunami-reduction, preferable when looking at the consequences of the structure itself?

In the MCA a value or score is attributed each alternative on basis of selected criteria. The methodology of the MCA is further explained in Appendix IV. The results and interpretation are presented in this paragraph.

6.4.1 Criteria

In the MCA the following criteria have been used:

Reliability

The performance of the structure in case of an (extreme) tsunami event depends on the reliability of the structure. The more complicated, the less reliable the structure is. So, a structure without gaps (thus gates, which have to be closed in case of a tsunami) is more reliable than a structure with gaps. For offshore structures the reliability is high compared to inland structures. This is based on the assumption that the current velocities are less offshore then at the coast or inland (steepness of the wave). The lower the structure, the less reliable, since a overtopping tsunamis induce much higher loads on the structure (stability of the rear-side) then fully reflected tsunamis.

Morphological consequences

The protection against tsunamis could induce changes in natural coastal processes. The alongshore and cross-shore currents can be changed or even blocked, causing sedimentation or erosion. Near river mouths, the change in alongshore currents can cause sedimentation of the

river mouth. The cross shore sediment transport only takes place in the active zone, which lies around the 4m bathymetry line in the Banda Aceh Region.

Environmental consequences
Changing or blocking existing currents can also change the water exchange nearby the coast. The water quality may become poor, because the retention time increases. Besides of that many fish ponds exist inland of the coastline. The productivity of these nurseries depends on the exchange of tide.

Social consequences
The presence of a large structure along the entire coast or inland of the coast will affect the daily life of people. The number of connections with the sea is reduced. For an inland barrier, only a few connections with the other part of the town remain. Besides of this, a high wall will prevent circulation of fresh air.

Maintenance
The structure is designed for extreme events, which probably means that it isn't tested for tens of years. However, in case of an extreme event, it has to function properly. Because maintenance requires a lot of attention and spare parts, a complicated structure is considered negative.
Although the main structure is not complicated (a sand/gravel body), gates and crossing with rivers/roads make it complicated. However, maintaining an offshore structure is more difficult then a structure on land.

Land acquisition
Land is scarce. Land acquisition is a complicated issue.

* Costs and damage
Obviously, the most important parameters are the costs of the structure in relation to the provided protection. Because it is hard to compare a value (like social acceptance or environment) with costs, this parameter is calculated separately; the total value of the structure (based on above described criteria) is then compared to the total costs and damage. This results in a certain *value for money* figure.

The damage caused by a tsunami depends on the inundation. The damaged is calculated as described in Paragraph 5.3.2.

6.4.2 Scores

In the MCA the different criteria are evaluated by attribution of a score. The scale is from 1 to 9, with:

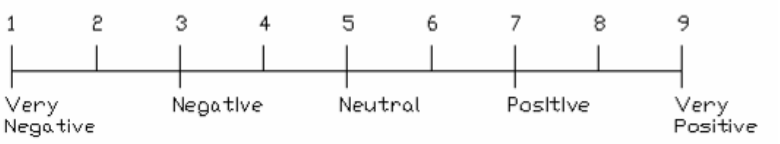

The scores for each alternative, based on the selected criteria are presented and discussed in Appendix IV.

6.4.3 Weighting factors

Weighting factors are attributed to each criterion to differentiate the importance of the various criteria. The morphological consequences, for example are less important then the social consequences.
The score of the individual criteria is multiplied by the weighting factor to obtain the final result of the MCA. See Appendix IV to know how the weighting factors are derived.

The results and a short reasoning are:

Reliability	5 →	Important because the structure is designed for extreme events and failure means high damage and loss of live
Morphological consequences	1 →	Morphological consequences can be controlled by sand nourishment of dredging. This criterion is of minor importance
Environmental consequences	2 →	The environmental issues can be controlled
Social consequences	6 →	Very important
Maintenance	4 →	The presence of a structure can affect the quality of life and as a consequence of that the development of the whole city
Land acquisition	3 →	The difficulties with land acquisition can affect the feasibility of the structure

6.4.4 Alternatives

The alternatives which are evaluated in this Multi Criteria Analysis are the alternatives as described in Chapter 5.

6.4.5 Results

In Appendix IV, the complete Multi Criteria Analysis is described, the attributed scores included. The costs are presented in Appendix V.

The weighted scores for each alternative are presented in Figure 6-12.

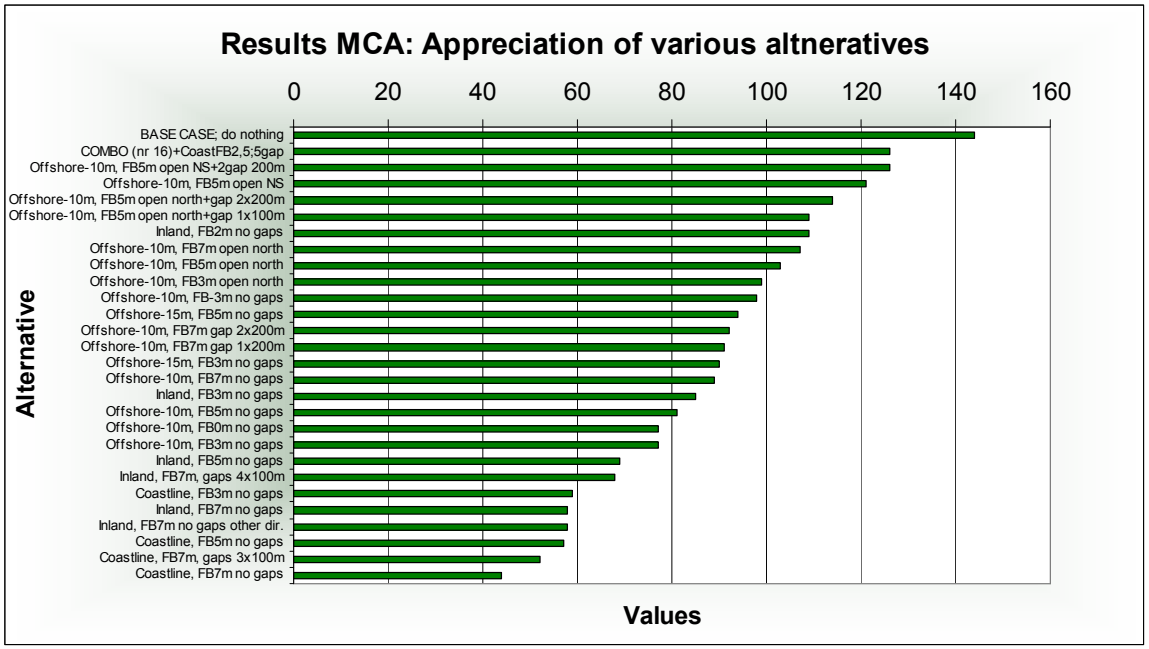

Figure 6-12 MCA results: the appreciation of various structures

The Base Case (i.e. the situation without structural measures), gives the highest value. Although this seems weird, it is logical. This analysis valuates for each alternative to what extend it causes negative consequences for society *except for its effectiveness in tsunami reduction.* Doing nothing is not implying social, environmental, morphological consequences and results therefore in the highest value. Above results mainly represent the social appreciation of the measures.

In general, offshore alternatives have much higher value than coastal and inland alternatives. This is mainly due to the negative impact of high structures on land due to blocking views and connections.

As mentioned before, the MCA primary adds up the *value* of various alternatives. Of course, selection of an alternative only on this basis is not sufficient. On the other hand, selection of an alternative only based on *costs and benefits* (CBA) is not fair either, because non-financial aspects (for instance, the social acceptance of a 7m high wall) can be of significant importance and directly influence the social feasibility of a tsunami barrier.

So, both methods have limitations. It is tried to combine the benefits of both methods. The value for each alternative, provided by the MCA is compared to the costs and damage as used in the CBA. This provides some feeling about the *value for money* ratio of each individual alternative.

The MCA-value is therefore simply divided by the costs. This results in a value/cost ratio for each alternative. A high value/cost (VC) ratio represents an alternative where a high value is acquired for a relatively low price:

$$VC\text{-}ratio = Value / Costs = Value / (Construction\ Costs + Damage)$$

Costs+Damage

The costs do not only represent the construction costs of the structure but also damage as caused by a Dec2004 Tsunami event. This damage is obtained from the 2D Tsunami Model runs, where the inundation volume is used as an indication for the resulting damage (see Chapter 5). The reference case is the Dec2004 Tsunami without any structural measure, where the resulting damage was $1,13 Billion. The construction costs are presented in Figure 6-7. The costs estimation is presented in Appendix V.

Remark

It should be noted that this straight comparison of values and costs is arbitrary. It suggests that doubling the value of the structure, allows doubling the costs of the structure. However, this can not be concluded from this analysis. Tsunamis do not only inflict economical damage but also personal damage. Therefore, the final conclusion regarding the value of a certain alternative in relation with the costs and damage should not be drawn by economists but by the involved people themselves.

To account for this sensitivity, two VC-ratios are presented:

1. Value/cost ratios based on the economical damage due to **1** Dec2004 tsunami-events during the lifetime of the structure
2. Value/cost ratios based on the economical damage due to **2** Dec2004 tsunami-events during the lifetime of the structure

An overview of the (weighted) scores, constructions costs, damage and resulting scores is given in Appendix V.

The value/cost ratios based on the economical damage due to **1** Dec2004 tsunami-events during the lifetime of the structure, is presented below.

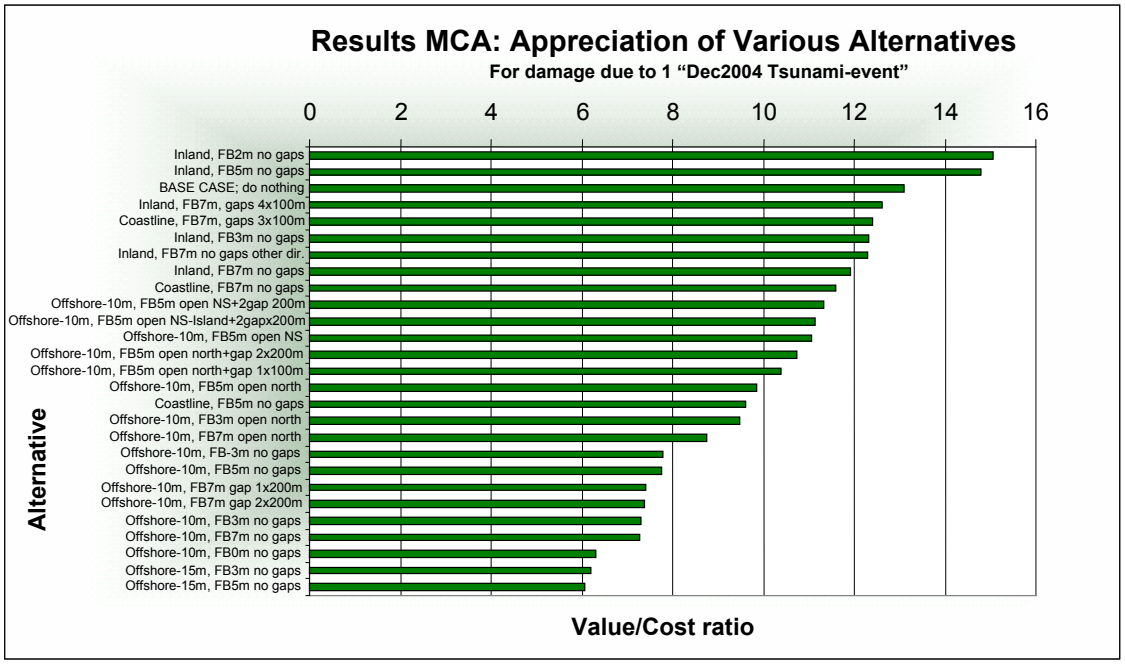

Figure 6-13 VC-ratio based on 1 Dec2004 Tsunami event

Under these conditions, building on land, on the coast or even doing nothing gives the highest value with respect to the costs. Offshore solutions are simply too expensive to justify the damage.

However, increasing the damage by factor 2 changes the picture completely. See Figure 6-14 below.

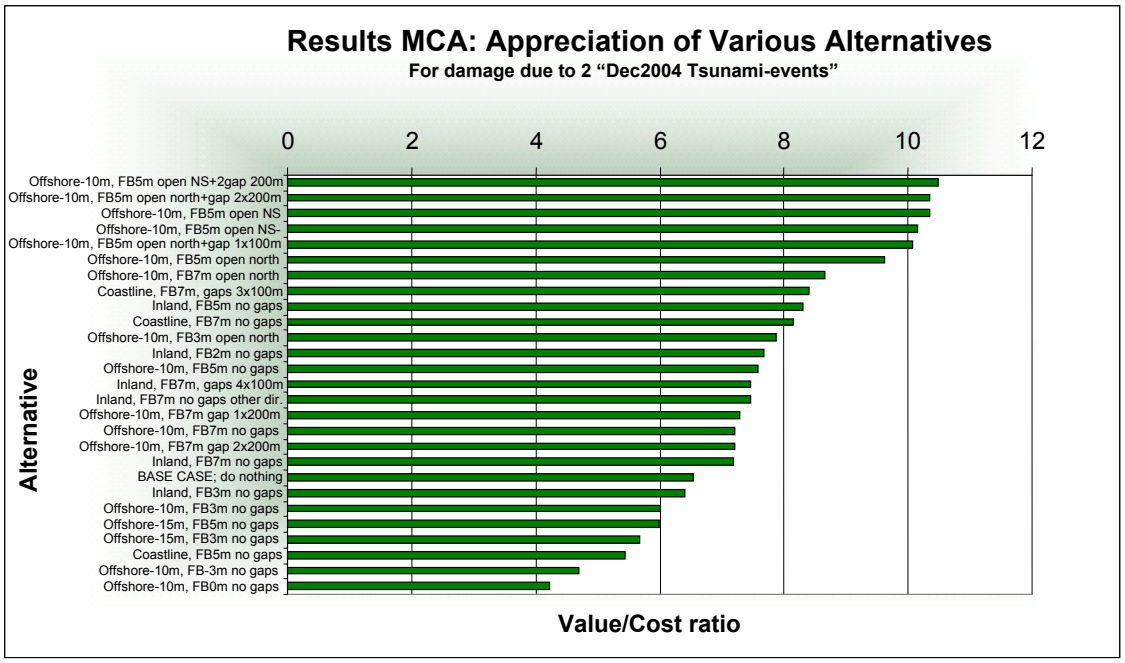

Figure 6-14 VC-ratio based on 2 Dec2004 Tsunami events

In this case offshore solutions at 10m water depth become preferable. The damage due to the tsunamis is evaluated higher than the construction costs of offshore solutions. Again, this does not necessarily mean that the damage really **is** higher, but that it is evaluated higher.

6.4.6 Conclusion MCA

This MCA made clear that purely based on the value of the alternatives, the offshore solutions have strong preference above structural measures on land. This is mainly due to the high social impact of high structures on land.
The fact that an offshore structure has much less impact on the every-day live was the most decisive criterion (social consequence). But also the lower steepness of the wave front offshore, and consequentially, the lower impact on the structure increases the value of these solutions (reliability). Of lower importance, but still considerable, was the advantage that for offshore construction no land acquisition is required.

However, when the value is compared to the total costs (construction costs + damage) the situation changes. If the damage due to tsunamis is evaluated as equal to the Dec2004 tsunami, inland structures or doing nothing becomes preferable. When damage is evaluated higher (2x) offshore solutions have the highest ranking.

6.5 SUMMARY AND CHOICE

The Cost Benefit Analysis showed that from an economical point of view the coastal and inland walls are more feasible than offshore alternatives but probably will still generate negative returns. Only under favourable conditions, a positive return can be expected in case of inland and coastal barriers. Offshore solutions are most expensive. This is due to the high construction costs involved with offshore works.

The used parameters have a high influence on the outcome of this method. Growth rates for 100years are not reliable anyhow. The positive effect on economical growth when Banda Aceh is well-protected is not taken into account. The assumption that if a tsunami is significantly higher than the structure height, the damage will be equal to a situation without protection is not realistic either. These points are in favour of the economical feasibility, especially for offshore barriers.

To account for the social consequences of large structures, a Multi Criteria Analysis was carried out. Logically, the offshore barriers have higher appreciation than structures on land, because land structures affect the daily live and development of the city. The MCA-values (although discussable) were compared to the cost to give some idea about the *value-for-cost* ratio. It was shown that when the (appreciation of the) damage due to tsunamis equals two Dec2004 tsunamis during the structure lifetime, offshore solutions still are preferable.

Conclusively, in economical terms, the low frequency of tsunamis and the rather low damage do not justify tsunami protection structures. Significant tsunamis require high structures, which will induce high costs. This accounts mostly for offshore barriers.
On the other hand, tsunamis inflict besides economical damage also personal damage. Due to the Dec2004 tsunami, almost 70.000 people died in Banda Aceh. Tsunamis affect the core of

society. The deaths, the physical and emotional suffering, the disruption of society and the remaining uncertainty about future tsunamis are all 'costs' which can not be simply added to the equation. Therefore, the final decision about tsunami protection is a political or societal process rather then the outcome of this analysis and should be made by the people involved.

Supposed that a positive decision is made, the MCA clearly indicates that offshore solutions will be the most feasible means of tsunami protection, from a social point of view. The presence of high structures on land (>7m), will affect the interaction between land and sea, ultimately affecting future economical development. It affects views and hence the aesthetical value and land use values in its vicinity. Thereby, tsunami height, run-up, velocities and impact are smaller in offshore conditions.

Another (soft) option would be to implement a Tsunami Early Warning System (TEWS). At this moment, a TEWS is being developed for Banda Aceh, in combination with a design for a network of sound refuge buildings. This will reduce the number of deaths in case of another tsunami. However, such systems do not prevent against economical damage. The anticipated reduction in tsunami victims could also be less, because:

- the fault-line is located very close to Banda Aceh, leaving little time left for refuge[17]
- the awareness of tsunami threat will become less in time,
- the proper functioning of tsunami early warning systems will be doubtful after several years: who is responsible for testing and organizing drills?

For these reasons it is decided to elaborate further on the design of an offshore tsunami barrier, despite the negative cost-benefit ratio. The design of this structure is worked out in Chapter 7.

[17] *The 2004 Tsunami hit the city approximately 20minutes after the earthquake.*

Chapter 7. DESIGN TSUNAMI BARRIER

7.1 INTRODUCTION

The previous Chapters dealt with various alternatives for a Tsunami Protection Barrier for Banda Aceh. It was assumed that offshore solutions, despite their high construction costs, are the only realistic means for tsunami protection. Protection against considerable tsunami heights requires high structures that will severely affect daily life in the city in case they are built on land or on the coastline.

In this Chapter a design will be presented for an offshore barrier at -10m bathymetry line. Various choices have been made regarding materials, armour layers, slopes, heads, etc. These choices are supported by calculations that are presented in Appendices VI to IX.

7.2 DESIGN CONSIDERATIONS

The design of the offshore barrier, both in plan view and cross-section, is based on a number of considerations:

- The structure's main function is to protect the entire city of Banda Aceh against significant flooding due to tsunamis. It should allow sufficient navigation from and to open sea. It should allow water refreshing by circulation. Latter criterion leads to the implementation of gaps/openings.
- The design tsunami is the Dec2004 Tsunami. If possible, the design should be made in such a way that higher tsunamis can be survived without significant damage.
- Due to the long life-time, the expected damage due to regular events should be minimized. (low damage number)
- Prior to a tsunami the structure is most likely attacked by an earthquake. The higher the earthquake the higher the expected tsunami. It is therefore evident that instability and collapse due to earthquakes may not occur, as there is no time to repair the damage before tsunami arrival (about 15-20min for Banda Aceh).
- Because the structure aims to protect against extreme events, medium damage is allowed due to the design tsunami. However, the structure should keep its primary retaining function. This leads to less strict damage criteria under tsunami attack then under regular wave attack.

These considerations will be translated in actual choices for the preliminary design in both plan view and cross section.

7.2.1 Plan view

In plan view, the following considerations are at stake:

- number and width of gaps
- location and configuration of the barrier

In order to reduce the hindrance for navigation and allow sufficient circulation of the enclosed sea-area, it is important that the barrier has a sufficient number of gaps. These openings however also allow water inflow in case of a tsunami. Various alternatives and configurations have been modelled. Finally, it was concluded that a small number of gaps in the barrier does not lead to excessive inundation of the hinterland. An open north and south also has limited effect on the final inundation volume. Based on the results of this modelling, a final plan view is presented. See Figure 7-1.

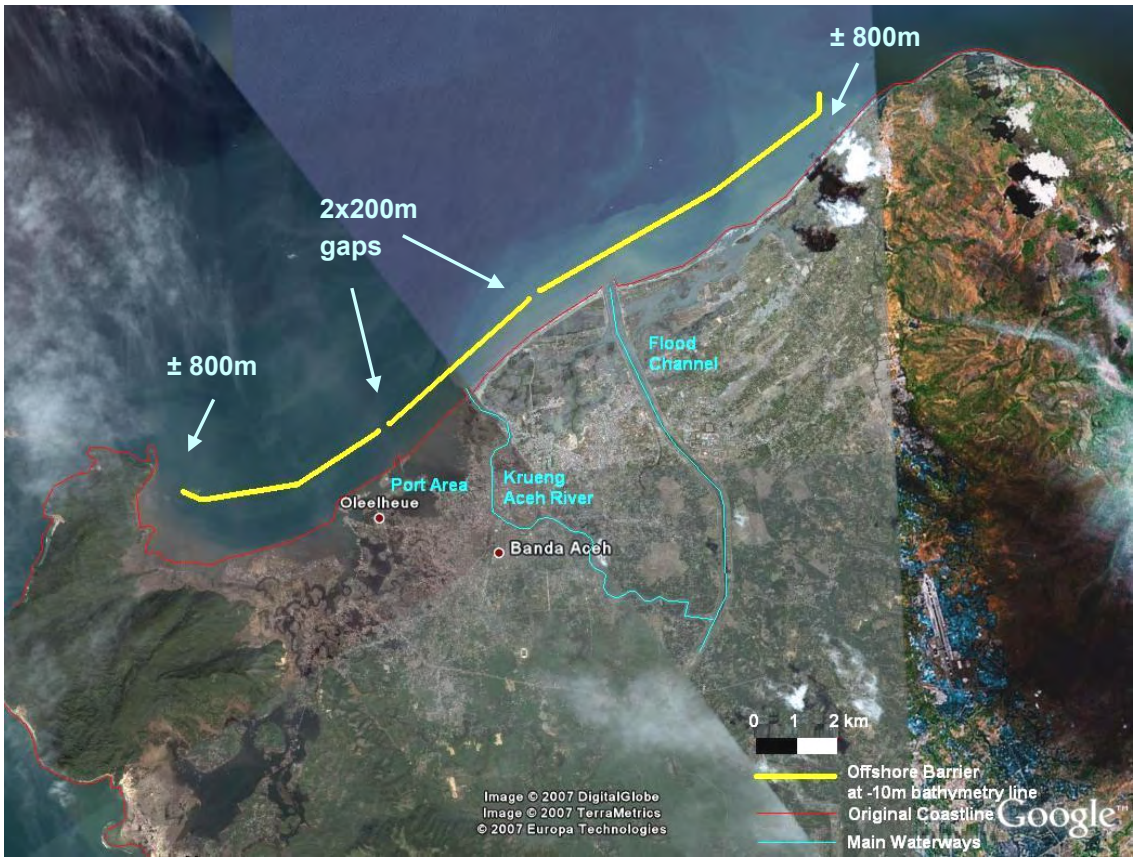

Figure 7-1 Plan view of Banda Aceh with Offshore Tsunami Barrier

The first gap of 200m is located in front of the present port area. The other gap (also 200m) is in between the Flood Channel and the Krueng Aceh River. The barrier is not attached to the coast to allow circulation of the water. The width of these openings is approximately 800m.

Other properties are:

- Freeboard height is 7m above Mean Sea Level
- Construction depth at 10m water depth
- The average distance of the barrier to the coast is 1km
- The total length of the barrier is 19,8km.
- The barrier reduces the open connection with the sea with 92%

7.2.2 Cross-section

In the cost calculation in Appendix V, a preliminary design was presented based on a number of assumptions:

- the core is built up with 2 bunds of Geocontainers, to increase stability and prevent liquefaction in case of earthquakes
- the slopes are quite steep (1:2 and 1:1,5) to reduce the volume
- a sunken toe because of high expected current velocities under tsunami attack
- an excavation of approximately 4m for soil improvement
- an heavy layer of concrete armour blocks on the front side
- berms are added

However, due to increased knowledge about the actual loads of tsunamis on offshore structures, this design has been changed. The main changes are:

- The entire slope is increased to 1:3.
- The Geocontainers are placed on top of the soil improvement instead on the original seabed.
- A slope protection is added on the rear side, for overtopping tsunamis
- The sunken toe is replaced by a toe placed on the seabed.

This changed design forms the starting point for the design of the tsunami barrier. Both designs are presented in Figure 7-2.

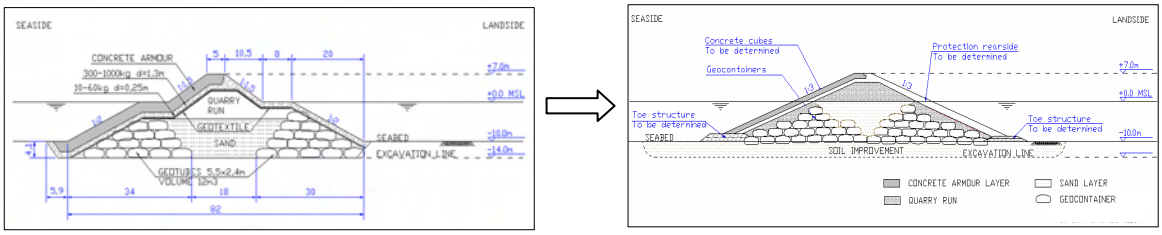

Figure 7-2 Initial cross section as used in cost calculation (left) and changed design as starting point for the detailed design in this chapter.

The choice for toe construction, structure slopes, slope protection, berms, core material, etc. depends on the loads on the structure.

These loads and possible failure mechanisms are determined in the following sections.

Note: the chosen retaining height of 7m is direct result from the economic analysis in 6.3.7.1. There it was found that the optimal protection level for offshore structures would be 10m, with an associated structure height of 16,3m. This figure is rounded to 17m, because it is expected that due to settlements the constructed height will decrease during time.

This optimal protection level corresponds with a tsunami of 10m at the coastline.

7.3 DESIGN LOADS

7.3.1 Normal wave attack

The offshore breakwater is located at 10m water depth. Storm waves (short period and swell) will attack the structure during its lifetime. In SDC, these wave conditions are studied for various location in front of Banda Aceh and for various return periods.
Because maintenance is costly, damage should be minimized. The waves with return period 1/100 year are used. Sea-level rise and tidal variation increase are taken into account. See Appendix VIII for details.

The design values for normal wave attack (RP=100year) are:

Design water level	*= 1,45m + MSL*
H_s	*= 2,7 m*
$H_{s;swell}$	*= 1,0m*
T_p	*= 7,7s*
$T_{p;swell}$	*= 18,2s*
Direction:	*= perpendicular to the breakwater*

7.3.2 Tsunami attack

The loads due to tsunami attack can be described with 2 parameters:

1. Velocities
    a) velocities through the gaps
    b) velocities before and over the structure
2. Water level differences

These loads can cause:
1. Instability of the structure as a whole (sliding)
2. Instability of structure parts due to erosion (of sand, stones, etc)
3. Failure of armour layer due to excess water pressures in case of fast fall / rise in water level

For the design tsunami the Dec2004 Tsunami is used. The velocities through the gaps and the water levels on both sides of the structure are calculated with the 2D Tsunami Model. The output-maps for the maximum water levels (Figure 7-3) and maximum velocity field (Figure 7-4) are presented below.

The resulting water levels for the Dec2004 Tsunami has been calibrated with satellite data (see Chapter 4). Therefore these values are assumed as sufficiently reliable.

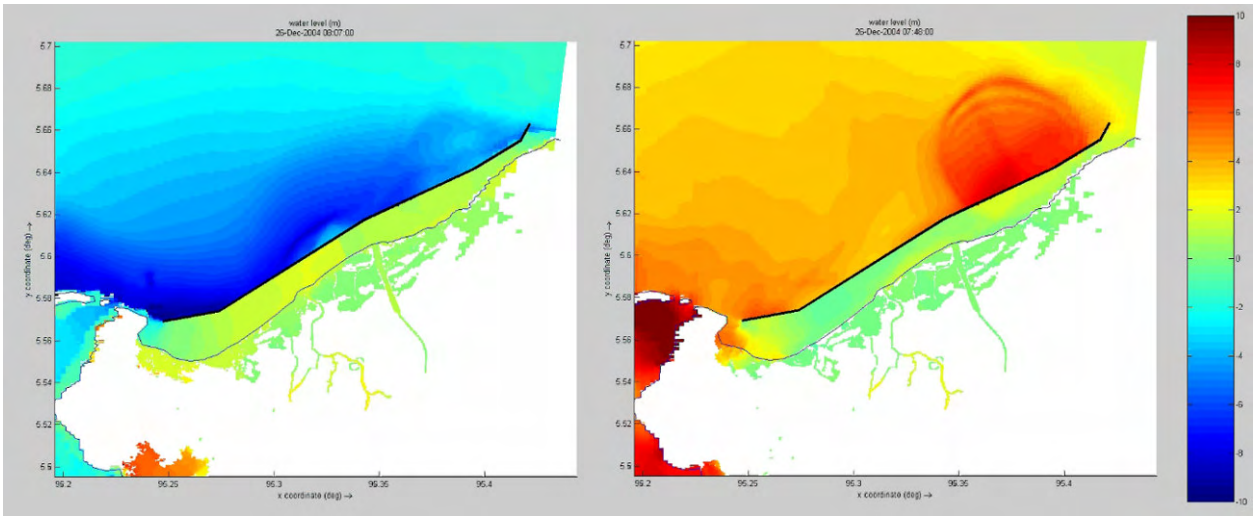

Figure 7-3 Two situations when sliding could occur. Left figure: increased water level at landside and dropdown at seaside; seaward sliding. Right figure: increased water level at seaside and lowering water level at landside; landward sliding. Scale in meters.

The maximum head differences are:

In the left figure: the maximum head difference is: -10 – 2 = -12m
In the right figure, the maximum head difference is: +7 (freeboard) - -2 = 9m

The initial dropdown of the water level is normative, with a head difference of 12m.
The velocity field due to the Dec2004 Tsunami is presented in Figure 7-4.

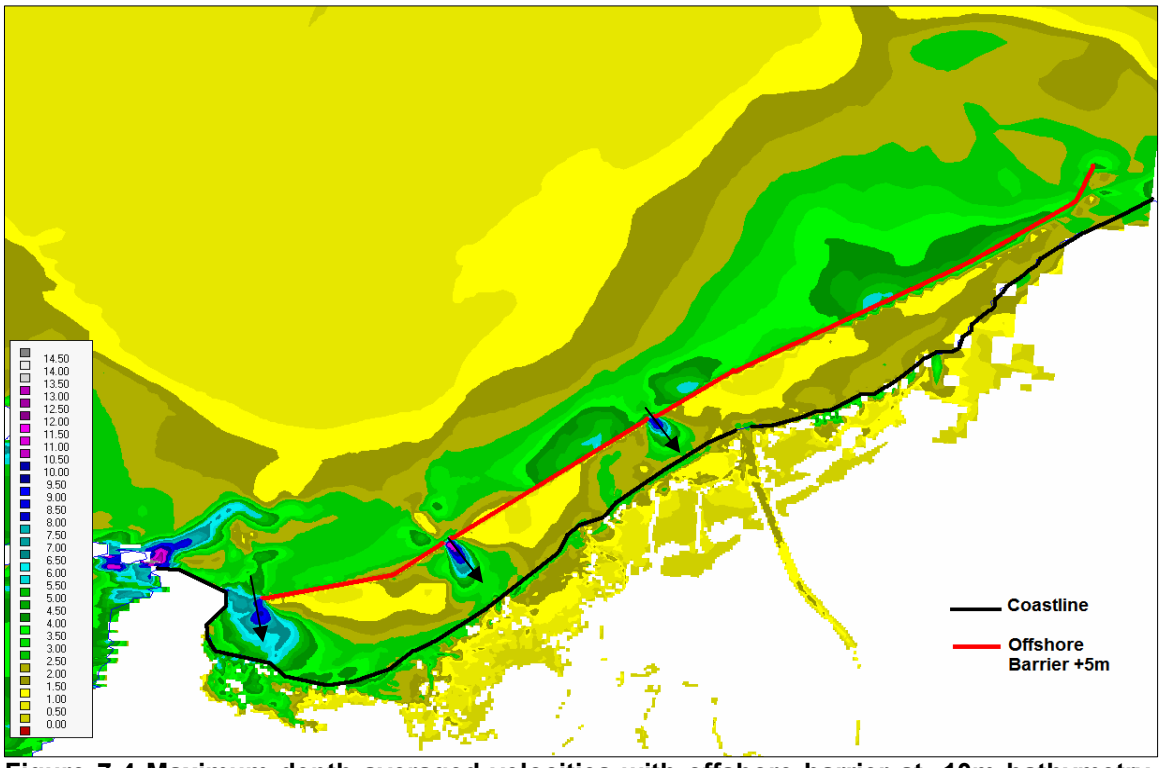

Figure 7-4 Maximum depth averaged velocities with offshore barrier at -10m bathymetry. Label in m/s

The maximum velocities obtained in this calculation are:

Velocity in gap:	12 m/s (in landward direction)
Velocity over the barrier	3,5 m/s

Reliability of these values

The total width of the gaps is 200m. With a grid size of 50m, the gap is modelled by 4 grids. It is therefore assumed that the resulting velocity of 12m/s is reasonably well represented by this model run. It is surprising that this velocity does not occur during the maximum head difference of 12m, which is in seaward direction, but are directed landward.

The magnitude can (roughly) be checked with a simple calculation. The flow through the gap can locally be considered as a flow acceleration area, with fixed water heads on upstream and downstream side Figure 7-5). For flow contraction situations, the law of energy-conservation accounts.

This conservation of energy (head) yields:

$$E_1 = E_2 \rightarrow h_1 + \frac{v_1^2}{2g} = h_2 + \frac{v_2^2}{2g} \Rightarrow v_2 = v_1 + \sqrt{2g(h_1 - h_2)}$$

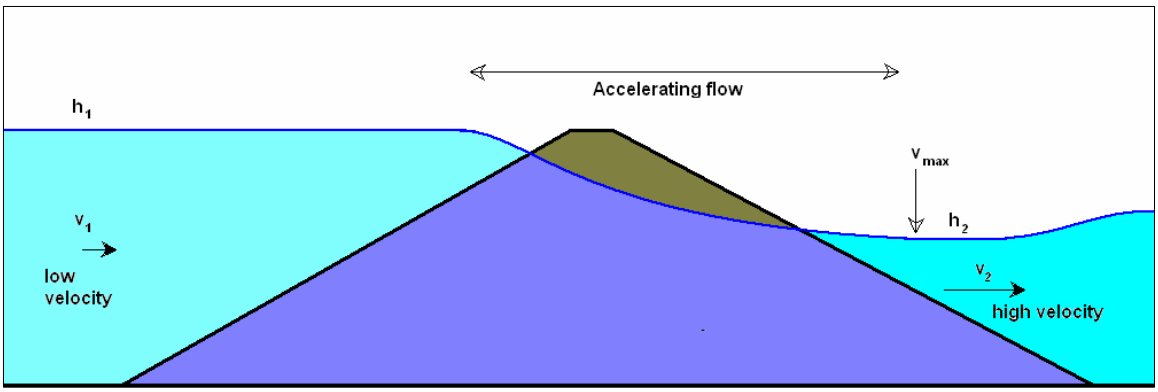

Figure 7-5 Definition sketch flow acceleration through gaps

With h_1=17m, h_2=10m, and $v_1 \leq 1{,}0 m/s$, v_2 becomes:

$v_2 = 1{,}0 + \sqrt{2g(17-10)} = 12{,}7\ ^m/_s$, which is in the same order of magnitude as indicated by the 2D-model.

For water flowing over the barrier the velocities are not reliable. As explained before in Chapter 4, the low-crested barriers are primarily calibrated with resulting water levels. Therefore, the resulting velocities over the crest of the barrier can not be considered as a reliable estimate. Additional modelling is necessary.

1D modelling for velocity over barrier

The velocities over the structure (along the slopes and crest) are calculated with a (semi) 1D-model in FORTRAN provided by Prof. Stelling. Appendix IX gives an overview of modelling activities, results and calibrations with this model. The structure is modelled by changing the

bottom profile. The overall grid size is 15m, but in the vicinity of the breakwater it decreases stepwise to 1m along the structure slopes.

Various structures were modelled to study the influence of geometry on the (depth-averaged!) velocities. General conclusions are:

- The maximum velocities occur at the rear side of the structure, on the water line.
- The velocities in front of the structure (toe) are low (<0,5 m/s)
- The shape or slope on the front side has no significant influence on the maximum velocities.
- Applying a berm on the rear side introduces high peak velocities on the edges.

The results of one model run are presented in Figure 7-6.

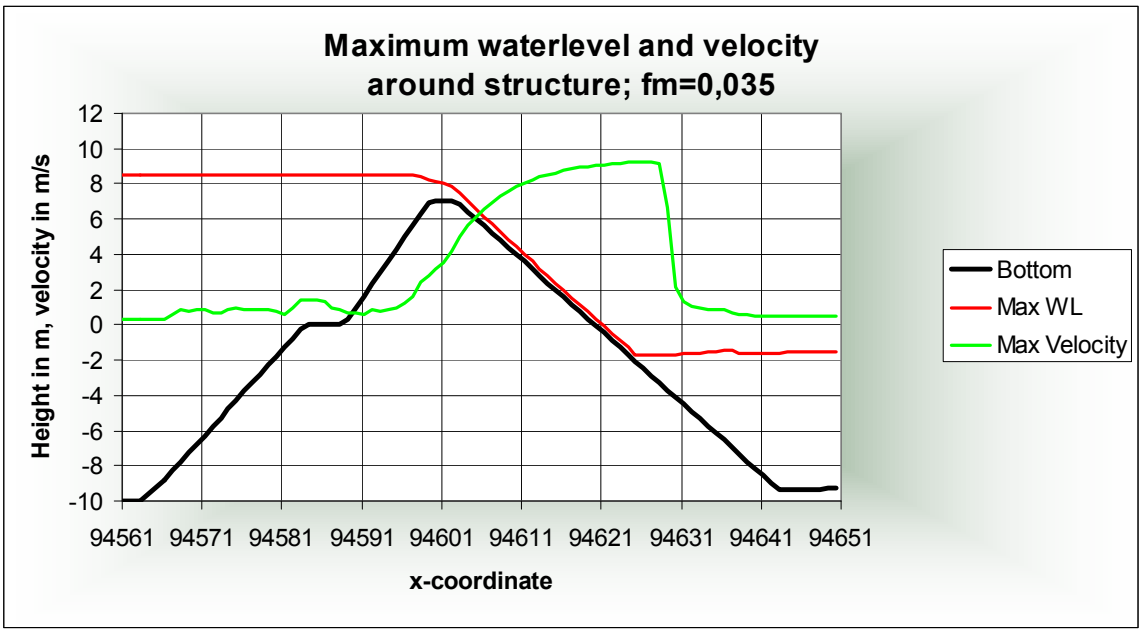

Figure 7-6 Maximum velocities and water levels for offshore breakwater

The maximum occurring velocity is 9,3 m/s. This velocity is horizontal. With correction along the slope, the velocity becomes 9,3/cos(α) =9,9m/s.

Conclusively, the design values for the maximum head difference and velocities are:

Maximum head difference	= 12m
Maximum (averaged) velocity in gaps	≈ 12 m/s
Maximum velocity over barrier; crest	≈ 5 m/s
Maximum velocity over barrier; rear-side	≈ 10 m/s

Further uncertainties in the numerical model results have not been taken into account by obtaining these design values. Corrections for turbulence have not been applied.

Additional loads due to reflected tsunami waves from the coast are negligible.

7.3.3 Earthquakes

Banda Aceh is prone to earthquakes. As discussed in Chapter 3, earthquakes occur more often than tsunamis. In general, 50% of the strong earthquakes generate a (local) tsunami.
Prior to a tsunami, the structure most likely experiences an earthquake. In order to provide good tsunami-protection it is therefore very important that this initial loading can be withstood by the structure.

So, earthquakes do occur more frequently then tsunamis but any earthquake could be followed by a tsunami. Therefore, thorough attention should be paid to prevent structural failure due to earthquake induced loadings. Liquefaction of the subsoil and structure body itself are the most likely failure mechanisms.

The design values for Banda Aceh are normally prescribed by the Indonesian Building Code (ref).

In this specific situation, the design earthquake is set to M_w=9,2 with peak ground accelerations of 0,3g.

Conclusively, the design values for earthquakes are:

Magnitude on Richter Scale, M_w	*= 9,2*
Peak ground acceleration	*= 0,3g ≈ 3 m/s^2*

7.4 FAILURE MECHANISMS

The described design loads can lead to failure of the structure. Possible failure mechanisms are:

- Instability due to direct loads from the tsunami wave. Especially the crest and rear side are vulnerable due to overtopping.
- Instability due to normal wave loading. Especially toe and armour layer on the front side are vulnerable.
- Instability due to long duration of tsunami wave, due to direct load on the structure (drag forces) or erosion of the seabed. This is especially important in the gaps, where the bottom is unprotected and extremely high velocities occur.
- Failure of the armour layer due to internal pressures
- Unequal settlements over axis of breakwater due to seismic activity, maybe resulting in liquefaction of seabed and/or structure body and unequal settlements along the axis of the breakwater leading to damage of armour layer.

These failure mechanisms are depicted in Figure 7-7.

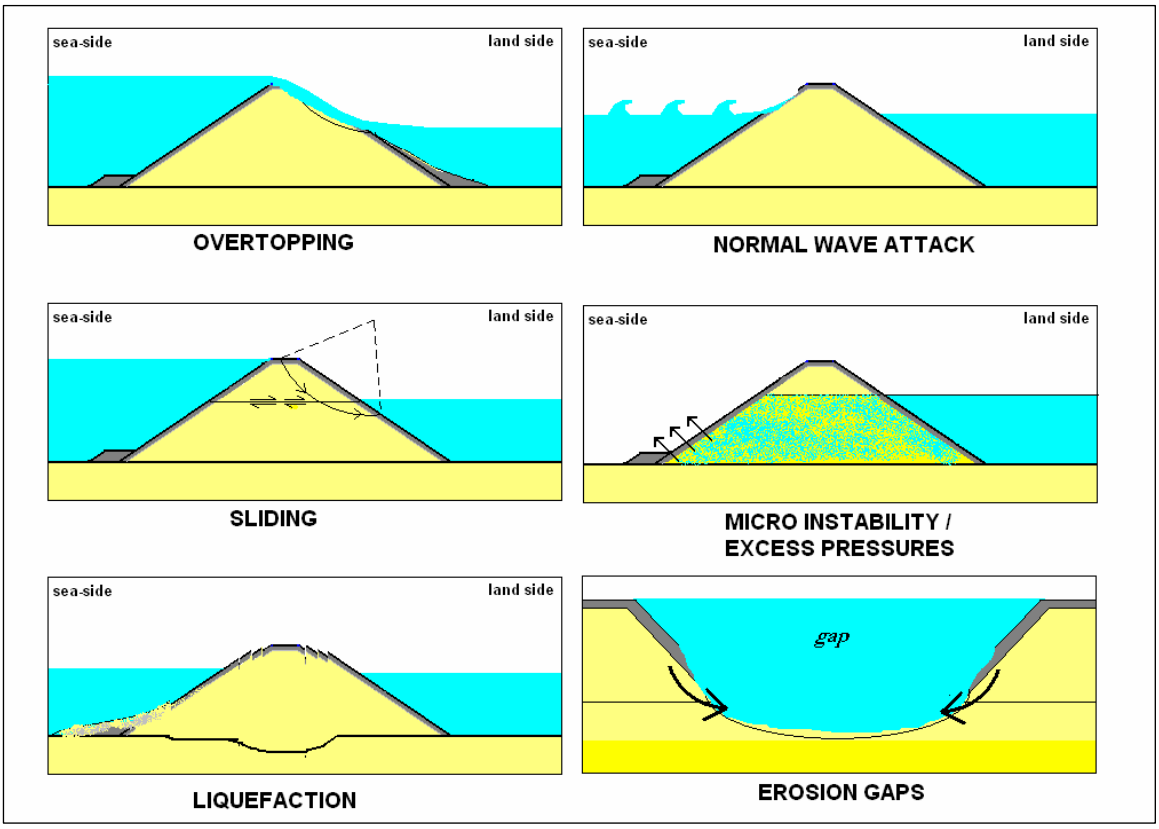

Figure 7-7 Failure mechanisms Offshore Tsunami Barrier Banda Aceh

Settlement does not necessarily lead to damage or collapse. However, it reduces the effective height of the breakwater. It is expected that due to settlement of the subsoil and structure itself, approximately 2 -3m height will be lost. This height should be added to the final design height to obtain the required construction height.

7.5 DESIGN OFFSHORE TSUNAMI BARRIER

7.5.1 Overtopping

Appendix VIII deals with the determination of the armour layer. It is found that under the extreme flow velocities on the rear side of the barrier, unrealistic stone diameters are required. Following the design consideration that a 'low damage' is not realistic, the 'CERC'-formula[18] [13] has been used. This method enables to allow certain damage, expressed in a number of moved blocks. But even with 20% damage ('CERC-formula'), a required stone weight of 33ton was calculated. With the Izbash formula, the required stone weight increases dramatically for flow velocities above 3-5m/s (W≈1800ton for *u=9m/s*)

[18] *This stability formula was originally developed by CERC and is therefore referred to as the CERC-formula. It was concluded by Japanese engineers in the design of the Kamaishi breakwater, that this formula accurately described the block movement due to tsunami currents.*

Therefore, other means of slope protection have to be proposed. It is possible to protect slopes against extremely high velocities. Various large scale tests ([6], [28]) have shown that stable slope protection is possible, even for flow velocities of 17-23m/s. Two possible solutions are shown in Figure 7-8. The use of block mats (like Armorflex) and the application of wedge-shaped blocks are both proven to be stable in high flow regions.

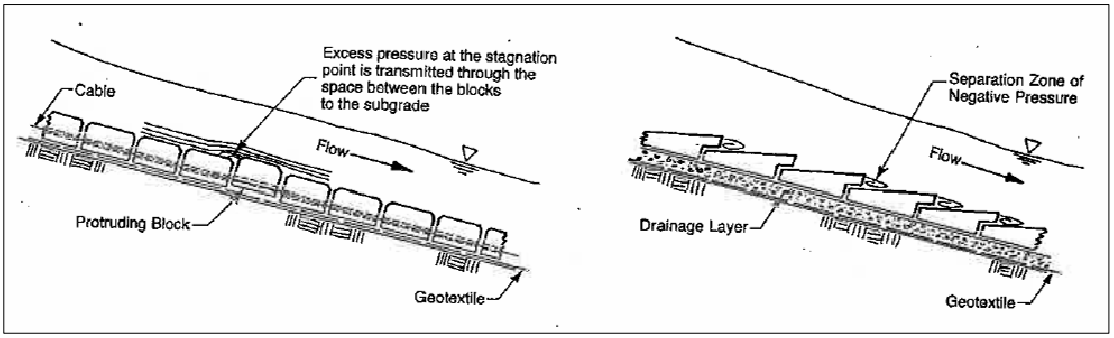

Figure 7-8 Left: a cabled concrete block revetment. Right: Wedge-shaped block system [6]

However, the durability of these solutions in this specific situation is questionable. Above mentioned solutions are often used in spillways, and constructed in dry circumstances. Offshore execution (and maintenance) is much more complicated. Generally, these solutions require extensive attention for details, which can not be guaranteed for offshore situations in Banda Aceh.

Therefore asphalt is proposed. Several mix types are possible [39],[40]. Two mix types are proposed in this situation:

1. *Grouting mortar / dense stone asphalt for the top layer and under water*
   Grouting mortars are hot-type mixes of sand, filler and bitumen and used for grouting stone revetments above and below water-level. Dense stone asphalt is a gap-graded mixture of stone, sand, filler and bitumen. The material is, like grouting mortars, water impermeable. Relatively expensive compared to lean sand asphalt.

2. *Lean sand asphalt as under layer for the dry part of the slope*
   Lean sand asphalt is a mixture of sand with 3%-5% bitumen. The permeability is very similar to sand after some time. It is much cheaper though and used as under layer, covered by dense stone asphalt.

In Appendix XIII, the required thickness is calculated, based on pressure differences that can cause uplift of the asphalt layer.

The following remarks are made about the use of asphalt:

- It necessary to extend the asphalt layer below MSL. The construction of grouting mortar under water is complicated and expensive. Special (mobile) mixing equipment is necessary at location.
- The pressure differences and suction forces of the flowing water require a thick layer. Rough calculations indicate at least 1,3m is necessary.

- Inspection and maintenance of the asphalt layer is costly and complicated (offshore conditions, under water). However, this also accounts for wedge-shaped blocks.
- Damage can arise by:
    - Deformation due to unequal settlement of the barrier due to seismic activity leading to cracks/grooves in and through the revetment
    - Poor connections and joints with other armour layer

Although complicated and costly a further study into the feasibility of asphalt in this situation is strongly recommended. The layer is mainly applied on the inner slope of the breakwater's trunk and therefore not prone to regular wave attack. This positively influences the durability of this solution.

It is important to consider a potential negative pressure zone on the downstream slope, especially directly below the crest. The flow over the crest could separate from the slope creating a low-pressure zone. The transition should be streamlined and not abrupt.

It is expected that the use of concrete blocks or rip-rap on the inner slope will not ensure stability during tsunami overtopping. Further study and physical model tests are required anyhow.

7.5.2 Normal wave attack

With the derived design values for the breakwater location, H_s = *2,7m,* T_p=*7,7s,* and the assumed slope of 1:3, the required armour layer was calculated, using the Van-der-Meer formula for cubes. The same calculation was done for the swell conditions, H_s = *1,0m,* T_p=*18,2s*, but this lead to smaller dimensions. Appendix VIII gives an elaborate overview of the calculation.

It is concluded that under these circumstances and with low damage criterion (N_{od} =0,2), 1 layer of 4,6-ton placed blocks are required. This armour layer is applied over the full height of the structure.

The toe on the front side is constructed of 2 layers 1000-3000kg. On the rear side, 2 layers 300-1000kg stones are applied. This heavy toe is applied due to uncertainties in the actual current velocities under tsunami waves. Additional (physical) modelling is recommended. The toe is placed on the seabed (no sunken toe).

7.5.3 Sliding

Sliding can occur when the force on a part of the structure exceeds the friction which can be generated by this structure part.

Two types of sliding are treated:

1. Horizontal sliding
2. Circular sliding (Bishop method)

Horizontal sliding can occur when a head difference generates a horizontal load on the structure. In Appendix VI, the normative situation is analysed. The horizontal wave impact is calculated with 3 methods:

1. The loads obtained from the 1D-model (integration of static and dynamic water pressures)
2. The loads calculated with Tanimoto (see section 2.6.1), which is a lower limit
3. The loads calculated with Kato (see section 2.6.2), which is an upper limit.

It is found that horizontal sliding can not occur with the assumed structural dimensions (slopes 1:2,7; crest width 5m). See Figure 7-9.

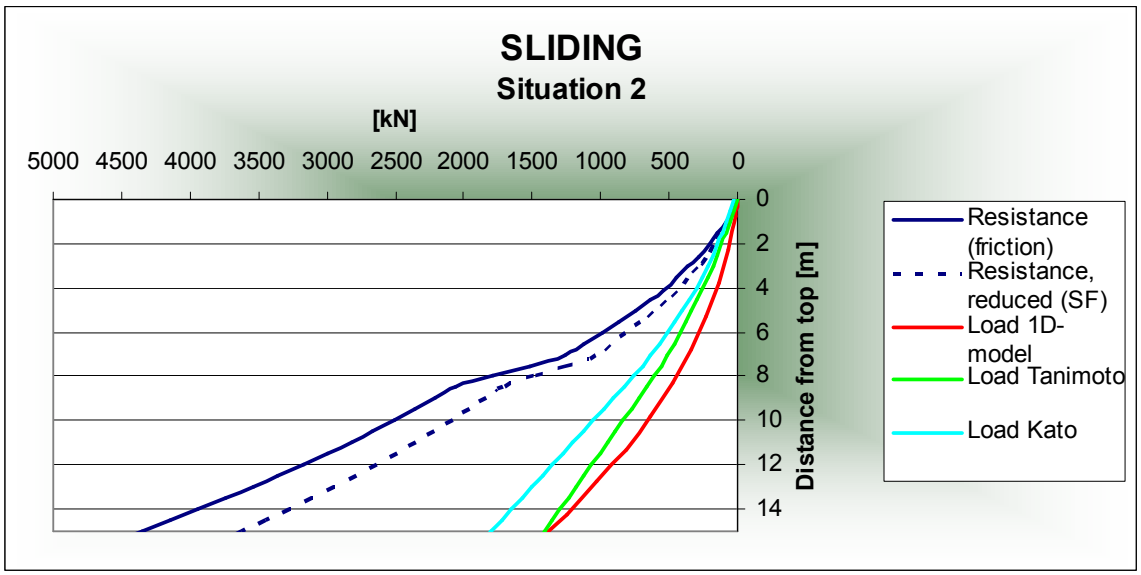

Figure 7-9 Sliding; Loads according to Tanimoto, Kato and 1D-model and resistance

The possibility of circular sliding is investigated with the use of MStab. The front slope shows the highest susceptibility to sliding in case of the outwardly directed head difference of 10m. Assuming that the structure is built up with GeoContainers, however, reduced the likelihood of sliding and MStab indicated that sufficient stability against circular sliding is found. The influence of a berm on the stability was found limited. Therefore, no berms are applied.

Additional study is necessary, because the actual composition of the breakwater is more complicated then assumed (Geocontainers and geotextiles are not modelled).

7.5.4 Excess water pressures / micro stability

Because the water head on the seaside will drop quite fast due to the negative tsunami wave, seepage through the dike can occur. The demand for stability in case of horizontal seepage is most strict:

$$\phi \geq 2\alpha$$

The permissible slope angle ϕ is half the angle of repose. With a breakwater built up with quarry-run (ϕ=40deg), the maximum slope becomes 20deg, which is 1:2,7. This slope should at least be applied on the entire rear side, and on the lower part of the front side.

The assumed slope of 1:3 over the entire structure height is sufficiently stable.

7.5.5 Liquefaction

In Appendix VII, the liquefaction potential is calculated for 5 locations along the planned axis of the Tsunami Barrier.

It was concluded that for 2 locations, a high likelihood of liquefaction exists. Several methods are available to decrease the liquefaction potential. Replacing the poor-graded soil and/or compaction are often-used methods. It was assumed without further reasoning, that replacement of a top-layer of 4m thickness will cover the costs to prevent against liquefaction.

The liquefaction potential of the structure body (for the saturated part) is not calculated, because in-situ data is required. The stability of the structure body is ensured by applying so-called GeoContainers. These 'sand-tubes' are placed under water at an angle of 1:3 or even more gentle. The slope is filled out with quarry run.

7.5.6 Gaps

The introduction of gaps also requires the construction of breakwater heads. In total, 6 heads have to be constructed. For normal wave attack, no systematic test results are available. The Shore Protection Manual recommends constructing a head with stones which are twice as heavy as in the trunk or, a head with a slope twice as gentle as the trunk's slope [30].

The gaps form the most difficult part of the entire structure, since the current velocities are extremely high (12m/s). Both breakwater heads and the bottom material are heavily exposed. Although damage is allowed, there should be a basic protection to prevent against entire collapse of the breakwater heads due to erosion. See Appendix VIII on some rough estimates about scour holes. The following measures are proposed to prevent severe damage to the breakwater heads:

- Slopes 1:6
- Asphalt layer that stretches entirely to the toe of the structure, thickness ≈1,5m
  - Grouted mortar for underwater part
  - Combination of lean asphalt and dense stone asphalt for upper (dry) part
  - The under water layer extends sufficiently far on the front side of the trunk ≈100-200m
- Concrete mattresses (GreenFlex or ArmorFlex) which stretch at least 50m towards sea- and landside of the breakwater.
  - The edges of these mattresses are protected with heavy concrete blocks, with streamlined shapes. This is to prevent removal of the mattresses when the flow reverses.

See the following section for drawings.

7.6 SUMMARY AND DRAWINGS

Due to the extreme nature of tsunamis, some damage is allowed as long as the primary function is maintained.

This damage is most of all concentrated on the crest and rear side of the breakwater, since high velocities do occur in case of tsunami overtopping. For the preliminary design, an asphalt layer is proposed. High velocities do also occur in the gaps. With gentle slopes of the heads and an extensive bottom protection the impact of the scour holes is reduced.

Instability of the breakwater itself due to sliding and liquefaction is mainly prevented by applying a core of GeoContainers. These containers prohibit liquefaction and the generation of sliding planes and circles.

The sea-side is designed against 'normal' waves, with low damage criterion. Toe structures are put into the design to support the armour layers on the slope. Direct wave attack on the toe's will not occur, due to the large depth they are constructed in.

In below figures the preliminary design is presented in both cross section and plan view of the gaps. It is stressed that many details require additional research. Physical modelling for such an expensive structure under such unsure circumstances is inevitable. Figure 7-10 and Figure 7-11 present the composition and dimensions of the offshore Tsunami Barrier. Figure 7-12 shows a plan view of the gap and a general layout of the proposed protection.

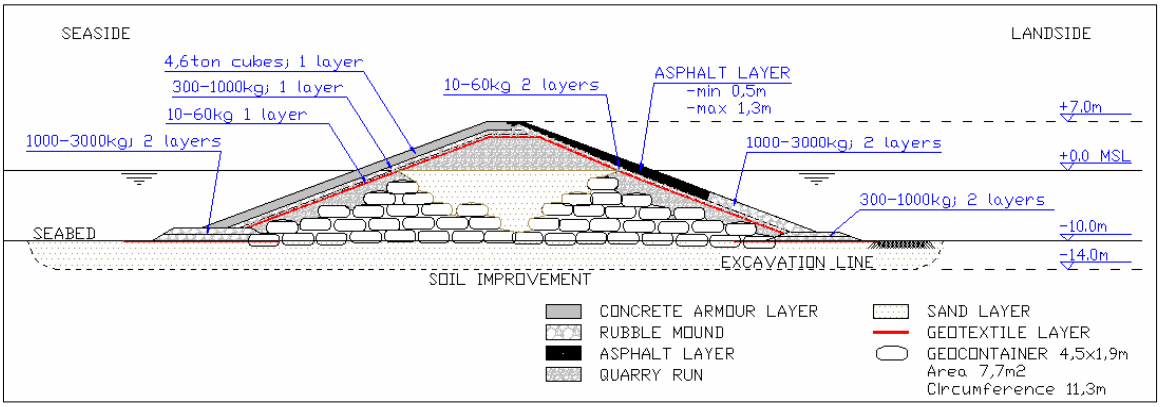

Figure 7-10 Cross section Offshore Tsunami Barrier; composition

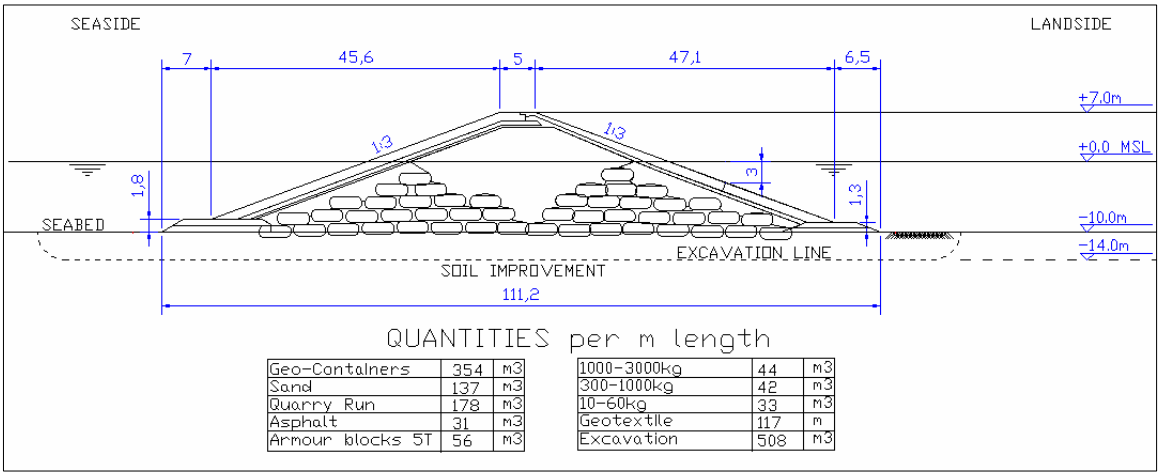

Figure 7-11 Cross section Offshore Tsunami Barrier; dimensions and quantities

Note: with this new cross section and quantities, the construction costs are changed slightly. For asphalt, a unit rate of \$250/m^3 is used. The 'new' construction costs for this design becomes \$1,17 Billion. This minor difference has no influence on the conclusions of the feasibility study,

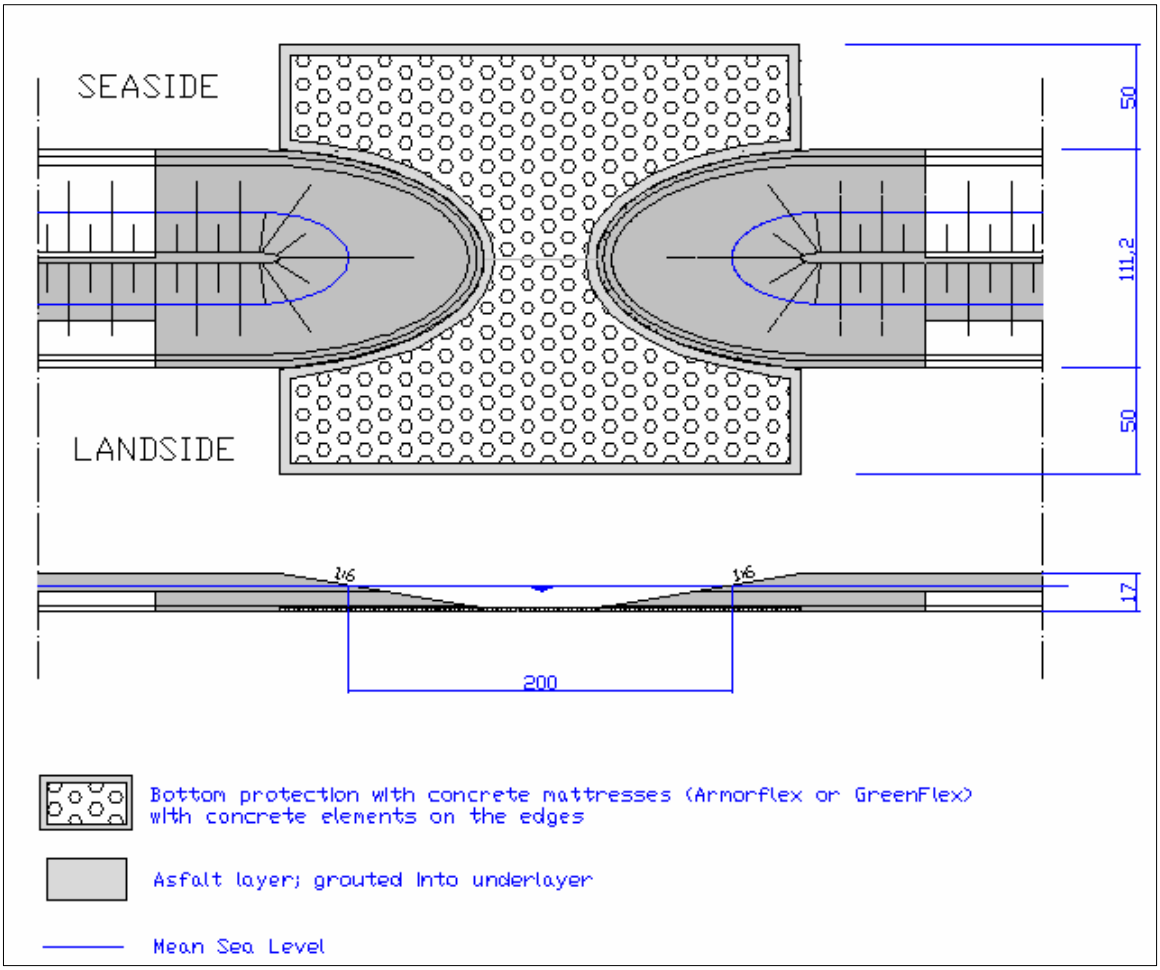

Figure 7-12 Plan view and cross section of gap and general layout of gap protection

Figure 7-13 and Figure 7-14 show 3D impressions of the designed tsunami barrier. Note that the heads are completely covered by an asphalt layer.

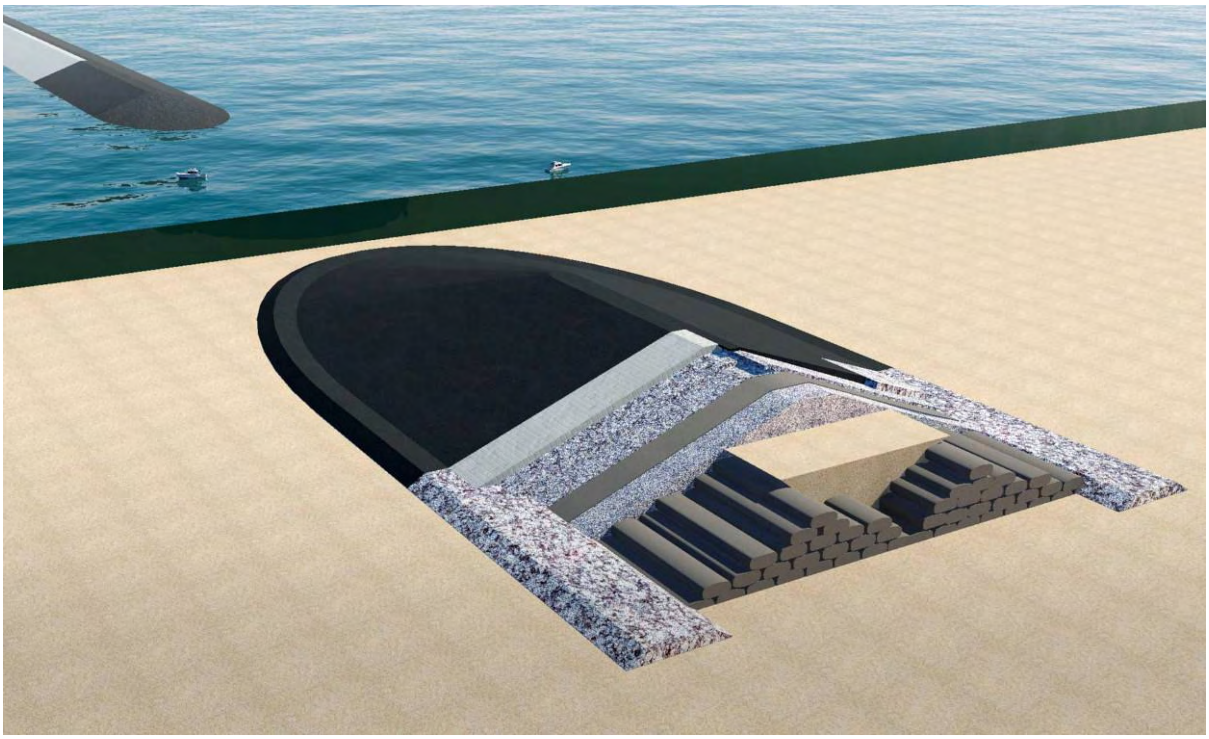

Figure 7-13 3-D impression of offshore tsunami barrier; gap

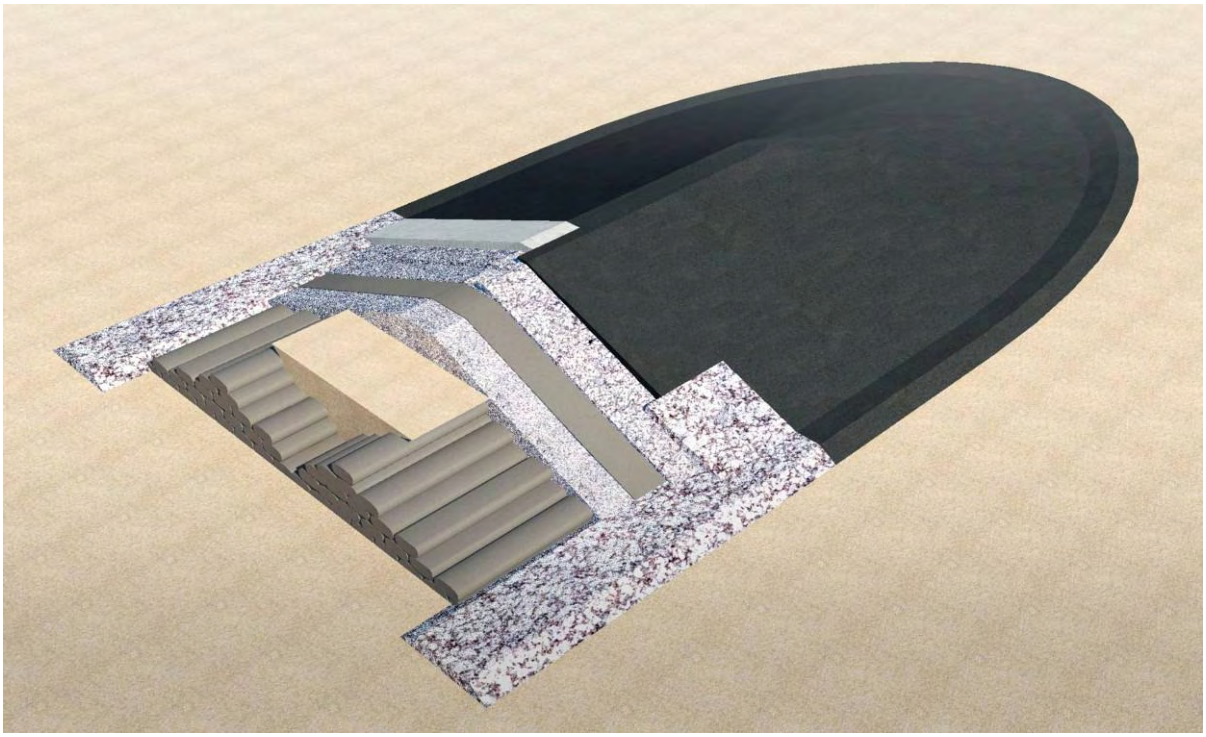

Figure 7-14 3-D impression of offshore tsunami barrier; composition

Chapter 8. CONCLUSIONS AND RECOMMENDATIONS

8.1 CONCLUSIONS

In this section the conclusions that were drawn throughout the research and that are relevant for the final conclusion, are stated in chronological order. Finally, the general conclusion on the objective that was formulated in section 1.3 is presented.

Tsunami theory and modelling

- The high variety in tsunami wave signal leads to a wide range of theoretical relations between magnitude, run-up height, inundation, impact force, current velocities, etc.
- General relations between earthquake magnitude, tsunami magnitude, wave run-up height are much to common to be used for specific design purposes
- Relations between tsunami height and impact force are indicative and can be used for preliminary design, but the definition of wave height, shape (broken/non-broken) and the location of the structure will induce different loads.
- The near-shore bathymetry was found to have a significant influence of the shoaling of the wave. Concave profiles lead to higher waves (and run-up against structures) then convex profiles.
- A negative wave (with initial dropdown of the water level) leads to higher run-up and impact
- The velocities and water levels around the structure, obtained from 1D-modelling, showed reasonable agreement with theory.
- Empirical relations between overtopping volume and structure height can not be used. The fact that successive waves ride on each other and penetrate farther was indicated as the main reason for this difference.

Tsunami protection alternatives

- Tsunami protection measures by means of mangrove trees or other vegetation are somewhat effective for tsunamis lower than 3m, but will be destroyed by higher tsunamis.
- Submerged breakwaters will only show minor effectiveness in tsunami protection, since they are aimed at dissipation of wave energy
- In general, tsunami protection should aim at reflection of the energy instead of dissipation.
- According to the 2D-model runs and analysis of tsunami risk, the following optimal structure heights are obtained
    - An offshore breakwater at -10m with a freeboard of 6,3m
    - A coastal structure of 12,6m height
    - An inland structure of 9,7m height
- The construction costs of these alternatives are estimated at:
    - An offshore breakwater at -10m with a freeboard of 6,3m: $ 1.140.000.000
    - A coastal structure of 12,6m height: $ 461.000.000
    - An inland structure of 9,7m height: $ 327.000.000

Feasibility of protection alternatives

- The Cost Benefit Analysis showed that none of the protection alternatives is feasible in economical terms, assuming moderate growth and discount ratios.
- The offshore barrier was least feasible (in economical terms), followed by a coastal and inland structure.
- Analysis of the alternatives on basis of non-financial criteria (MCA) suggested that offshore structures are the only realistic means of tsunami protection from a social point of view. The presence of high structures on land will disrupt socio-economic development of the city of Banda Aceh.
- Considering the small escape time in case of a tsunami warning and decreasing awareness in time, it can still be a good choice to choose for extensive tsunami protection structures in Banda Aceh.

Design Offshore Tsunami Barrier

- An offshore tsunami barrier at -10m water depth and a freeboard of 7m is designed. The anticipated reduction of inundation volume for a Dec2004 Tsunami amounts to 95%.
- The average distance to the coast is 1km, and in total 4 gaps (2x200m;2x800m) are included in the design to allow navigation and circulation.
- Based on model runs, maximum velocities of 12m/s in the gaps and 10m/s along the rear-slope are expected. Maximum head differences amount to 12m in seaward direction.
- The slopes of the trunk are 1:3 (v:h); the slopes of the head is 1:6.
- The front side of the barrier is protected against 'normal' storm waves, because tsunamis induce low loads of the front side.
- The core is built up of two bunds consisting of GeoContainers to increase stability against liquefaction. The top is constructed of quarry run.
- The rear-slope is protected with an asphalt layer to -3m MSL to prevent erosion due to overtopping tsunamis. This layer is constructed on top of several layers rip-rap to ensure a high permeability to prevent internal pressure built-up.
- Toes are constructed to support the slopes. The toes have a high permeability.
- A geotextile layer is put on the core material.
- Soil improvement in required to prevent liquefaction.
- The heads are protected with (grouted) asphalt stretching entirely to the toe. The bottom in the gaps is covered with geotextile, with cabled concrete mattresses on top.

The objective that was formulated at the start of this research is:

> *Provide insight into the feasibility of tsunami protection measures for Banda Aceh and set up a preliminary design for a tsunami protection structure.*

The general conclusion is:

> *In economical terms, tsunami protection measures for Banda Aceh are not feasible. The costs do not outweigh the prevented damage or benefits.*
>
> *In social terms, the only realistic means for extensive structures are offshore solutions. A preliminary design has been made for an offshore structure at 10m water depth with a freeboard of +7m MSL and 4 gaps. It is expected that this structure reduces flooding to tsunami-events like the Dec2004 tsunami with approximately 95%.*

8.2 RECOMMENDATIONS

The conclusions drawn in the previous section are based on numerical models and analyses that have their limitations. The most limitations are already discussed throughout the report. The recommendations following from these discussions are presented here.

Recommendations regarding the feasibility of tsunami protection for Banda Aceh
Very little data is available about the probability of tsunamis. Historical records are short and not always reliable. However, much more is known about the probability of earthquakes. Because submarine earthquakes are the most likely cause of tsunamis worldwide, it is recommended to:

- Study the relation between earthquake (fault-type, magnitude) and the excitation signal of tsunamis in more detail in order to indirectly derive a more reliable probability distribution for tsunamis.

With the help of numerical models, the propagation of the excitation signal can be calculated. Although models are available that accurately account for wave shoaling, reflection, dispersion, etc., extensive CPU-time is required to simulate tsunami wave fields. Therefore, some tsunami hazard mapping methods are based on simple shoaling laws (Green). This law however, is not accurate for near-shore wave development. Because tsunami hazard is related with the tsunami wave height *at the coast*, it is recommended to:

- Study the influence of near-shore bathymetry on tsunami wave development in more detail. Initial modelling indicates a significant difference between convex and concave profiles.

The likelihood of earthquake-generated tsunamis is related with the amount of built-up stresses in a fault. Earthquakes go along with stress release, consequently indicating that after a major earthquake the likelihood of (large) tsunamis is immediately decreased. And so is the risk.
Although it is logical that the need for a detailed study into tsunami protection measures arises after a big disaster, it would be wiser to:

- Focus on locations were earthquake activity was low for an unusual long period

The near-future risk is much higher for these locations. In various studies it was indicated that the amount of slip (measure for the stress release) in the southern part of the Sunda Trench was less then in the north for the Dec2004 earthquake. This indicates that the tsunami threat in this region is higher than north. Cities like Padang (South Sumatra, almost 1 million inhabitants) probably show a higher vulnerability for the coming 100 years then Banda Aceh.

It was concluded that the costs of extensive tsunami protection structures for Banda Aceh are (much) higher than the benefits. The probability of tsunamis together with the sustained damage is too low to justify such investments in economical terms. Considerations about the little escape time for Banda Aceh, the positive influence of a sound protection scheme on economical

development and the valuation of deaths could still lead to a rational decision in favour of large tsunami protection measures. Nevertheless, for Banda Aceh it seems better to:

- Investigate the feasibility of other types of protection, like mangrove trees in combination with a sound Tsunami Early Warning System and a network of refuge buildings

These measures would prevent economical damage due to low tsunamis (<3m) and will save lives, also for high tsunamis. The economical damage could be reduced further by:

- Building reinforced concrete structures, especially at the coast, that allow flow-through of the tsunami wave (e.g. large windows facing the sea)

Recommendations regarding the design of an offshore rubble-mound tsunami barrier

For Banda Aceh
The design is based on analysis of theoretical relations, model runs and existing designs. Several uncertainties remain due to lack of data and time. It is recommended to:

- Obtain more soil data to determine the likelihood of liquefaction in more detail
- Study the effect of the breakwater on the retention time of waste water disposed by the Krueng Aceh River. Enough circulation should be obtained.
- Study the effect of the breakwater on normal wave transmission and changes in sediment transport
- Assess the width of the gaps in case of increased navigation

It is obvious that for the detailed design of such an extensive structure, it is necessary to:

- Carry out physical model tests with the proposed barrier design for both trunk and heads/gaps.

In general
The design of a rubble-mound tsunami barrier yields some specific problems, mainly related with the stability of the rear-slope and high current velocities in gaps (if applied). To gain more insight in the physics of tsunami wave attack on rubble mound structures, it is necessary to:

- Carry out physical modelling to study the
  - Local velocities (turbulence) around structure, but mainly at rear-side and the stability of several slope protections (armour layer, asphalt, etc.)
  - Flow through the barrier
  - Degree of scouring around the structure and mainly in the gaps and the effectiveness of scour-protection measures
  - Impact forces of a broken or breaking tsunami.

Especially the protection of the rear side and the heads and bottom of the gaps are points of points of concern.

LIST OF REFERENCES

[1] BAPPENAS (2005), Indonesia: Preliminary Damage and Loss Assessment, The December 26, 2004 Natural Disaster, *The Consultative Group on Indonesia*, January 19-20, 2005.

[2] BATTJES, J.A. (2002), Vloeistofmechnica, *faculty of Civil Engineering Delft University of Technology, Delft*.

[3] BRYANT, E. (2001), TSUNAMI: The Underrated Hazard, *Cambridge University Press, Cambridge*

[4] CAMFIELD, F.E. (1980), Tsunami Engineering, *U.S. Army, Corps of Engineers, Coastal Engineering Research Center, Fort Belvair.*

[5] CHU, K.K., ABE, T (1981), Tsunami Run-Up and Back-Wash on a Dry Bed, *Terra Scientific Publishing Company, Tokyo*

[6] CLOPPER, P.E., (1991), Protecting Embankment Dams with Concrete Block Systems, *Hydro Review,* Volume X, No. 2, April 1991, pages 54-67

[7] CUYPERS, K., (2004) Breakwater stability under tsunami attack, for a site in Nicaragua. *Final Thesis Report, Delft University of Technology, Delft.*

[8] © CUR-PUBLICATIE 214, Geotextiele zandelementen, 2004, *Stichting CUR, Gouda.*

[9] © CUR-PUBLICATIE 168A, Oeverbeschermingsmaterialen, 1994, *Stichting CUR, Gouda.*

[10] EDWARD, P.J.K., TERAZAKI, M., YAMAGUCHI, M., The impact of tsunami in coastal areas: Coastal protection and disaster prevention measures; experiences from Japanese coasts, *Coastal Marine Sciences 30(2):414-424*, 2006.

[11] GEIST, L.E, (2001), Complex earthquake rupture and local tsunamis, *Journal of Geophysical Research, Vol. 107. No. B5, U.S. Geological Survey, Menlo Park, California, USA.*

[12] HARADA, K., KAWATA, Y. (2004) Study of the effect of coastal forest to tsunami reduction, Annuals of Disaster Prevention, *Research Institute of Kyoto Univ., No.47C, Kyoto.*

[13] HITACHI, S., KAWADA, M., TSURYA, H., (1994), Experimental studies on tsunami flow and armorblock stability for the design of a tsunami protection breakwater in Kamaischi Bay, *Hydro-Port 1994 Vol. I., Coastal Development Institute of Technology*, pages 765-783.

[14] HOFFMANS, G.J.C.M, VERHEIJ, H.J. (1997) Scour Manual, *Balkema, Rotterdam*.

[15] HORRILLO, J, KOWALIK, Z (2006), Wave dispersion study in the Indian Ocean Tsunami of December 26, 2004. *Science of Tsunami Hazards*, Vol. 25, No. 1, page 42.

[16] JICA STUDY TEAM, 2005, Study on the Urgent Rehabilitation and Reconstruction Plan for Banda Aceh City in the Republic of Indonesia. *Banda Aceh.*

[17] KAMEL, A.M., (1970), Laboratory study for design of tsunami barrier, Journal of the Water ways, *Harbours and Coastal Engineering Division, ASCE, Reston*, page 766-779.

[18] KATHIRESAN, K., RAJENDRAN, N., 2005. Coastal mangrove forests mitigated tsunami. *Estuarine, Coastal and Shelf Science 65*, 601-606.

[19] KATO, F., INAGAKI, S. AND FUKUHAMA, M. (2006) Wave Force on Coastal Dike due to Tsunami. World Scientific Publishing, *COASTAL ENGINEERING 2006; Proceedings of the 30th International Conference, San Diego, California, USA.*
Abstract available at http://www.pwri.go.jp/eng/ujnr/joint/37/paper/13kato.pdf

[20] KERR, A.M., BAIRD, H., CAMPBELL, S.J., 2006. Comments on "Coastal mangrove forests mitigated tsunami". *Estuarine, Coastal and Shelf Science 67*, 539-541.

[21] IDA, K. (1981), Tsunamis: their Science and Engineering, Ida, K., Iwasaki, T., *Terra Scientific Publishing Company, Tokyo.*

[22] IKENO, M., MORI, N. AND TANAKA, H.(2001), Experimental Study on Tsunami Force and Impulsive Force by a Drifter under Breaking Bore like Tsunamis, *Proceedings of Coastal Engineering,* JSCE, Vol. 48, 2001.

[23] IKENO, M., TANAKA, H.(2001), Experimental Study on Impulsive Force and Tsunami Running up to Land, *Proceedings of Coastal Engineering,* JSCE, Vol. 50, 2003.

[24] MANGKUSUBROTO, K.,et al, (2005), Rebuilding a better Aceh and Nias, *Report of a joint team of BRR and World Bank, Banda Aceh.*

[25] MATSUTOMI, H., et al. (2005), Aspects of Inundated Flow due to the 2004 Indian Ocean Tsunami, Coastal Engineering Journal, Vol. 48, No. 2 (2006) 167-195, *World Scientific Publishing Company, Tokyo.*

[26] NATAWIDJAJA, D.H, Neotectonics of the Sumatran Fault and Paleogeodesy of the Sumatran Subduction Zone, PhD thesis, *California Institute of Technology, Pasadena, California*, 2002. Available from http://etd.caltech.edu/etd/available/etd-05222003-155554/unrestricted/DHN_ Thesis.pdf

[27] PILARCZYK, K.W. (2003), Design of low-crested (submerged) structures –an overview –, *6th International Conference on Coastal and Port Engineering in Developing Countries, Colombo, Sri Lanka*.

[28] POWLEDGE, G.R., PRAVDIVETS, Y.P., (1994), Experiences with Embankment Dam Overtopping Protection, *Hydro Review*, February 1994, pages 1-6.

[29] RITSEMA, A.R. (1976), Tsunamis; alles verwoestende vloedgolven, *Natuur en techniek, jrg. 44*, *nr. 3,*1976, pp 164-179.

[30] SCHIERECK, G.J. (2001), Introduction to bed, bank and shoreline protection; engineering the interface of soil and water, *Delft University Press, Delft*

[31] SEA DEFENCE CONSORTIUM (Feb. 2007), Coastal Baseline Study Report, Vol II; Hydraulic Conditions, *SDC-R-60014.*

[32] SEA DEFENCE CONSORTIUM (Feb. 2007), Coastal Baseline Study Report, Vol III; Tsunami Modelling and Risk Assessment, *SDC-R-60014.*

[33] SEA DEFENCE CONSORTIUM (Feb. 2007), GEOTEKNIKA KONSULINDO, Draft report of geotechnical site investigation for Banda Aceh, Volume II, *SDC-RD-70016.*

[34] SPIELVOGEL, L.Q. (1976), Run-up of Single Waves on a Sloping Beach, in Tsunami Research, Heath, R.A., Cresswell, M.M., *Royal Society of New Zealand, Wellington*, pp 113-119.

[35] STEIN, S. OKAL, E.A. (January 2007), Ultralong Period Seismic Study of the December 2004 Indian Ocean Earthquake and Implications for Regional Tectonics and the Subduction Process, *Bulletin of the Seismological Society of America, Vol. 97*, No. 1A, pp S279-S295.

[36] STELLING, G.S. DUINMEIJER, S.P.A. (2003), A Staggered Conservative Scheme for every Froude Number in Rapidly Varied Shallow Water Flows, *International Journal for Numerical Methods in Fluids;* **43**:1329-1354.

[37] SYNOLAKIS, C.E. (1990), Tsunami Run-up on Steep Slopes: How Good Linear Theory Really Is, in Tsunami Hazard; a practical guide for tsunami hazard, Bernard, E.N., *Kluwer, Dordrecht*, pp 221-234.

[38] TANIMOTO, K (1981), On the Hydraulic Aspects of Tsunami Breakwaters in Japan, *Terra Scientific Publishing Company, Tokyo,*.

[39] TAW (1985), The use of asphalt in hydaulic engineering, Technical Advisory Committee on Waterdefences, *Rijkswaterstaat, The Hague.*

[40] TAW (2002), Technisch Adviescommissie voor Waterkeren, Technisch Rapport Asfalt voor Waterkeren, november 2002.

[41] THIO, H. K.,ICHINOSE, G., SOMERVILLE, P., (2005), Probabilistic Tsunami Hazard Analysis, *Risk Frontiers Quarterly Newsletter*, Vol. 5, Issue 1, July 2005.

[42] VERRUIJT, A. (1999) Grondmechanica, *Delft University Press, Delft*.

[43] VRIJLING, H. et al (1997), Probability in Civil Engineering; Part 1: The Theory of Probabilistic Design*, faculty of Civil Engineering Delft University of Technology, Delft*.

[44] WALTERS, R.A., (2005). A semi-implicit finite element model for non-hydrostatic (dispersive) surface waves, *International Journal for Numerical Methods in Fluids;* **49**: 721-737.

[45] WARD, N. (2000). Landslide tsunami, *Institute of Geophysics and Planetary Physics, University of California, Santa Cruz.*

[46] WARD, N. Tsunamis. *Institute of Tectonics, University of California, Santa Cruz.* Article for publication in Encyclopedia of Physical Science and Technology, Academic Press. Available from http://www.es.ucsc.edu/~ward/papers/tsunami_ency.pdf

[47] WILKINSON, F. (2005), Coastal design and Tsunami Mitigation, *United Nations High Commissioner for Refugees,* ISBN 085 825 796 3

[48] YAMAMOTO, Y, et al (2005), Verification of the Destruction Mechanism of Structures in Sri Lanka and Thailand due to the Indian Ocean Tsunami, in *Coastal Engineering Journal, Vol. 48,* No. 2 (2006) 117-145, *World Scientific Publishing Company and Japan Society of Civil Engineers.*

Sites on World Wide Web

[49] http://www.eri.u-tokyo.ac.jp/

[50] http://www.ngdc.noaa.gov
Tsunami Event Database of the National Geophysical Data Centre

[51] http://www.waveofdestruction.org

[52] http://www.asiantsunamivideos.com

[53] http://www.nerc-bas.ac.uk/tsunami-risks

[54] http://www.geophys.washington.edu/tsunami/general/physics/characteristics.html

[55] http://www.wldelft.nl

[56] http://earthquake.usgs.gov/

[57] http://www.nae.edu
National Academy of Engineering. Article by Robert A. Dalrymple and David L. Kriebel, Lessons in Engineering from the Tsunami in Thailand.

[58] http://www.infoplease.com/ipa/A0107634.html

[59] http://www.worldbank.org
[60] http://www.earth.northwestern.edu/people/seth/research/sumatra2.html
[61] http://www.ew.govt.nz/enviroinfo/hazards/naturalhazards/coastal/tsunami.htm
[62] http://intern.forskning.no/arnfinn/tsunami/tsunami_english.swf
Nice simulation of plate tectonics (subduction) and relation with tsunami wave
[63] http://www.thaiappraisal.org/pdfNew/Monthly_Forum/MF31_Land%20Seminar-Mr.%20Uji%20Hino.pdf
Interesting slide-show with many pictures of tsunami protection measures in Japan
[64] www.icdp-online.org/.../hawaii/Ringof_Fire.gif
Website of the International Continental Scientific Drilling Program
[65] http://news.bbc.co.uk/1/shared/spl/hi/pop_ups/05/sci_nat_enl_1111709134/html/1.stm
[66] http://www.andaman.org/mapstsunami/tsunami.htm
Website with lot of information about earthquakes and tsunamis around the Andaman and Nicobar Islands, northwest of Sumatra.
[67] http://www.dcrc.tohoku.ac.jp/index.html
Disaster Control Research Center of Tohoku University, Japan
[68] http://www.noort-innovations.nl/

APPENDICES

BELONGING TO THE FINAL THESIS REPORT:

"*A STUDY INTO THE FEASIBILITY OF TSUNAMI PROTECTION STRUCTURES FOR BANDA ACEH*
&
A PRELIMINARY DESIGN OF AN OFFSHORE RUBBLE-MOUND TSUNAMI BARRIER"

Author: Ton van der Plas, BSc.
Date: November 15, 2007

APPENDIX; TABLE OF CONTENTS

APPENDIX I. TSUNAMI THEORY 7

I - 1 TSUNAMI GENERATION 7
I.1.1 Tsunami intensity and magnitude scale 7
I.1.2 Fault types 8
I.1.3 Effect of landslide velocity on tsunami generation 10
I - 2 TSUNAMI PROPAGATION 11
I.2.1 Derivation tsunami wave speed and shoaling law 11
I.2.2 Typical refraction pattern 12
I - 3 SHORELINE INTERACTION 13
I.3.1 Comparing Bryant's breaking criterion with Iribarren number 13
I.3.2 Velocities 13
I - 4 INTERACTION WITH STRUCTURES 14
I.4.1 Tanimoto: wave pressure distribution (unbroken tsunami) 14
I.4.2 Cross: tsunami wave pressure distribution (bore) 16
I.4.3 Low-crested structures: overtopping volume Kaplan 17
I.4.4 Submerged structures; effectiveness in tsunami conditions 17
I.4.5 Soft measures; effectiveness in tsunami conditions 18

APPENDIX II. 1D-MODELLING WITH DELFT3D 21

II - 1 MODEL DESCRIPTION 21
II - 2 INUNDATION VOLUME; THEORY 22
II - 3 COMPARISON 23
II - 4 ADDITIONAL 1D-MODELLING 28
II - 5 FINDINGS 36

APPENDIX III. OVERVIEW 2D-MODEL RUNS 39

APPENDIX IV. MULTI-CRITERIA ANALYSIS 43

IV - 1 CRITERIA 43
IV - 2 SCORES 43
IV - 3 WEIGHTING FACTORS 45
IV - 4 VALUE / COST RATIO 46
IV - 5 SUMMARY 50

APPENDIX V. COST ANALYSIS FOR VARIOUS ALTERNATIVES 51

V - 1 OFFSHORE TSUNAMI BARRIER 51
V - 2 COASTAL TSUNAMI BARRIER 53
V - 3 INLAND TSUNAMI BARRIER 54
V - 4 OVERVIEW 55

APPENDIX VI. STABILITY CALCULATION; SLIDING 57

VI - 1 SLIDING ALONG ANY HORIZONTAL PLANE 57
VI - 2 SLIDING ALONG ANY CIRCULAR PLANE 64

APPENDIX VII. STABILITY CALCULATION; LIQUEFACTION 67

VII - 1 WHAT IS LIQUEFACTION? 67
VII - 2 HOW TO DETERMINE THE LIKELIHOOD OF LIQUEFACTION 67
VII - 3 RESULTS 69

APPENDIX VIII. STABILITY CALCULATION; ARMOUR LAYER 75

VIII - 1 ARMOUR LAYER FRONT SIDE 75
VIII - 2 TOE STRUCTURE 79
VIII - 3 REQUIRED BREAKWATER HEIGHT UNDER STORM CONDITIONS 79
VIII - 4 CONSIDERATIONS ARMOUR LAYER REAR SIDE 80
VIII - 5 ASPHALT LAYER REARSIDE 83
VIII - 6 ARMOUR LAYER ON THE BREAKWATER HEADS 85
VIII - 7 DRAWINGS 87

APPENDIX IX. 1D-PROGRAM (FORTRAN) 91

IX - 1 THEORY 91
IX - 2 MODELLING 91
IX - 3 OUTPUT 94
IX - 4 VALIDATION 97
IX - 5 FINDINGS STRUCTURE MODELLING 101
IX - 6 FINDINGS ABOUT INFLUENCE BATHYMETRY ON INUNDATION 102

LIST OF REFERENCES 104

APPENDIX; LIST OF FIGURES

Figure I-1 Dip-slip and strike-slip faults and associated angels [56], [32] 9
Figure I-2: Different wave shapes for equal earthquake magnitudes [46] 10
Figure I-3 Tsunami height vs. slide thickness as function of relative velocity [45] 11
Figure I-4 Refraction in a bay, at a headland and around an island [53] 12
Figure I-5 Wave pressure distribution due to non-breaking long-period waves [38] 14
Figure I-6 Definition sketch of submerged breakwater [27] 17
Figure I-7 Reduction of waves by submerged breakwaters [27] 18
Figure I-8 Coastal forest width and reduction rate of inundation [12] 19
Figure II-1: Cross-sectional and schematic view of the model area 21
Figure II-2 Overview of the possible sea defence measures 22
Figure II-3 Cross section and definitions 22
Figure II-4 Correlation 1D-model results with Kaplan; Seawall 24
Figure II-5 Correlation 1D-model results with Kaplan; Breakwater 24
Figure II-6 Correlation 1D-model results with Kaplan; Mangrove 25
Figure II-7 Inundation length with Kaplan compared with 1D-model results for 2 structure types (because H is at the shoreline, the wave heights for the breakwater are adjusted to account for shoaling) 26
Figure II-8 Successive penetration of 3 waves for the case H=10m, h=5m. The red line indicates the maximum water level in case there is no structure. The blue line is the maximum water level for the simulated case with structure. 27
Figure II-9 1D model: Maximum water levels for varying bathymetry. $H_{boundary}$=6m. 29
Figure II-10 Maximum water level with Lhok'Gna profile 30
FigureII-11 Offshore Breakwater: Maximum run-up for 1D-profile (existing run, see upper part) and maximum run-up for 2D-profile (lower part) 31
FigureII-12 Coastal Barrier. 1D model: Maximum run-up for 2 different profiles 31
FigureII-13 Inland Barrier. 1D model: Maximum run-up for 2 different profiles 31
FigureII-14 Various tsunami shape signals as applied on the open (left) boundary of the model 33
FigureII-15 1D model: Maximum water levels for varying signal shape. H_c=10m. 33
FigureII-16 Timeframe of a run with two opposite signals running up a linear slope 34
FigureII-17 Comparison between effectiveness of seawall +4m, inland wall +4m and combined measure. 35
FigureII-18 Comparison between effectiveness of offshore barrier+5m, seawall+5m and combination 36
Figure III-1 Inundation level - Offshore barrier of 7 metres with 2 x 200 metre openings [32]. 41
Figure III-2 Inundation level - Coastline barrier of 11 metres with 3 x 100 metre openings [32]. 41
Figure III-3 Inundation level - Inland barrier of 7 metres with 4 x 100 metre openings [32]. 42
FigureIV-1 Scores for each alternative 44
Figure IV-2 Results MCA: Appreciation of various alternatives 46
Figure IV-3 Total Value and Ranking for various alternatives 48
Figure IV-4 Value/cost ratios for various alternatives; Case 1 49
Figure IV-5 Value/cost ratios for various alternatives; Case 2 49
Figure V-1 Cross-section Offshore Tsunami Barrier at -10m Bathymetry line 51
Figure V-2 Overview construction- and additional costs for the main alternatives 56
Figure VI-1 Two situations when sliding could occur. Left figure: increased water level at landside and dropdown at seaside; seaward sliding. Right figure: increased water level at seaside and lowering water level at landside; landward sliding. 57
Figure VI-2 Two considered situations 57
Figure VI-3 Resistance against sliding for each distance from crest breakwater 59
Figure VI-4 Sliding; resistance and load according to Tanimoto 59
Figure VI-5 Maximum waterlevel, velocity and energyhead around the structure 61
Figure VI-6 Definitions according to Tanimoto 61

Figure VI-7 Resistance against sliding; Kato, Tanimoto and 1D-model 63
Figure VI-8 Resistance against sliding; Kato; Tanimoto and 1D-model. ZOOM 64
Figure VI-9 Stability against circular sliding for Load Case 2. Output from MStab. 65
Figure VII-1 Definitions of area boundaries according to Japanese Standard 68
Figure VII-2 Overview offshore SPT locations. Location B-06 is at -13m. 69
Figure VII-3 SPT-values for 6 offshore locations 70
Figure VII-4 Results N_{eq} versus a_{eq} in Japanese Standard Graphs for 6 boreholes 72
Figure VII-5 Grain size distribution for boreholes B-01 and B-04 73
Figure VII-6 Total vertical stresses at seabed level. Values in kN/m^2. 74
Figure VIII-1 Cross section of offshore barrier; starting point for technical design. 75
Figure VIII-2 Maximum water level, velocity and energy head around structure 76
Figure VIII-3 Overview of SWAN output-locations [33] and breakwater location 77
Figure VIII-4 Maximum water level, velocity and energy head around structure 80
Figure VIII-5 Duration of peak velocities over structure. 81
Figure VIII-6 Relation between *D* and *y* 82
Figure VIII-7 Required stone diameter with Izbash and “CERC-formula” 83
Figure VIII-8 Definition parameters h_1, h_2, d and α 84
Figure VIII-9 Velocity field (maximum) for Dec2004 Tsunami and offshore barrier +5m. Scale is in m/s. 85
Figure VIII-10 General layout of scour and flow pattern in gap. Source [14] 86
Figure VIII-11 Cross section Offshore Tsunami Barrier; composition 88
Figure VIII-12 Cross section Offshore Tsunami Barrier; dimensions and quantities 88
Figure VIII-13 Plan view and cross section of gap and general layout of gap protection 89
Figure VIII-14 3-D impression of offshore tsunami barrier; gap 90
Figure VIII-15 3-D impression of offshore tsunami barrier; composition 90
Figure IX-1 Typical foreshore bathymetry Banda Aceh 92
Figure IX-2 Original and schematized signal at -20m. 92
Figure IX-3 Foreshore bathymetry with structure. 94
Figure IX-4 Maximum water level and velocity over structure. 95
Figure IX-5 Maximum water level, velocity and energy head around structure, fm=0,035 95
Figure IX-6 Maximum water level, velocity and energy head around structure, fm=0,035 96
Figure IX-7 Maximum momentum per grid cell 96
Figure IX-8 Duration of peak velocities over structure. 97
Figure IX-9 Maximum velocities and water levels for offshore breakwater 98
Figure IX-10 Detailed view on the crest and output points 99
Figure IX-11 Wave overtopping definition sketch (after Schűttrumpf et al. [7]) 100
Figure IX-12 Velocities with Schűttrumpf and 1D-model 101
Figure IX-13 Maximum shoaling at the coast for various foreshore bathymetries 103

APPENDIX; LIST OF TABLES

Table I-1: Earthquake magnitude, Tsunami Magnitude, Intensity and Tsunami Run-up Heights 7
Table III-1: Overview model runs for offshore alternatives, all for M_w = 9,2. 39
Table III-2: Overview model runs for the coastal alternatives, all for M_w = 9,2. 39
TableIII-3: Overview model runs for inland alternatives, all for M_w = 9,2. 40
TableIV-1: Determination of weighting factors 45
TableV-1: Cost estimation offshore tsunami barrier at -10m bathymetry line 51
TableV-2: Cost estimation coastal tsunami barrier, 11m height 53
TableV-3: Cost estimation Inland tsunami barrier, 8m height 55
TableVII-1: Overview bore locations 74
Table VIII-1: Design wave heights, periods and water levels for various return periods [31] 77
Table IX-1: Depths and velocities on the crest 98
Table IX-2: Velocities on the back side with Schűttrumpf 101

Appendix I. TSUNAMI THEORY

This Appendix presents some background information for Chapter 2. To make it readable on its own, some parts will be similar to the text in Chapter 2.

I - 1 TSUNAMI GENERATION

I.1.1 Tsunami intensity and magnitude scale

The most common cause of tsunami is seismic activity. However, not every earthquake is powerful enough to trigger a tsunami.

In order to define the quantity of energy involved in a tsunami, a tsunami scale is introduced. Imamura and Iida proposed a magnitude scale, where the magnitude is linked to the maximum tsunami run-up.

$$m_{II} = \log_2 H_{r;\max}$$

m_{II} = Imamura-Iida tsunami magnitude scale [-]
$H_{r;max}$ = the maximum tsunami run-up height

An empirical relation between m and the earthquake magnitude M_w is[29]:

$$m = (2{,}6 \pm 0{,}2)M_w - (18{,}4 \pm 0{,}5)$$

The margins are in the order of 2%-8% and due to differences in depth and fault-type.

In Table I-1 the tsunami magnitude m and the corresponding run-up is listed and related to an earthquake magnitude on Richter scale. Only earthquakes of magnitude 7,0 or greater are responsible for significant tsunami waves with run-ups in excess of 1m. However, as an earthquake's magnitude rises above 8,0, the run-up height and destructive energy increases dramatically.

Table I-1: Earthquake magnitude, Tsunami Magnitude, Intensity and Tsunami Run-up Heights

Earthquake Magnitude Richter Scale	Tsunami Magnitude m_{II}	Maximum Run-up [m]	Intensity *I*	Mean Run-up [m]
6.0	-2	<0,3	- 2	0,2
6.5	-1	0,5-0,75	-1	0,4
7.0	0	1,0-1,5	0	0,8
7.5	1	2,0-3,0	1	1,5
8.0	2	4,0-6,0	2	3
8.2	3	8,0-12,0	3	6

Earthquake Magnitude Richter Scale	Tsunami Magnitude m_{II}	Maximum Run-up [m]	Intensity *I*	Mean Run-up [m]
8.5	4	16,0-24,0	4	12
8.8	5	>32,0	5	24

Solovies and Go (Soloviev and Go, 1975) [11] proposed an intensity scale i that is based on the mean tsunami run-up height $\overline{H}_r$ along a section of the coastline:

$$i = \log_2(\overline{H}_r \sqrt{2})$$

Comparison between the two definitions suggests that the maximum run-up height is √2 times the mean run-up height along a stretch of the coast.

Besides the earthquake magnitude as important variable in explaining the initiation of tsunamis, also the focal depth (i.e. the depth of the epicenter) is of importance.

Ritsema [29] listed 2 conditional expressions for the generation of tsunamis:

$$M(m \geq 1) = 6{,}3 + 0{,}015 D_f$$
$$M(m \geq 2) = 7{,}7 + 0{,}009 D_f$$

where D_f = focal depth of the earthquake in [km] and M is the earthquake magnitude on Richter scale which is required to generate a tsunami magnitude higher than mentioned in the argument. For example, to generate a tsunami of at least magnitude 2, with a focal depth of 30km, one needs at least an 8.0 magnitude earthquake.

I.1.2 Fault types

Two main fault types can be distinguished: a dip-slip and a strike slip fault. A dip-slip earthquake can be on a vertical or a dipping plane, where the latter is called a thrust-dip. These fault types can be in normal and reverse direction, see Figure I-1

In each case rupturing can occur at any point along the fault line. This point is known as the focal depth of the epicentre. The hypocenter is the centre of the earthquake and the epicentre is its perpendicular projection on the Earth's surface. The distance in between defines the depth of the earthquake.

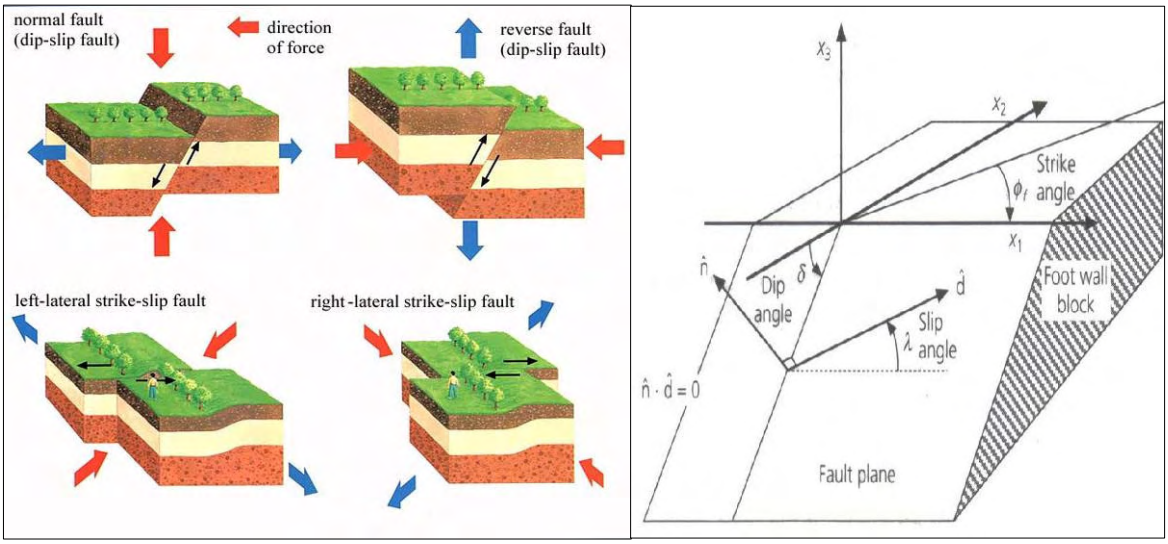

Figure I-1 Dip-slip and strike-slip faults and associated angels [56], [32]

The orientation of the rupture plane depends on two angles. The direction of the fault plane relative to the Earth's local surface is defined by the dip angle δ. The strike angle Φ_f is the clockwise angle between the geographical north and the strike. The classification of an earthquake is determined by the slip angle λ, which indicates the direction in which the upper block moves with respect to the lower block. The main types are the dip-slip (λ=±90°) and strike-slip (λ=0°, 180°). The magnitude of an earthquake is associated with the amount of the movement along the plane, the so-called slip.

While the vertical dip-slip (with δ ≈ 90°) mechanism seems to be a logical one for tsunami generation because it abruptly displaces large sections of the seafloor vertically, the area of uplift cancels out the area of subsidence, resulting in small or non-existent tsunami. But this mechanism is still better at producing tsunami than the strike-slip pattern. The thrust dip-slip fault is the most preferred fault mechanism for tsunami generation. Shallow subduction zones earthquakes are one of the most common sources of destructive tsunamis in the world. Subduction zones typically have average dip values of δ ≈ 25° ± 9°, with the largest tsunami associated with higher dip values. As the dip-angle (δ) decreases, the tsunami is more likely to have a leading trough.

Tsunami wave characteristics are highly variable. Figure I-2 shows that a same earthquake magnitude can result in widely different waves: a deep fault movement produces a wave with lower amplitude than a shallower one.

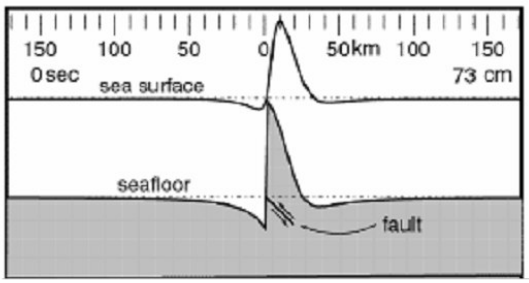

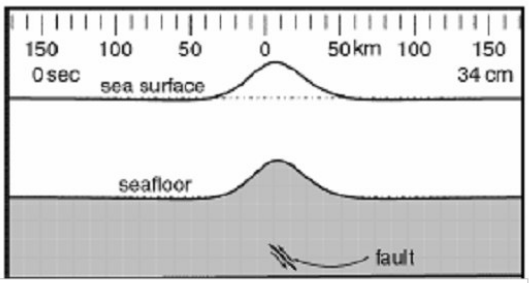

Left: tsunami from a M7.5 thrust earthquake. The fault strikes north-south (into the page) and the sections are taken east-west.

Right: tsunami from the M7.5 thrust earthquake of **left fig.**, now buried 30 km. Deeper earthquakes make smaller and longer wavelength tsunamis.

Figure I-2: Different wave shapes for equal earthquake magnitudes [46]

This indicates that (general) relations between earthquake and resulting tsunami magnitude, intensity or run-up are not suited for design purposes.
This is also illustrated by another event: on Friday 17 July 1998, the Pacific Tsunami Warning Centre detected the Papua New Guinea earthquake with a magnitude of 7.1 and an aftershock of 5.75. The Warning Centre issued an innocuous tsunami information message about an hour later. In the meantime a devastating tsunami struck the Sissano coastline (Papua New Guinea). The inundation depth averaged 10m along 25km of coastline, reaching a magnitude of 17,5m elevation. The penetration length was about 4km. Over 2200 people lost their lives [3], [49].

I.1.3 Effect of landslide velocity on tsunami generation

Wave generation by landslides depends primarily upon the volume of the material moved and submerged, the speed of the landslide and the mechanism of movement.
Wave size increases with landslide volume, not only because the obvious reason that a greater volume contains more energy, but also because larger landslides experience less basal friction and turbulent drag in relation to their size and therefore move further and faster [45].
The efficiency of wave generating increases with the speed of the landslide, typically to the point where the landslide velocity equals the velocity of the waves that it produces. At this point, wave resistance will prevent further acceleration. Above this point, the tsunami height decreases again. Slides that happen too fast or too slow are inefficient tsunami generators. Ward [45] has investigated this and the results of his modelling are depicted in Figure I-3, where the relative wave height (tsunami height divided by landslide thickness) is shown as a function of the relative velocity (slide velocity divided by tsunami velocity i.e. $\sqrt{gd}$)

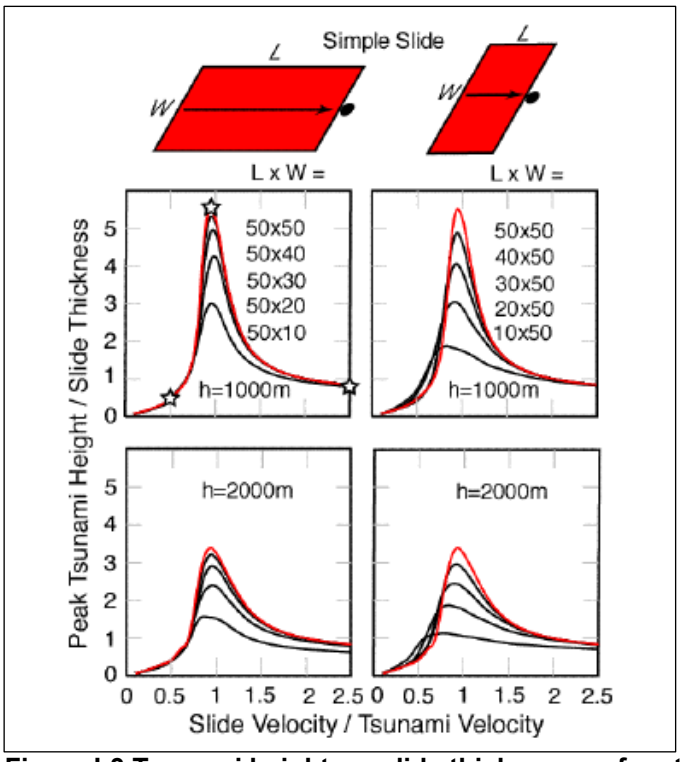

Figure I-3 Tsunami height vs. slide thickness as function of relative velocity [45]

Generally, the wavelengths and periods of landslide-generated tsunami range between 1 and 10km and 1 and 5 minutes respectively. These values are much shorter than those produced by earthquakes.

I - 2 TSUNAMI PROPAGATION

I.2.1 Derivation tsunami wave speed and shoaling law

The simplest means of analyzing the wave motion, where the ratio of wave height to water depth (H/d) is small, is to use the shallow water equations.

For small values of H/d: $$c^2 = \frac{gL}{2\pi}\tanh\left(\frac{2\pi d}{L}\right)$$

Tsunamis are shallow waves (L>>d) so, letting d/L → 0, $$\tanh\left(\frac{2\pi d}{L}\right) \to \frac{2\pi d}{L}$$

Combining this (after substitution): $$c = \sqrt{gd}$$

In this approach, the velocity of the wave depends only on the water depth. In deep oceans, the wave travels with a speed comparable of that of jet planes.

Because the wave celerity is independent of the wave period, all waves travel at the same speed. This means that no dispersion occurs. Some remarks on this assumption will be described later.

For small amplitude waves, the energy can be calculated by: $E = \frac{1}{8}\rho g H^2 L$.

In case of an un-refracted wave, energy conservation yields:

$$E_1 = E_2 \rightarrow \left(\frac{1}{8}\rho g H^2 L\right)_1 = \left(\frac{1}{8}\rho g H^2 L\right)_2 \rightarrow \frac{H_2}{H_1} = \sqrt{\frac{L_1}{L_2}}$$

but as $L = cT$, and T is assumed to be constant, and as $c = \sqrt{gd}$ for shallow water waves, the change in wave height becomes:

$$\frac{H_2}{H_1} = \left(\frac{d_1}{d_2}\right)^{\frac{1}{4}}$$

This equation is the well-known Green's Law and describes the shoaling process of waves propagating in decreasing water depth.

I.2.2 Typical refraction pattern

See Figure I-4 for typical refraction pattern.

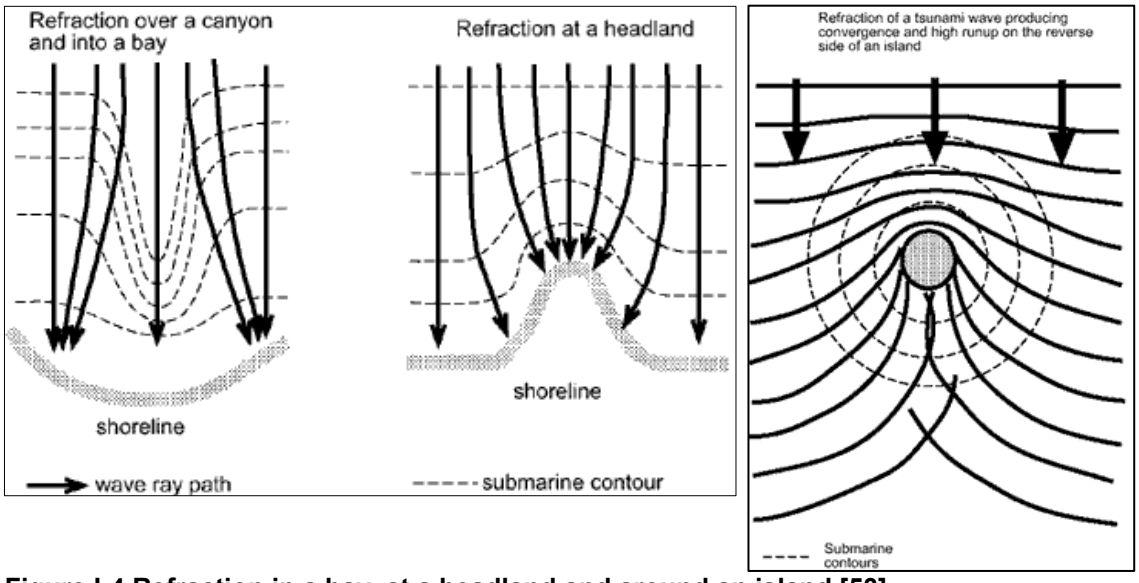

Figure I-4 Refraction in a bay, at a headland and around an island [53]

I - 3 SHORELINE INTERACTION

I.3.1 Comparing Bryant's breaking criterion with Iribarren number

Bryant presents a breaking criterion for tsunami waves on a slope [3]:

$$B_r = \frac{\varpi^2 H}{g \tan^2 \beta}$$

The angular frequency $\varpi = \frac{2\pi}{T}$ and β is the slope of the bottom. If B_r > 1 the waves break down. Although this equation is presented as a specific tsunami-breaker criterion, the similarity with the well-known Iribarren-parameter is surprising. This parameter reads [30]:

$$\xi = \frac{\tan \beta}{\sqrt{H / L_0}}$$

Where $L_0 = \frac{gT^2}{2\pi}$. The transition between breaking and non-breaking lies around ξ = 3-5, where a higher value indicates non-breaking conditions. Writing the Iribarren parameter in an opposite way, it is comparable to Bryant's expression. Rewriting the Iribarren parameter gives:

$$\left(\frac{1}{\xi}\right)^2 = \frac{H}{\tan^2 \beta \cdot L_0} = \frac{2\pi \cdot H}{gT^2 \tan^2 \beta} = \frac{\frac{2\pi}{T^2} \cdot H}{g \tan^2 \beta} = \frac{1}{2\pi} \cdot \frac{\varpi^2 H}{g \tan^2 \beta} = \frac{B_r}{2\pi}$$

Comparing ξ with Br finally gives $\xi = \sqrt{\frac{2\pi}{B_r}} \approx 2{,}51$. Bryant's expression is similar to the Iribarren expression with a breaking limit of 2,51 instead of 3 to 5. This indicates that tsunami waves show almost the same behaviour as wind or swell waves. Only, the very long wavelength and period of tsunami changes the notions 'steep' and 'gentle' completely. This is clearly illustrated by the fact that most tsunami do not break on beaches with slopes of 1:100 and steeper, but surge onto shore and are even reflected. For a tsunami of 6m-height and a period of 20min, a slope of 1:100 is just as steep as a slope of 1:1 is for a wave with a period of a few seconds.

I.3.2 Velocities

For surge run-up on a dry bed, Keulegan (1950) gives $u = 2\sqrt{gh}$, while Fukui (1963) gives a lower value of [4]:

$$u = 1{,}83\sqrt{gh}$$

Latter equation yields velocities of 5,4m/s for 3m high tsunami. Slope and bed roughness can be incorporated as follows:

$u = \frac{H_c^{0,7}\sqrt{\tan\beta_w}}{n}$, where β_w is the slope of the water surface in degrees. Typical values range between 0,001 and 0,0025, increasing with slope.

This yields velocities of 2 á 3 m/s for 3m high tsunami with n=0,035.

For tsunami waves propagating inland, Iizuka and Matsutomi (2000) [47] proposed to use:

$$u = 1{,}1\sqrt{gh}$$

With h is the inundation depth. Yamamoto [47] investigated the damage to structures in Sri Lanka on basis of this expression and they found a good agreement with observations.

I - 4 INTERACTION WITH STRUCTURES

I.4.1 Tanimoto: wave pressure distribution (unbroken tsunami)

To determine the forces on a vertical wall due to tsunami forces, Tanimoto studied the wave pressure distribution for different values of h/L. Based on these results and Goda's formula for storm waves, a wave pressure distribution to calculate tsunami forces on a vertical wall is proposed. This method is only valid for relatively deep water offshore, so that no breaking tsunami occurs.

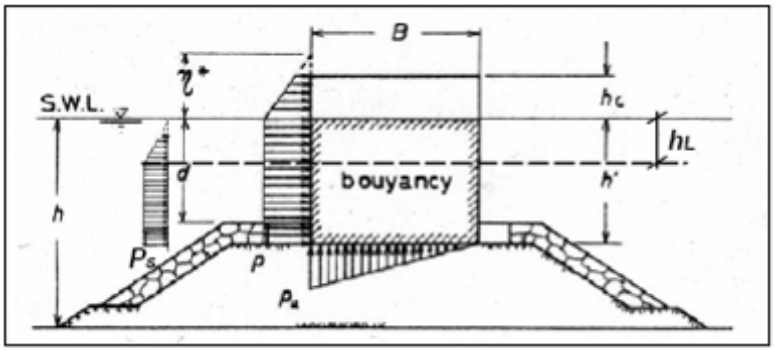

Figure I-5 Wave pressure distribution due to non-breaking long-period waves [38]

$$\eta^* = 1{,}5H$$
$$p = p_u = 1{,}1 w_0 H$$

where η^* is the height above the still water level at which the wave pressure intensity is zero, p is the wave pressure intensity which acts uniformly on the vertical wall below the still water level, and p_u is the intensity of the toe uplift pressure. The total horizontal wave force P, uplift force U, and the overturning moment around the heel of the caisson, MP, and MU, are expressed as follows:

$$P = \left\{1 + \left(1 - \frac{h_c^*}{3H}\right)\frac{h_c^*}{h'}\right\} ph'$$

$$M_P = \left\{\frac{1}{2} + \left(1 - \frac{h_c^*}{3H}\right)\frac{h_c^*}{h'} + \left(\frac{1}{2} - \frac{4}{9}\frac{h_c^*}{H}\right)\left(\frac{h_c^*}{h'}\right)^2\right\} ph'^2$$

$$U = \frac{1}{2} p_u B$$

$$M_U = \frac{1}{3} p_u B^2$$

Where $h_c^* = \min\{\eta^*, h_c\}$

Tanimoto also incorporated the influence of a water-lowering at the backside of the structure (h_L, see Figure I-5). This lowering causes a decrease of the resisting water pressure at the backside, but on the other hand increases the structure weight. The horizontal force P_s due to the lowering is (so, acting in the direction of the tsunami force!),

$$P_s = w_0 h_L \left(h' - \frac{1}{2} h_L\right)$$

The arm, to the heel of the caisson, associated with this force is:

$$X_{P_s} = \frac{k}{2} + \frac{h_L}{24k}$$

with $k = \left(h' - \frac{1}{2} h_L\right)$. Consequently the moment can be calculated by:

$$M_{P_S} = w_0 h_L \left\{\frac{1}{2}\left(h' - \frac{1}{2} h_L\right)^2 + \frac{1}{24} h_L\right\}$$

The safety factors against sliding, $S_{sliding}$, and against overturning, $S_{overturning}$, are examined as follows:

$$S_{sliding} = \frac{\mu(W_0 - U)}{P + P_s}$$

$$S_{overturning} = \frac{W_0 X_{W_0} - M_u}{M_P + M_{P_s}}$$

Where W_0 is the weight of the structure under water, taking the lowering of the water level into account and μ is the friction between the concrete (of the caisson) and the rubble mound of which it is founded. Typically this value is taken to 0,6.

I.4.2 Cross: tsunami wave pressure distribution (bore)

The velocities within non-broken tsunami are relatively low. Most of the initial damage of such tsunami will be due to buoyancy and hydrostatic forces. The withdrawal of the tsunami occurs in many cases much more rapidly than the runup, also causing more damage than the initial wave loading.

When the tsunami forms a borelike wave, the current velocities are much higher. The dynamic water pressure will increase too. Another important parameter is the inclination of the face of the bore. The steeper the face of the bore, the higher is the impact on a structure.

Cross (1967) in [4] showed that the force per unit length of a vertical wall, from the leading edge of a surge impinging normally to the wall, could be given as:

$$P = \frac{1}{2}\rho g H^2 + C_F \rho u^2 H$$

With H the height of the surge, $1{,}83\sqrt{gH} < u < 2{,}0\sqrt{gH}$, and:

$$C_F = (\tan\theta)^{1,2} + 1$$

Where θ is the inclination of the water surface relative to a horizontal line
C_F accounts for both inertial and drag forces. After some derivation, the relation becomes:

$$P = \frac{1}{2}\rho g H^2 + \left[\left(\frac{4gn^2}{H^{1/3}}\right)^{1,2} + 1\right]\rho u^2 H$$

With n is the Manning roughness coefficient. For a typical value of n = 0,035, H = 6,0, the coefficient C_F becomes 1,012. This is quite low, but the high velocities (up to $2{,}0\sqrt{gH}$) used by Cross makes the hydrostatic component a relatively small part of the total force.

I.4.3 Low-crested structures: overtopping volume Kaplan

Kaplan [4] developed an empirical equation for the volume of overtopping of a seawall at the shoreline. This equation is written as:

$$V = \frac{21{,}65\left(KH_c - h_w\right)^3}{K^2 H_c}$$

where V is the quantity of overtopped water, h_w the height of the seawall and $K = \frac{H_r}{H_c}$, with H_r the vertical height of the wave run-up on a similar wall high enough to prevent overtopping.

For H_c = 8m, h_w = 4m, and K = 2, the volume per m^1 length (for a single wave!) becomes 1170m^3. For a wave period of 10 minutes, this amounts to 1950 litres / second for every meter length. However, the total inundation volume due to a tsunami wave train is much more, as shown in Appendix I. This is mainly due to the fact that a tsunami consists of several waves.

I.4.4 Submerged structures; effectiveness in tsunami conditions

Another way of reducing waves is by submerged structures (breakwaters, artificial reefs, etc). Pylarczyk [27] gives an overview of formulas to determine the wave transmission coefficient KT for different values of the relative crest width, B/L_0, and crest height, R_c/H_{si}, where R_c is the height of the breakwater above water level and H_{is} the incident significant wave height.

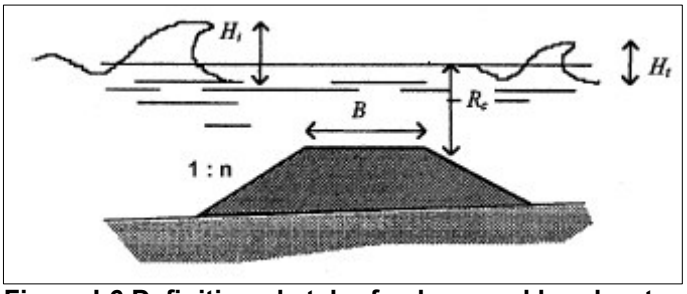

Figure I-6 Definition sketch of submerged breakwater [27]

The original formula of d'Angremond&Van der Meer&de Jong complies rather well with the measurement depicted in Figure I-7. The formula reads:

$$K_T = -0{,}4\frac{R_c}{H_i} + \left(\frac{B}{H_i}\right)^{-0{,}31}\left[1 - \exp\left(-0{,}5\xi\right)\right]\cdot C$$

With ξ the Iribarren parameter and C=0,64 for permeable and 0,8 for impermeable structures.

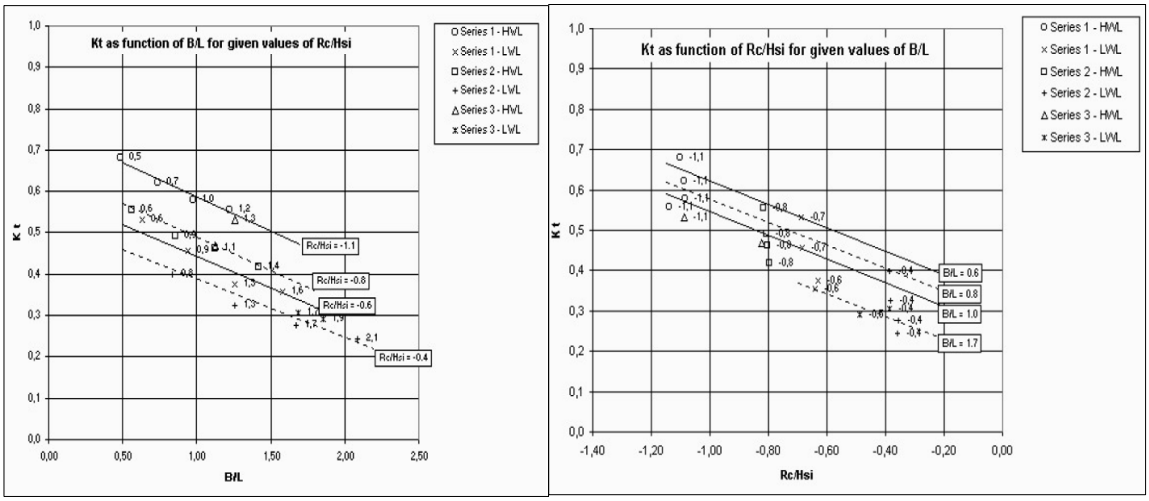

Figure I-7 Reduction of waves by submerged breakwaters [27]

From both graphs in Figure I-7 it becomes clear that the effectiveness of a submerged structure depends on the ratio B/L and R_c/H_{si}. Decreasing these ratios will increase the transmission and thus decrease the effectiveness of the structure.
Therefore, it is expected that for tsunami with wave lengths in the order of kilometres, the effectiveness of submerged structures is limited. The ratio B/L is almost zero, which corresponds with a high transmission.

I.4.5 Soft measures; effectiveness in tsunami conditions

Instead of hard structures, trees and other dense vegetation may offer some protection against tsunami. Groves of trees can dissipate tsunami energy and reduce surge heights, but may also be sheared off and add debris to the flow.

For limited tsunami heights, the reduction rate of the inundation depth is studied by Harada and Kawata,[12]. The resulting reduction rates for different tsunami heights are presented in Figure I-8.

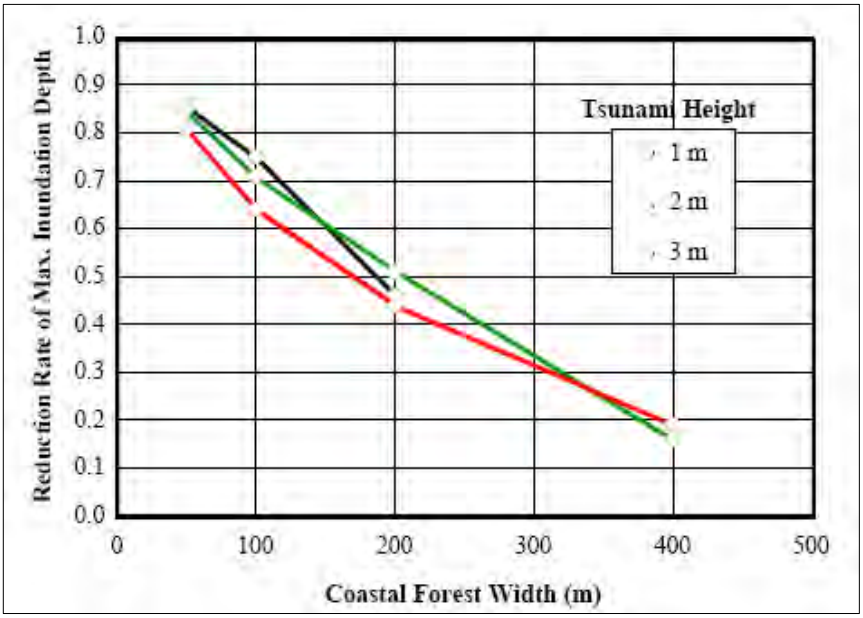

Figure I-8 Coastal forest width and reduction rate of inundation [12]

In this study, the density of the forest is 30 trees per 100m^2 and the trunk diameter 15cm. It was found that coastal forest is generally collapsed by tsunami of over 4m height. According to this study, the coastal forest could reduce tsunami inundation depth with 50-60% and flow velocity to 40-60% in case of a tsunami wave height of 3m

Surveys and analysis of field data ([16][18][20]) on one hand indicate that forests can be effective in tsunami reduction but on the other hand argue the effectiveness.

Appendix II. 1D-MODELLING WITH DELFT3D

II - 1 MODEL DESCRIPTION

The model covers a sea area up to 20m-depth line from the coast and it has a length, Ls, that equals approximately 3 km (see Figure II-1). Approximately 7 km (L) stretch of land is included in the model to allow this area to be (partly) inundated. Within this area one or more sea defence structures will be incorporated.

The friction parameters resemble typical values for offshore, vegetated and build-up areas. See Chapter 2.

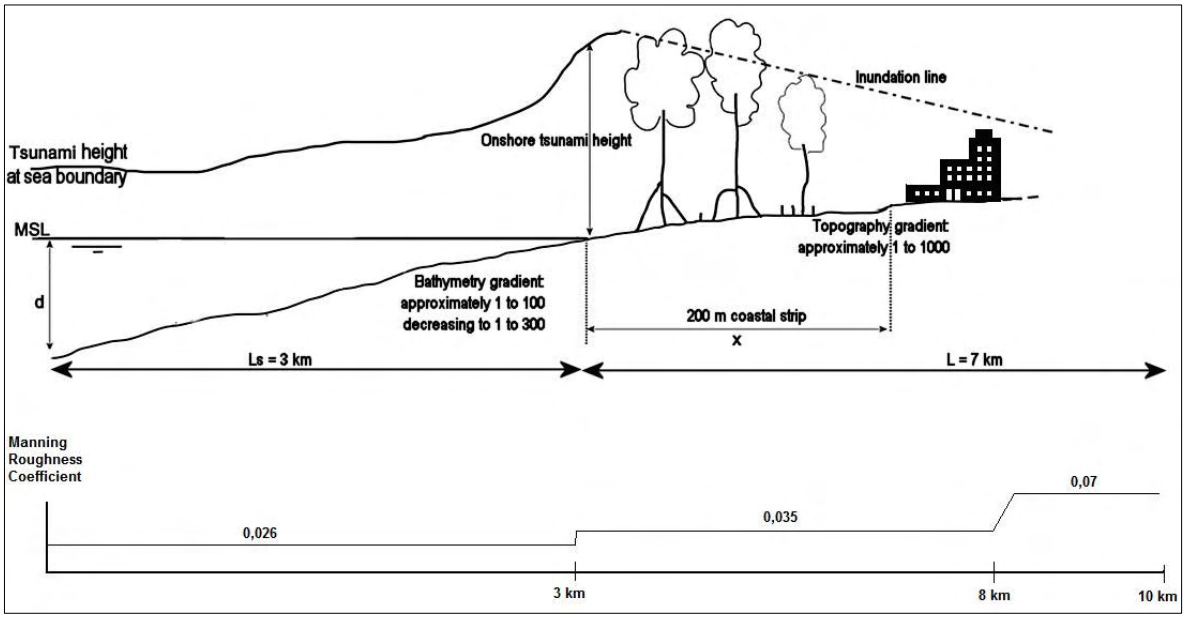

Figure II-1: Cross-sectional and schematic view of the model area

Three separate defence measures that may be applied independently or in combination, are contemplated in this study (see Figure II-2):

- Building of a near shore breakwater at 10m depth with respectively freeboard dimensions: -5m, 0m, 5m, 10m and 13m. The slope that is applied in the scenarios amounts to 3:2.
- Building of a seawall with a height of approximately 2 and 5 meters at 200 m distance from coastline. The slope that is applied in the scenarios amounts to 3:2.
- Cultivate a mangrove forest with a width of 200m, 100m and 50m behind the shore line

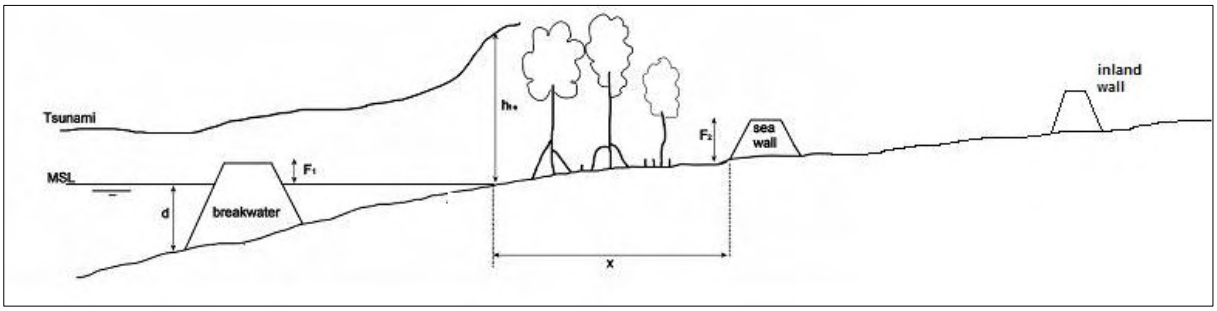

Figure II-2 Overview of the possible sea defence measures

In total 27 runs are carried out. They will not be listed here, since these runs already existed. The conclusion is presented in Chapter 4.

II - 2 INUNDATION VOLUME; THEORY

The existing 1D-model results are compared with the (overtopping) theory presented in Chapter 2. The equation proposed by Kaplan for the overtopping volume for a single wave reads:

$$V = \frac{21{,}65(KH - h)^3}{K^2 H}$$

Where H is the tsunami height at the shoreline, h the structure height, K the ratio H_r / H, with H_r the run-up of the wave against a structure high enough to prevent overtopping.

The bathymetry as defined in enables to derive a simple relation between the overtopping volume and inundation length L.

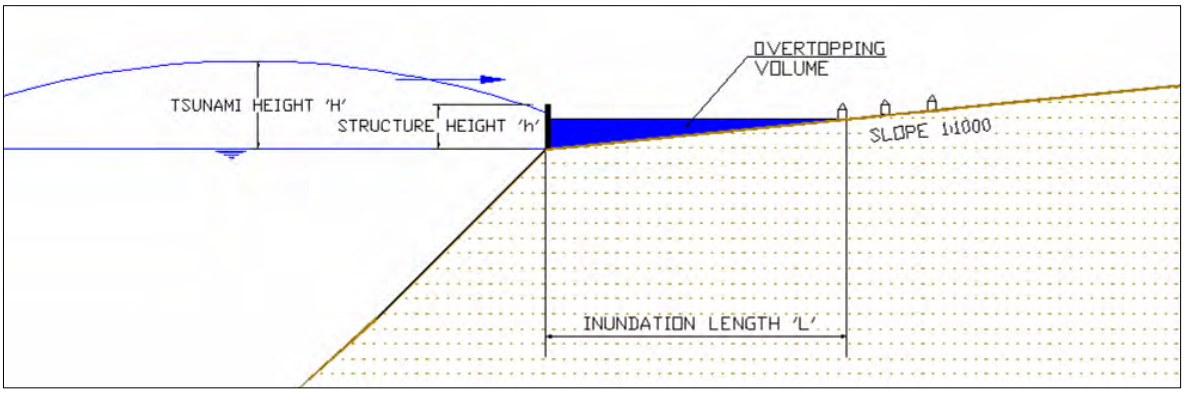

Figure II-3 Cross section and definitions

The inundation length L is related with overtopping volume V as follows (see also Figure II-3):

$$V = \frac{1}{2}\tan\beta \cdot L^2 \rightarrow L = \sqrt{\frac{2V}{\tan\beta}}$$

With V written according to Kaplan and tan β = 1/1000, the relation between tsunami height, structure height and K becomes:

$$L = 208{,}1\sqrt{\frac{(KH-h)^3}{K^2H}}$$

It must be noted that this overtopping corresponds to a single wave. For the overtopping of several successive waves no theoretical relation exist.

II - 3 COMPARISON

The correlation between $\sqrt{\frac{(KH-h)^3}{K^2H}}$ and the 1D-model inundation results is investigated for different values of K (2 to 5). The best fit was found with K=2, corresponding with a run-up of twice the incoming wave height. The results are presented in Figure II-4 to Figure II-6. Negative freeboards (i.e. submerged structures) are not taken into account.

Although the reduction of the wave height and inundation by mangrove is due to another mechanism (friction instead of reflection), the correlation is still presented in order to give a complete overview of the model results.

The R-squared value between Kaplan's expression and the 1D-model results varies between 0,74 and 0,84. The lowest value corresponds with overtopping of mangrove. Although the amount of data points is somewhat low (especially for the seawall runs), the agreement between theory and model results is reasonable.

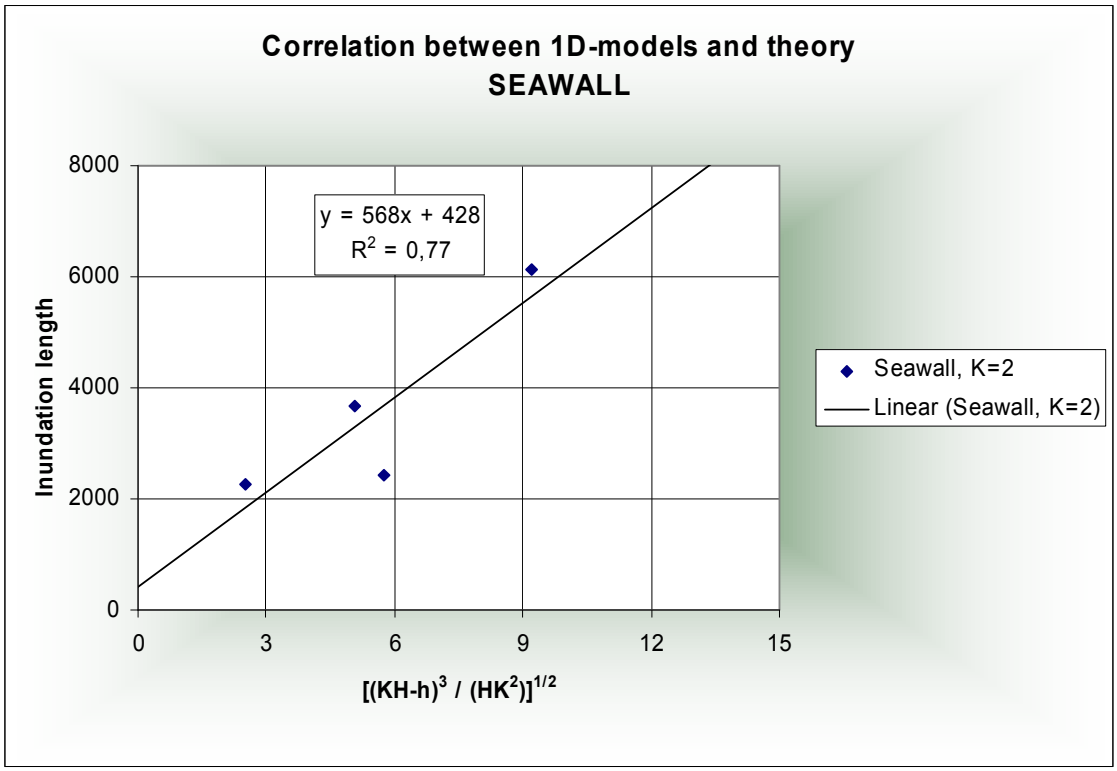

Figure II-4 Correlation 1D-model results with Kaplan; Seawall

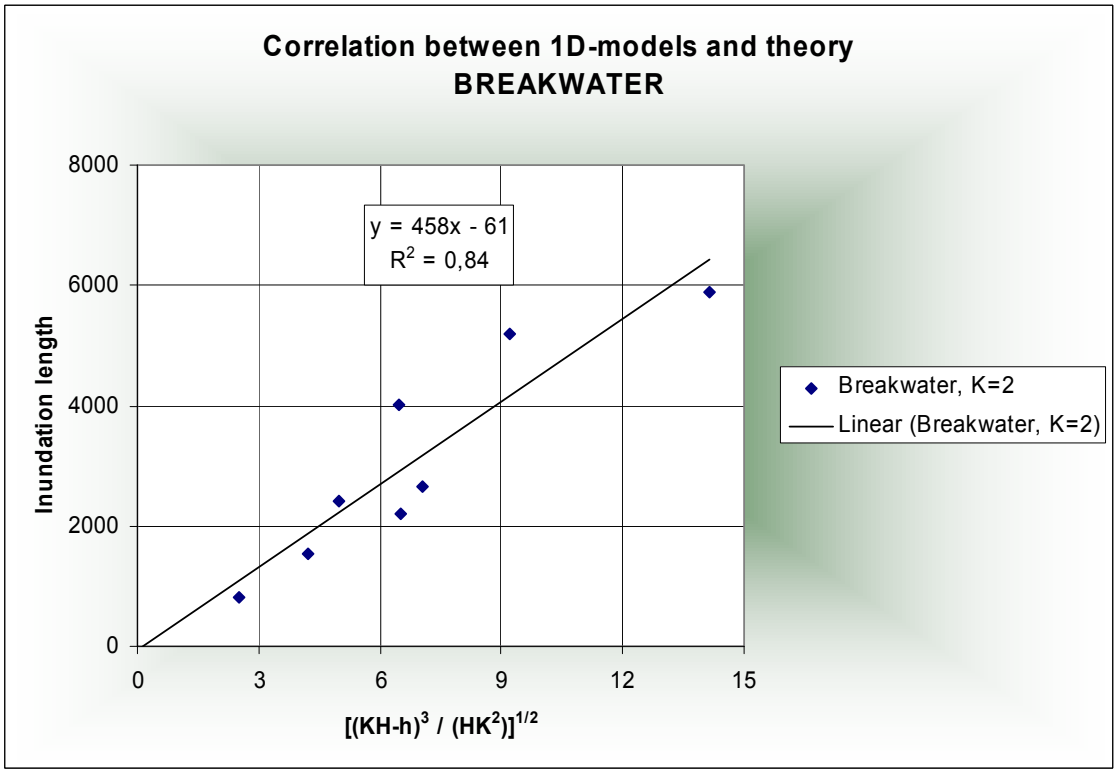

Figure II-5 Correlation 1D-model results with Kaplan; Breakwater

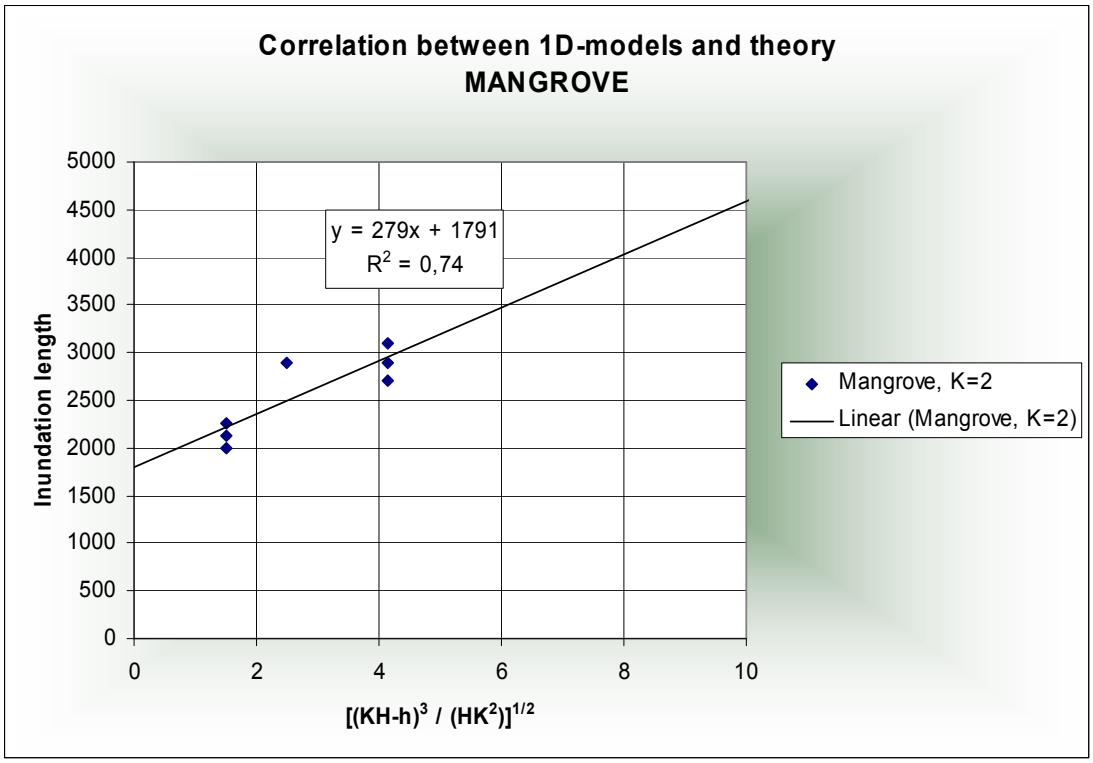

Figure II-6 Correlation 1D-model results with Kaplan; Mangrove

Comparison of the fitted trend lines (formulas are depicted in the graphs) with Kaplan's formula, shows the same trend, but the inundation length predicted by Kaplan is about 1/3 of the inundation length. The inundation length by Kaplan must be multiplied by factor 3(!) to give reasonable accordance with the obtained results, see Figure II-7

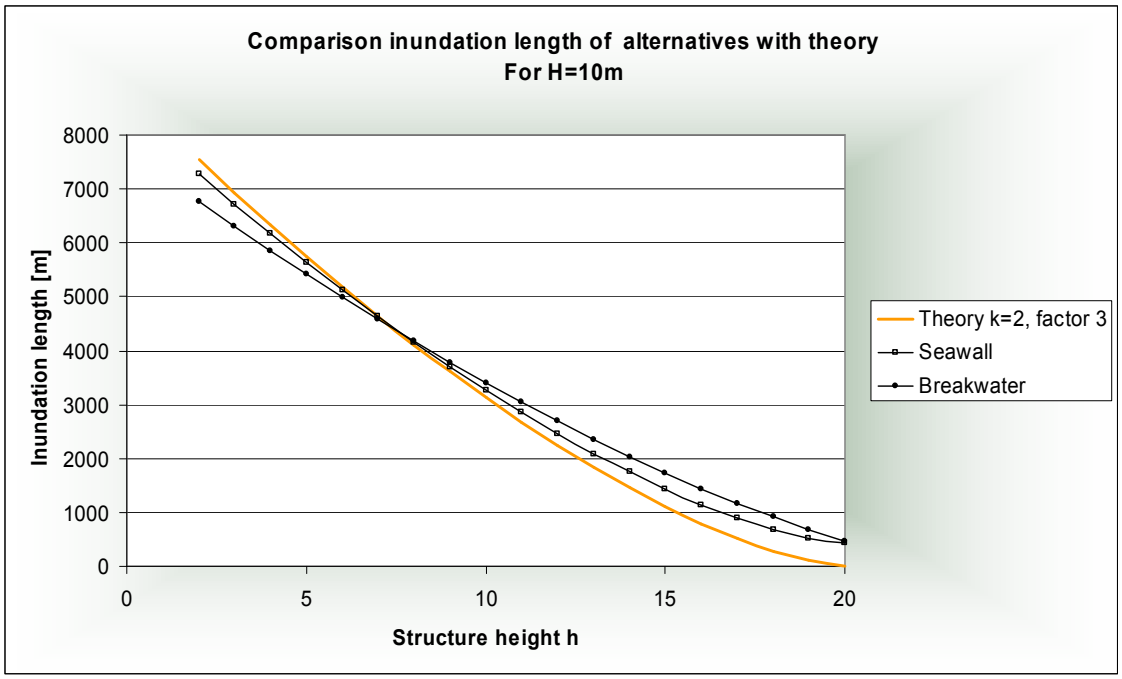

Figure II-7 Inundation length with Kaplan compared with 1D-model results for 2 structure types (because H is at the shoreline, the wave heights for the breakwater are adjusted to account for shoaling)

An increase of factor 3 in inundation length means an increase of factor 9 (!) in the overtopping volume. This cannot be explained by the fact that this tsunami wave train consist of 3 successive waves.

The penetration of the successive waves is depicted for the case H=10m and seawall height h=5m.

Frames of the 1D-model run with H=10m and a seawall of 5m at the coast	**Explanation**
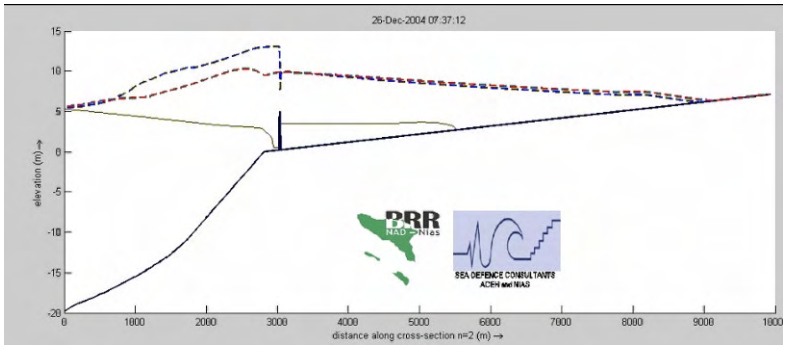	First wave height, H_1=6,7m L_1= 2,4 km According to Kaplan: (k=2) L_1= 0,98 km According to Kaplan: (k=5) L_1= 2,4 km

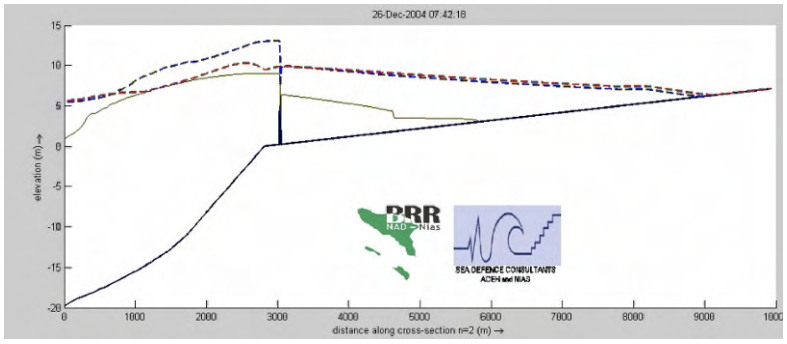

2^{nd} wave height, H_2=7m

L_{1+2}= 3,7 km

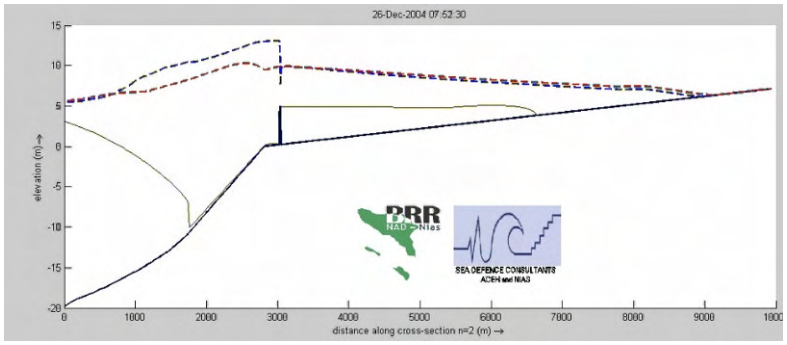

According to Kaplan: (k=2)

L_{1+2}= 1,4 km

According to Kaplan: (k=5)

L_{1+2}= 3,6 km

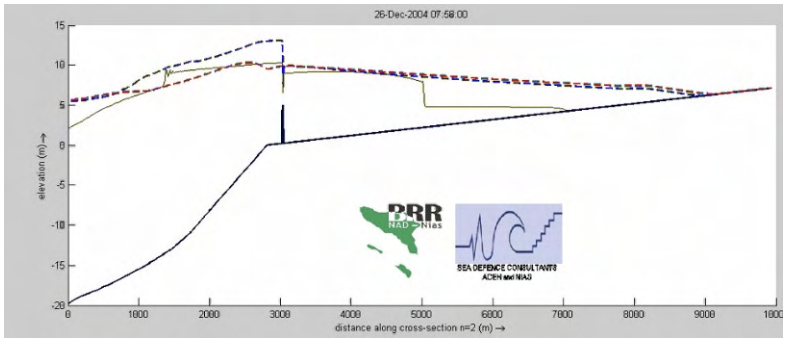

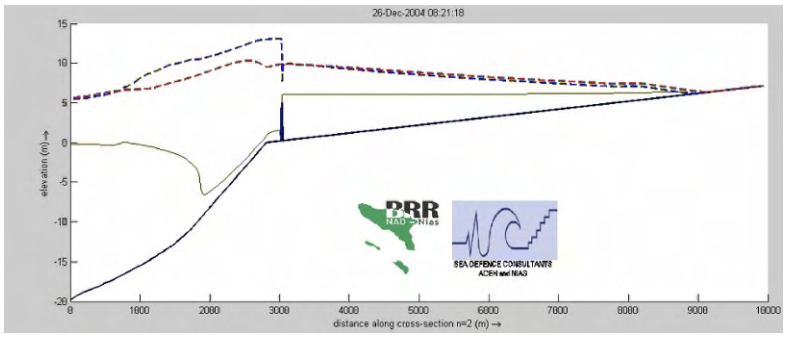

3^{rd} wave height, H_2=9,9m

L_{1+2+3}= 6,1 km

According to Kaplan: (k=2)

L_{1+2+3}= 2,4 km

According to Kaplan: (k=5)

L_{1+2+3}= 5,3 km

Figure II-8 Successive penetration of 3 waves for the case H=10m, h=5m. The red line indicates the maximum water level in case there is no structure. The blue line is the maximum water level for the simulated case with structure.

Although the overtopping volumes predicted by Kaplan (with K=2) show the same behaviour as and has reasonable correlation with the 1D-model results, an average factor of 3 is necessary to get the same inundation length. For the investigated case in Figure II-8 it becomes clear that Kaplan's prediction is significantly lower than the predicted inundation, except a run-up factor K=5 is applied. However, applied on all model results, this factor gives poor correlation ($R_{K=5}^2$ = 0,16). But even with K=5, the prediction of Kaplan lags behind the predicted penetration. While the first wave experience the full friction of the ground behind the seawall, it can clearly be seen that the 2nd and 3rd wave easily penetrate because they 'ride' on the 1st wave. Because backflow of the water is not possible, every next wave just adds an additional amount of water to the hinterland. In the final situation the overtopping volume simply equals the storage capacity of the area behind the seawall.

From the video frames it can also be seen that the highest water level (the heading up) above the seawall is about 13m (blue line). It is expected that the run-up against a structure, high enough to prevent overtopping, will not exceed 20m. This corresponds with factor K ≤ 2. This is most likely the reason that a run-up factor of 5 gives poor correlation with the model results.

Conclusion
Reasonable agreement was found between Kaplan's prediction of overtopping volumes (with K=2) and the 1D-model results. However, overtopping volumes should be multiplied by factor 9 (3^2) to obtain the same penetration length. This is not only due to the fact that 3 successive waves overtopped the seawall, as also the first wave penetrates much farther than predicted with Kaplan. Although a run-up ratio of K=5 gave a good prediction in the investigated case, the overall correlation was poor. This is supported by the indication that the required structure height to prevent overtopping approximately equals twice (K=2) the incoming wave height.

II - 4 ADDITIONAL 1D-MODELLING

The influence of the near-shore bathymetry (shape) on the wave development (without structures)
The initial reason to investigate the influence of the near-shore bathymetry was the fact that the existing 1D-modelling gave much higher wave heights at the shore than the 2D-model runs. And this happens for identical tsunami signals. The only possible explanations could be the influence of spatial effects (bays, islands etc.) either the bathymetry.

Various profiles were modelled with the same boundary conditions. The applied tsunami signal has the same shape as in the existing 1D-model runs. The height at the model boundary is H=6m. The resulting (maximum) wave heights are depicted in Figure II-9.

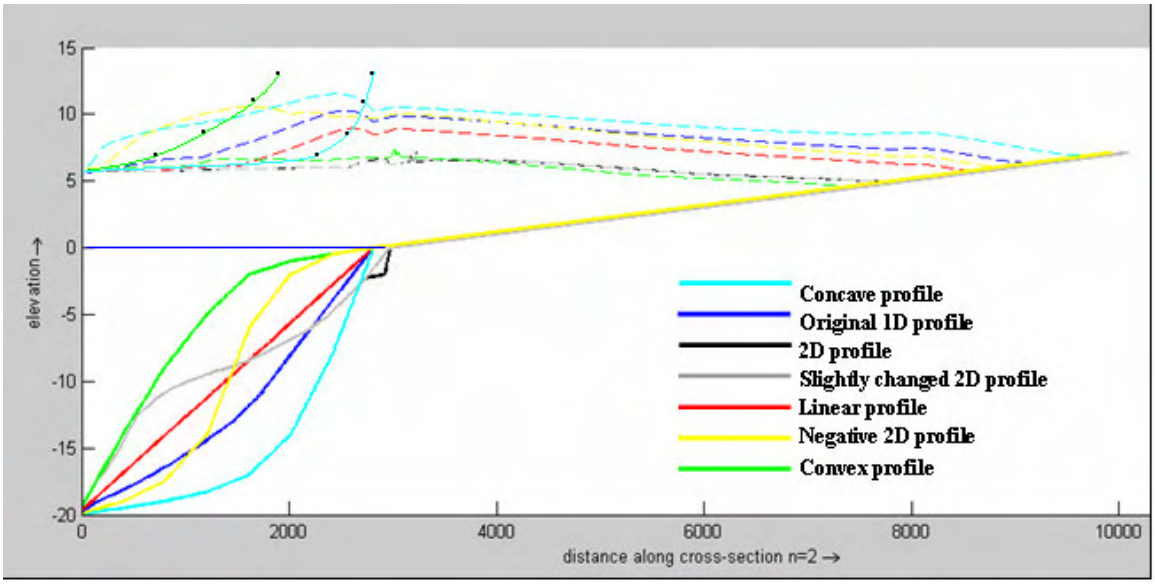

Figure II-9 1D model: Maximum water levels for varying bathymetry. $H_{boundary}$=6m.

In this figure, the so-called '2D-profile', is obtained from the 2D-model, where the actual bathymetry is used. The profile called 'original 1D-profile' is the profile as used in the existing 1D-model runs.

The dashed lines in Figure II-9 indicate the maximum water level during the entire run. The black-dotted green line indicates the theoretical shoaling[1] for the convex profile and the black-dotted blue line represents the theoretical shoaling for the concave profile. It is clear that the wave development close to the shore cannot be described by this simple law. Non-linear effects play an important role.

The difference for the two profiles used in the models is:

The maximum height for the original 1D-profile	=	10,3m
The maximum height for the 2D-profile	=	6,7m
The factor difference	=	1,54

Conclusion

The near-shore bathymetry has a major influence on the development (or shoaling) of the wave. Where a concave profile (light blue line) causes the wave to increase approx. factor 2 towards the coast, the wave height hardly increases in case of a convex profile (green lines).
The big difference between the wave heights associated with the 2D-profile and the 1D-profile explains the difference between both models. The actual profile in front of Banda Aceh is more convex (at least the first part) then concave, as was assumed in the original 1D model runs.

[1] *Theoretical shoaling means the wave growth according to Green's Law, following* $(d_2/d_1)^{0.25}$. *See Chapter 2 on this matter.*

This analysis also explains the much higher wave heights in Lhok'Gna. Applying this bathymetry in the 1D-model gives a wave height at the coast of almost 20m. Note that this is for the tsunami-signal as occurred in Banda Aceh where the waves were lower. However, the important finding is that the fore-shore bathymetry is of significant influence on the final wave height at the coast. See Figure II-10.

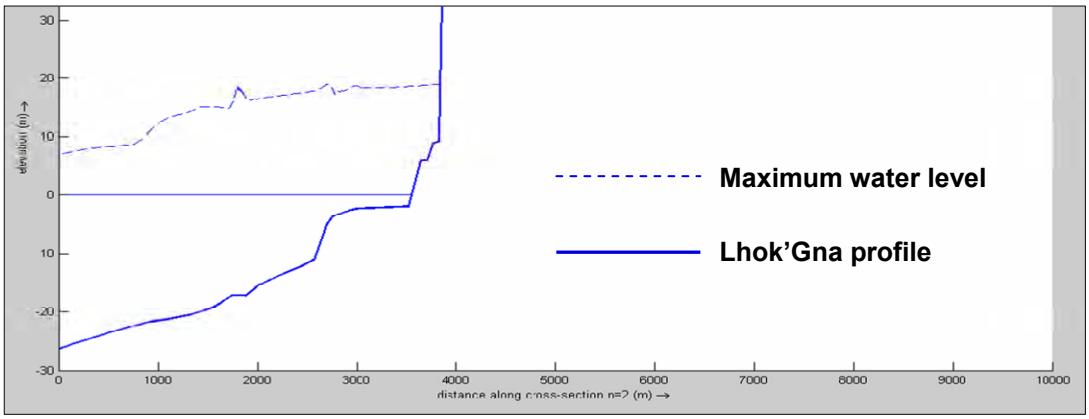

Figure II-10 Maximum water level with Lhok'Gna profile

The influence of bathymetry (shape) on the run-up against structures

The question arose whether this bathymetric influence also accounts for the run-up against structures. For this purpose, three structures were modelled in both the 1D- and 2D-profile.

Offshore Tsunami Barrier (see FigureII-11)

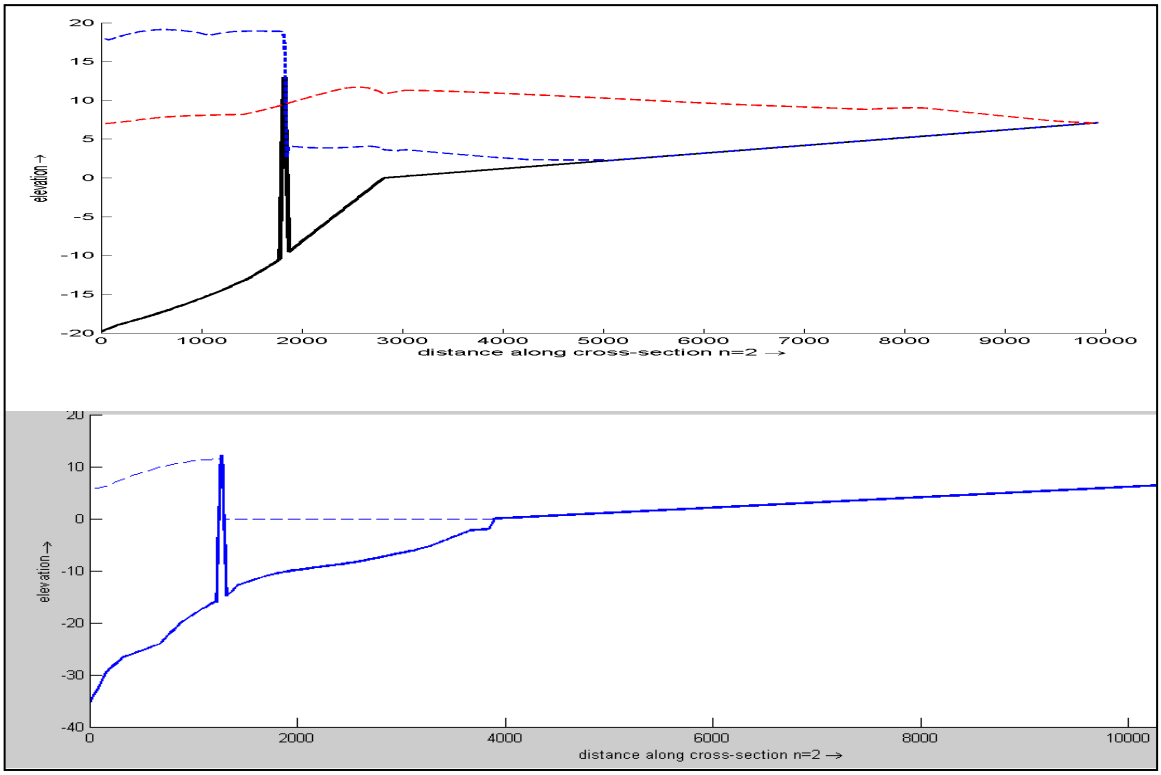

FigureII-11 Offshore Breakwater: Maximum run-up for 1D-profile (existing run, see upper part) and maximum run-up for 2D-profile (lower part)

The maximum run-up in case of the 1D-profile is: 17m
The maximum run-up for the 2D-profile is: 9,5m

Factor difference = 1,79

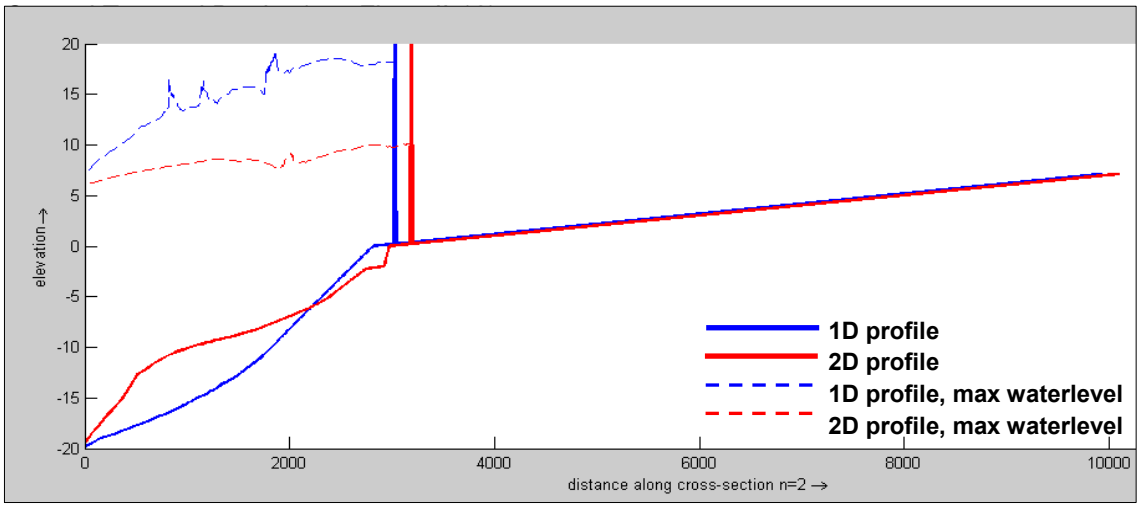

FigureII-12 Coastal Barrier. 1D model: Maximum run-up for 2 different profiles

The maximum run-up in case of the 1D-profile is: 18,2m
The maximum run-up for the 2D-profile is: 10,2m

Factor difference = 1,78

Inland Tsunami Barrier (see FigureII-13)

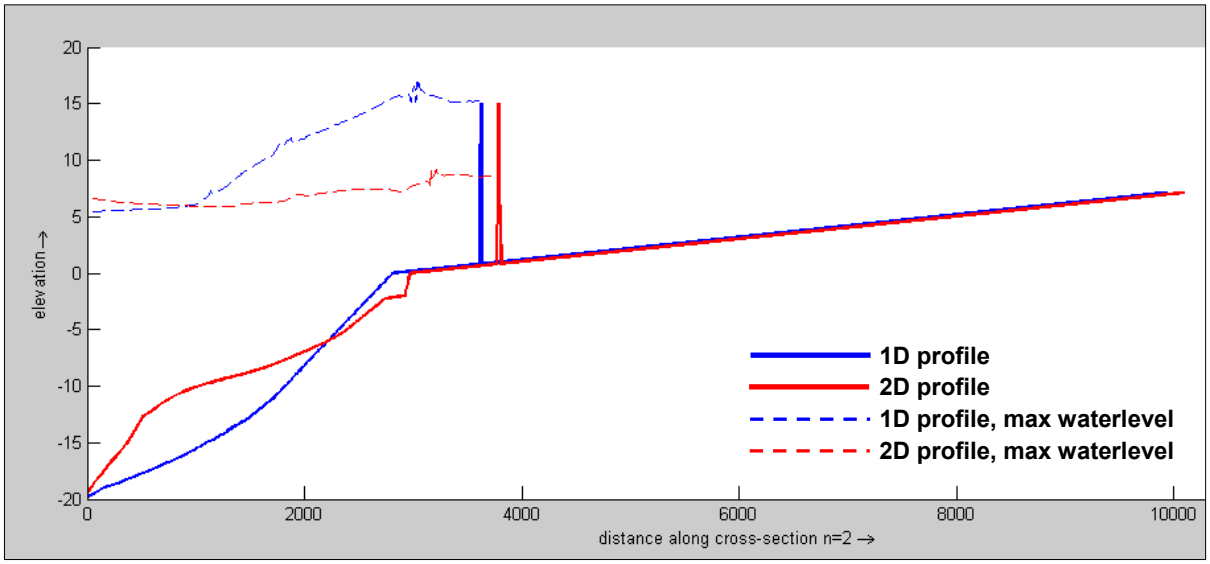

FigureII-13 Inland Barrier. 1D model: Maximum run-up for 2 different profiles

The maximum run-up in case of the 1D-profile is:	15,3m
The maximum run-up for the 2D-profile is:	8,7m
Factor difference =	1,76

Conclusion

The run-up against a structure depends mainly on the height of the incoming wave. As we have seen that the wave height increases much more with a concave profile than with a convex profile, it is expectable that the run-up shows the same behaviour.

The run-up against the same structure and with the same tsunami signal at the boundary is more then 1,7times higher in case of the 1D-profile (concave) then with the 2D-profile (more convex).

Where the difference in maximum wave height at the coast differed factor 1,5 for the runs without structure, this difference obviously increases in the run-up (factor 1,7). Apparently, also the velocity of the wave is higher. This can be explained by considering that the velocity decreases with decreasing depth and because a concave profile maintains its depth longer, the velocity of the wave running over it, will be maintained longer. This most probably results in a higher impact and run-up.

The influence of tsunami shape signal on structures

The original signal has been used in the existing models to simulate the effect of structures. This signal was rescaled to model different tsunami heights.

In the additional modelling, various signals have been used as boundary condition, see FigureII-14

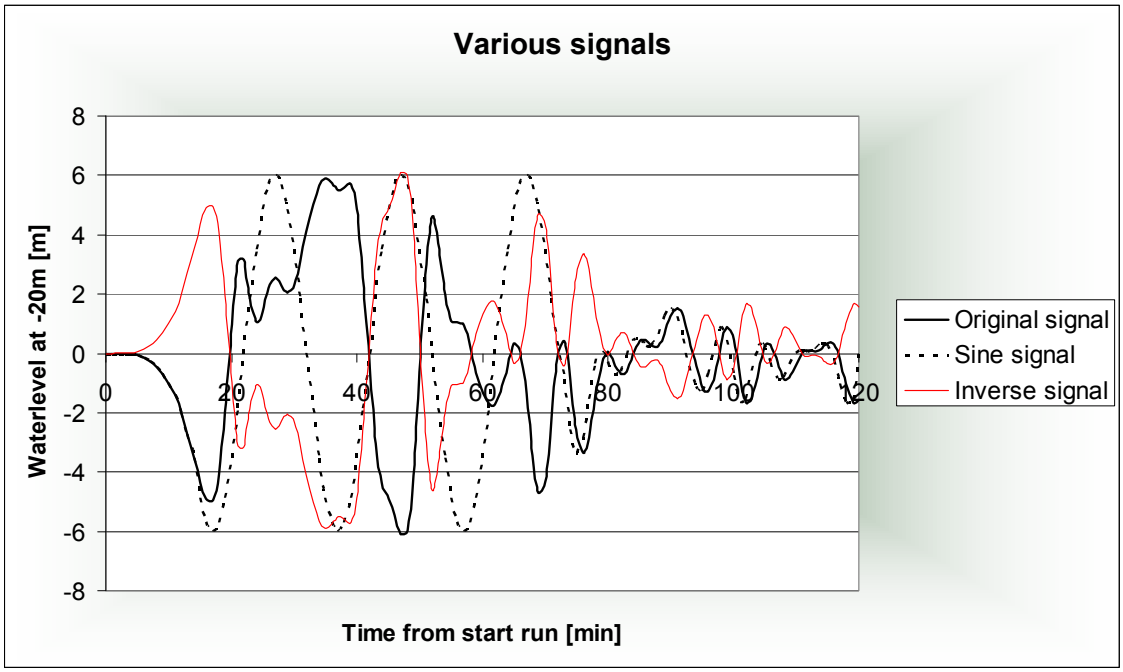

FigureII-14 Various tsunami shape signals as applied on the open (left) boundary of the model

Three different signals have been modelled. Although Banda Aceh will only receive tsunamis with preceding troughs (see 'original signal'), the influence of a tsunami with preceding crest is investigated to gain more insight (see' inverse signal', which is the inverse of the 'original signal'). Thereby a pure sine-signal, with preceding trough is applied.

The maximum water levels for the various signals (and profiles) are depicted in FigureII-15.

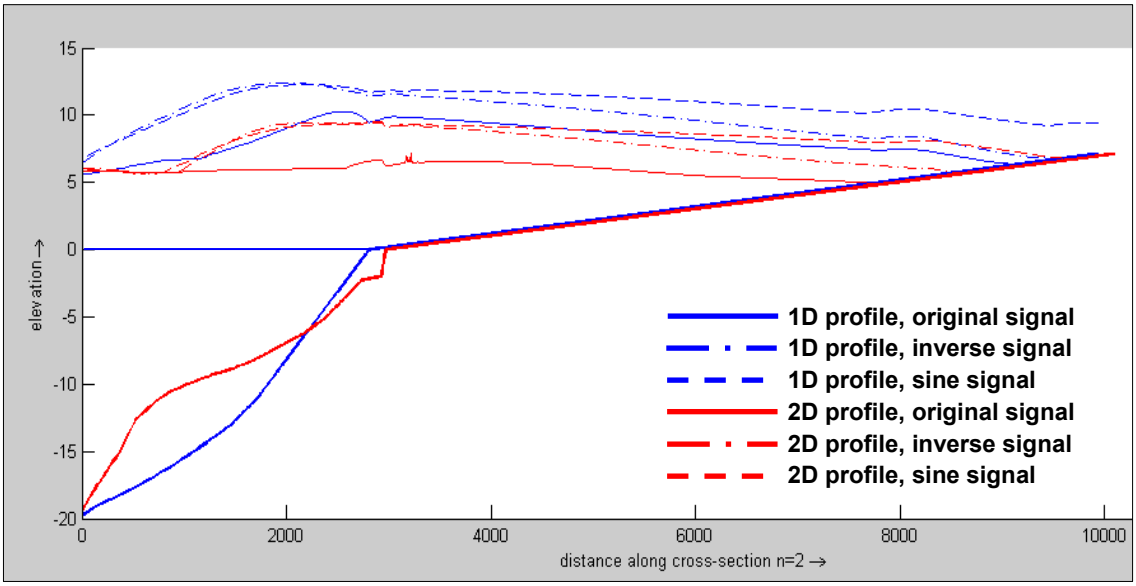

FigureII-15 1D model: Maximum water levels for varying signal shape. H_c=10m.

Conclusions

The results indicate that whatever tsunami signal is applied, the maximum water levels are higher for the 1D-(concave)-profile then for the 2D-(convex)-profile. This is in line with the previous findings for concave and convex profiles.

The sine-signal with preceding trough gives the highest water levels and penetration. The reason is that the 3 successive waves are all the same size and represent much more volume then the (positive) part of the other signals. It is simply a matter of volume.

The inverse signal of the 'original signal' causes higher water levels and consequently more penetration than the original signal. This seems to indicate that an initial crest will cause higher water levels then an initial trough.

However, more runs have been made with positive and negative signals, see FigureII-16, and with a linear bathymetry. Two identical (but opposed) sine-signals were used. In the frame it is visible that the red (negative) wave has finally a higher run-up then the blue (positive) wave. The most obvious reason is that the wave front for negative waves is much steeper. As run-up is also related with the steepness of the wave front, (see Chapter 2), this is the most logical explanation.

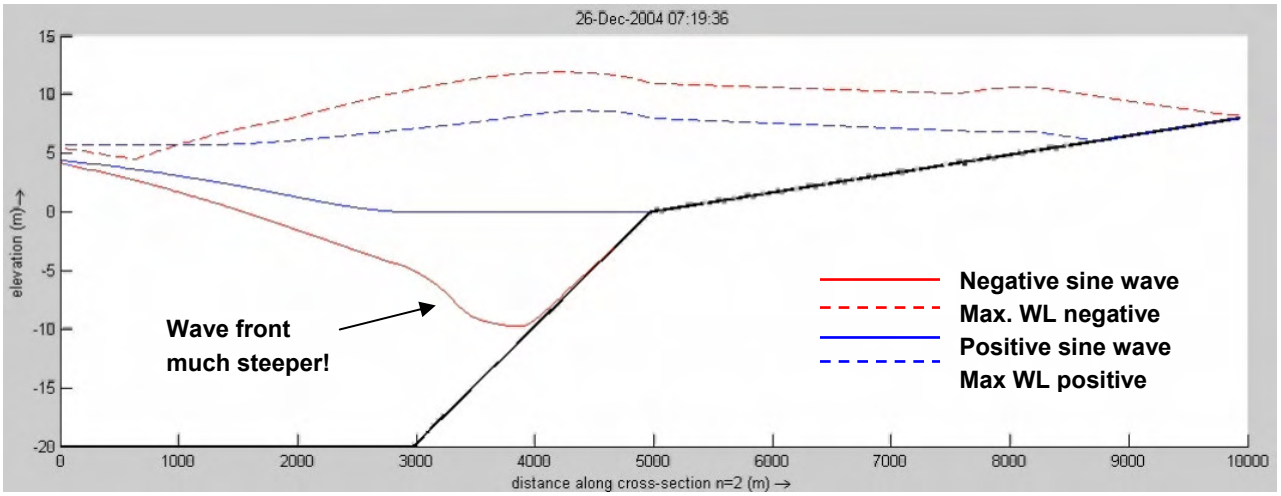

FigureII-16 Timeframe of a run with two opposite signals running up a linear slope

For pure sine signals, the difference between positive and negative waves is clear. However, various profiles and signals make it more difficult to find the right parameters which describe the behaviour of the wave development.

In general it is accepted that tsunamis which first retreat from the coast (negative) have a higher impact on the coast then identical waves without preceding trough. The higher run-up is nevertheless not associated with higher wave heights, but with higher steepness.

Combined measure versus separate measures

The effectiveness of separate and combined measure is shown in FigureII-17 by means of maximum water levels.

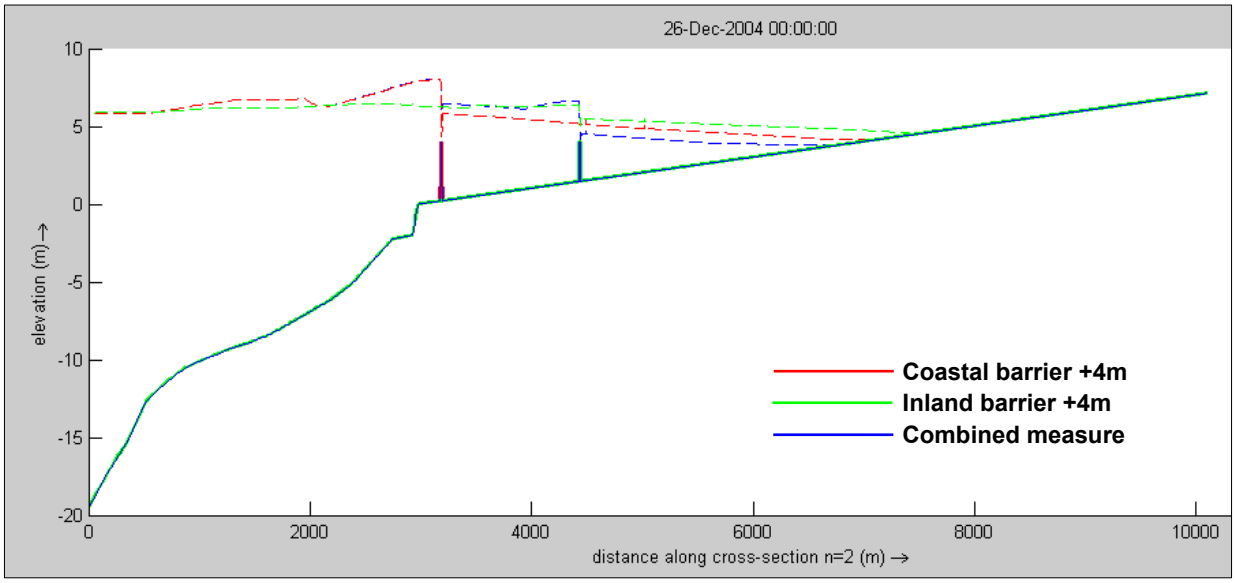

FigureII-17 Comparison between effectiveness of seawall +4m, inland wall +4m and combined measure.

Both measures (inland and coastal barrier) have a retaining height of + 4m MSL. One would expect that the inland barrier is more effective to protect the hinterland, because the tsunami waves are lower inland.

However, from this results it must be concluded that a coastal barrier of +4MSL is more effective (see red line) than an inland barrier of +4MSL (green line). Again, the steeper wave inland causes a higher run-up and consequently more overtopping.

The effect of a combined measure is very limited. The first wave overtops the coastal barrier and fills up the area in between. The successive wave will simply 'ride over' the stored water and overtop the 2nd barrier. It seems much more effective to invest in making one (high!) structure instead of two structures with limited heights.

FigureII-18 shows the additional effect of a seawall 5m on the existing offshore barrier +5m. The reduction is more significant, but still disappointing. Placing the 5m seawall on top of the breakwater will be more effective in flood reduction.

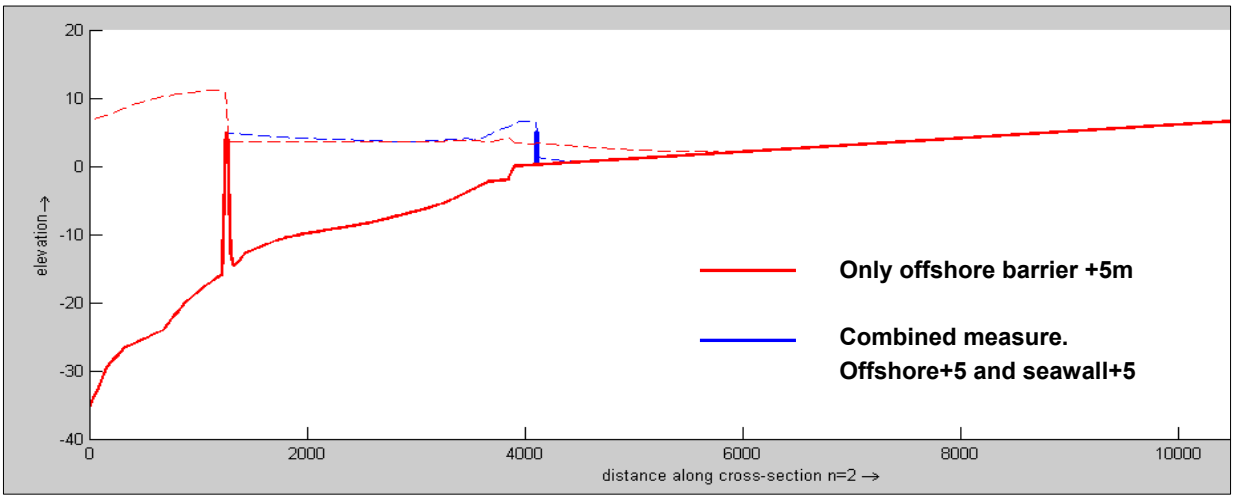

FigureII-18 Comparison between effectiveness of offshore barrier+5m, seawall+5m and combination

II - 5 FINDINGS

Findings existing runs

It was concluded that protection against high tsunami events is difficult to achieve with any type of measure. Offshore breakwaters and seawalls both require a freeboard about equal to the tsunami height on the shoreline. The effectiveness of an offshore breakwater at this height is better than of a seawall. This makes sense considering that the tsunami height at about 10 m deep will be lower than on the shoreline. Mangroves have shown hardly any effectiveness for tsunami heights > 3m.

To obtain any significant effect a seawall must be at least and preferably higher than 5 meters. But negative side effects will increase with height (more about this in Chapter 2). For an offshore breakwater the negative side effects are less, especially if gaps are applied. However an offshore breakwater with a freeboard higher than 5m is much more expensive than a seawall with a 5 m height. The breakwater would be 15 m high, considering quadratically increasing costs with the height of such structures and the construction under water the difference in costs will be significant.

Summarizing, stand alone mangrove zones are not considered effective in tsunami protection. An offshore breakwater or seawall might be an option, potentially in combination with mangrove zones.

The empirical expression of Kaplan (see section I.4.3) for overtopping of low-crested structures has been used to validate the model results. It turned out that this theory consequently underestimates the overtopping volume as calculated by the 1D-model. Although reasonable agreement was found between Kaplan's prediction of overtopping volumes (with K=2) and the 1D-model results, overtopping volumes had to be multiplied by factor 9 (3^2) to obtain the same penetration length. This is not only due to the fact that 3 successive waves overtopped the

seawall, as also the first wave penetrates much farther than predicted with Kaplan. Although a run-up ratio of K=5 gave a good prediction in the investigated case, the overall correlation was poor. This is supported by the indication that the required structure height to prevent overtopping approximately equals twice (K=2) the incoming wave height. This is the normal value for standing waves.

Findings additional model runs

The near-shore bathymetry has a major influence on the development (or shoaling) of the wave. In case of a concave profile the run-up is approximately 1,5 times as high as in case of a convex profile, where the wave hardly shoals towards the coast. The run-up against the same structure and with the same tsunami signal at the boundary is more then 1,7times higher in case of the 1D-profile (concave) then with the 2D-profile (more convex).

Where the difference in maximum wave height at the coast differed factor 1,5 for the runs without structure, this difference obviously increases in the run-up against structures (factor 1,7). Apparently, also the velocity of the wave is higher. This can be explained by considering that the velocity decreases with decreasing depth and because a concave profile maintains its depth longer, the velocity of the wave running over it, will be maintained longer. This most probably results in a higher impact and run-up.

The results indicate that whatever tsunami signal is applied, the maximum water levels are higher for the 1D-(concave)-profile then for the 2D-(convex)-profile.

The inverse signal of the ‘original signal’ causes higher water levels and consequently more penetration than the original signal. This seems to indicate that an initial crest will cause higher water levels then an initial trough. However, more runs with linear profiles and pure sine-signals indicate the opposite. Tsunamis with preceding trough have higher impact (water levels etc.) than positive tsunamis. The higher run-up is nevertheless not associated with higher wave heights, but with higher steepness.

For pure sine signals, negative waves cause much higher run-ups. However, various (combinations of) profiles and signals could change the actual overtopping and flooding.

The effect of combined measures is very limited. The first wave(s) overtops the first barrier and fills up the area to the 2nd barrier. The successive wave(s) will simply ‘ride over’ the stored water and overtop the 2nd barrier. It seems much more effective to invest in making one (high!) structure instead of two structures with limited heights.

Appendix III. OVERVIEW 2D-MODEL RUNS

In Table III-1: Overview model runs for offshore alternatives, all for M_w = 9,2., an overview is provided for all model runs made with offshore alternatives. Table III-2 shows the same for all coastal alternatives and TableIII-3 lists the runs with inland alternatives.

Table III-1: Overview model runs for offshore alternatives, all for M_w = 9,2.

Depth	Retaining height	Specification	Inundation Volume [10^6 m^3]	Effectiveness
-	-	BASE CASE (DEC2004 TSUNAMI)	106	0%
-15M	3M	NO GAPS	13,1	87,7%
-15M	5M	NO GAPS	1,73	98,4%
-10M	-3M	NO GAPS	80,1	24,4%
-10M	0M	NO GAPS	58,1	45,2%
-10M	3M	NO GAPS	21,5	79,7%
-10M	5M	NO GAPS	2,34	97,8%
-10M	7M	NO GAPS	1,06	99,0%
-10M	7M	GAP 1X200M	1,75	98,4%
-10M	7M	GAP 2X200M	3,10	97,1%
-10M	3M	OPEN NORTH	20,5	80,7%
-10M	5M	OPEN NORTH	2,47	97,7%
-10M	7M	OPEN NORTH	1,12	98,9%
-10M	5M	OPEN NORTH + GAP 1X100M	2,94	97,2%
-10M	5M	OPEN NORTH + GAP 2X200M	3,92	96,3%
-10M	5M	OPEN NORTH/SOUTH	7,23	93,2%
-10M	5M	OPEN NORTH/SOUTH + GAP 2X200M	8,79	91,7%
-10M	5M	OPEN NORTH/SOUTH_ISLAND + GAP 2X200M	10,64	90,0%

The variant with no gaps are modelled to gain insight in the general behaviour of the alternative. The absence of gaps means either a fully closed structure either a structure with gates that can be closed in case of a tsunami warning. Both options are regarded as non-feasible. The construction, maintenance and operation of offshore gates for extreme events will be extremely difficult and costly.

Table III-2: Overview model runs for the coastal alternatives, all for M_w = 9,2.

Retaining height	*Specification*	*Inundation Volume [10^6 m^3]*	*Effectiveness*
-	BASE CASE (DEC2004 TSUNAMI)	106	0%
3M	NO GAPS	89,5	15,5%
5M	NO GAPS	43,8	58,7%
7M	NO GAPS	15,4	85,5%

Retaining height	*Specification*	*Inundation Volume [10^6 m^3]*	*Effectiveness*
11M	NO GAPS	1,45	95,8%
7M	GAPS 3X100M	19,2	81,9%

The variant with no gaps are modelled to gain insight in the general behaviour of the alternative. The absence of gaps means either a fully closed structure either a structure with gates that can be closed (fast) in case of a tsunami warning. For coastal structures it is possible to have gates in the entrances (rivers and channels). However, since the operation and maintenance of such gates is difficult, one run is made with gaps. The gap width of 100m is possible, considering the absence of big ships. The influence of the constriction of the discharge-channels in case of a torrential rainfall is simulated with an available SWAN-model. For 1/100-year conditions, no flooding was caused by the decreased discharge openings.

TableIII-3: Overview model runs for inland alternatives, all for M_w = 9,2.

Retaining height	**Specification**	**Inundation Volume [10^6 m^3]**	**Effectiveness**
-	BASE CASE (DEC2004 TSUNAMI)	106	0%
2M	NO GAPS	67,0	36,8%
3M	NO GAPS	61,7	41,8%
5M	NO GAPS	35,1	66,8%
7M	NO GAPS	30,9	70,8%
FR	FULL REFLECTION	28,7	73,0%
7M	NO GAPS, OTHER DIRECTION	29,5	72,2%
7M	GAPS 4X100M	35,9	66,1%

For some model runs, the inundation maps are shown in Figure III-1 (offshore), Figure III-2 (coastal) and Figure III-3 (inland).

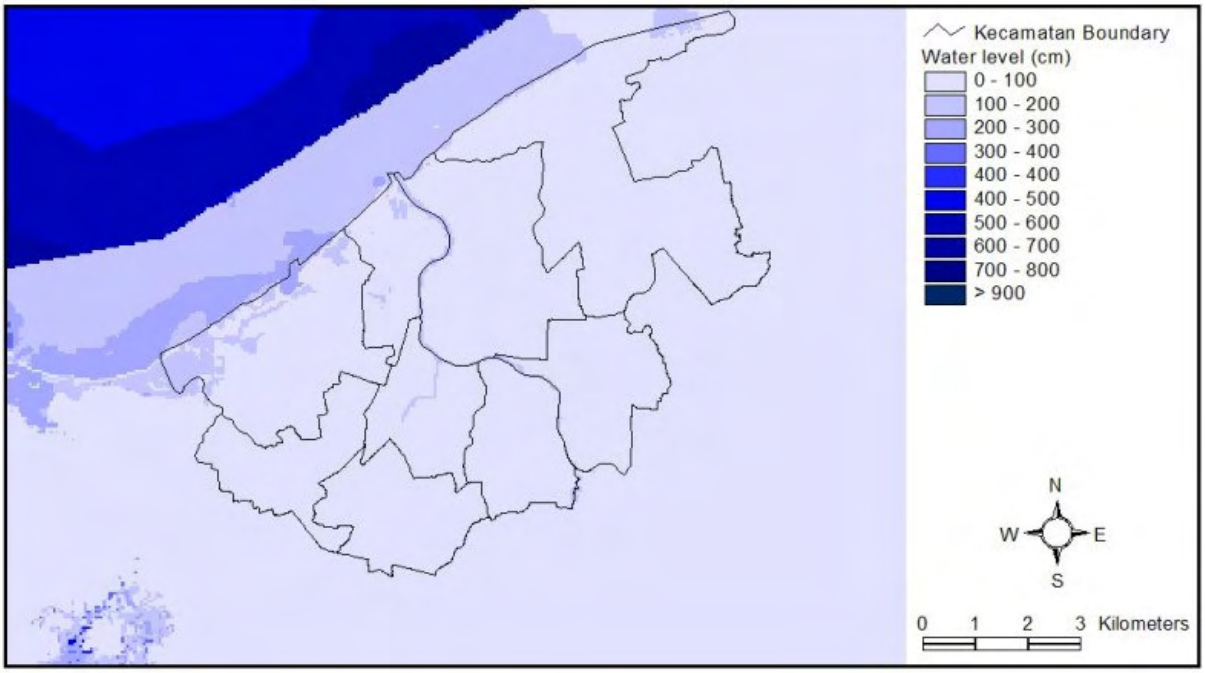

Figure III-1 Inundation level - Offshore barrier of 7 metres with 2 x 200 metre openings [32].

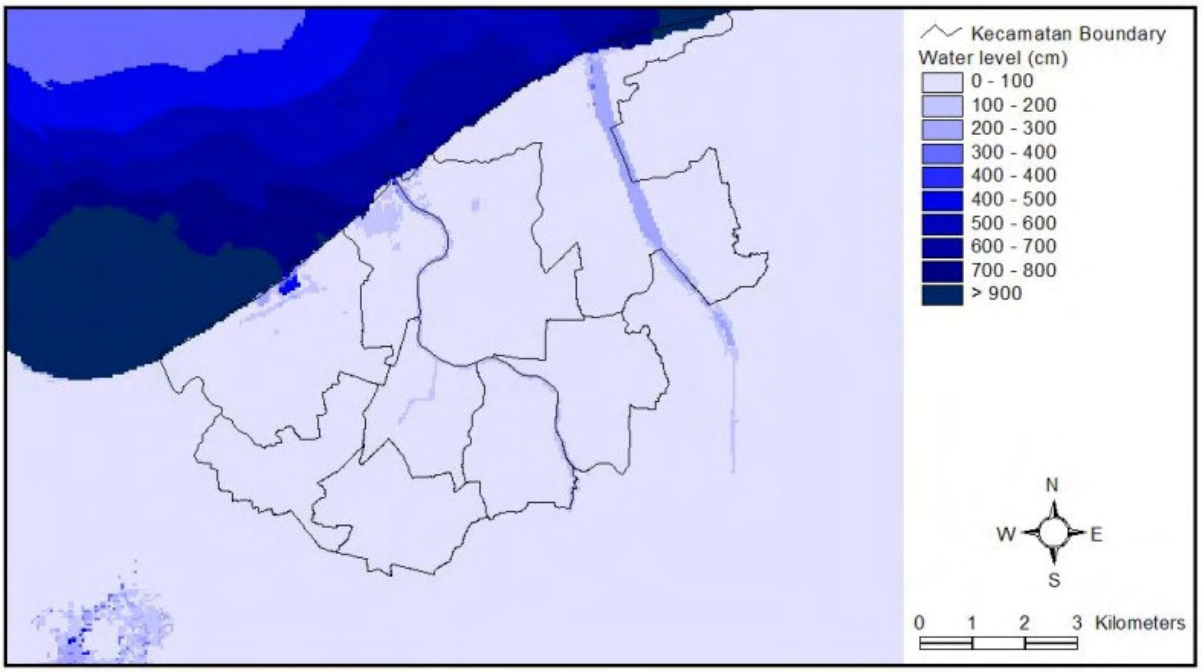

Figure III-2 Inundation level - Coastline barrier of 11 metres with 3 x 100 metre openings [32].

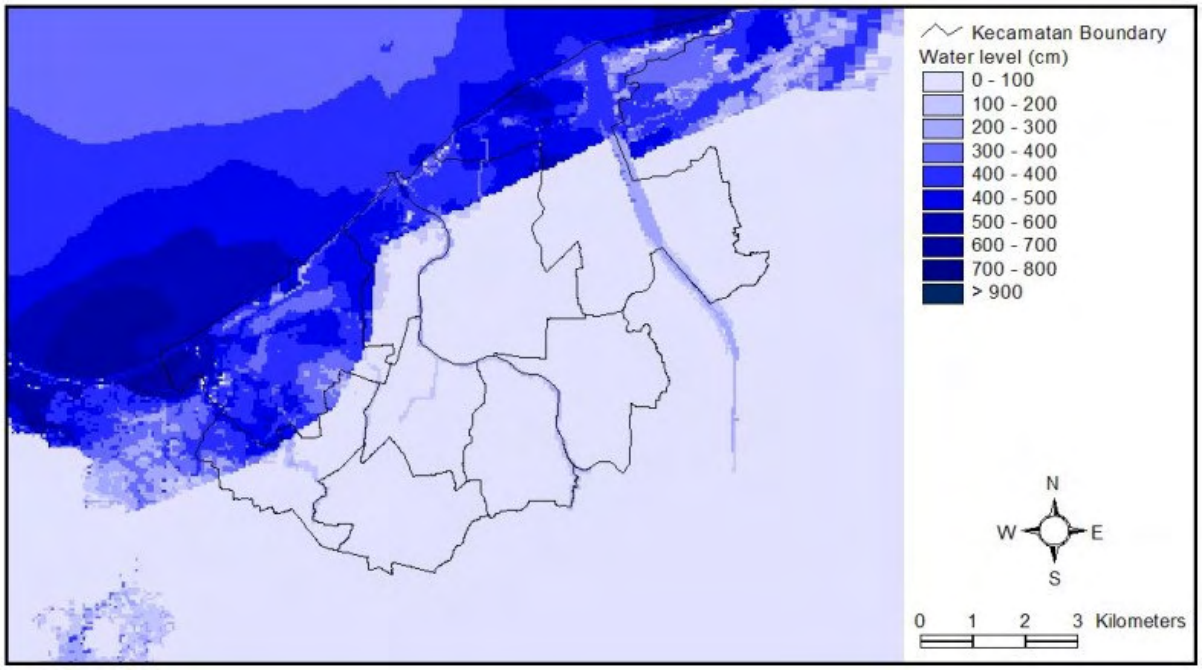

Figure III-3 Inundation level - Inland barrier of 7 metres with 4 x 100 metre openings [32].

Appendix IV. MULTI-CRITERIA ANALYSIS

The Multi-Criteria-Analysis (MCA) is a method to evaluate alternatives on basis of selected criteria. Because often the consequences of activities can not be expressed in costs either benefits, the Cost-Benefit-Analysis (CBA) does not give a full picture of reality. With the MCA it is possible to account for these non-financial consequences, finally giving a certain value for each alternative. Although this value in itself neither presents a full picture, it is helpful to become aware of other non-financial aspects associated with the various alternatives.

This final value is obtained by attributing scores to various alternatives, on basis of selected criteria. To account for the fact that certain criteria are more important then others, a weighting factor could be applied. The method is elaborated in this Appendix, and the results are presented and discussed.

IV - 1 CRITERIA

The selected criteria are:

- Reliability
- Morphological consequences
- Environmental consequences
- Social consequences
- Maintenance
- Land acquisition
-

The reason to select these criteria is explained in Chapter 6. Note that the effectiveness of the structure (i.e. one of the most important criteria) is not listed. This will be done later, since the effectiveness is measured in damage, which is a *financial* parameter and can not be compared with *value*.

IV - 2 SCORES

In the MCA the different Criteria are evaluated by attribution of a score. The scale is from 1 to 9, with:

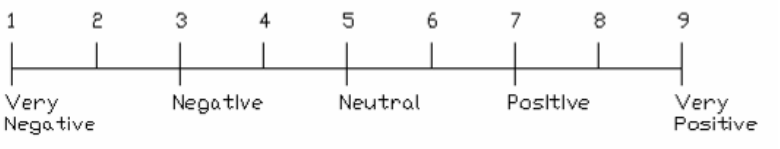

In FigureIV-1 the scores are shown for each alternative and criterion. The alternatives are listed left and are similar to the runs which are made with the 2D-DELFT 3D model. The used names should be read in the following way, for instance:

Offshore-15m, FB3m no gaps

This is an offshore barrier built at -15m bathymetry line, with a freeboard (FB) of 3m. The structure is fully closed, which means that no gaps are present where through the water could penetrate. This means that in reality movable gates have to be constructed, which should be closed in case of a tsunami-event.

The open north or south refers to barriers which are not attached to the coast. The gap between the head of the breakwater and the coast line is approximately 800m. *Open NS*, means a breakwater with both an open north and an open south.

In case of gaps, the number of gaps and the width is mentioned.

No	SCORES FOR EACH ALTERNATIVE	Reliability	Morphological consequence	Environmental consequence	Social consequence	Maintenance	Land acquisition
0	**BASE CASE; do nothing**	9	9	9	9	9	9
1	Offshore-15m, FB3m no gaps	4	2	3	8	1	9
2	Offshore-15m, FB5m no gaps	5	2	3	8	1	9
3	Offshore-10m, FB-3m no gaps	2	8	8	9	1	9
4	Offshore-10m, FB0m no gaps	3	4	5	5	2	9
5	Offshore-10m, FB3m no gaps	4	2	1	5	3	9
6	Offshore-10m, FB5m no gaps	5	2	1	5	3	9
7	Offshore-10m, FB7m no gaps	7	2	1	5	3	9
8	Offshore-10m, FB7m gap 1x200m	7	4	1	5	3	9
9	Offshore-10m, FB7m gap 2x200m	7	4	2	5	3	9
10	Offshore-10m, FB3m open north	7	4	4	6	3	9
11	Offshore-10m, FB5m open north	8	4	4	6	3	9
12	Offshore-10m, FB7m open north	9	4	4	6	3	9
13	Offshore-10m, FB5m open north+gap 1x100m	8	4	5	7	3	9
14	Offshore-10m, FB5m open north+gap 2x200m	8	7	7	7	3	9
15	Offshore-10m, FB5m open NS	8	8	8	8	3	9
16	Offshore-10m, FB5m open NS+2gap 200m	8	8	8	9	3	9
17	Offshore-10m, FB5m open NS-Island+2gap200m	8	8	8	9	3	9
18	Coastline, FB3m no gaps	1	6	6	6	2	3
19	Coastline, FB5m no gaps	2	6	6	5	3	2
20	Coastline, FB7m no gaps	4	6	6	1	4	1
21	Coastline, FB7m, gaps 3x100m	5	6	6	1	6	1
22	Inland, FB2m no gaps	2	9	9	8	8	9
23	Inland, FB3m no gaps	2	8	8	6	8	5
24	Inland, FB5m no gaps	3	8	8	3	7	4
25	Inland, FB7m no gaps	4	8	8	1	6	3
26	Inland, FB7m no gaps other dir.	4	8	8	1	6	3
27	Inland, FB7m, gaps 4x100m	5	8	8	1	9	3
28	COMBO (nr 16)+CoastFB2.5;5gap	8	8	8	9	3	9

FigureIV-1 Scores for each alternative

The Base Case is the situation where no structural measures are applied. As this is the reference situation, it has the highest scores (all score 9).

The justification of the scores can be derived from the description of the criteria in Chapter 6.

IV - 3 WEIGHTING FACTORS

Weighting factors are attributed to each criterion to differentiate the importance. The score of the individual criteria is multiplied by the weighting factor to obtain the overall result of the MCA

The factors can be determined by comparing the criterions with each other. In TableIV-1 this has been done by attributing '0' or '1', where '1' means that the horizontal criterion is more important then the vertical one. For each row, the factors are added up (sum).

TableIV-1: Determination of weighting factors

	Reliability	Morphological	Environmental	Social	Maintenance	Land acquisition	Sum	Sum+1
Reliability		1	1	0	1	1	**4**	**5**
Morphological	0		0	0	0	0	**0**	**1**
Environmental	0	1		0	0	0	**1**	**2**
Social	1	1	1		1	1	**5**	**6**
Maintenance	0	1	1	0		1	**3**	**4**
Land acquisition	0	1	1	0	0		**2**	**3**

Because one criterion is considered as the least important, this one would result in a 'weighting factor' of zero. Therefore, applied weighting factors are taken equal to the sum+1. A short reasoning for the attributed weighting factor is given in Chapter 6.3.3.

Applying these factors on the scores, and adding up the individual scores for each criterion, results in a total score, or value, for each alternative.

The results are presented below (Figure IV-2) in descending order.

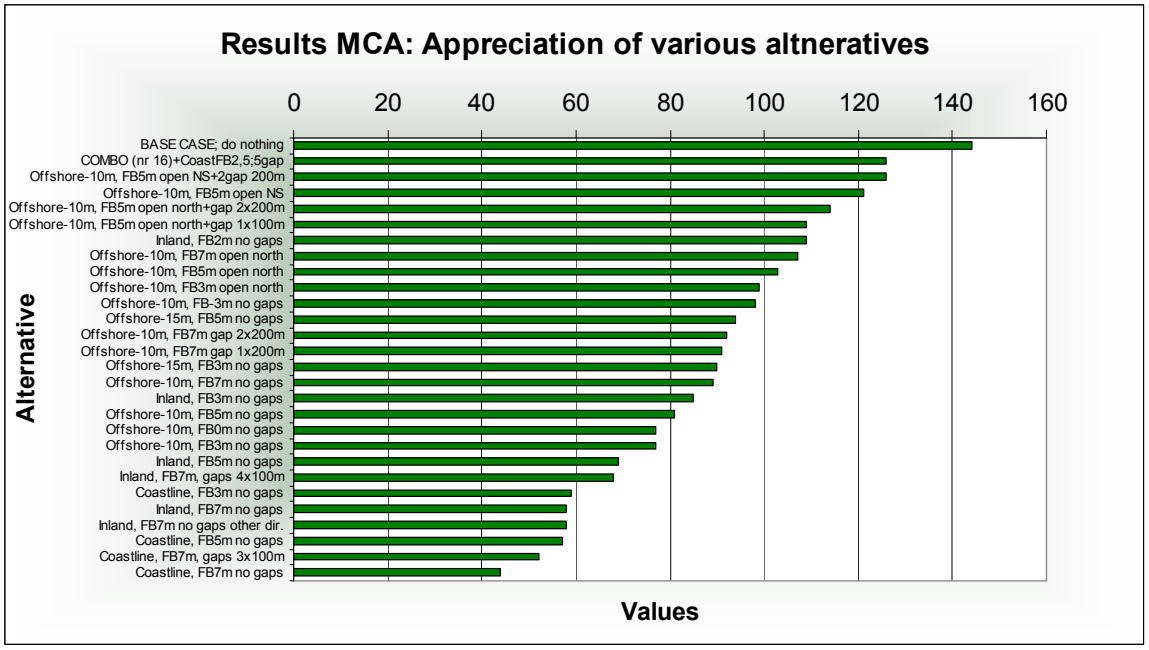

Figure IV-2 Results MCA: Appreciation of various alternatives

In general, offshore alternatives have much higher value than coastal and inland alternatives. This is mainly due to the high social impact of high structures on land.

IV - 4 VALUE / COST RATIO

As mentioned before, the MCA primary adds up the *value* of various alternatives. Selection of the alternative only on this basis is not sufficient.
On the other hand, selection of an alternative only based on *costs and benefits* (thus financial terms) is not fair either, because non-financial aspects (for instance, the social acceptance of a 7m high wall) can be of significant importance.

So, both methods have limitations. In this Appendix it is tried to combine the benefits of both methods. The value for each alternative, provided by the MCA is compared to the costs and damage as used in the CBA. This will not give final answers, but at least will provide an answer to the question: what are the costs for a certain value?

The MCA-value is therefore simply divided by the costs. This results in a value/cost ratio for each alternative. A high value/cost (VC) ratio represents an alternative where a high value is acquired for a relatively low price:

$$VC\text{-}ratio = Value / Costs = Value / (Construction\ Costs + Damage)$$

Costs+Damage

The costs do not only represent the construction costs of the structure but also damage as caused by a Dec2004 Tsunami event. This damage is obtained from the 2D-DELFT3D model runs, where the inundation volume is used as an indication for the resulting damage (see Chapter 5). The reference case is the Dec2004 Tsunami without any structural measure, where the resulting damage was $1,13 Billion. The construction costs are presented in Appendix V.

Remark

It should be noted that this straight comparison of values and costs is arbitrary. It suggests that doubling the value of the structure, allows doubling the costs of the structure. However, this can not be concluded from this analysis. Tsunamis do not only inflict economical damage but also personal damage. Therefore, the final conclusion regarding the value of a certain alternative in relation with the costs and damage should not be drawn by economists but by the involved society itself.

To account for this sensitivity, two VC-ratios are presented:

1. Value/cost ratios based on the economical damage due to **1** Dec2004 tsunami-events during the lifetime of the structure
2. Value/cost ratios based on the economical damage due to **2** Dec2004 tsunami-events during the lifetime of the structure

An overview of the (weighted) scores, constructions costs, damage (in red) and resulting scores is given in the following Figure IV-3.

No	ALTERNATIVE	Reliability	Morphological consequences	Environmental consequences	Social consequences	Maintenance	Land acquisition	Total Value	Construction costs [M USD]	Damage [M USD]-> 1xDec2004 event	Total value / (Costs+Damage)	Ranking
0	BASE CASE; do nothing	36	9	9	45	18	27	144	0	1100	13,1	3
1	Offshore-15m, FB3m no gaps	16	2	3	40	2	27	90	1314	136	6,2	26
2	Offshore-15m, FB5m no gaps	20	2	3	40	2	27	94	1532	18	6,1	27
3	Offshore-10m, FB-3m no gaps	8	8	8	45	2	27	98	429	832	7,8	19
4	Offshore-10m, FB0m no gaps	12	4	5	25	4	27	77	617	603	6,3	25
5	Offshore-10m, FB3m no gaps	16	2	1	25	6	27	77	833	223	7,3	23
6	Offshore-10m, FB5m no gaps	20	2	1	25	6	27	81	1020	24	7,8	20
7	Offshore-10m, FB7m no gaps	28	2	1	25	6	27	89	1212	11	7,3	24
8	Offshore-10m, FB7m gap 1x200m	28	4	1	25	6	27	91	1212	18	7,4	21
9	Offshore-10m, FB7m gap 2x200m	28	4	2	25	6	27	92	1212	32	7,4	22
10	Offshore-10m, FB3m open north	28	4	4	30	6	27	99	833	212	9,5	17
11	Offshore-10m, FB5m open north	32	4	4	30	6	27	103	1020	26	9,9	15
12	Offshore-10m, FB7m open north	36	4	4	30	6	27	107	1212	12	8,7	18
13	Offshore-10m, FB5m open north+gap 1x100m	32	4	5	35	6	27	109	1020	30	10,4	14
14	Offshore-10m, FB5m open north+gap 2x200m	32	7	7	35	6	27	114	1020	41	10,7	13
15	Offshore-10m, FB5m open NS	32	8	8	40	6	27	121	1020	75	11,0	12
16	Offshore-10m, FB5m open NS+2gap 200m	32	8	8	45	6	27	126	1020	91	11,3	10
17	Offshore-10m, FB5m open NS-Island+2gapx200m	32	8	8	45	6	27	126	1020	110	11,1	11
18	Coastline, FB3m no gaps	4	6	6	30	4	9	59	69	929	5,9	28
19	Coastline, FB5m no gaps	8	6	6	25	6	6	57	138	455	9,6	16
20	Coastline, FB7m no gaps	16	6	6	5	8	3	44	220	160	11,6	9
21	Coastline, FB7m, gaps 3x100m	20	6	6	5	12	3	52	220	199	12,4	5
22	Inland, FB2m no gaps	8	9	9	40	16	27	109	28	695	15,1	1
23	Inland, FB3m no gaps	8	8	8	30	16	15	85	49	640	12,3	6
24	Inland, FB5m no gaps	12	8	8	15	14	12	69	102	365	14,8	2
25	Inland, FB7m no gaps	16	8	8	5	12	9	58	166	321	11,9	8
26	Inland, FB7m no gaps other dir.	16	8	8	5	12	9	58	166	306	12,3	7
27	Inland, FB7m, gaps 4x100m	20	8	8	5	18	9	68	166	373	12,6	4
28	COMBO (nr 16)+CoastFB2,5;5gap	32	8	8	45	6	27	126	1020	54	11,7	9

Figure IV-3 Total Value and Ranking for various alternatives

The value/cost ratios based on the economical damage due to **1** Dec2004 tsunami-events during the lifetime of the structure, is presented below, see Figure IV-4.

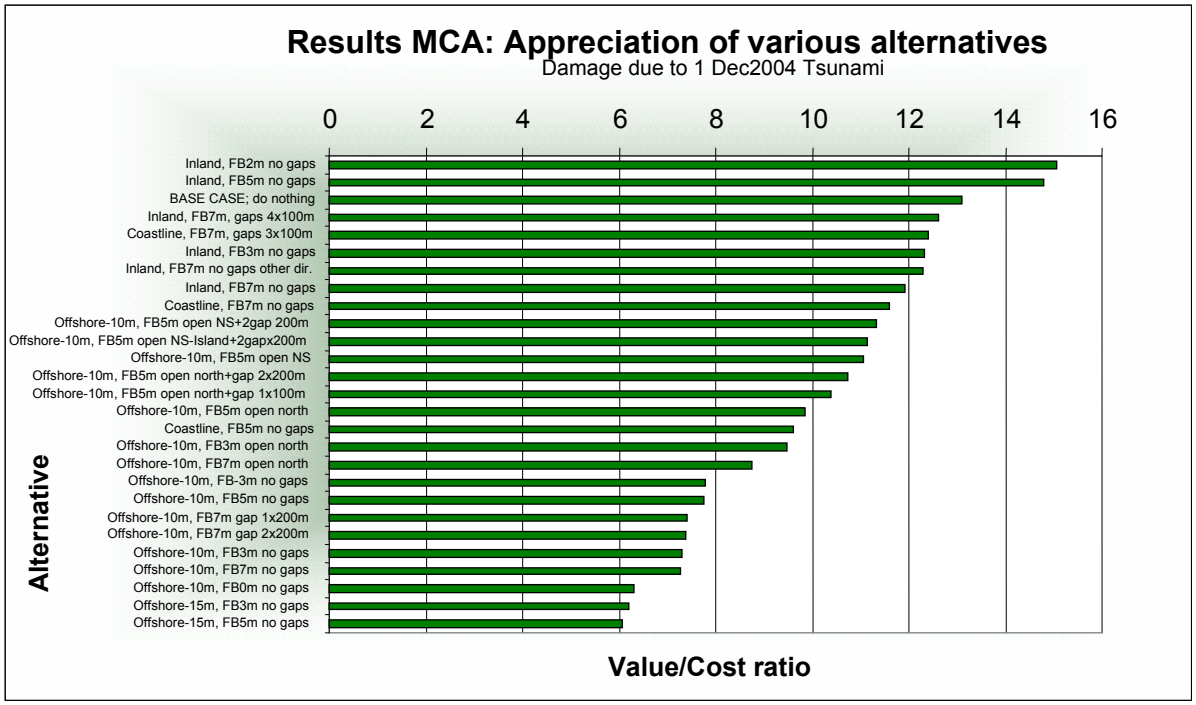

Figure IV-4 Value/cost ratios for various alternatives; Case 1

Under these conditions, building on land, on the coast or even doing nothing gives the highest value with respect to the costs. Offshore solutions are simply too expensive to justify the damage. However, increasing the damage by factor 2 changes the picture completely, see Figure IV-5.

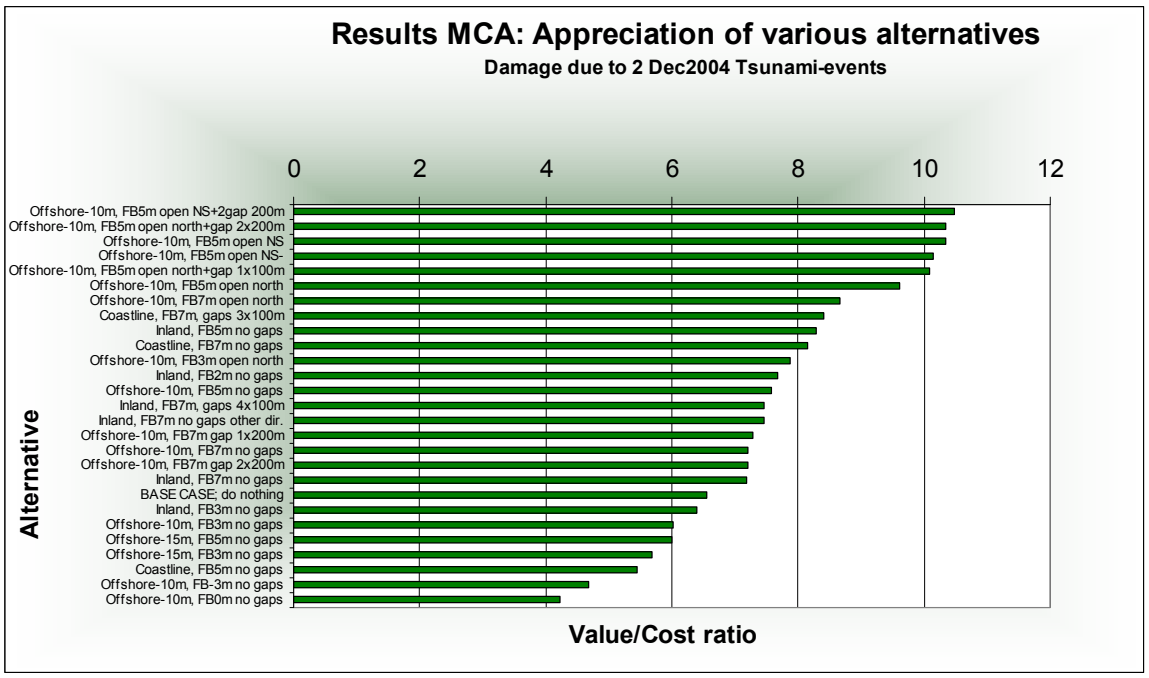

Figure IV-5 Value/cost ratios for various alternatives; Case 2

In this case offshore solutions at 10m water depth become preferable. The damage due to the tsunamis is evaluated higher than the construction costs of offshore solutions. Again, this does not mean that the damage really **is** higher, but that it is evaluated higher.

IV - 5 SUMMARY

This MCA made clear that in case a structure is built, the offshore solutions have strong preference above structural measures on land. This is mainly due to the high social impact of high structures on land.

When the value is compared to the total costs (construction costs + damage) the picture changes. If the damage due to tsunamis is evaluated as equal to the Dec2004 tsunami, inland structures or doing nothing becomes preferable. However, when damage is evaluated higher (2x) offshore solutions have the highest ranking.

Appendix V. COST ANALYSIS FOR VARIOUS ALTERNATIVES

The cost-calculation for the presented cross-sections presented is based on three reference designs of which the height is chosen more or less randomly:

- An offshore barrier of 17m height (7m retaining height in 10m water depth)
- A coastal barrier of 11m height
- An inland barrier of 8m height

These cost estimates are compared and a relation between structure height and costs is obtained for the three alternatives for a wider range of structure heights.

on up-to-date unity rates for material and labour. The length of all alternatives is approximately the same, 22km. Although the finally chosen design, proposed in Chapter 7 of the main report, differs slightly from the design used in this analysis, this will not change the results of the analyses where the costs are used for.

V - 1 OFFSHORE TSUNAMI BARRIER

The cost calculation for the offshore barrier is based on the cross section of Figure V-1.

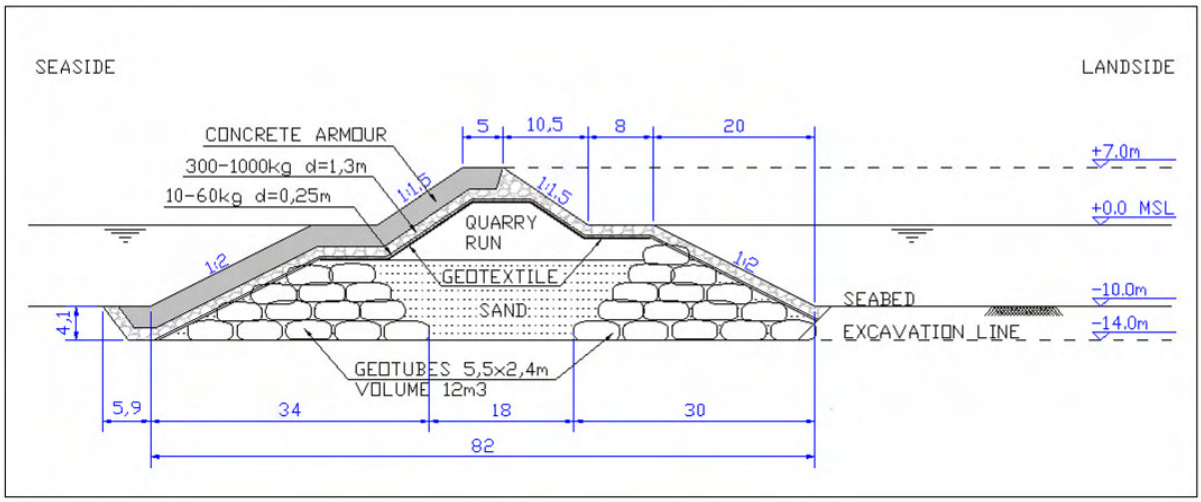

Figure V-1 Cross-section Offshore Tsunami Barrier at -10m Bathymetry line

In TableV-1, the costs are estimated based on volumes and up-to-date unit rates. Costs are expressed in US Dollars ($).

TableV-1: Cost estimation offshore tsunami barrier at -10m bathymetry line

No	Description	Unit	Quantity	Unit rate	Costs/m	Total costs
I	OFFSHORE BARRIER					
	Concrete Armour Layer (not reinforced)	m^3/m	134	$90,00	$ 12.060	

No	Description	Unit	Quantity	Unit rate	Costs/m	Total costs
	Stone 300-1000kg	m^3/m	130,7	$32,00	$ 4.182	
	Stone 10-60kg	m^3/m	22,5	$32,00	$ 720	
	Sand	m^3/m	300	$8,00	$ 2.400	
	Quarry Run	m^3/m	149,3	$25,00	$ 3.733	
	Excavation Area	m^3/m	354	$8,00	$ 2.832	
	Geocontainers (12m2 each)	m^3/m	348	$30,00	$ 10.440	
	Smoothening layer on Geocontainers	m^3/m	10	$32,00	$ 320	
	Geotextile on quarry run	m^2/m	44	$5,50	$ 242	
	TOTAL	**m^3/m**	**1094,5**		**$ 36.929**	
II	GENERAL	%	2		$ 739	
III	OTHERS	%	5		$ 1.846	
	SUM				**$ 39.514**	
	Tax	%	10		$ 3.951	
	Profit	%	10		$ 3.951	
	Contingency	%	15		$ 5.927	
	TOTAL CONSTRUCTION COSTS per m				**$ 53.344**	
	TOTAL CONSTRUCTION COSTS FOR ENTIRE BARRIER (22,5km)					**$ 1.200.000.000**
	Construction costs per m^3 volume of offshore barrier					$ 48,7 / m^3
IV	ADDITIONAL COSTS					
	Design and supervision of the barrier; estimated at 5% of construction costs					$ 60.000.000
	Study of morphology/environment/navigation, etc. for implementation of barrier into the area, estimated at 5% of construction costs					$ 60.000.000
	Execution of mitigating measures to guarantee environment, employment in the area, estimated at $200 million					$ 200.000.000
	TOTAL COSTS INCLUDING ADDITIONAL COSTS					**$ 1.520.000.000**
	Total costs per m^3 volume of offshore barrier					$ 61,7 / m^3
V	MAINTENANCE COSTS PER YEAR					
	Maintenance costs of barrier per year, estimated at 1% of construction costs:					$ 12.000.000
	Maintenance costs of mitigating measured per year, estimated at 2,5% of execution costs:					$ 5.000.000
	TOTAL OF MAINTENANCE COSTS PER YEAR					**$ 17.000.000**

Notes

- All rates include mobilization and demobilization of equipment
- Volumes are brute volumes including voids
- Rates take into account voids

- The unit rate for Geocontainers is bases on correspondence with Ten Cate and evaluation of completed projects with Geocontainers [8].

V - 2 COASTAL TSUNAMI BARRIER

The cost calculation for the coastal barrier is shown in TableV-2 and is based on the following characteristics:

- Height of the barrier: 11m
- Crest width 8m
- Slopes 1:2
- Footprint width = 11*2*2 + 8 = 52m
- Length 22.000m

For the used unit rates:

- Rock and concrete on shoreline barrier is 15% cheaper than for offshore barrier
- No Geocontainers, but instead bund walls have to be made for hydraulic fill

TableV-2: Cost estimation coastal tsunami barrier, 11m height

No	Description	Unit	Quantity	Unit rate	Costs/m	Total costs
I	COASTAL BARRIER					
	Concrete Armour Layer (not reinforced)	m^3/m	106	$76,5	$8.109	
	Stone 300-1000kg	m^3/m	53	$27,2	$1.442	
	Stone 10-60kg	m^3/m	26	$27,2	$707	
	Sand	m^3/m	220	$8,0	$1.760	
	Geotextile	m^2/m	57	$5,5	$314	
	Geotextile mattress along shoreline	m^2/m	8	$30,0	$240	
	Provision for bund walls	LS	1		$300	
	TOTAL	**m^3/m**	**405**		**$12.871**	
II	GENERAL	%	2		$257	
II		%				
I	OTHERS		5		$644	
	SUM				**$13.772**	
	Tax	%	10		$1.377	
	Profit	%	10		$1.377	
	Contingency	%	15		$2.066	
	TOTAL CONSTRUCTION COSTS per m				**$18.593**	
	TOTAL CONSTRUCTION COSTS FOR ENTIRE BARRIER (22km), rounded					**$425.000.000**
	Construction costs per m^3 volume of offshore barrier					$ 46 / m^3

No	Description	Unit	Quantity	Unit rate	Costs/m	Total costs
IV	ADDITIONAL COSTS					
	Design and supervision of the barrier; estimated at 5% of construction costs					$21.250.000
	Land acquisition. IDR300.000 / m^2 = \$33,3 / m^2					
	Total required: 22000*54 m^2 = 1.188.000m^2					
	Total land acquisition costs: 1.188.000 * \$33,3 =					$39.600.000
	TOTAL COSTS INCLUDING ADDITIONAL COSTS					**$485.850.000**
	Total costs per m^3 volume of offshore barrier					\$ 54,5 / m^3
V	MAINTENANCE COSTS PER YEAR					
	Maintenance costs of barrier per year, estimated at 1% of construction costs:					$4.250.000
	TOTAL OF MAINTENANCE COSTS PER YEAR					**$4.250.000**

Notes

- All rates include mobilization and demobilization of equipment
- Volumes are brute volumes including voids
- Rates take into account voids

The same cost estimate is made for a coastal barrier of 14m height. It was concluded that the coastal barrier gets \$2,00 / m^3 cheaper for each meter that the barrier is higher. The overall unit rate for the 11m barrier is \$46/m^3.

The unit rate for the construction costs of a barrier of 14m height becomes: (46 – 3 * 2) = \$40 / m^3
The volume = 550m^2/m, this results in \$484.000.000 total construction costs.

V - 3 INLAND TSUNAMI BARRIER

For the inland barrier, no geotextile mattresses are required and the toe structure is less compared to the coastal barrier. However, the overall construction type of the inland barrier is identical to the coastline barrier. Therefore, the same assumption as mentioned above is used. For each meter higher the unit rate for the inland wall becomes \$2,00/m^3 lower.

For an inland wall with the following characteristics:

- Height of the inland barrier 8m
- Crest width 5m
- Slopes 1:2
- Footprint width = 8*2*2 + 5 = 37 m
- Length 22.000m
- volume is 168m^3.

The unit rate becomes: 46 + (11-8) * 2 = \$ 52 / m^3. The cost calculation is presented in TableV-3.

TableV-3: Cost estimation Inland tsunami barrier, 8m height

No	Description	Unit	Quantity	Unit rate	Costs/ m	Total costs
I, II & III	Construction costs	m^3	168	$ 52	$8.736	
	TOTAL CONSTRUCTION COSTS per m				**$8.736**	
	TOTAL CONSTRUCTION COSTS FOR ENTIRE BARRIER (22km), rounded					**$200.000.000**
	Construction costs per m^3 volume of offshore barrier					$ 52 / m^3
IV	ADDITIONAL COSTS					
	Design and supervision of the barrier; estimated at 5% of construction costs					$10.000.000
	Land acquisition. IDR500.000 / m^2 = $55,6 / m^2.					
	Total required: 22000*47 = 1.034.000m^2.					
	Total land acquisition costs: 1.034.000 * $55,6 =					$57.490.400
	TOTAL COSTS INCLUDING ADDITIONAL COSTS					**$267.490.400**
	Total costs per m^3 volume of offshore barrier					$ 72,4 / m^3
V	MAINTENANCE COSTS PER YEAR					
	Maintenance costs of barrier per year, estimated at 1% of construction costs:					$2.000.000
	TOTAL OF MAINTENANCE COSTS PER YEAR					**$2.000.000**

Notes

- All rates include mobilization and demobilization of equipment
- Volumes are brute volumes including voids
- Rates take into account voids

V - 4 OVERVIEW

The costs (construction costs, additional costs and maintenance costs) for each elaborated alternative are:

Offshore Tsunami Barrier at -10m water depth. Total height: 17m.

- Construction costs $ 1.200.000.000
- Additional costs $ 320.000.000
- Maintenance costs $ 17.000.000 / year

Coastal Tsunami Barrier. Height: 11m

- Construction costs $ 425.000.000
- Additional costs $ 60.850.000
- Maintenance costs $ 4.250.000 / year

Inland Tsunami Barrier. Height: 8m

- Construction costs $ 200.000.000
- Additional costs $ 67.500.000
- Maintenance costs $ 2.000.000 / year

An attempt has been made to extend this cost estimate to an estimation of the costs for a range of structure heights.

For the construction costs, the overall costs per m^3 are calculated, based on the previous analysis. With this figure, the costs for the other structure heights are simply calculated, based on the volume of the structure.

Although this approach entails some rough assumptions, it provides a good tool to analyse the feasibility of the alternatives. For an overview, see Figure V-2.

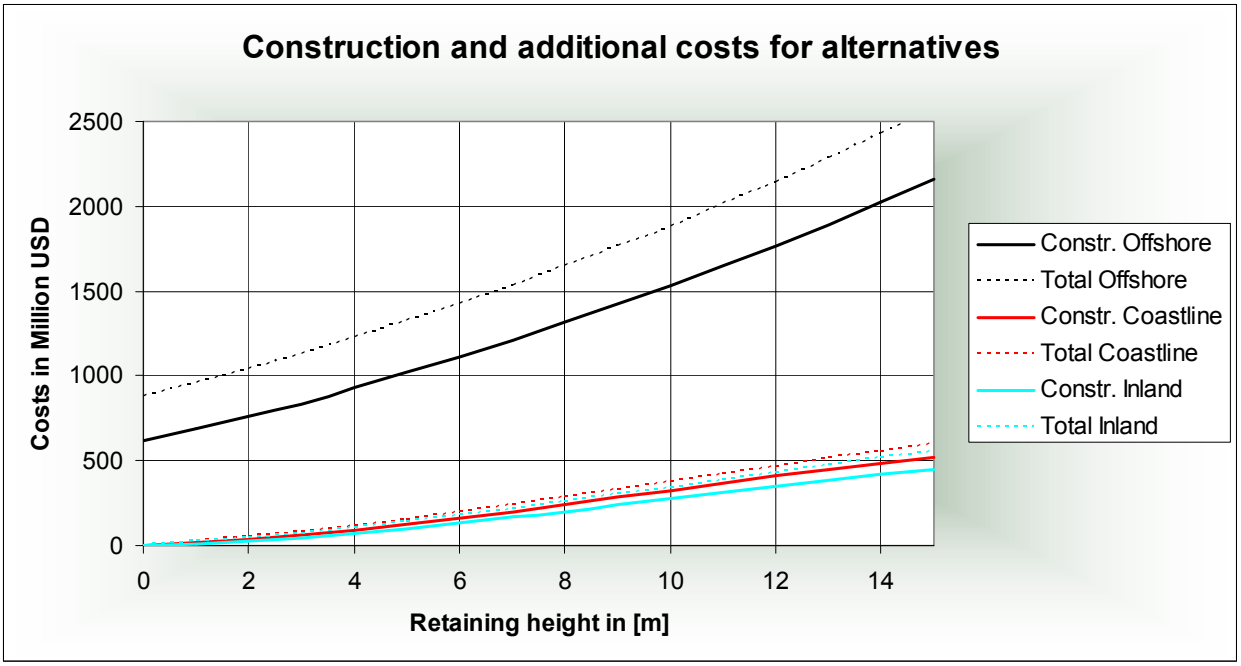

Figure V-2 Overview construction- and additional costs for the main alternatives

The horizontal axis shows the retaining height. This can also be seen as the visible height of the structure. An offshore breakwater at -10m water depth with no retaining height, or visible height, still has construction costs around USD $600 million. These are the costs for constructing the under-water-part of the structure.

Appendix VI. STABILITY CALCULATION; SLIDING

VI - 1 SLIDING ALONG ANY HORIZONTAL PLANE

Due to horizontal water pressures, the structure could collapse due to sliding. Two situations are considered, as shown below in Figure VI-1.

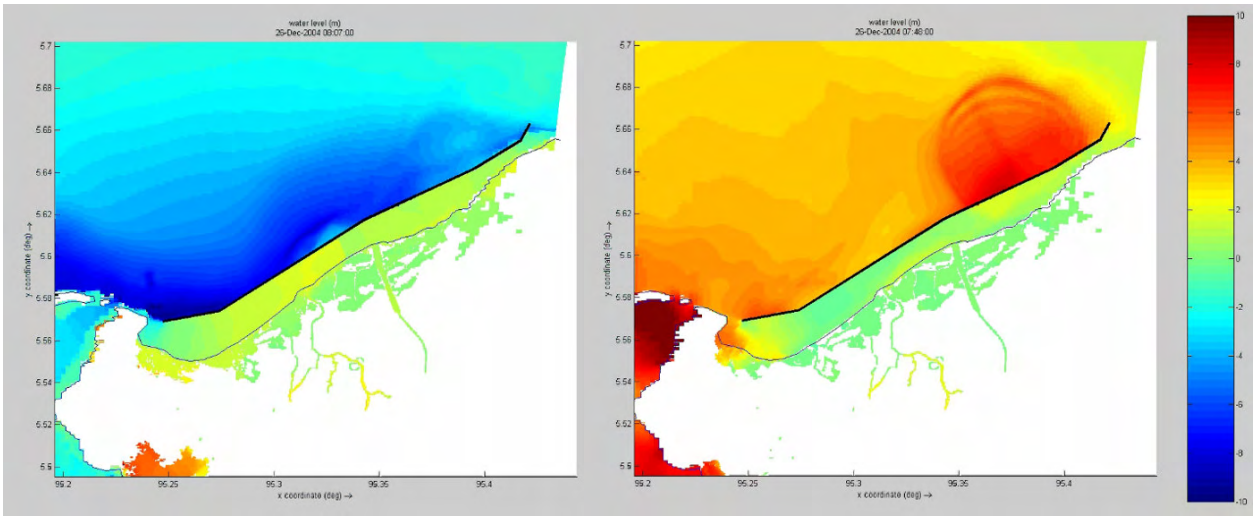

Figure VI-1 Two situations when sliding could occur. Left figure: increased water level at landside and dropdown at seaside; seaward sliding. Right figure: increased water level at seaside and lowering water level at landside; landward sliding.

In situation 1, the maximum head difference becomes: -10 – 2 = -12m
In situation 2, the maximum head difference becomes: +7 (freeboard) - -2 = 9m

In these situations water pressures acting in horizontal direction could cause sliding of the structure. Two possibly decisive situations are depicted in Figure VI-2.

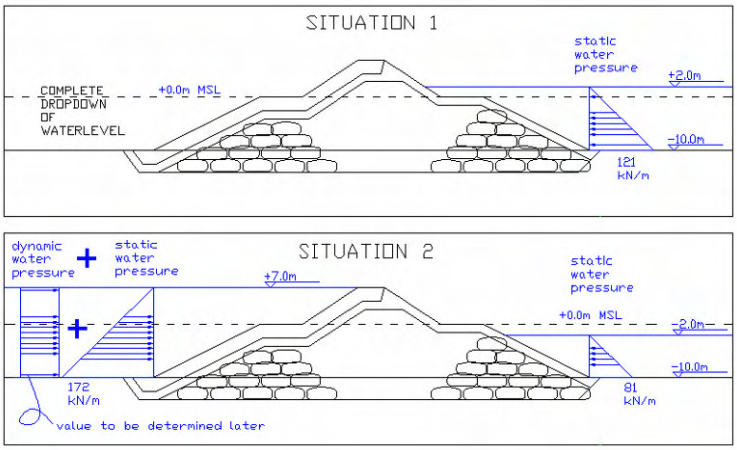

Situation 1
Only hydrostatic force acting in seaward direction

Situation 2
Seaside: hydrostatic force + dynamic force over entire height.
Landside: hydrostatic force with lowered water level.

Figure VI-2 Two considered situations

The dynamic water pressure in situation 2, acting in landward direction is discussed later, as this highly depends on the velocity of the tsunami impact.

Resistance

The resistance of the structure depends on the effective vertical weight (if submerged, the effective weight is smaller than the total weight because of buoyancy) multiplied by a friction factor. This friction factor is calculated by:

$$f = c + \tan(\phi)$$

Where *c* is the cohesion and ϕ is the angle of repose. For rubble mound (in the top) a conservative value of 30° is assumed. For the underlying sand layer the same value is taken, which corresponds with densely packed sand (30-33°). The sand is not cohesive, so *c* = 0. The friction factor *f* then becomes:

$$f = 0 + \tan(30) = 0{,}58$$

It is assumed that the structure is completely dry from the lowered water level up to crest level. Buoyancy can only occur below the lowered water level.

The following densities are used:

Concrete:	24kN/m^3
Rubble-mound:	18kN/m^3
Sand, dry:	18kN/m^3
Sand, wet:	20kN/m^3

With above values the resistance of the structure-body against sliding along any horizontal plane can be determined. For safety reasons, the strength is reduced by factor 1,2. The results are presented below (Figure VI-3).

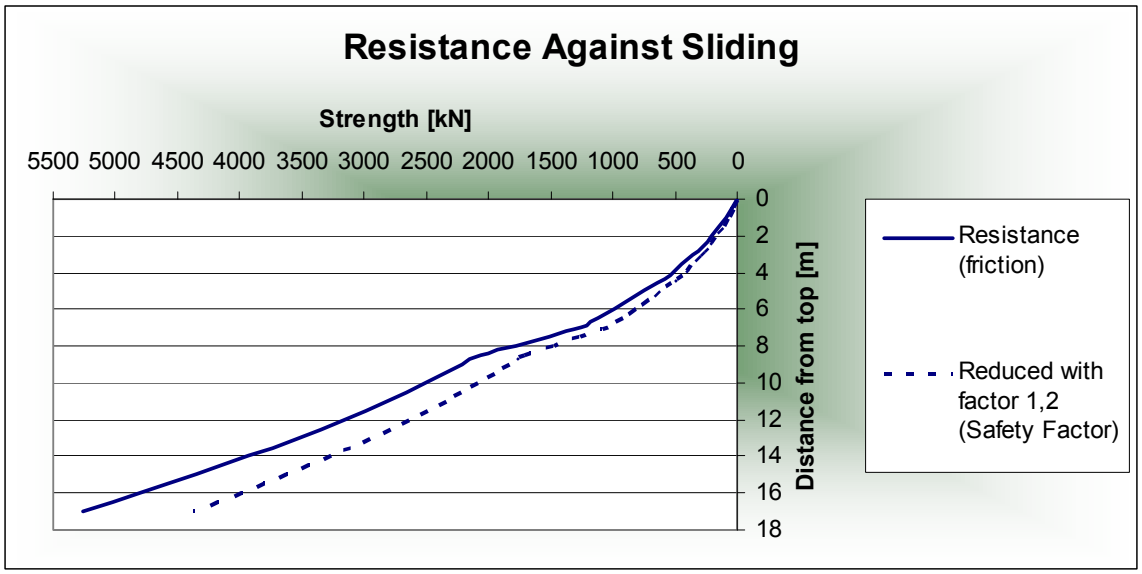

Figure VI-3 Resistance against sliding for each distance from crest breakwater

Load case, situation 1

In this situation only hydrostatic forces occur. The loads due to hydro-static water pressures can easily be calculated by:

$F_{hydrostatic} = ½ \rho g h^2$

The *h* is the water level in front of or behind the structure.
The resulting forces (red line) and resistance (blue line) are shown in Figure VI-4.

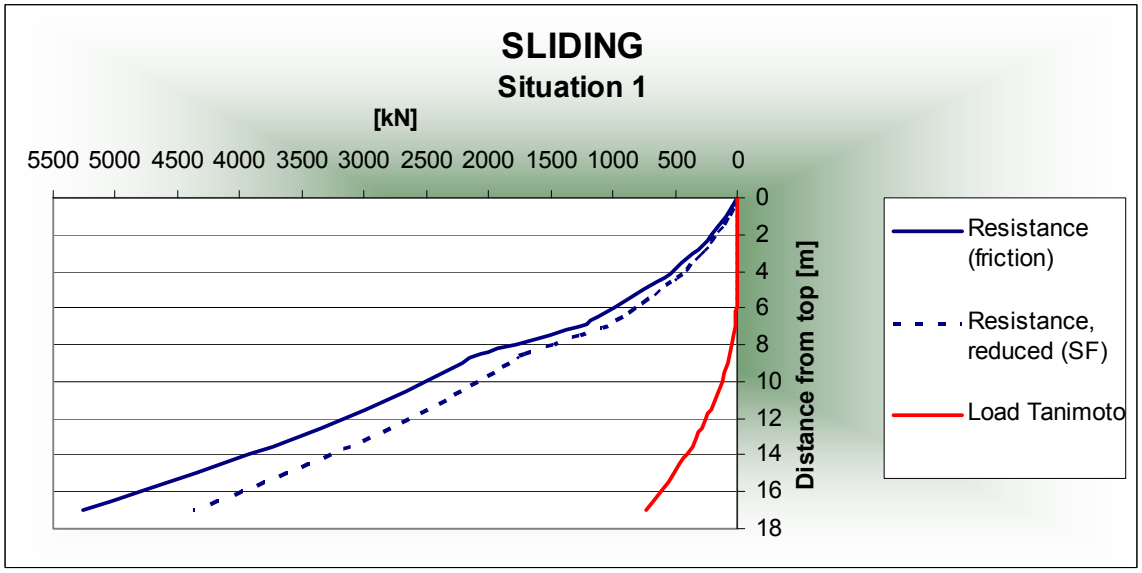

Figure VI-4 Sliding; resistance and load according to Tanimoto

Conclusion

The hydrostatic forces acting in seaward direction during initial and complete drawback of the water in front of the structure do not exceed the resistance of the structure.

Load case, situation 2

The loads due to hydro-static water pressures can easily be calculated by:

$F_{hydrostatic} = ½ \rho g h^2$

The *h* is the water level in front of or behind the structure.

The dynamic force over a certain height can be obtained by:

$F_{dynamic} = \rho u^2 h$

The velocity *u* is an important parameter. In Chapter 4 it was concluded that on land (for Banda Aceh) the velocities did not exceed about 1,3√(gh). The velocities in open areas, closer to the seas, even showed lower velocities. However, as the breakwater is located offshore at 10m water depth, it is expected that even lower velocities can be used to calculate the dynamic water pressure.

To support this idea, two approaches are worked out and compared

A. Horizontal water pressures based on 1D modelling of the structure
B. Horizontal load according to the method of Tanimoto (for non-breaking tsunamis)
C. Horizontal load according to the method of Yamamoto (calibrated for bores running on land)

Approach A

The 1D-model is used to obtain velocities and water levels along the entire slope of the breakwater structure. The grid size is locally decreased from 15m to 3m at the structure location. For each grid, velocities and water levels are extracted. The results are presented in Figure VI-5.

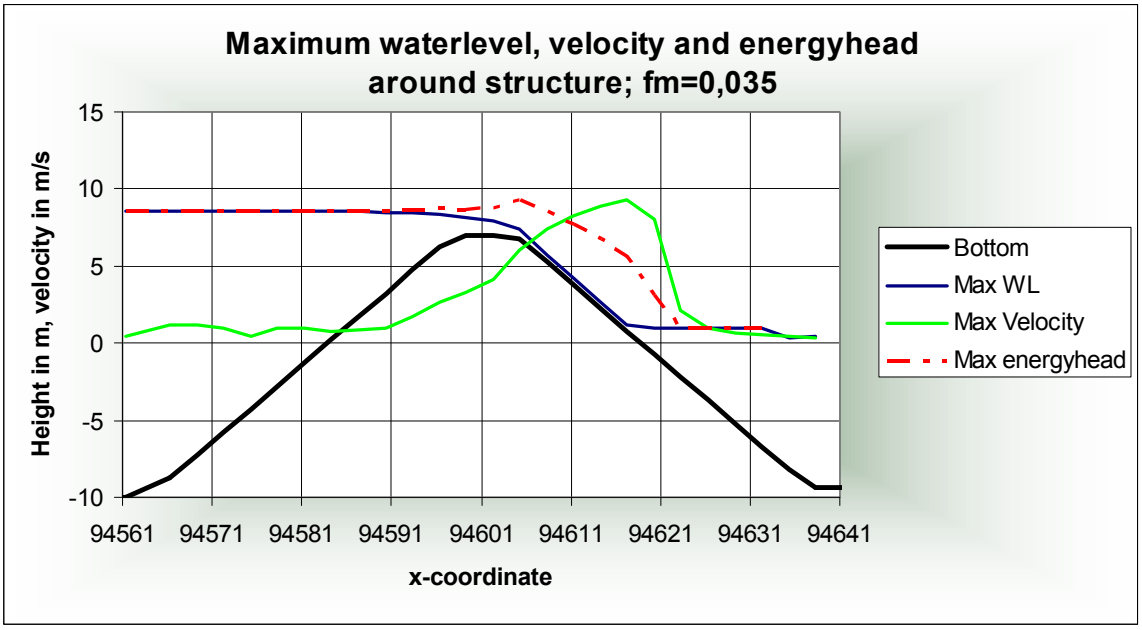

Figure VI-5 Maximum waterlevel, velocity and energyhead around the structure

It is clear that velocities on the seaside (left side) of the structure are quite low compared to the land side. Values vary between 0,5 and 2m/s on the front side, but at the back side, velocities up to 9 m/s do occur.

However, for sliding only the velocities in the front of the structure are important. For each grid, the total horizontal water pressure ($F_{hydrostatic}$ + $F_{dynamic}$) is calculated. The resulting horizontal loads on the structure are presented later.

Approach B

In Chapter 2, the method of Tanimoto is presented for stability calculations concerning caisson-type breakwaters. Although this structure is a rubble-mound structure, the horizontal load should be comparable. The used formulas and definitions (see Figure VI-6):

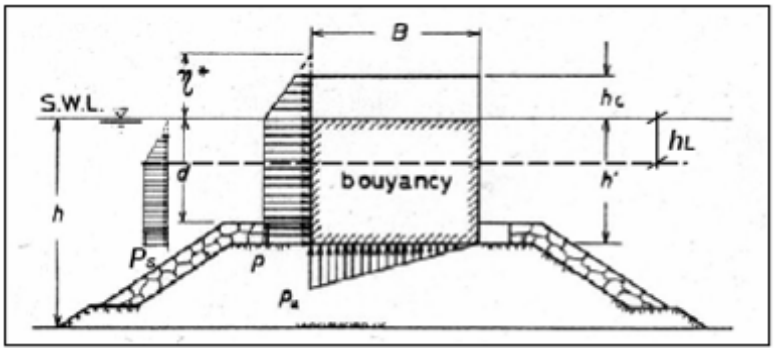

Figure VI-6 Definitions according to Tanimoto

$$\eta^* = 1{,}5H$$
$$p = p_u = 1{,}1 w_0 H$$

where η^* is the height above the still water level at which the wave pressure intensity is zero, *p* is the wave pressure intensity which acts uniformly on the vertical wall below the still water level.

$$P = \left\{1 + \left(1 - \frac{h_c^*}{3H}\right)\frac{h_c^*}{h'}\right\} p h'$$

Where $h_c^* = \min\{\eta^*, h_c\}$

Tanimoto also incorporated the influence of a water-lowering at the backside of the structure. The horizontal force due to the lowering is:

$$P_s = w_0 h_L \left(h' - \frac{1}{2} h_L\right)$$

The most difficult parameter is the tsunami height H. Tanimoto proposed to use the reflected wave height. As from the model runs can be concluded, the maximum reflected tsunami wave is:

H = 8,5m

With a lowering at the land side of 2m, the pressure distribution is known and the total horizontal force can be determined.

Approach C

Yamamoto *et al* [48] (see Chapter 2), investigated the damage for structure on land. He found that it could be well described by assuming a drag force equal to:

$$p_{dyn} = 0{,}5 C \rho u^2$$

with $u = 1{,}1\sqrt{gh}$, *h* is the inundation depth, *ρ* is the density of sea water (kg/m^3) and C is a shape coefficient (=2 for rectangle sections and 1,2 for circular sections).

In the investigated cases the structure is completely surrounded by water, flowing with velocity *u.* For the flow over the offshore barrier, the situation is different. The water is stacked up in front of the barrier. Applying a velocity relative to the local depth would result in a decelerating flow towards the crest of the barrier (in reality this flow is accelerating). See figure below.

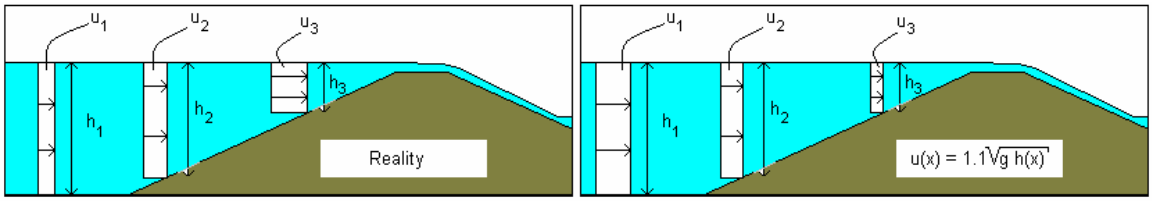

Therefore, Yamamoto's approach would lead to unrealistic values. However, this method can be used to estimate the velocity on the crest. According to the 1D-modelling, the maximum water depth on top = 1,5m ≈ 2,0m. This leads to:

$$u_{crest} = 1{,}1\sqrt{2{,}0g} \approx 5{,}0m/s$$

Applying this velocity over the total height for all cross-sections in above graph, the dynamic force according to Yamamoto can be calculated. It was also found in Chapter 2.5 that a safe upper limit for tsunami-forces is the method of Kato. This method yield loads which are approximately 1,13 times higher then Yamamoto's method.
It is believed that this approach leads to conservative values, since the depth-averaged velocity will be lower in on the slopes of the barrier.

For load case 2, the impact of the positive wave on the structure, these three approaches are elaborated and the loads are calculated and presented in the following 2 graphs (Figure VI-7 & Figure VI-8).

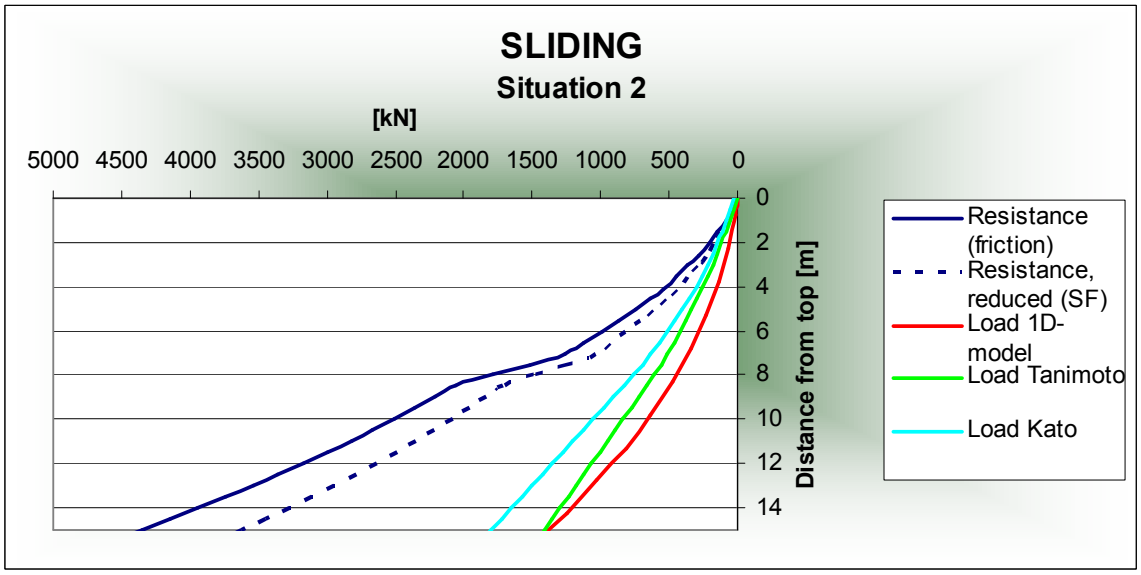

Figure VI-7 Resistance against sliding; Kato, Tanimoto and 1D-model

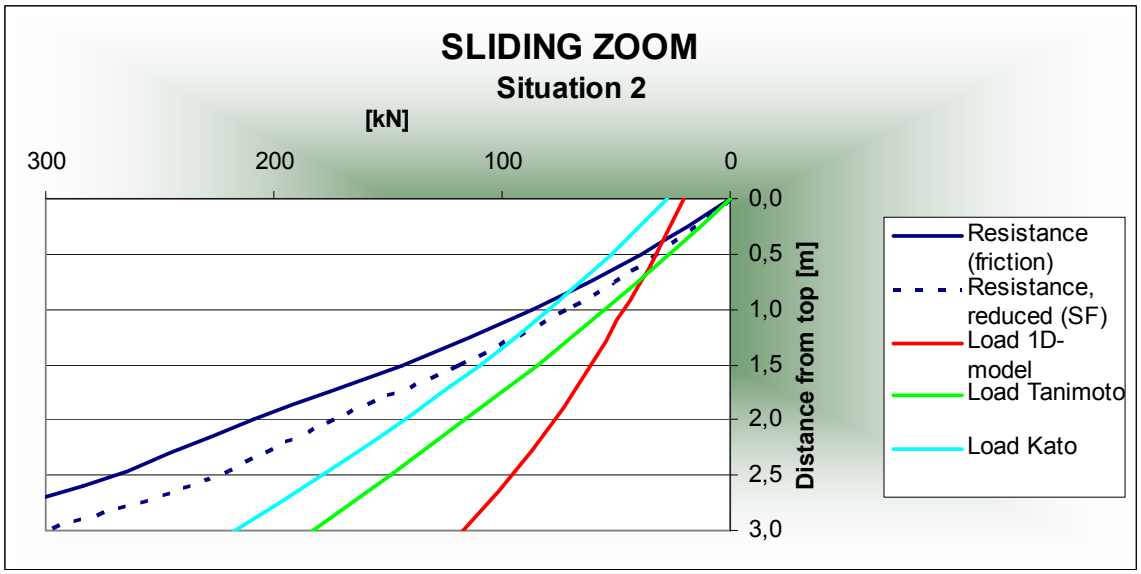

Figure VI-8 Resistance against sliding; Kato; Tanimoto and 1D-model. ZOOM

Over the total height of the structure the (reduced) resistance against sliding is higher than the loads as calculated by Tanimoto. For the first meter, the loads obtained from the 1D – model and calculated with Kato exceed the resistance. Increasing the crest width is not helpful in this case, because the overload is cause by the force of the overlying water mass. But the development of a horizontal sliding plane in the first meter can easily be prohibited by applying armour stones or rock with a diameter greater then 1m.

The 1-D model results, gives results smaller then the other methods. This is because the hydrostatic forces are dominant with respect to the dynamic forces. This indicates that the velocities are low, and the tsunami attack can be well described as a rapidly rising tide in stead of an impinging wave.

Conclusion
Although load case 2 is normative, the loads do not exceed the resistance.

In all load cases the breakwater design is safe against sliding along any horizontal plane below 1m beneath the crest. On the crest, blocks greater then 1m should be applied.

VI - 2 SLIDING ALONG ANY CIRCULAR PLANE

The stability against sliding along a circular plane can be investigated with the Bishop method. Because a large number of calculations is required, this failure mechanism is studied with MStab. The studied load cases are:

1. Equal water levels on both sides (+ 0,0 MSL)
2. High outer water level (+7.0 MSL) and lower inner water level (-2.0 MSL)
3. Low outer water level (complete drying -10.0 MSL) and average inner level.

The influence of slope angle, core material, berms and crest-width has been studied. The results for load case 2 are shown below. Green means an safety factor higher then 1,5.

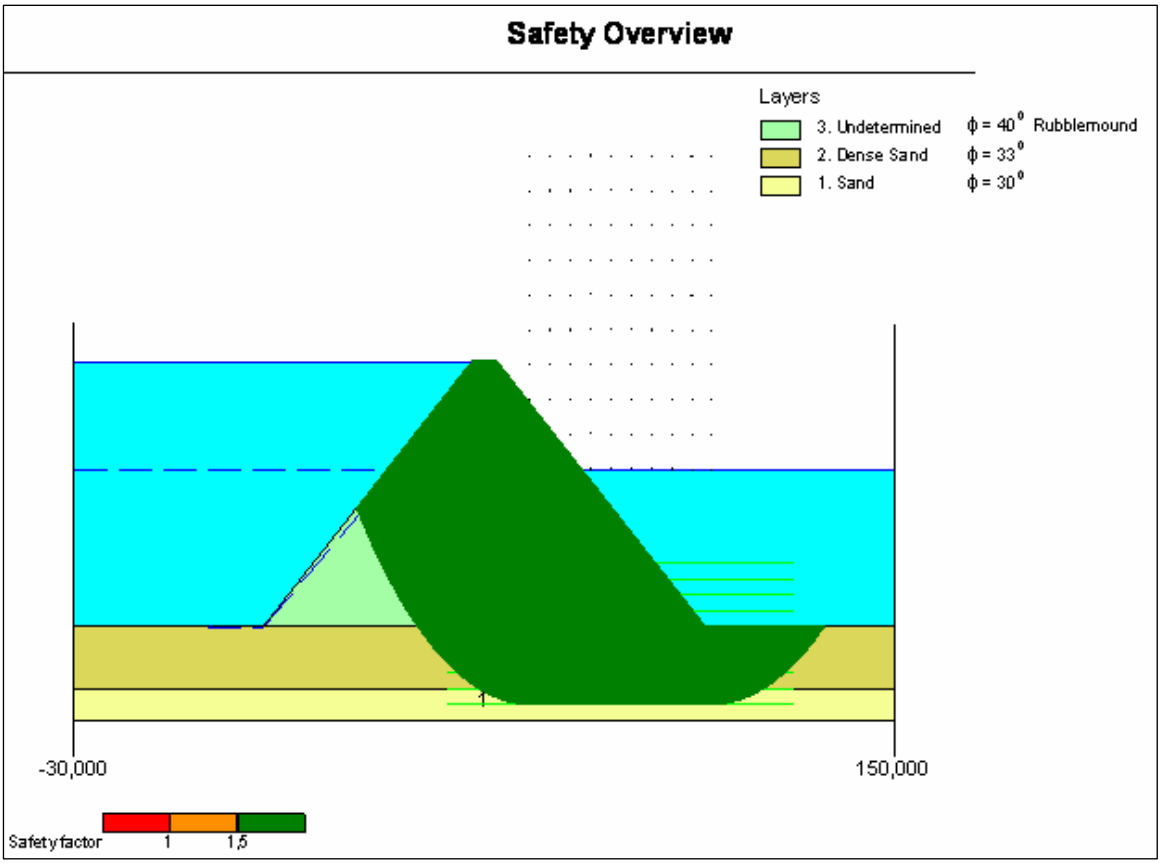

Figure VI-9 Stability against circular sliding for Load Case 2. Output from MStab.

Load case 1 and 2 do not show any susceptibility to circular sliding. For load case 3, with a head difference of 10m, sliding circles could possibly occur. However, constructing the lower part of the structure with (big) geo-containers will prevent against development of a sliding circle.

A berm (5m width) has some positive effect on the stability of the upper part of the slope.

Conclusion

In general the structure seems sufficiently stable against circular sliding. However, the assumptions made in above calculations are rough. Therefore, for detailed design, the actual composition of the structure has to be modelled more accurate.

Appendix VII. STABILITY CALCULATION; LIQUEFACTION

VII - 1 WHAT IS LIQUEFACTION?

Liquefaction refers to a situation in granular material where pore pressures are generated to such a degree that intergranular contact is lost. The entire medium loses its shear strength and behaves like a thick fluid. Under these circumstances any shear loading will cause stability failure. The types of sediments, which are most susceptible for liquefaction, are clay-free deposits, sand and silts. The ground layer must be saturated (and often under ground water level). Well graded soil is less likely to liquefy than uniformly graded soil.

Liquefaction occurs when the structure of loose, saturated sand breaks down due to some rapidly applied loading. Especially earthquakes generate load situations under which liquefaction is likely to occur. As earthquakes regularly occurs in Banda Aceh and, moreover, could be followed by tsunamis, the barrier (and its foundations) should be able to withstand the shear loads induced by the dynamic loads. Failure of the barrier due to a heavy earthquake will directly induce a high risk because the possibility of an arriving tsunami, with no time to restore the damage.

VII - 2 HOW TO DETERMINE THE LIKELIHOOD OF LIQUEFACTION

To be able to study the dynamic behaviour of the soil, cyclic load tri-axial compression tests or cyclic load simple shear tests should be carried out. These tests are not available. Nevertheless it is possible to make certain comments on the liquefaction potential, by using the relations between CPT and liquefaction resistance. Normally, the likelihood of liquefaction is determined by:

$$LP = \frac{CRR}{CSR}$$

where

LP = Liquefaction Potential
CRR = Cyclic Resistance Ratio
CSR = Cyclic Stress Ratio

The resistance is determined by use of the N-value, the number of blows per feet in a Standard Penetration Test. This value is corrected for the equipment used, the so-called N1(60)-value.

By plotting the CSR-(N1)60 pairs for cases in which liquefaction was and was not been observed, a curve that bounds the conditions at which liquefaction has historically been observed can be drawn. This curve, when interpreted as the maximum CSR for which liquefaction of a soil with a given penetration resistance can resist liquefaction, can be thought of as a curve of cyclic resistance ratio (CRR). Then, the potential for liquefaction can be evaluated by comparing the earthquake loading (CSR) with the liquefaction resistance (CRR) - this is usually expressed as a factor of safety against liquefaction,

When the LP-factor is higher then 1, the resistance exceeds the load and the soil will not liquefy. A method which is based on this idea, but less conservative is proposed in the Japanese Standard.

This method combines for each layer of sand the combination of load (a_{eq}) and resistance (N_{eq}). The result is a point in Figure VII-1.

Area I = high likelihood of liquefaction
Area II = likelihood of liquefaction
Area III = small likelihood of liquefaction
Area IV = very small likelihood of liquefaction

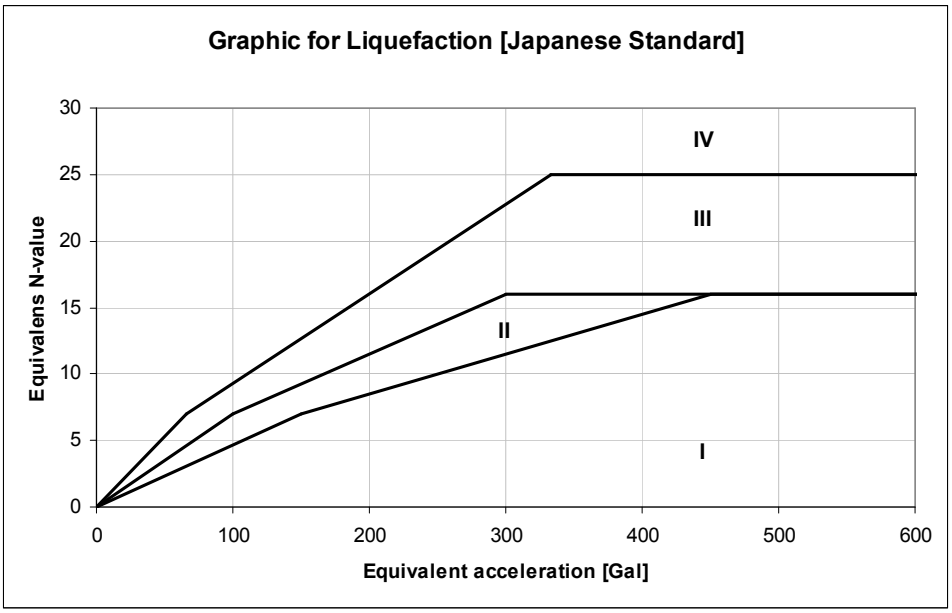

Figure VII-1 Definitions of area boundaries according to Japanese Standard

a_{eq} is the equivalent acceleration [in Gal] which induces shear stresses and can be calculated by:

$$a_{eq} = 0{,}7 \cdot 980 \cdot \left(\frac{\tau_{\max}}{\sigma'_v} \right)$$

with $\tau_{\max} = \sigma_v \cdot a \cdot r_d(z)$

σ'_v = effective vertical stress at depth z
a = horizontal acceleration at $z=0$ expressed in g
r_d = stress reduction factor according to:

$r_d(z)$ = Stress reduction factor, $r_d = \begin{cases} 1{,}0 - 0{,}00765z & for \quad z \le 9{,}15m \\ 1{,}174 - 0{,}0267z & for \quad 9{,}15 \le z \le 23m \\ 0{,}744 - 0{,}008z & for \quad 23 \le z \le 30m \\ 0{,}5 & for \quad z > 30m \end{cases}$

VII - 3 RESULTS

The strength depends on the SPT-value. For the offshore location at -10m bathymetry line, 5 SPT's are available [source]. See Figure VII-2.

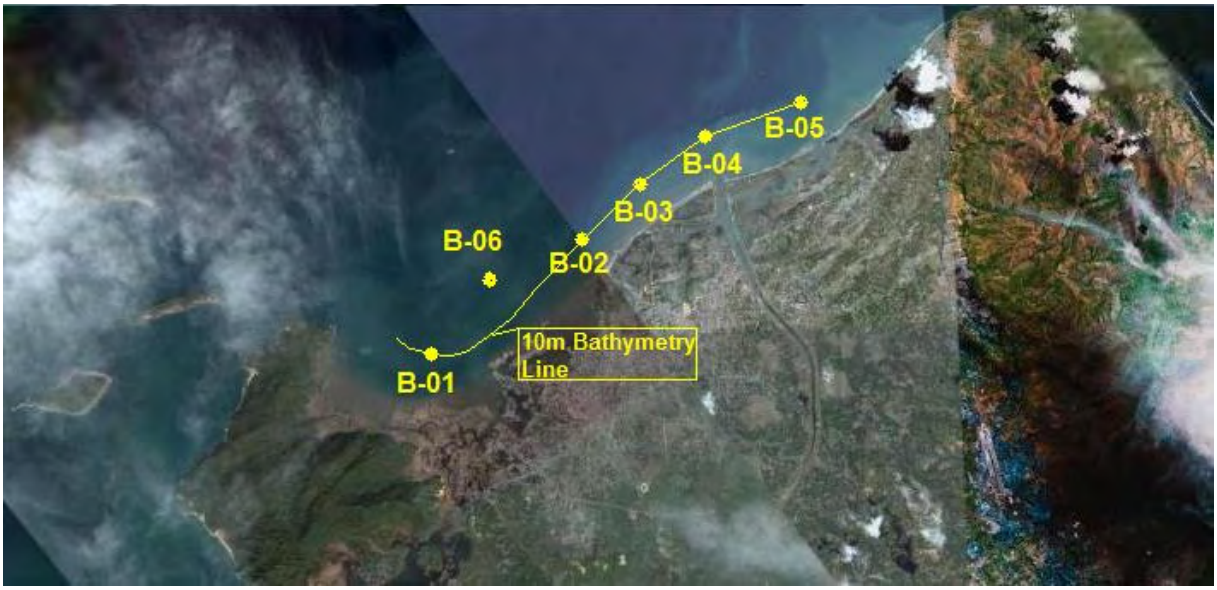

Figure VII-2 Overview offshore SPT locations. Location B-06 is at -13m.

The actual N-values for these locations can be found in [33] and are displayed below. Figure VII-3.

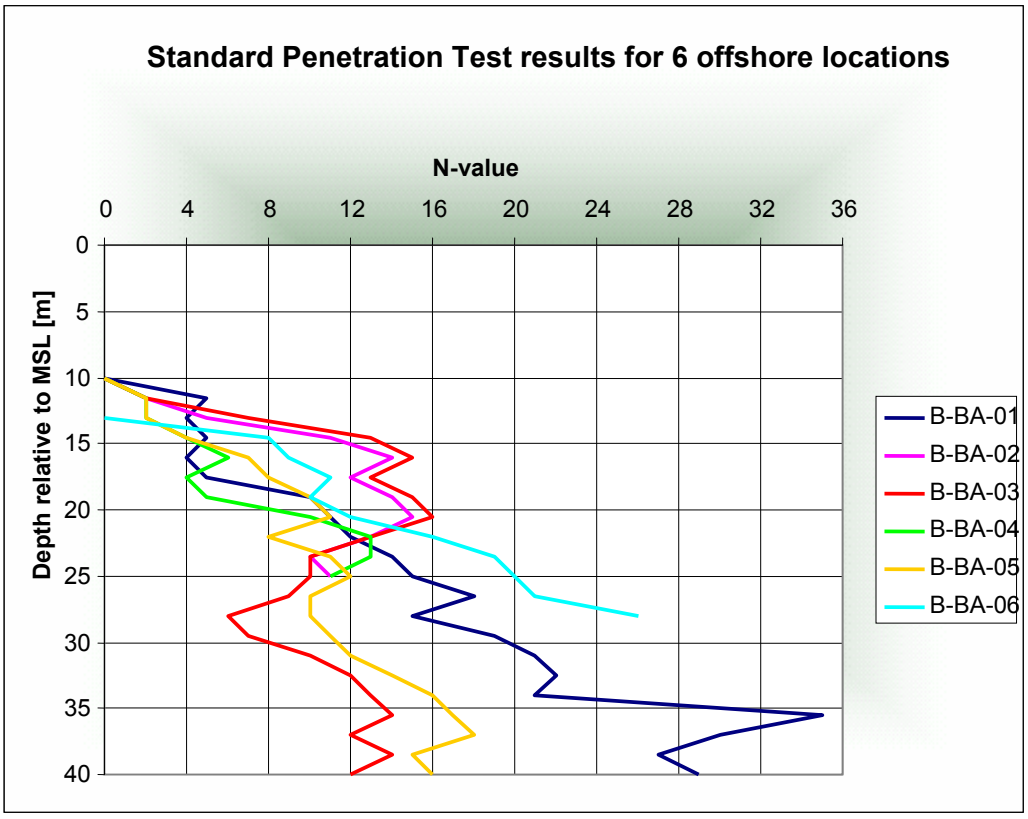

Figure VII-3 SPT-values for 6 offshore locations

These values are corrected to the equivalent value by:

$N_{eq} = N_{65} / C_N$

With $$N_{65} = \frac{(N - 0.019(\sigma'_v - 65))}{(0.0041(\sigma'_v - 65) + 1)}$$

And $C_N = 0{,}5$

Due to the structure's weight, the (shear-) stresses will increase and subsequently the N-value. However, these values are not available. The results for liquefaction as presented below belong therefore to an unloaded situation. In the present state, the results are (Figure VII-4):

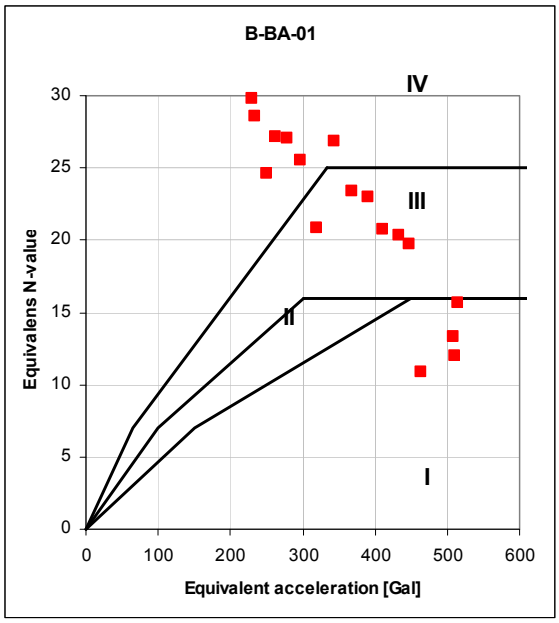
B-BA-01
Equivalens N-value
Equivalent acceleration [Gal]
I
II
III
IV
0
5
10
15
20
25
30
0
100
200
300
400
500
600

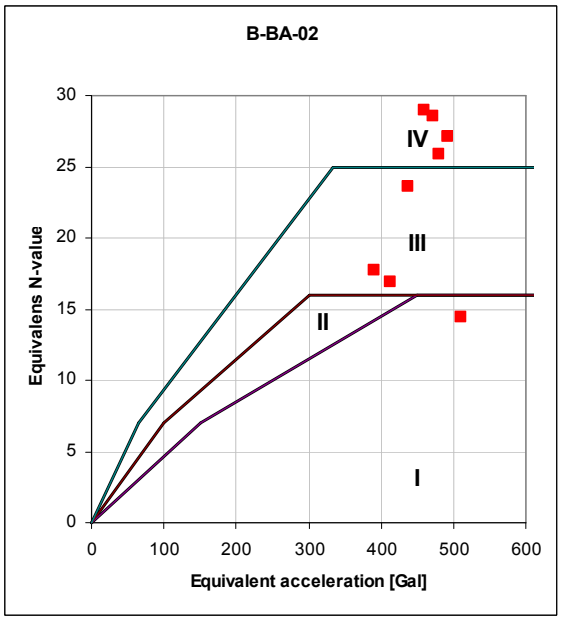
B-BA-02
Equivalens N-value
Equivalent acceleration [Gal]
I
II
III
IV
0
5
10
15
20
25
30
0
100
200
300
400
500
600

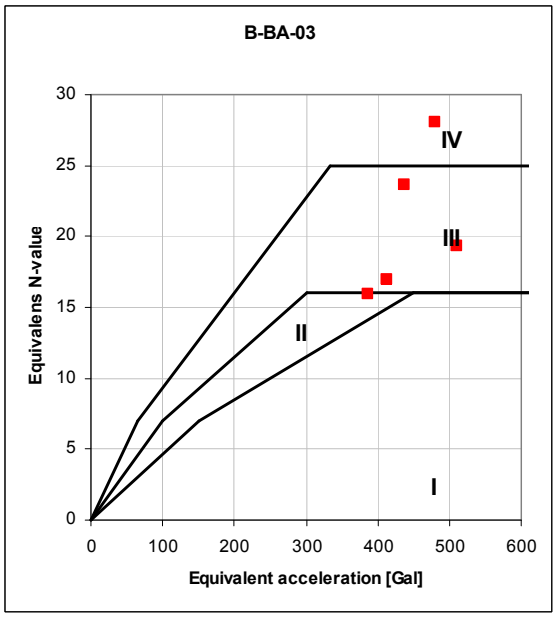
B-BA-03
Equivalens N-value
Equivalent acceleration [Gal]
I
II
III
IV
0
5
10
15
20
25
30
0
100
200
300
400
500
600

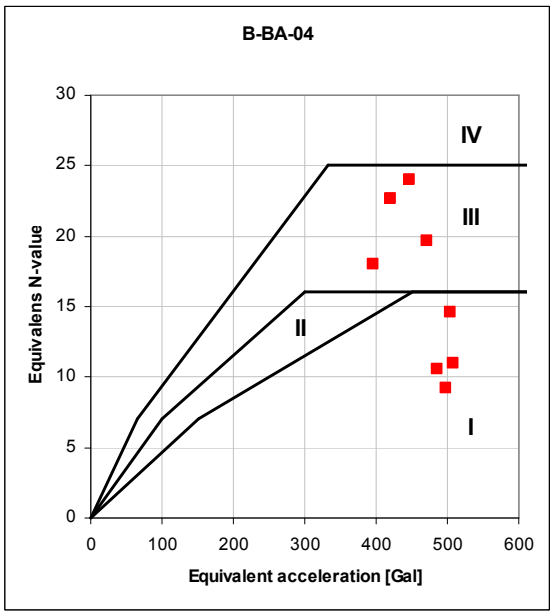
B-BA-04
Equivalens N-value
Equivalent acceleration [Gal]
I
II
III
IV
0
5
10
15
20
25
30
0
100
200
300
400
500
600

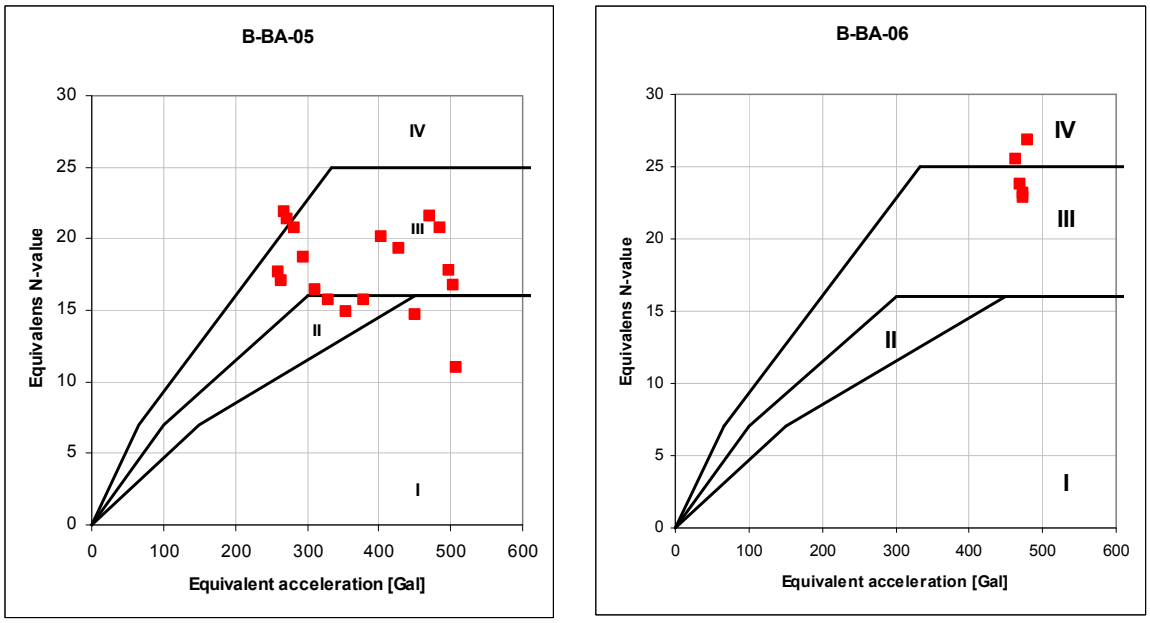

Figure VII-4 Results N_{eq} versus a_{eq} in Japanese Standard Graphs for 6 boreholes

As can be seen from Figure VII-4, boreholes B-01 and B-04 show susceptibility to liquefaction. The first 5 to 7 meters show low resistance.

Another tool to assess the likelihood of liquefaction is the grain size distribution. For both boreholes and the first 5-6 meters these are depicted in Figure VII-5.

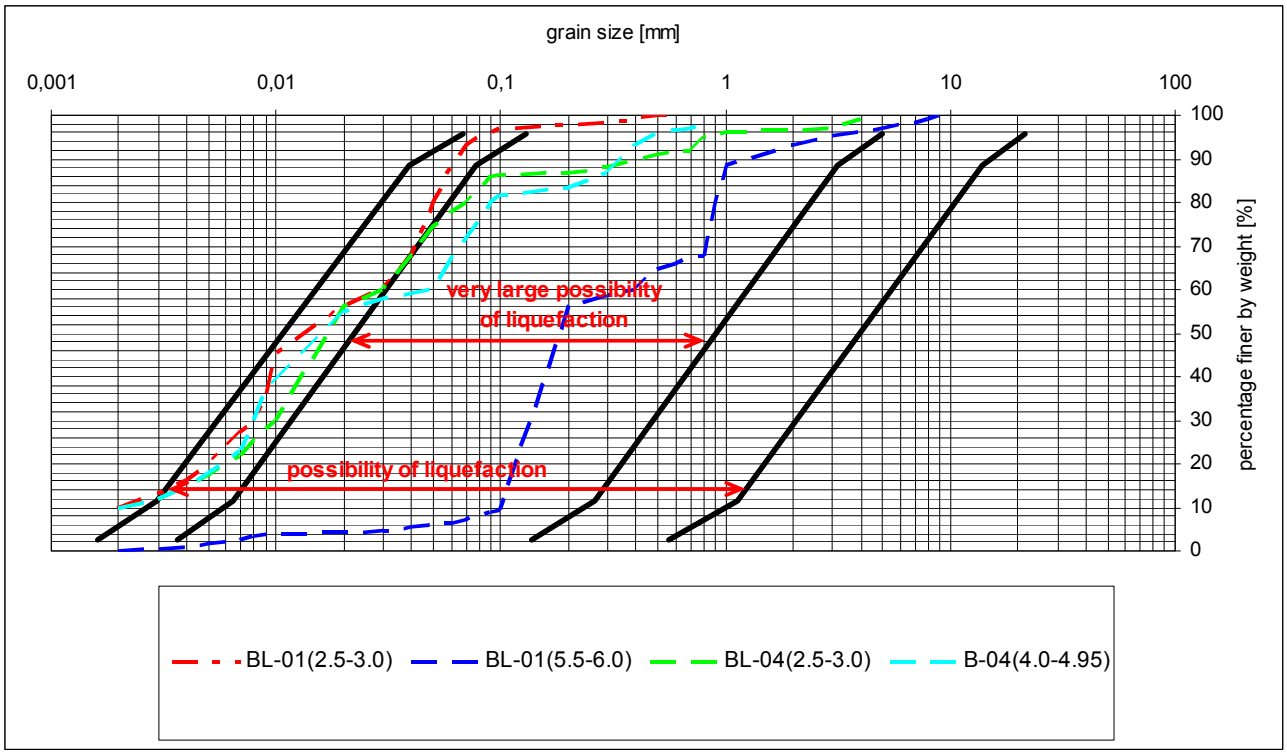

Figure VII-5 Grain size distribution for boreholes B-01 and B-04

As stated before, well-graded soil is less likely to liquefy. The boundaries in the grain size distribution graph are shown (black lines). Only the deeper layer for Borehole BL-01 lies in between all boundaries, indicating that with this soil-type a high possibility for liquefaction exists.

However, above analysis does not account for the positive effect of increased upper load by the presence of the breakwater structure. Due to the weight of the structure, the vertical effective stresses will increase and thereby enhancing the soil properties (density). Consequently the SPT-values will increase. The stress distribution (total stress) at seabed level is presented in Figure VII-6 .

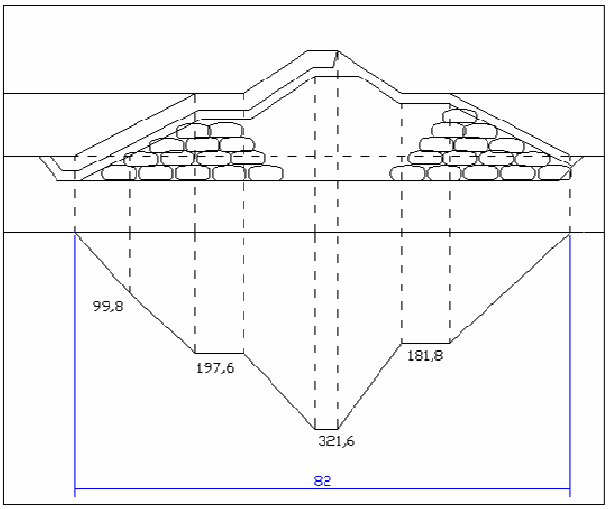

Figure VII-6 Total vertical stresses at seabed level. Values in kN/m^2.

The average vertical stress is 169kN/m^2. It is expected that the shear strength will increase with 30%. The results of this calculation for each bore hole are listed in TableVII-1

TableVII-1: Overview bore locations

SPT	Thickness bad layer	Action
B-01	0-5	DREDGING 4M
B-02	0-2	DREDGING 4M
B-03	0	DREDGING 4M
B-04	0-5	DREDGING 4M
B-05	0-3	DREDGING 4M
B-06	0	OUTSIDE BREAKWATER AREA

The seabed around B-01 is more likely to liquefy than the rest of the coastline. This is because it is located in a bay. At B-02, outside the vicinity of the bay, the resistance of the soil is much higher.
B-04 also shows a liquefiable layer of about 5m. This most probably is due to the sediments disposed by the river.

It is assumed for the time being that dredging and replacing the first 4m over the total length of the barrier will cover the costs required for soil improvement.

Appendix VIII. STABILITY CALCULATION; ARMOUR LAYER

In this Appendix the calculations are shown which are used to design the armour layer on all sides of the offshore breakwater. The main loads on a stone in an armour layer are gravity and the impact of waves and currents. For the latter load, the velocity is the most important parameter.

Two load cases are elaborated:

1. The water levels and velocities as exist under tsunami attack. For this case, the Dec2004 Tsunami conditions have been used as starting point.
2. 'Normal' wave attack under storm conditions.

The starting point for the design is the cross section as depicted in Figure VIII-1.

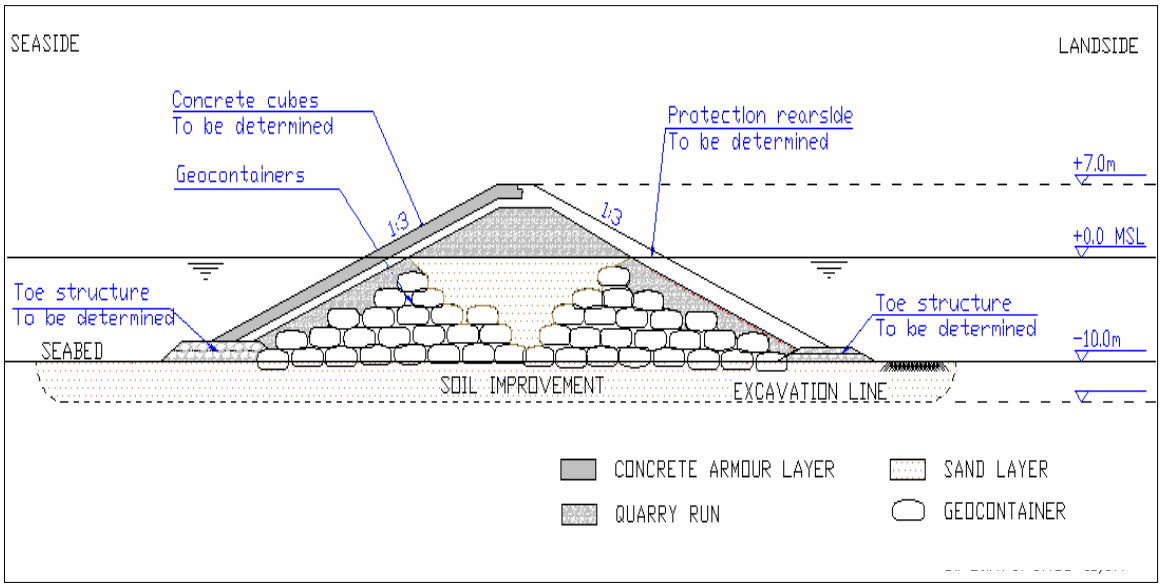

Figure VIII-1 Cross section of offshore barrier; starting point for technical design.

The excavation depth is determined in the previous Appendix and amounts to 4m below seabed.

VIII - 1 ARMOUR LAYER FRONT SIDE

On the front side (seaside) of the offshore barrier, the loads under tsunami conditions are limited. As shown in Figure VIII-2 below, the velocities do not exceed 3m/s up to the crest of the offshore barrier.

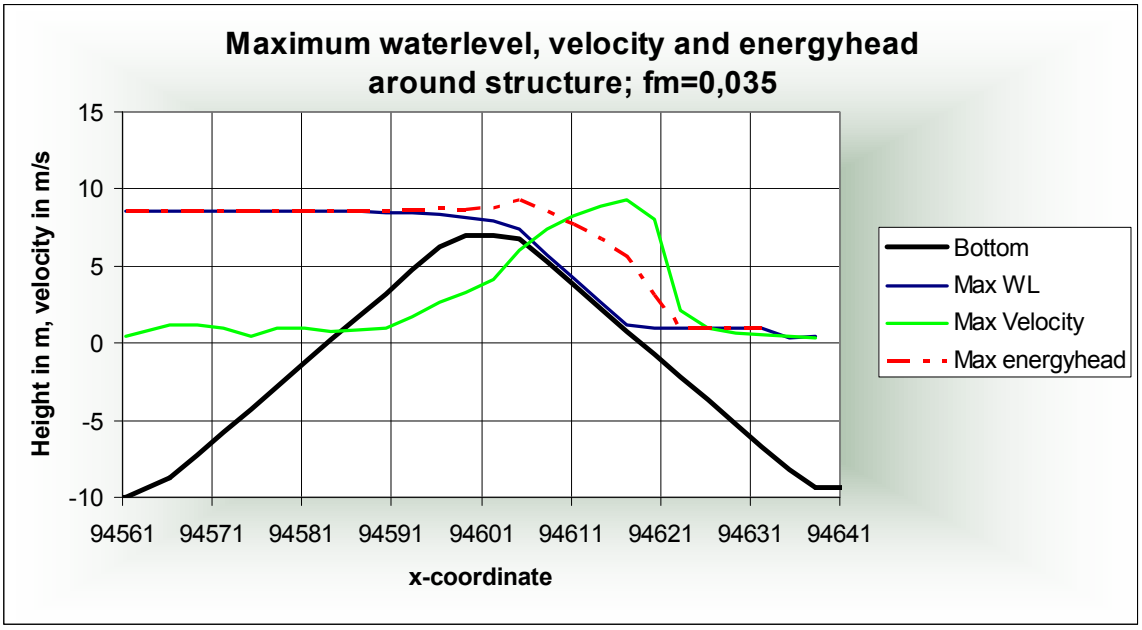

Figure VIII-2 Maximum water level, velocity and energy head around structure

Therefore, the load under normal wave attack is normative. Within the SDC-project, wave conditions for various return periods were computed for Banda Aceh [31]. This has been done with SWAN for numerous locations along the Sumatran coast, see Figure VIII-3. For each selected output-point, 15 scenarios with different wave and wind conditions are computed. Various swell conditions are combined with varying winds.
In Figure VIII-3, an overview of the output locations around Banda Aceh is presented.

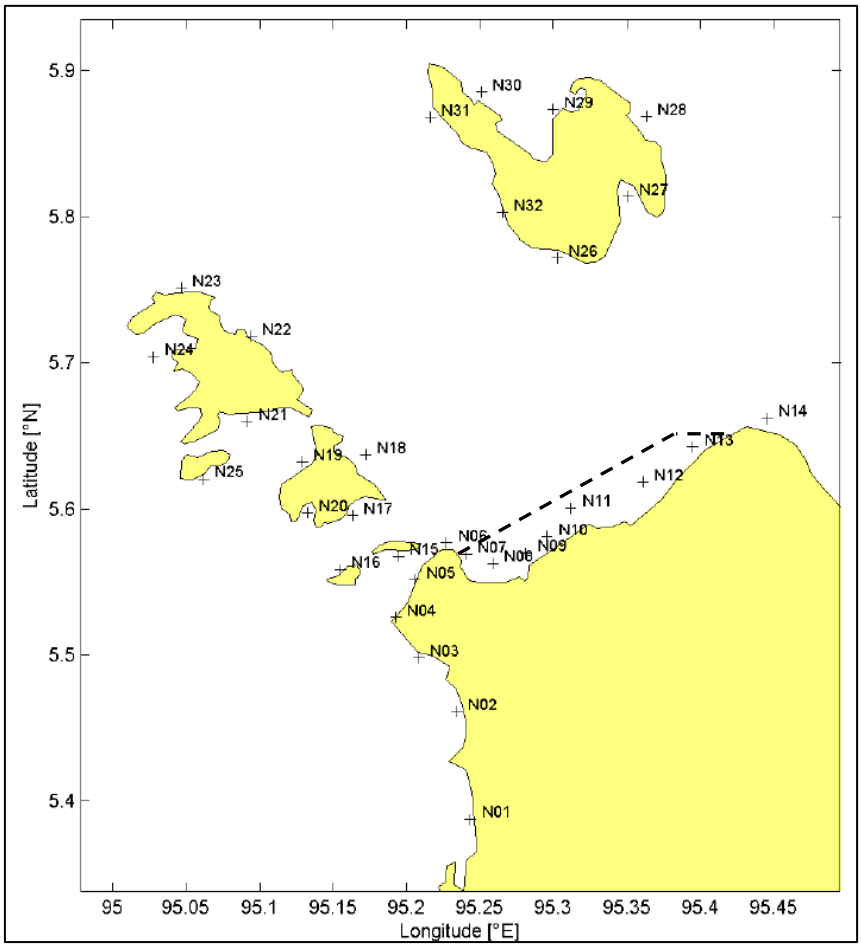

Figure VIII-3 Overview of SWAN output-locations [33] and breakwater location

Table VIII-1: Design wave heights, periods and water levels for various return periods [31]

Location	HHWS	RP 1/1 year			RP 1/25 year			RP 1/100 year		
		H_s	T_p	Dir	H_s	T_p	Dir	H_s	T_p	Dir
n06	0,85	2,1	7,7	35	2,6	8,5	36	2,8	8,5	36
n07	0,85	1,8	5,8	31	2,2	6,4	30	2,4	6,4	30
n08	0,85	1,6	5,3	24	1,9	6,4	23	2,1	5,8	23
n09	0,85	1,6	6,4	312	1,9	7,0	313	2,1	7,0	314
n10	0,85	1,7	6,4	306	2,1	7,0	307	2,3	7,0	308
n11	0,85	1,9	6,4	297	2,4	7,0	298	2,6	7,0	300
n12	0,85	1,9	8,5	11	2,5	8,5	10	2,7	9,3	9
n13	**0,9**	**1,9**	**6,4**	**295**	**2,5**	**7,0**	**298**	**2,7**	**7,7**	**300**
n14	0,9	2,7	7,7	47	3,3	8,5	48	3,6	9,3	49

In this design, a return period of 100 years is used. The maximum significant wave height in the location of the breakwater occurs at point n13 (n06 and n14 are outside the breakwater region) and is 2,7m with a peak period of 7,7s.

The peak period T_p = 7,7s. The ratio T_m / T_p ranges from 0,71-0,87. Her an average value of 0,79 is used.

It should be noted that above presented results are the maximum wave heights out of the 15 calculated scenarios. However, for the stability of armour layers, the highest wave does not necessarily induce the highest loads. Long (swell) waves, although lower, can give a higher load. Therefore, at least two load situations have to be checked. For output point n13, the extreme (1/100 year) long swell waves have the following characteristics:

H_s = 1,0m, T_p = 18,2s, Dir = 311^0 N.

Thanks to its favourable location, Banda Aceh is rather protected against long swell waves.

The extreme design water level in the Aceh Region = maximum spring tide level (HHWS) + 0.2 m (addition for long-term tidal variation) + 0,35 m (addition for sea level rise 100 years). The design parameters become:

Design water level = 0,9+0,2+0,35	= 1,45m + MSL		
Design significant wave height H_s	= 2,7 m	*or*	1,0 m
Design peak period T_p	= 7,7s		18,2 s
Design mean period T_m	= 6,1s.		
Direction:	= perpendicular to the breakwater		

The required stone diameter under these conditions can be determined with the help of the Van-der-Meer-formula [30]. A protection layer of armour blocks is chosen, so the Van-der-Meer-formula for armour blocks has to be used:

$$\frac{H_s}{\Delta D_n} = \left(6{,}7 \frac{N_{od}^{0,4}}{N^{0,3}} + 1{,}0 \right) \cdot s_{0m}^{-0,1}$$

with:

d_n	=	required cube size [m]	→	to be determined
Δ	=	relative density $(\rho_c - \rho_w)/ \rho_w$	→	(2400-1030)/1030 = 1,33 ($\rho_{concrete}$ = 2400kg/m^3)
H_s	=	design wave height [m]	→	2,7m
N_{od}	=	number of damaged units	→	0,2 (minor damage, due to complicated maintenance conditions offshore)
N	=	number of waves [-]	→	7000, maximum value
s_{0m}	=	wave steepness [-]	→	s_{0m} = H_s / L_{0m} = H_s / ($gT_m^2/2\pi$) = 0,046 (with T_m)

For the combination H_s=2,7m and T_p=7,7s, the required stone diameter is: D_n = 1,20 m
This corresponds with a stone weight of: W = 4,6 ton

The same calculation with the swell conditions (H_s=1,0m, T_p=18,8s), the required diameter becomes 0,42m. The first calculation is therefore normative.

Conclusion
For the seaside slope a single layer of 4,6-ton cubes (d = 1,20m) is applied.

VIII - 2 TOE STRUCTURE

The toe's main function is to support the armour layer of the slope. The stability of the stones in a toe increases with increasing depth. The water depth above the toe, h_t, the total water depth, h_m, and the required stone diameter d_{n50} are related with: [30]

$$\frac{H_s}{\Delta d_{n50}} = 8{,}7\left(\frac{h_t}{h_m}\right)^{1{,}4}$$

Due to the large depth, a sunken toe is not necessary. The toes are placed on the seabed.
For low LLWL (MSL -1,1m), and with an assumed toe thickness of 2,5m ($2*d_{50}$ of slope armour layer), the relative depth h_t/h_m = 0,72. The required stone diameter d_{n50} would become 0,31m.

However, the actual current velocities under the successive tsunami waves are uncertain. 1D-modelling does not provide clear values for the expectable loads due to attacking and retreating tsunami waves. The amount of turbulence is also unknown.

Due to these uncertainties, a heavier toe structure is proposed then would be necessary for protection against normal waves. The actual loads on the toe due to the tsunami waves have to be obtained from physical modelling.

Due to uncertainties, a double layer of 1000-3000kg stones is proposed (d_{total} = 2*0,92=1,84m).

On the rear side a smaller toe is proposed: 2 layers of 300-1000kg stones, d_{total} = 2*0,63 = 1,26m.

VIII - 3 REQUIRED BREAKWATER HEIGHT UNDER STORM CONDITIONS

For armoured rubble slopes, special formulae have been derived from tests with rough rubble slopes, including the effect of structure permeability to determine the run-up.

$R_{u2\%}/H_s = \xi_p$ for $\xi_p < 1.5$
$R_{u2\%}/H_s = 1.1\ \xi_p^{0.46}$ for $\xi_p > 1.5$

Where the run-up for permeable structures (P> 0.4) is limited to a maximum of:

$R_{u2\%}/H_s = 1.97$

The minimum crest height z should be
$z = h + Ru_{2\%}$

with:

h = design water level [m]
$Ru_{2\%}$ = design wave run-up level [m]

$\xi_p = 4{,}0$ (with T_p=7,7 s), so $R_{u2\%}/H_s$ = 1,1*4,0$^{0.46}$ = 2,1. $R_{u2\%}$ becomes 5,5m and the minimum crest height *z*:

z = h + $Ru_{2\%}$ = 1,45 + 5,5 = 6,95m +MSL.

The assumed crest height = 7m + MSL, which is sufficient under storm conditions.

Conclusion: A concrete armour layer of 4,6ton cubes is strong enough to withstand the design waves and the assumed crest height is high enough.

VIII - 4 CONSIDERATIONS ARMOUR LAYER REAR SIDE

The 1D-modelling indicates (depth averaged) velocities up to 9m/s for a retaining height of 7m. The existing modelling which was already available before this final thesis work, indicated velocities up to 15m/s. However, the assumed bathymetry was not realistic and the modelled structure had a freeboard of 5m. Therefore, the velocity profile as in Figure VIII-4 is used.

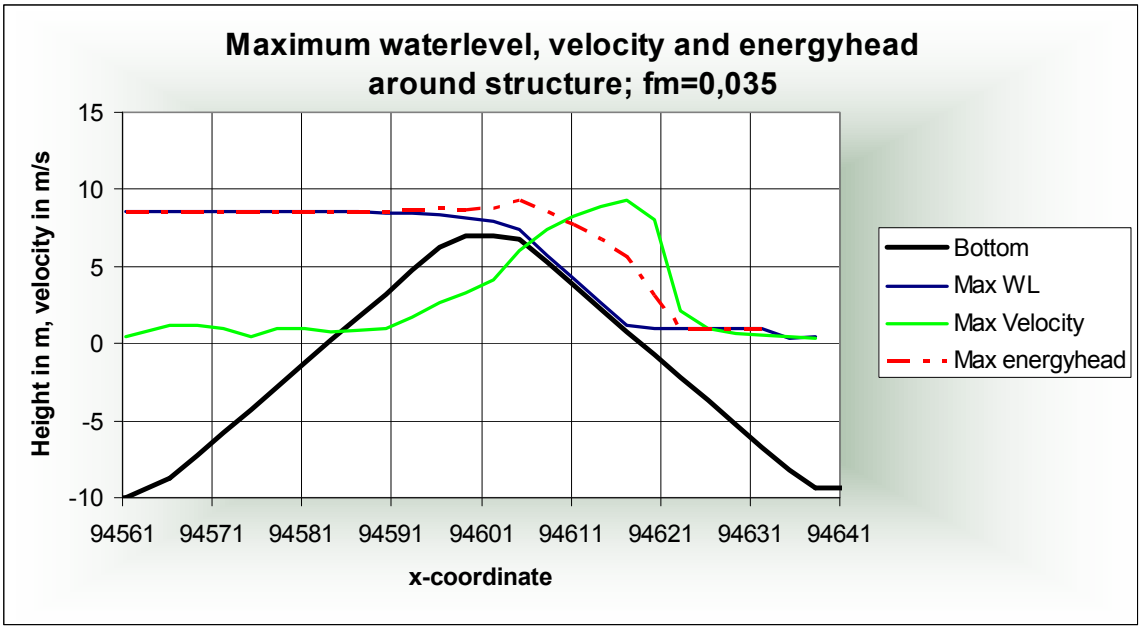

Figure VIII-4 Maximum water level, velocity and energy head around structure

The duration of these velocities is shown in Figure VIII-5. See Appendix IX for the calculation.

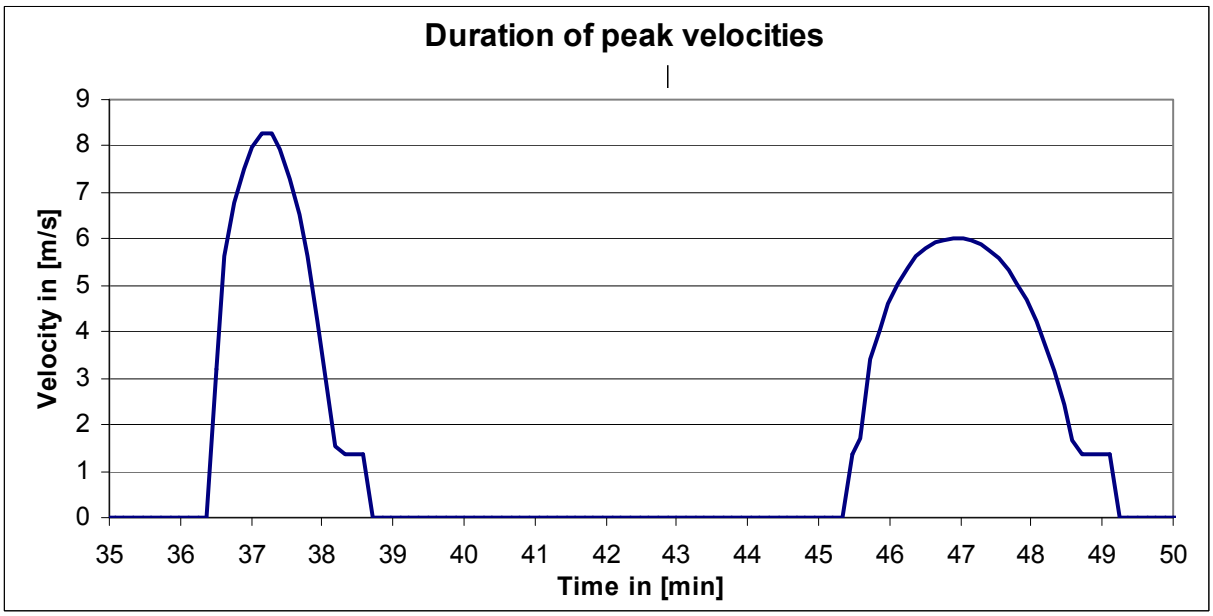

Figure VIII-5 Duration of peak velocities over structure.

The duration of velocities does not vary for structure slope but depends mainly on the tsunami excitation signal. The time-velocity distribution of the design showed in above graph will therefore be similar for the chosen design. The duration of high velocities (>3 m/s) is approx. 2 minutes for the initial peak, and approx. 3min for the 2nd peak. The design velocity is taken to 10m/s along the slope (see Figure IX-8 in Appendix IX).

Izbash

The design velocity for overtopping tsunamis is 10m/s along the rear slope of the structure. This velocity can be seen as a uniformly developed flow. Izbash formulated an empirical formula for stone stability under currents [30]:

$$u_c = 1{,}2\sqrt{2\Delta g d}$$

The critical velocity, u_c, gives a limit for the stone immobility and depends on the relative density, $\Delta = (\rho_s - \rho_w)/\rho_w = 1{,}57$, and the stone diameter *d*.

For stones on a slope, a reduction factor should be applied. This factor reads:

$$K(\alpha_{//}) = \frac{\sin(\phi - \alpha)}{\sin\phi}$$

With a slope of 1:2,5 ($\alpha = 23{,}6\,\deg$) and an angle of repose of $\phi = 30\,\deg$, the required stone diameter can be calculated for various velocities.

"CERC-formula"

During the design and physical modelling of the Kamaishi breakwater in Japan, an empirical formula was used to calculate the stability of a stone under currents [13], [7]. The results were compared with measurements and a good match was found. Because this formula was originally developed by the Coastal Engineering Research Centre (CERC), it will be referred to as the

"CERC-formula" in this study. It is used in this design, because it enables to allow some damage. The relation reads:

$$W = \frac{\pi \rho_s U_d^6}{48 y^6 g^3 (\rho_s / \rho_w - 1)^3 (\cos\alpha - \sin\alpha)^3}$$

The required stone diameter is determined in combination with a damage ratio *D (%),* which account for the numbers of moved armour blocks in a certain reference zone. This ratio is expressed in a constant *y* according to Figure VIII-6.

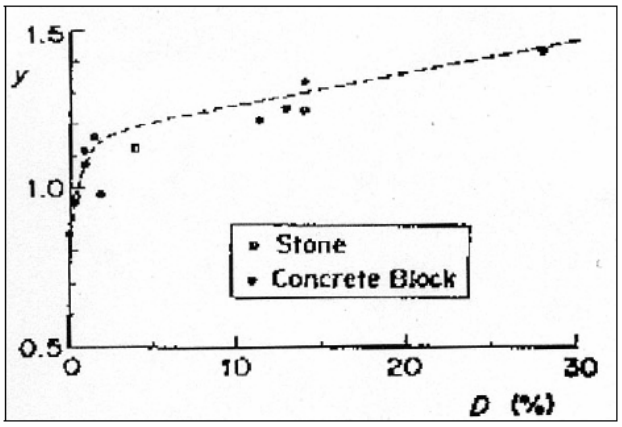

Figure VIII-6 Relation between *D* and *y*

U_d is the flow velocity acting on the stones. The other constants are supposed to be known. A description about this method is given in [13], [7].

These two methods give quite different results, see Figure VIII-7.

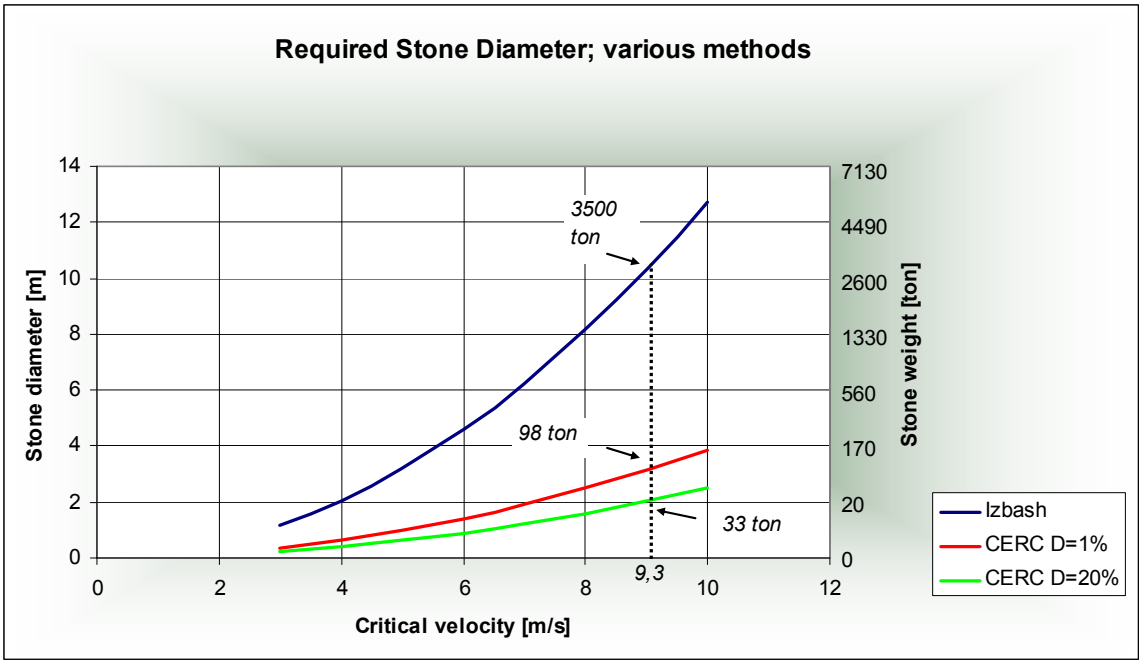

Figure VIII-7 Required stone diameter with Izbash and "CERC-formula"

Using the Izbash formula will lead to unrealistic stone dimensions. Even the "CERC-formula", which gives much favourable values, leads to stones of 33ton in weight (d=2,3m).

These blocks are too big to be feasible. The construction required very heavy equipment. Therefore, the use of asphalt is advised.

VIII - 5 ASPHALT LAYER REARSIDE

Two types of asphalt-mixture types are used: 1) a cheap but permeable *lean-sand asphalt layer* and 2) an expensive but impermeable *grouted mortar layer.*

The total layer thickness is calculated in this section. The weight of the layer must counterbalance the excess water pressures which can cause sliding of the layer (by exceeding the friction along the slope) or uplift of the layer. The latter situation is normative in the design circumstances.
Excess water pressure can rise due to Head differences between the phreatic line inside the barrier and the outer water level (see Figure VIII-8).

When the under-layer and the revetment below the impermeable asphalt layer (e.g. quarry run, rip-rap) are sufficiently permeable, then the pressure differences are limited.

For conservative design, the required layer thickness is calculated assuming a rather impermeable under-layer:

Required thickness due to head differences

Although non-stationary programs are required to determine the exact groundwater flow pattern through the dike, an approximate, analytical solution is available:

$$H = \frac{h_1}{\pi}\arccos\left[2\left(\frac{h_1 + d\cos\alpha}{h_1 + h_2}\right)^{\frac{\pi}{\arctan(\cot\alpha)+\pi/2}} - 1\right]$$

With parameters as indicated in Figure VIII-8.

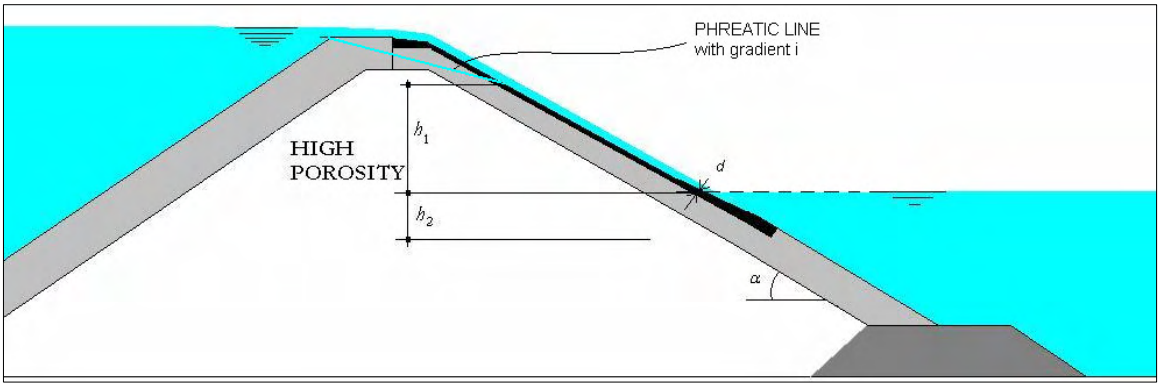

Figure VIII-8 Definition parameters h_1, h_2, d and α

The resulting layer thickness *d* can be calculated with:

$$\frac{H}{\Delta d} = \cos\alpha$$

Above the water level $\Delta = \rho_{asphalt} \approx 2200 kg/m^3$. The determination of the hydraulic gradient *i,* is normally done with computer programs[2]. The top of the barrier is made of quarry run, which has a high porosity. In this preliminary calculation it is assumed that h_1 = *5m.* For the design water levels, a slope of 1:3 and h_2 = *3m*, H becomes 2,6m and the required layer thickness (maximum at inner water level) becomes:

$$d_{required} = 1{,}3m$$

This thickness includes that part of the underlying stones that are fully grouted and from one whole with the overlying asphalt layer. The layer thickness can be decreases along the other sections of the slope.

For instance MSEEP. In this case however, a non-stationary outer water level should be applied to study the development in time of the phreatic line. In stationary situations the final gradient i = 1:7 for sand. It takes hours to reach this situation. For this tsunami-barrier it is assumed that the maximum gradient is 1:4,5, because the duration of this maximum water level is less then 10min. This means a lowering of 2m. H_1 becomes 5m in that situation. For detailed design the groundwater flow should be studied with the help of (non-stationary) computer programs

It is important to consider a potential negative pressure zone on the downstream slope, especially directly below the crest. The flow over the crest could separate from the slope creating a low-pressure zone. The transition should be streamlined and not abrupt.

VIII - 6 ARMOUR LAYER ON THE BREAKWATER HEADS

The current velocities trough the gap can not be obtained from 1D-modelling. Therefore, the 2D-model (Delft3d) is used. The grid size is 50m while the gaps have a width of 200m. This means that for each gap 4 grids are available, which is assumed to be sufficient for preliminary stability calculations.

The velocity field under the Dec2004 Tsunami conditions (for a structure height of 5m), is presented in Figure VIII-9.

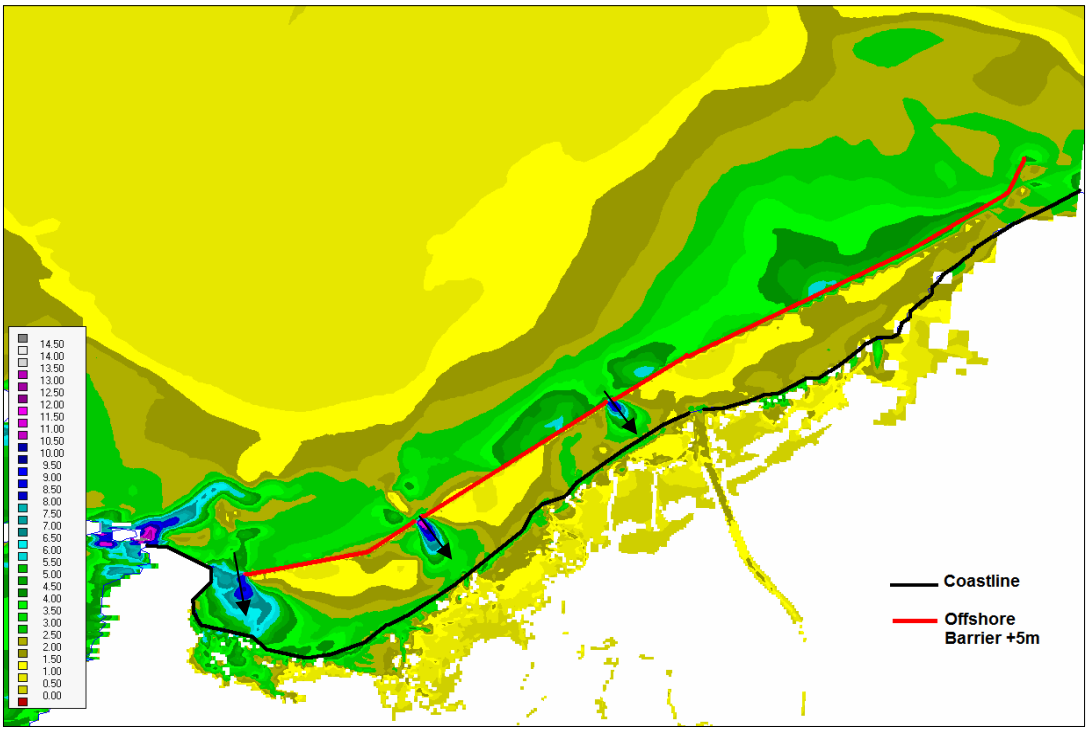

Figure VIII-9 Velocity field (maximum) for Dec2004 Tsunami and offshore barrier +5m. Scale is in m/s.

The maximum velocity in the gap is 12 m/s. The highest velocities are in landward direction. Note that this velocity is depth-averaged and for a 50m grid. The local velocities can be much higher, also due to turbulence.

The gaps form the most difficult part of the entire structure, since the average current velocities are extremely high (12m/s). During tsunami attack, severe erosion is expected. The breakwater head can be seen as abutments or groynes and the erosion patterns are expected to be similar. See Figure VIII-10.

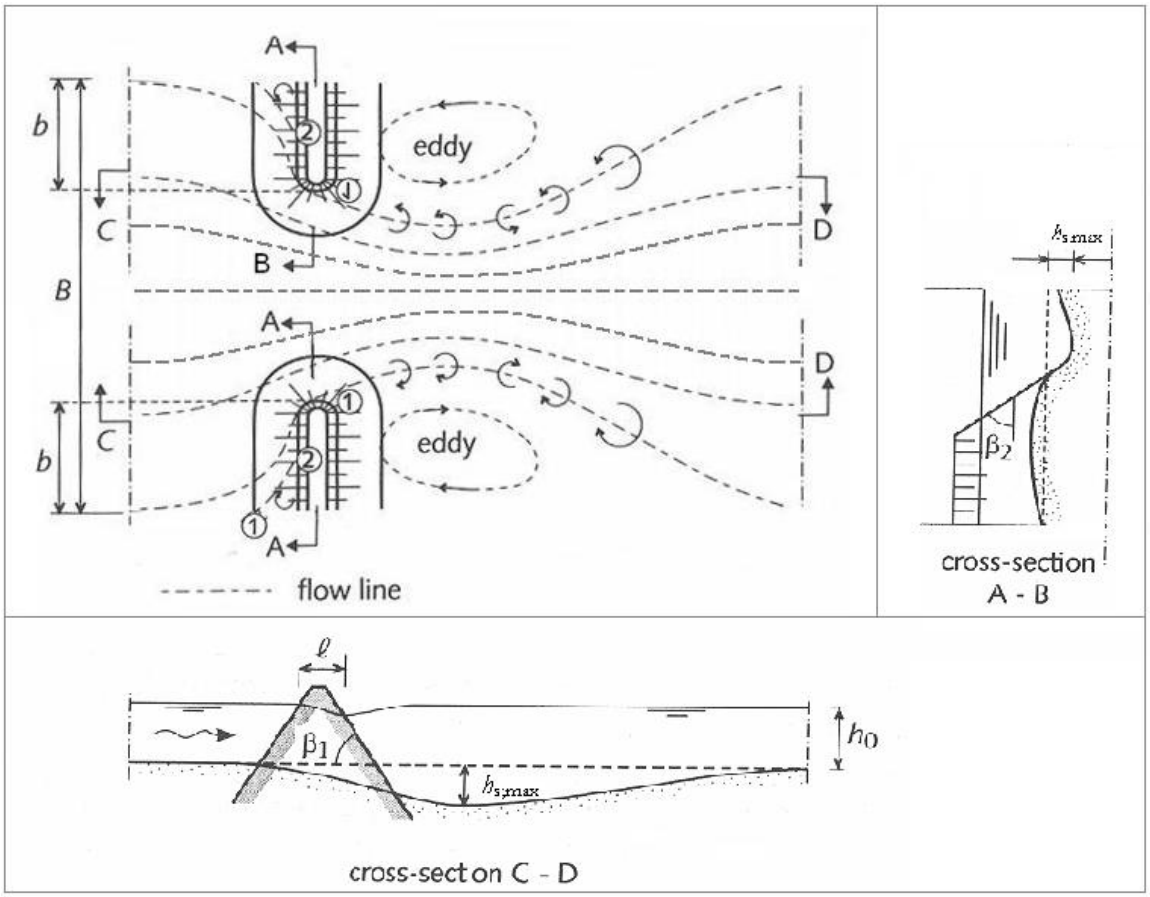

Figure VIII-10 General layout of scour and flow pattern in gap. Source [14]

To provide a rough idea about the expected scour depth during tsunami attack, an empirical expression is used. This expression is developed with several hundreds of test during the Deltaproject [30]. Although developed for situations with scour behind a scour protection, it gives an order of magnitude:

$$h_s(t) = \frac{(\alpha \cdot \bar{u} - \bar{u}_c)^{1,7} h_0^{0,2}}{10\Delta^{0,7}} t^{0,4}$$

in which $h_s(t)$ is the maximum depth in the scour hole as a function of time t (in hours). $\bar{u}$ is the vertically averaged velocity at the beginning of the erosion area (≈12m/s) and α is a correction factor representing turbulence and increases the effective velocity. $\bar{u}_c$ is the mean critical velocity:

$$\bar{u}_c = u_{*,c} C / \sqrt{g} \text{ , with } C = 18\log(12R/k_s)$$

For $d_{50} = 0{,}2mm$, $k_s = 3d_{50}$, and $R \approx 10m$, $\bar{u}_c$ becomes 0,21m/s.

The duration of this velocity is about 3minutes. Before and after this peak velocity, high velocities do occur, but in varying direction. Therefore it is assumed that the scour hole caused by this current is an upper limit. The scour depth after 3min tsunami wave can be calculated. The average velocity is taken to 12m/s and the 'turbulence-factor α is taken to 3. The scour depth after (3/60) hours becomes:

$$h_s(t) = \frac{(3 \cdot 12 - 0{,}21)^{1{,}7} 10^{0{,}2}}{10 \cdot 1{,}65^{0{,}7}} \left(\frac{3}{60}\right)^{0{,}4} = 14{,}7m$$

Increasing the duration to 5min increases the depth to 18m. Other expressions (Breusers/Raudkivi, 1991 in [30]) give equilibrium scour depths of about 12m.

Although the velocities and the flow situation differ from the range wherein these formulas are developed, it gives an idea about the expectable scour holes during tsunami attack. These holes undermine the slope of the breakwater heads and will lead to partial collapse of the heads. Besides that, the head itself is severely attacked by the currents.

In the design considerations it was mentioned that due to the extreme nature of significant tsunamis, the damage-criterion is not as strict as in normal situations. Although maintenance is complicated, it would be unrealistic to demand a 'no damage' or even 'low damage' criterion.

To account for the heavy loads on the breakwater heads, the slopes are made 1:6. The breakwater heads, including a sufficiently large part of the trunk, is protected with grouted mortar, which extends entirely to the bottom or toe of the structure. This grouted section should extend sufficiently far on the front side of the trunk (≈ 100-200m).

To reduce the erosion in the gaps, the bottom is protected with concrete mattresses. This could be done with (among others) ArmorFlex or GreenFlex mattresses. The concrete elements are connected with (stainless/galvanized) steel wires.
This bottom protection extends at least 50m outside the breakwater, in both seaward and landward direction. Directly after the edges of the protection, erosion holes will develop. When the flow reverses, these edges are heavily exposed to the flow and will probably be rolled up. Therefore, the edges have to be protected with lines of streamlined and heavy concrete elements.

VIII - 7 DRAWINGS

The proposed breakwater design is presented in this section.

Due to the extreme nature of tsunamis, some damage is allowed as long as the primary function is maintained.

This damage is most of all concentrated on the crest and rear side of the breakwater, since high velocities do occur in case of tsunami overtopping. For the preliminary design, an asphalt layer is proposed. High velocities do also occur in the gaps. With gentle slopes of the heads and an extensive bottom protection the impact of the scour holes is reduced.

Instability of the breakwater itself due to sliding and liquefaction is mainly prevented by applying a core of GeoContainers. These containers prohibit liquefaction and the generation of sliding planes and circles.

The sea-side is designed against 'normal' waves, with low damage criterion. Toe structures are put into the design to support the armour layers on the slope. Direct wave attack on the toe's will not occur, due to the large depth they are constructed in.

In below figures the preliminary design is presented in both cross section and plan view of the gaps. It is stressed that many details require additional research. Physical modelling for such an expensive structure under such unsure circumstances is inevitable. Figure VIII-11 and Figure VIII-12 present the composition and dimensions of the offshore Tsunami Barrier. Figure VIII-13 shows a plan view of the gap and a general layout of the proposed protection.

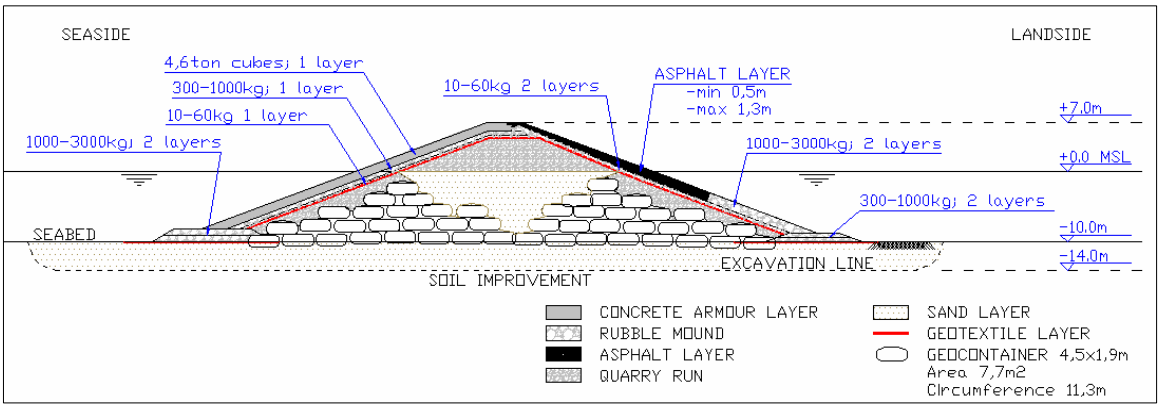

Figure VIII-11 Cross section Offshore Tsunami Barrier; composition

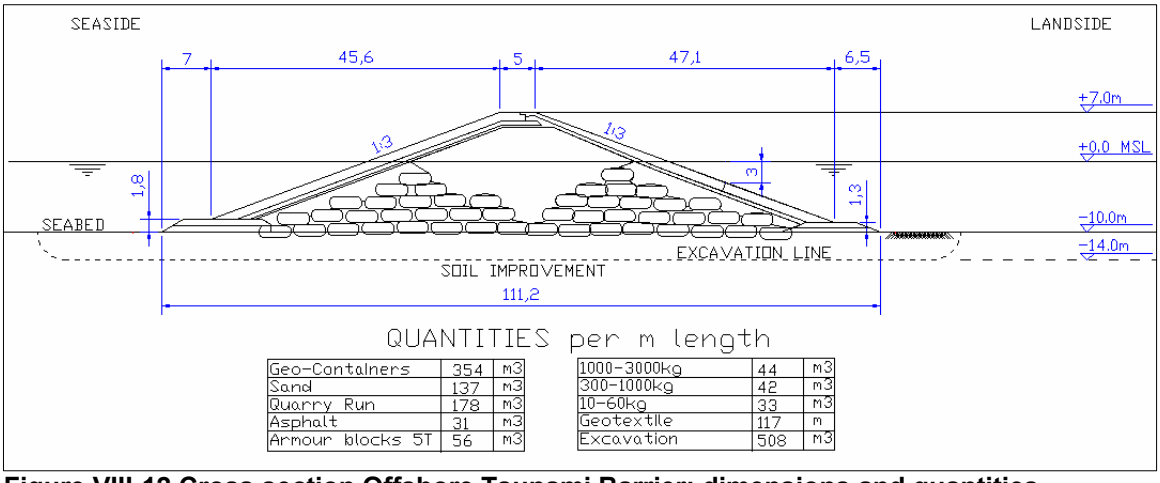

Figure VIII-12 Cross section Offshore Tsunami Barrier; dimensions and quantities

Note: with this new cross section and quantities, the construction costs are changed slightly. For asphalt, a unit rate of \$250/m^3 is used. The 'new' construction costs for this design becomes \$1,17 Billion. This minor difference has no influence on the conclusions of the feasibility study,

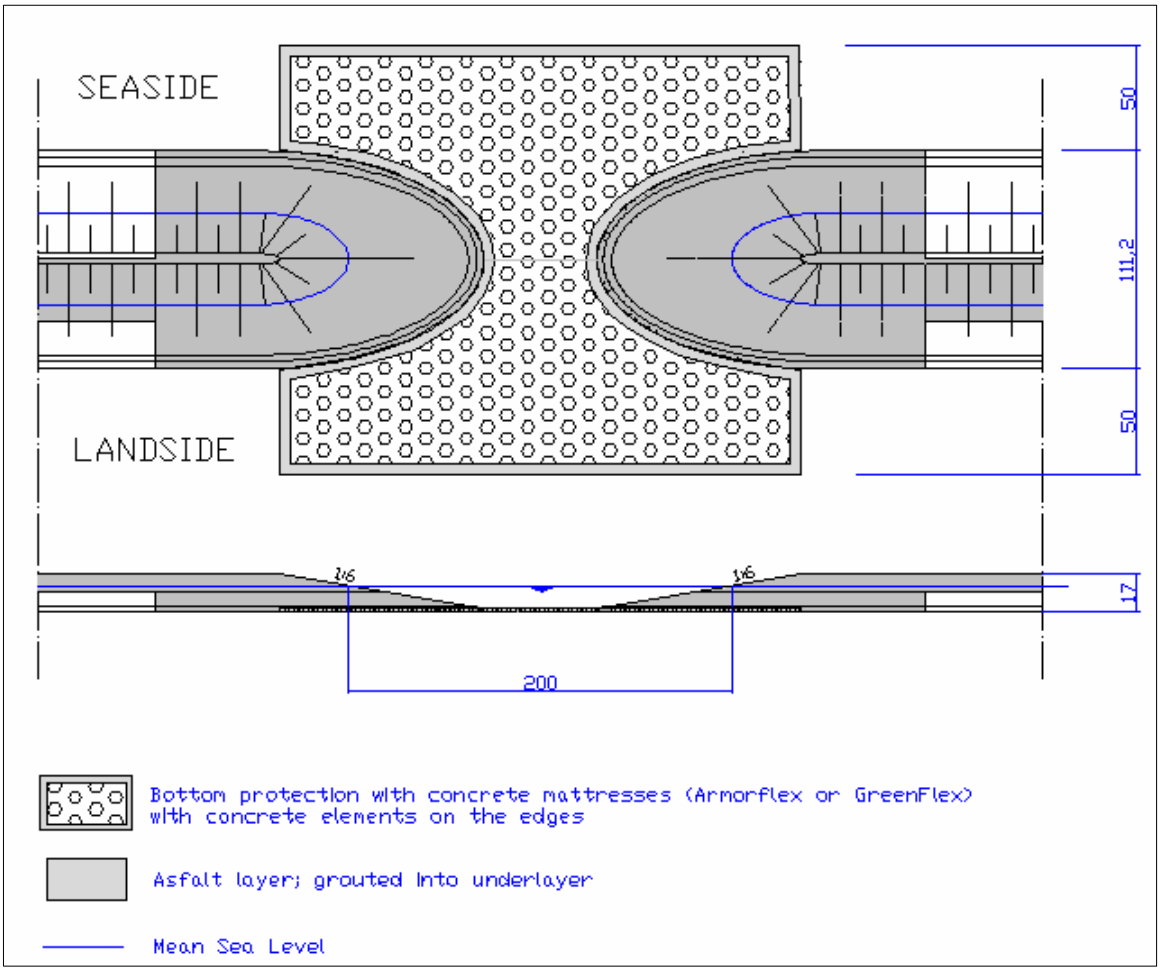

Figure VIII-13 Plan view and cross section of gap and general layout of gap protection

Figure VIII-14 and Figure VIII-15 show 3D impressions of the designed tsunami barrier. Note that the heads are completely covered by an asphalt layer.

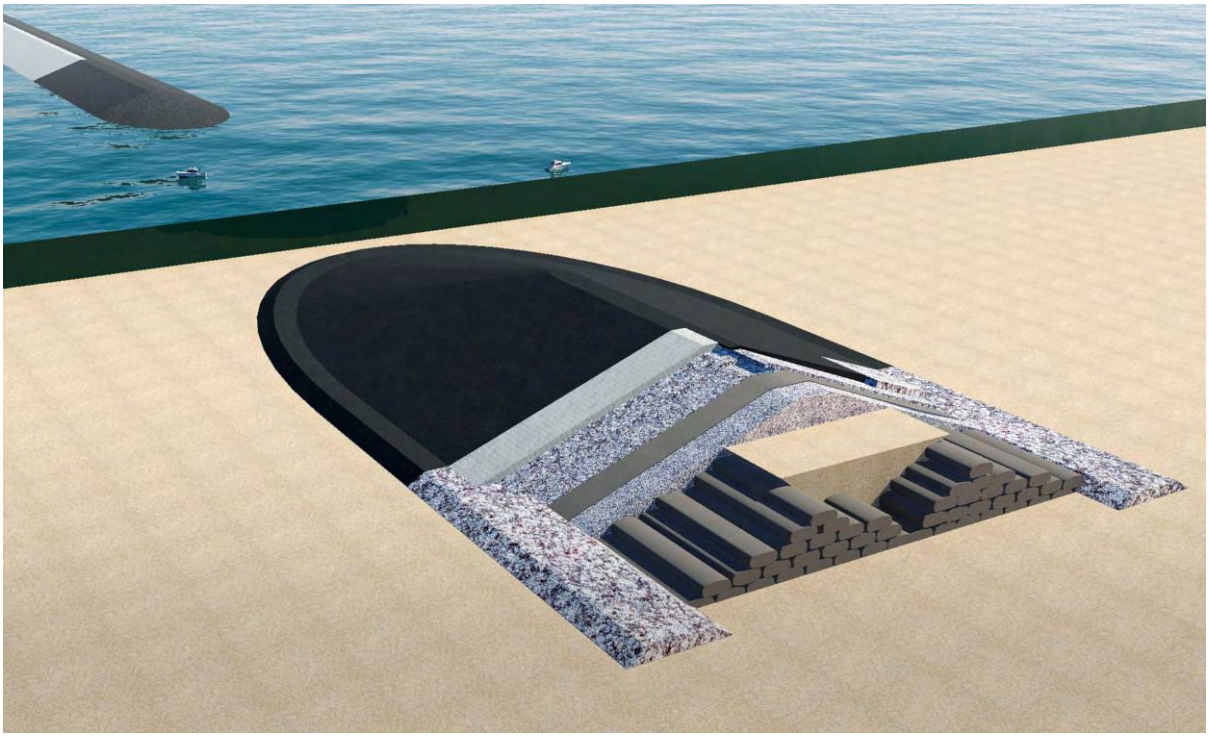

Figure VIII-14 3-D impression of offshore tsunami barrier; gap

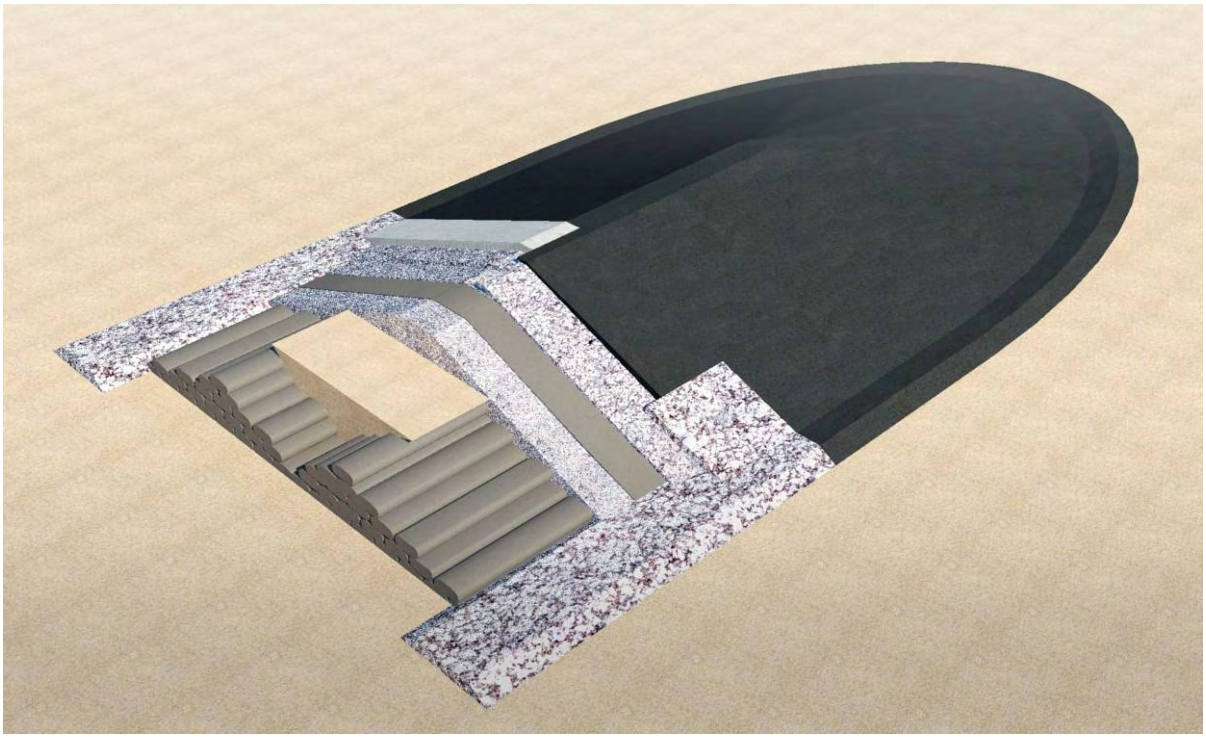

Figure VIII-15 3-D impression of offshore tsunami barrier; composition

Appendix IX. 1D-PROGRAM (FORTRAN)

IX - 1 THEORY

In this appendix an attempt is made to model the offshore Tsunami Barrier in an 1D-program, running in Fortran. The model is based on the 1D-nonlinerar shallow water equations which have been implemented by Prof. G.S. Stelling (member of thesis-committee) into this 1D-model.

The 1D nonlinear shallow water equations are divided in an equation of momentum and continuity:

Momentum:
$$\frac{\partial V}{\partial t} + V\frac{\partial V}{\partial x} = -g\frac{\partial \eta}{\partial x} - C_f \frac{V|V|}{d+\eta}$$

Continuity:
$$\frac{\partial (d+\eta)}{\partial t} = -\frac{\partial [(d+\eta)V]}{\partial x}$$

V	=	depth averaged horizontal velocity vector [m/s]
η	=	water elevation [m]
d	=	water depth [m]
C_f	=	non-dimensional friction coefficient [-]
g	=	gravitational acceleration [m/s$_2$]
t	=	time [s]
x	=	distance [m]

The coast and the open ocean boundary are modelled as closed boundaries (V=0). A description of the numerical technique used in this model can be found in reference [36].

The model was primarily used to study the general effect of bathymetry, signal, etc. on (for instance) the shoaling of the tsunami wave. For this purpose the model is used to obtain local (depth-averaged) velocities and water levels around the structure.

IX - 2 MODELLING

Bathymetry

The bathymetry in front of Banda Aceh is obtained from the 2D-model, which is based on recent survey-data. A typical profile is drawn in Figure IX-1.

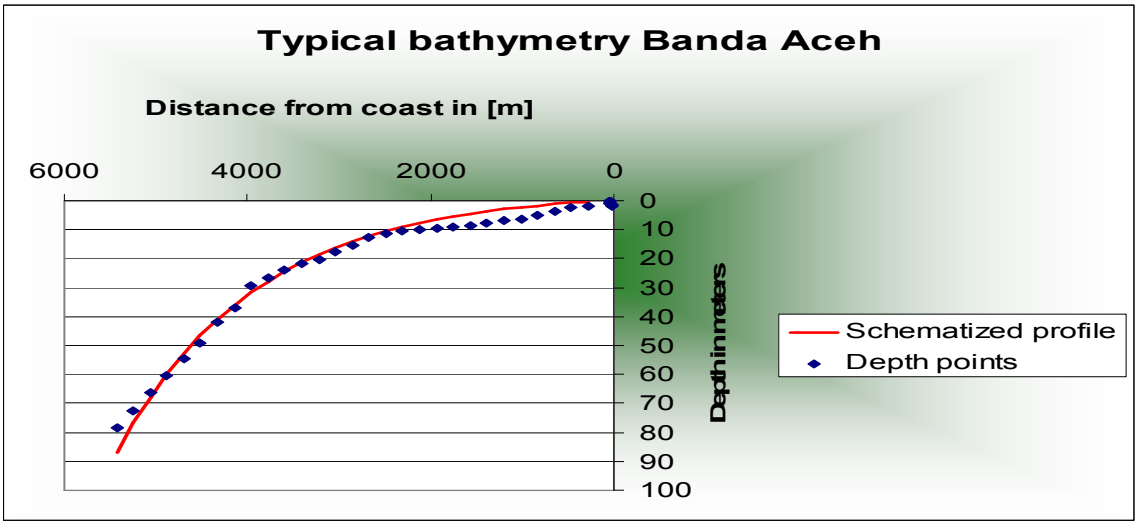

Figure IX-1 Typical foreshore bathymetry Banda Aceh

From d=80m, the profile is schematized by the next formula (see also the red line in above figure):

$$d = 2{,}7 \cdot e^{\left(\frac{0{,}97\,xl - x(m)}{1550}\right)} - 3$$

Tsunami signal

The tsunami signal at -20m depth is obtained from the 2D-model. Because in this 1D-model the signal is applied at the -1000m bathymetry line, and the signal close to the shore is a superposition of transmitted and reflected waves, it is not easy to reproduce the signal.

With trial and error the best-fit was obtained as depicted in Figure IX-2.

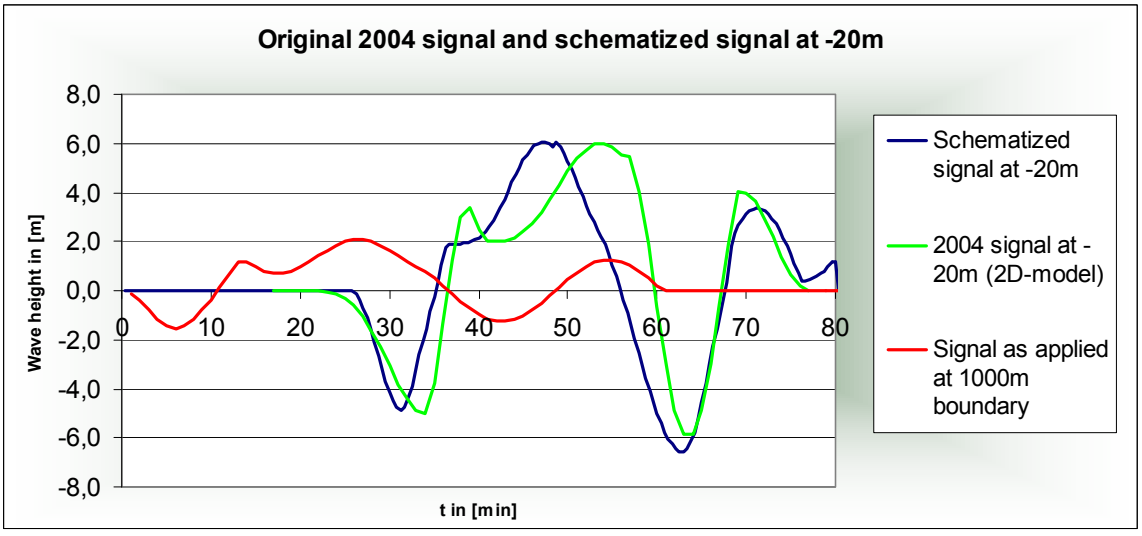

Figure IX-2 Original and schematized signal at -20m.

The red line is the signal as how it is applied at the -1000m bathymetry line. Due to shoaling the wave height increases towards the coast. The height at -20m is the blue line in above graph. The original signal (the green line) is reasonably well reproduced by this signal.

The increase in wave height, or shoaling, is (on average):

Shoaling positive water level	= 6/2,1	= 2,86
Shoaling negative water level	= 4,5/1,26	= 3,57

The theoretical shoaling from -1000 to -20m would be (Green's Law):

Theoretical shoaling	= (1000/20)^0,25	= 2,66

Green's Law does not account for reflection from the ocean's bottom. That is why the shoaling in the model is higher then the theoretical shoaling (see also Chapter 2 on this matter).

The signal consists of a combination of mathematical functions.

Modelling the structure

The structure or breakwater has been modelled by changing the bottom profile. The structure starts at the -10m bathymetry line.
The grid size is refined to 1m at the structure's position, step wise going down from 15m.

Various structures has been modelled, with varying slopes and retaining heights. For an idea of the scale, have a look at Figure IX-3.

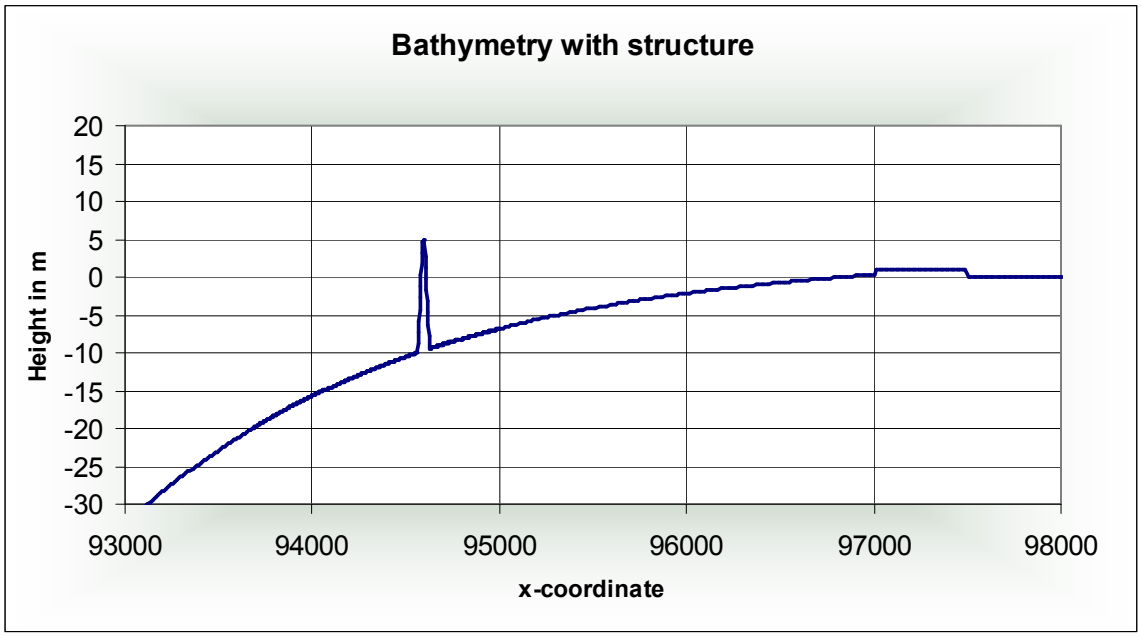

Figure IX-3 Foreshore bathymetry with structure.

The horizontal grid size is locally refined.

From -1000m to -30m → grid size = sqrt(g*d) (for 30m this is equal to 17m grid)
From -30m to -10m → step wise decrease from 17, 10, 5, 3, to 1m.
Around structure → 1m

With this fine grid, the slope of the structure is well-modelled. For each grid, the water level and velocity are generated as output.

IX - 3 OUTPUT

Although numerous model runs has been made, the results for a few runs are shown. See Figure IX-4 and next figures.

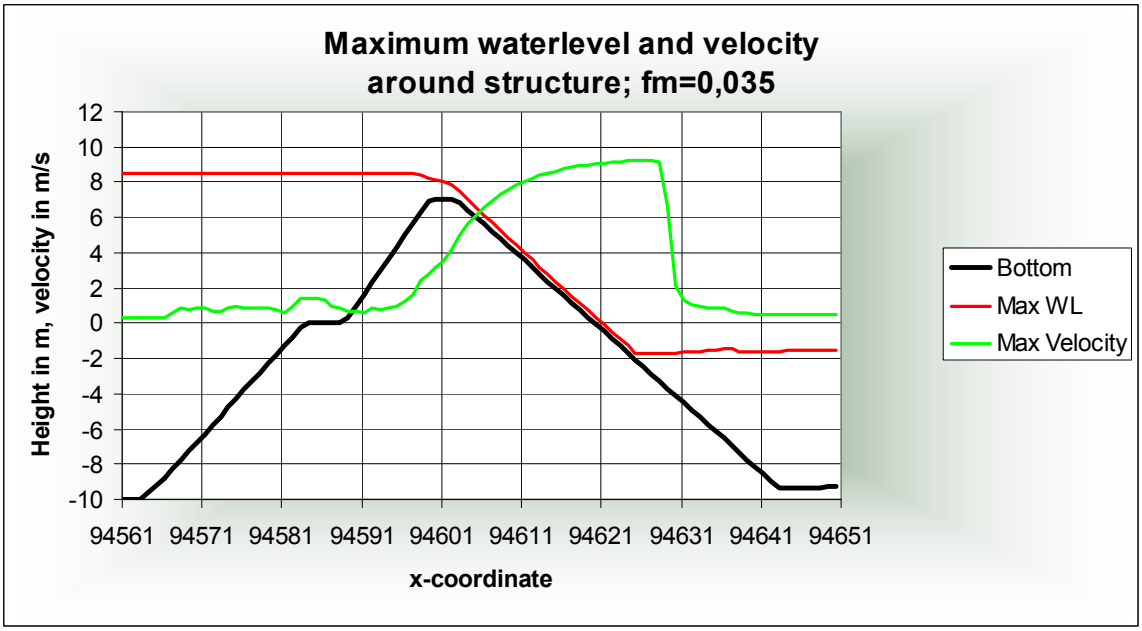

Figure IX-4 Maximum water level and velocity over structure.

With the same conditions as above, but a higher friction along the slope of the breakwater (f_m=0,035), the following parameters are obtained; see Figure IX-5.

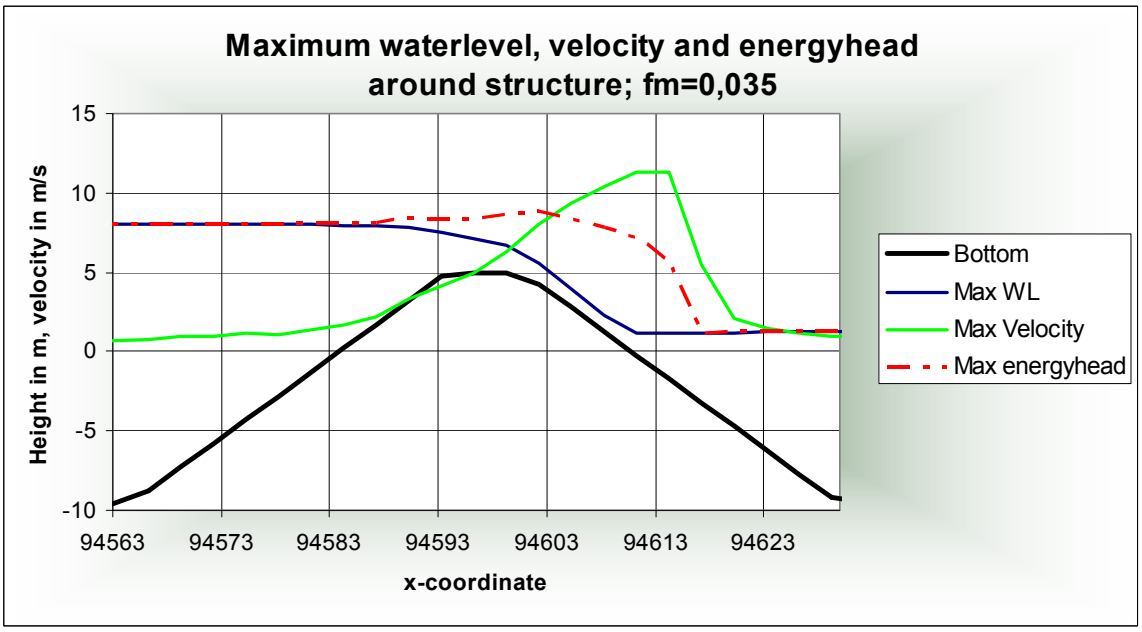

Figure IX-5 Maximum water level, velocity and energy head around structure, fm=0,035

With the same conditions as above, but only a freeboard 7m instead of 5m, one obtains the following water levels and velocities (Figure IX-6):

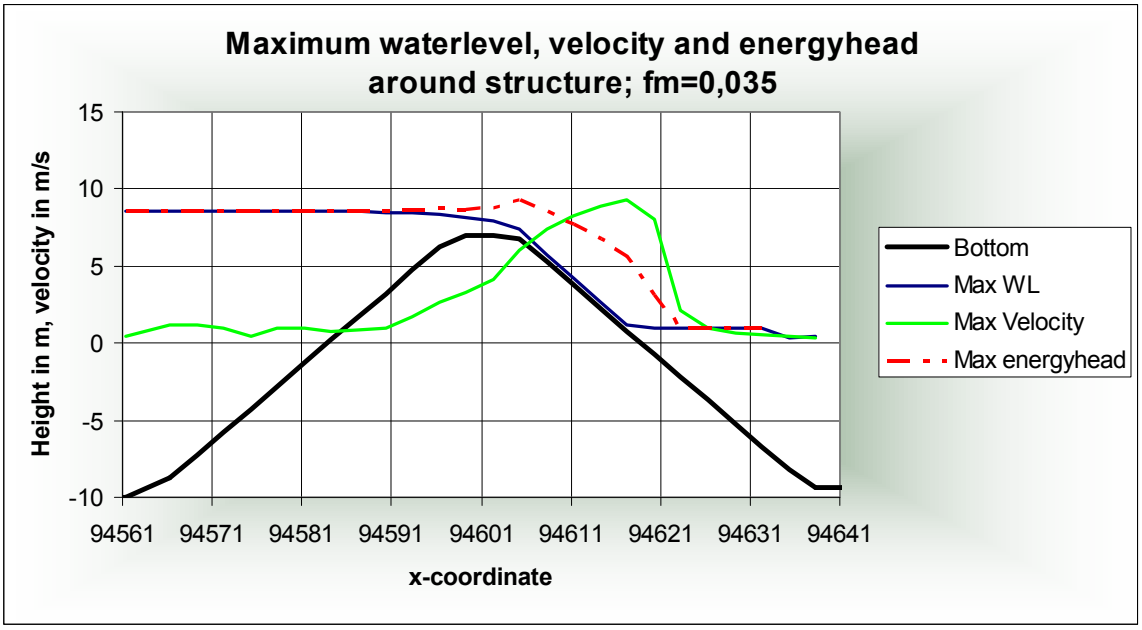

Figure IX-6 Maximum water level, velocity and energy head around structure, fm=0,035

The corresponding momentum is depicted in Figure IX-7.

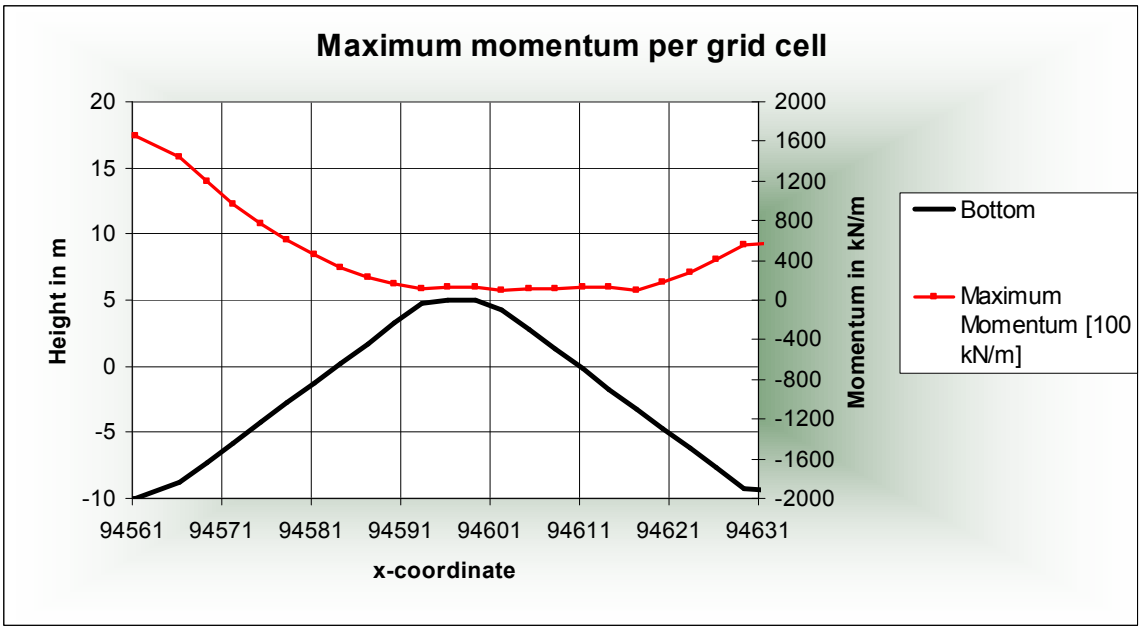

Figure IX-7 Maximum momentum per grid cell

With this momentum, the actual force on the structure can be calculated by integration of the height of the structure for the normative combination of water level and velocity. The results are presented in Appendix VI.

The time distribution of the velocities on the rear side of the barrier is also obtained from this modelling. The results are depicted in Figure IX-8.

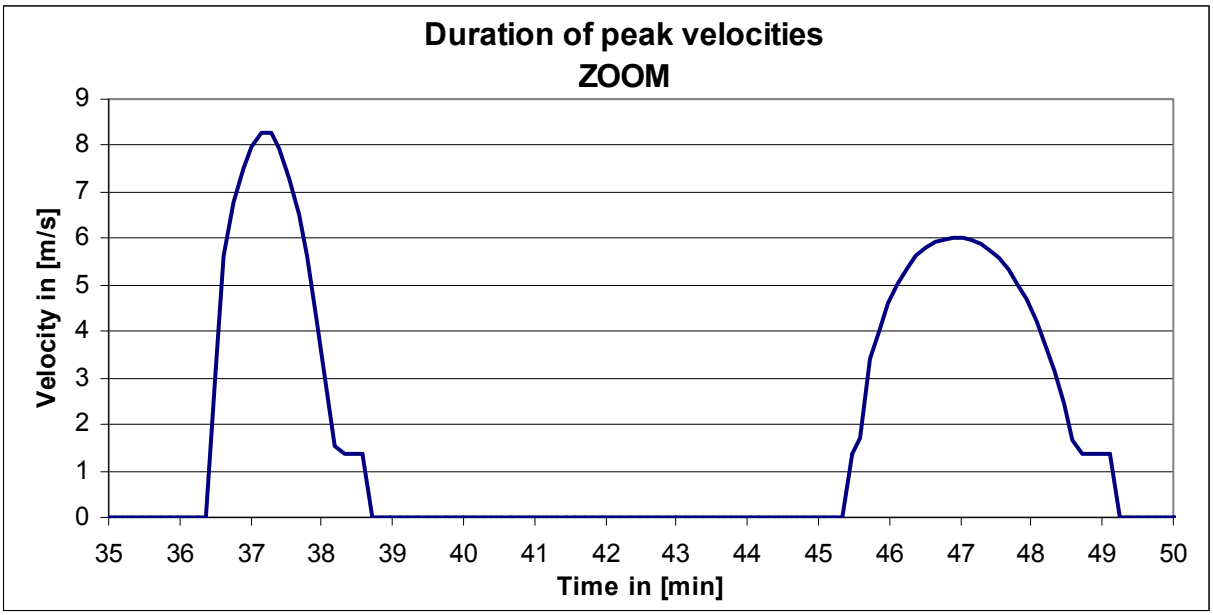

Figure IX-8 Duration of peak velocities over structure.

The duration of velocities does not vary for structure slope but depends mainly on the tsunami excitation signal. The time-velocity distribution of the design showed in above graph will therefore be similar for the chosen design. The duration of high velocities (>3 m/s) is approx. 2 minutes for the initial peak, and approx. 3min for the 2nd peak.

IX - 4 VALIDATION

The results of one model run are presented in Figure IX-9. This model represents the chosen breakwater design being attacked by the design tsunami (Dec2004 Tsunami).

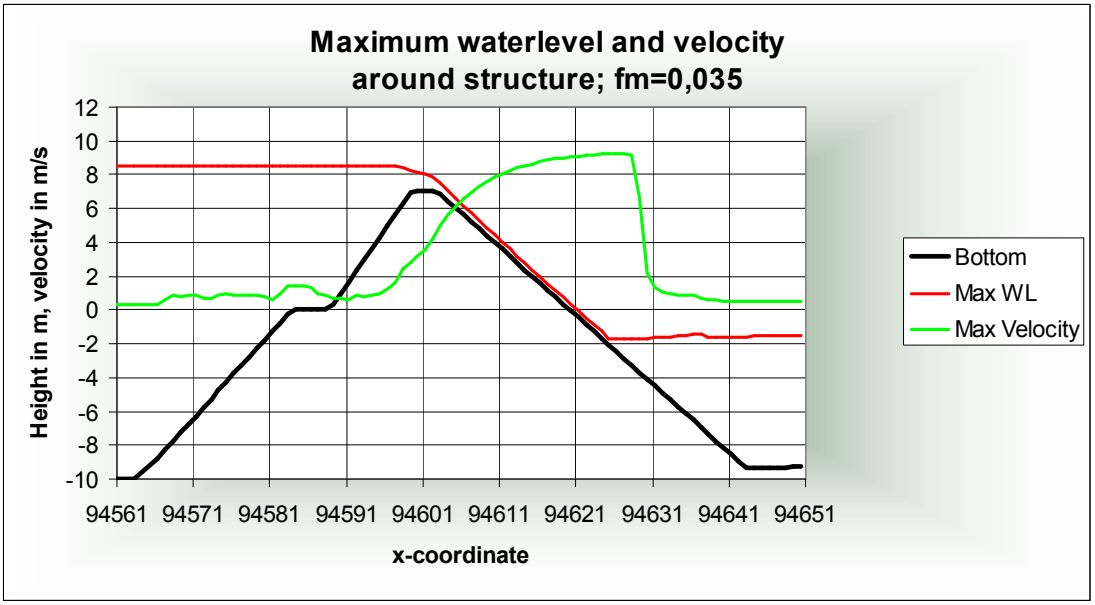

Figure IX-9 Maximum velocities and water levels for offshore breakwater

The maximum occurring velocity is 9,3 m/s.

In Figure IX-10, a zoom on the crest is presented, together with the location of the output points. The obtained values are presented in Table IX-1.

Table IX-1: Depths and velocities on the crest

Output point	Water depth [m]	Velocity	Discharge q [m^2/s]	Froude number $= \sqrt{gd}$
1	1,29	2,82	3,63	0,79
2	1,12	3,13	3,51	0,94
3	1,01	3,50	3,54	1,11
4	0,85	4,14	3,52	1,43
5	0,71	4,96	3,52	1,88

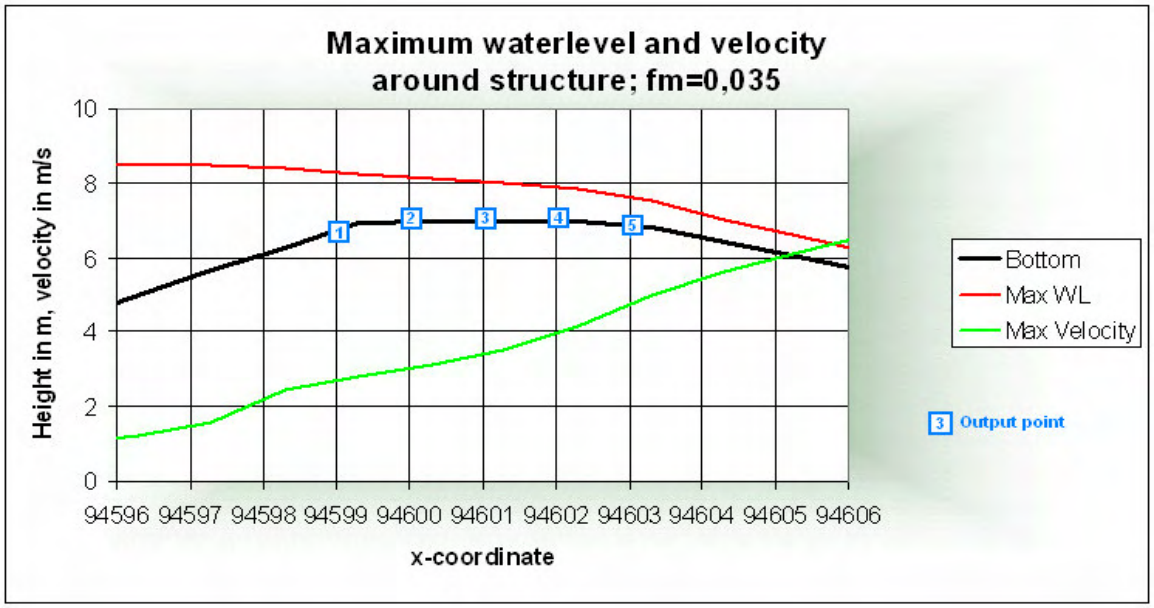

Figure IX-10 Detailed view on the crest and output points

The model results are checked by calculating the Froude-number, $Fr = \frac{u}{\sqrt{gd}}$, which shows a transition from tranquil flow in front of the barrier (Fr < 1,0; sub-critical) to rapid flow conditions on the rear side (Fr > 1,0; super critical).

The transition (Fr = 1,0; critical flow) lies on the crest of the barrier. This is an important property of the 'free-discharge weir' (*volkomen overlaat* in Dutch, [2]). Another property is the definition of the so-called critical depth, d_c. According to this theory, the critical depth is given by:

$$d_c = \frac{2}{3} E_{crest},$$

with

$$E_{crest} = H - a$$

H= energy head in front of the weir
a = height of the crest

Because the velocities in front of the breakwater (weir) are relatively low (<0,5m/s according to the model), the contribution of the velocity to the total energy head is negligible. $0{,}5^2$ / (2*g) = 0,01m. The energy head in front of the barrier, *H,* is therefore equal to the water depth, 18,5m. With a crest elevation of 17m above sea bottom, the critical depth becomes:

$$d_c = \frac{2}{3} E_{crest} = \frac{2}{3} \cdot (18{,}5 - 17) = 1{,}0m$$

This theoretical value gives good agreement with the numerically calculated water depth in the middle of the crest (output point 3; *1,01m*) in Table IX-1.

Consequently, the related discharges are consequently is also correct.

Another study, carried out by Schűttrumpf *et al* (in [7]), related the velocity and water depth on the crest with the velocities on the rear-slope. He developed an equation to calculate the velocity of a steady flow, and confirmed it with model experiments. This method can be compared with the 1D-model results.

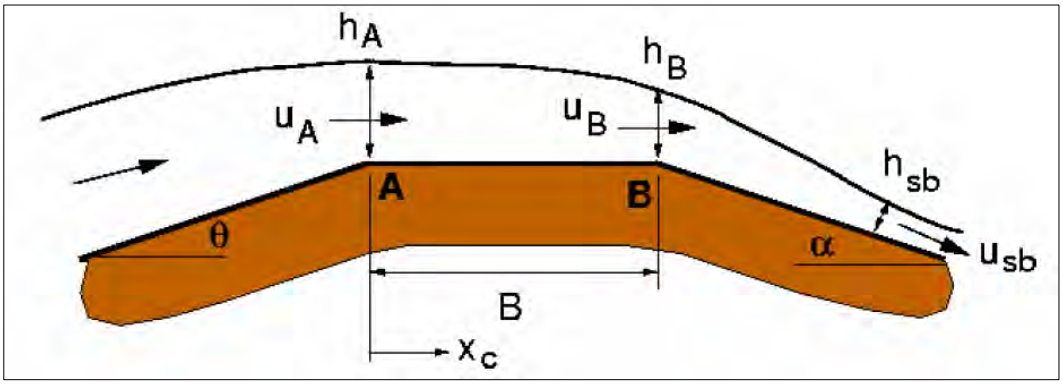

Figure IX-11 Wave overtopping definition sketch (after Schűttrumpf et al. [7])

The velocity on the backside is:

$$v_{sb} = \frac{v_B(0) + \frac{k_1 h_B}{f} \cdot \tanh\left(\frac{k_1 t}{2}\right)}{1 + \frac{f \cdot v_b(0)}{k_1 h_B} \cdot \tanh\left(\frac{k_1 t}{2}\right)}$$

with

$$t \approx -\frac{v_b(0)}{g \sin\beta} + \sqrt{\frac{v_b{}^2(0)}{g^2 \sin^2\beta} + \frac{2 s_B}{g \sin\beta}}$$

and

$$k_1 = \sqrt{\frac{2 f g \sin\beta}{h_B}}$$

The velocity $v_B(s_B)$ [m/s] is the velocity at distance s_B [m] from the crest, measures along the slope. The thickness of the water layer is denoted as h_B [m], β is the slope angle and f [-] represents a non-dimensional friction coefficient.

For 6 output points, the velocities are calculated (an iterative procedure is required). The friction coefficient is set to f=0,035, as in the model runs. See Table IX-2 and Figure IX-12 for the output.

Table IX-2: Velocities on the back side with Schűttrumpf

Output point along slope	Height [m] to MSL	Velocities 1D model along slope [m/s]	Velocity Schuttrumpf [m/s]	Error [%]
A	+7.00	4,12	4,12	0
B	+6,78	6,48	6,05	7,1
C	+5,28	7,88	7,22	8,9
D	+3,78	8,83	7,88	11,5
E	+2,28	9,49	8,27	13,7
F	+0,78	9,92	8,51	15,1

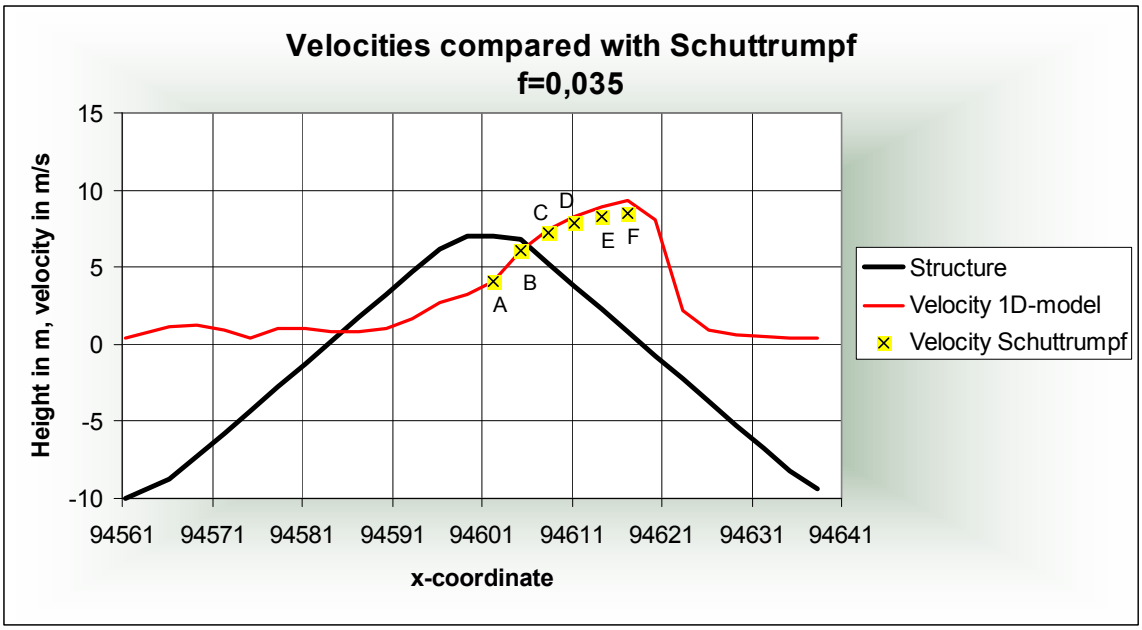

Figure IX-12 Velocities with Schűttrumpf and 1D-model

The maximum error is 15% for the lowest output point. The error increases down slope. However, the error-percentage falls within reasonable margins for a preliminary design and the 1D-model velocities are higher, so on the safe side.

IX - 5 FINDINGS STRUCTURE MODELLING

General conclusions are:

- The maximum velocities occur at the rear side of the structure, on the water line.
- The velocities in front of the structure (toe) are low (<0,5 m/s)
- The shape or slope on the front side has no significant influence on the maximum velocities.
- Applying a berm on the rear side induces high peak velocities (and logically more turbulence) at the transitions.

The design velocity is taken to 9,3 m/s in horizontal direction. Corrected along the slope this yields a velocity of approximately 10 m/s. The water depth associated with this velocity is 1,1m.

IX - 6 FINDINGS ABOUT INFLUENCE BATHYMETRY ON INUNDATION

For 3 different profiles, the inundation volume at the coast line is studied. This research is parallel with the 1D-Delft3D modelling with various profiles and forms and attempts to reproduce the same findings.

The input is given below. Three profiles are investigated; a linear, convex and concave profile.

Signal t1=8.0*60 if (t<t1) then a1=1.0 s1(1)=-a1*sin(2*pi*t/t1) else s1(1)=0.0	Linear profile d1=dpt-dpt*x(m)/(0.97*xl) d(m)=min(dpt,d1) if (d(m)<0.0) d(m)=-1.0

Convex profile/2D profile
d1=dpt-dpt*x(m)/(xl)
d2=2.7*exp((0.97*xl-x(m))/1550)-3
if (d(m)>84.0) d(m)=min(dpt,d1)
if (d(m)<84.0) d(m)=d2
if (d(m)<0.0) d(m)=-1.0
	Concave profile
	d1=dpt-dpt*x(m)/(xl)
	d2=-6.3e-10*(x(m)-0.92*xl)**3+1.1e-06*(x(m)-0.92*xl)**2-5.8e-03*(x(m)-0.92*xl)+80.00
	if (d(m)<80.0) d(m)=min(dpt,d2)
	if (d(m)<0.0) d(m)=-1.0

The maximum shoaling belonging to these profiles, and the theoretical shoaling (Green's Law) are depicted in Figure IX-13..

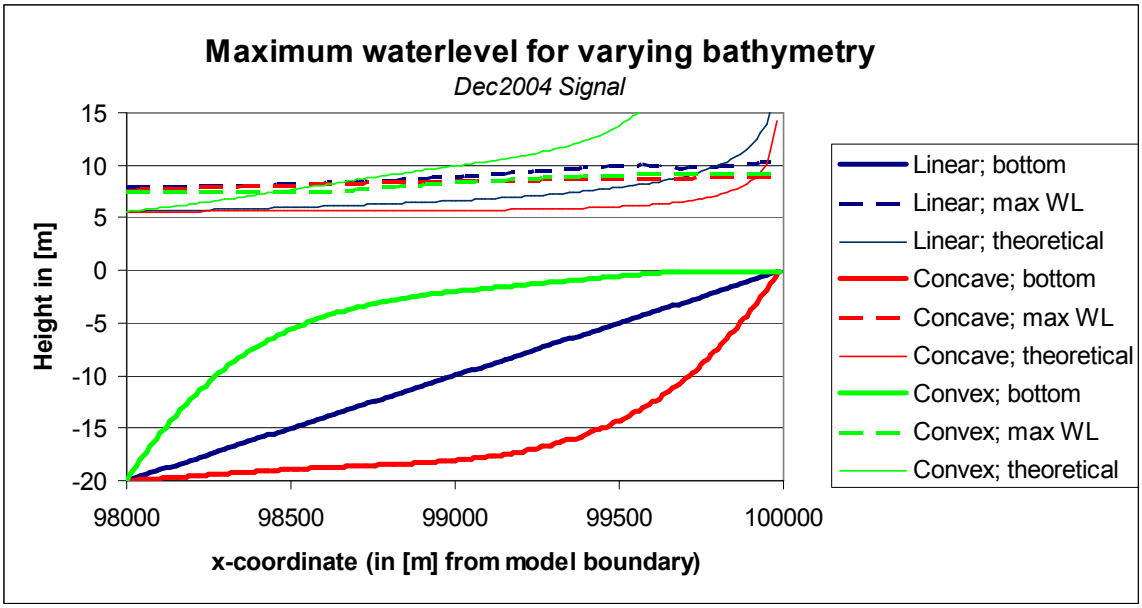

Figure IX-13 Maximum shoaling at the coast for various foreshore bathymetries

It must be concluded that based on this small research, the findings of the 1D-Delft3D modelling are not consistent with the semi-1D-modelling.
The shoaling heights do differ for various profiles. However, where the semi-1D modelling (see Chapter 4.3 in the main report) suggests a maximum shoaling for convex profiles, in this model the linear profile provides the highest waves. Furthermore, the concave profile is the lowest while in the semi-1D modelling it was found that this profile induces the highest waves.
The differences between various profiles are much smaller.

Unfortunately, a more detailed study into this matter falls beyond the scope of this thesis work. It is strongly recommended however that the influence of the bottom profile on the wave development (shoaling vs. reflection) is studied in more detail. Because Green's shoaling law is obviously not accurate in the last hundreds of meters before the coast, tsunami risk assessments (often based on simple shoaling laws) can not be trusted either.

LIST OF REFERENCES

[1] BAPPENAS (2005), Indonesia: Preliminary Damage and Loss Assessment, The December 26, 2004 Natural Disaster, *The Consultative Group on Indonesia*, January 19-20, 2005.

[2] BATTJES, J.A. (2002), Vloeistofmechnica, *faculty of Civil Engineering Delft University of Technology, Delft*.

[3] BRYANT, E. (2001), TSUNAMI: The Underrated Hazard, *Cambridge University Press, Cambridge*

[4] CAMFIELD, F.E. (1980), Tsunami Engineering, *U.S. Army, Corps of Engineers, Coastal Engineering Research Center, Fort Belvair.*

[5] CHU, K.K., ABE, T (1981), Tsunami Run-Up and Back-Wash on a Dry Bed, *Terra Scientific Publishing Company, Tokyo*

[6] CLOPPER, P.E., (1991), Protecting Embankment Dams with Concrete Block Systems, *Hydro Review,* Volume X, No. 2, April 1991, pages 54-67

[7] CUYPERS, K., (2004) Breakwater stability under tsunami attack, for a site in Nicaragua. *Final Thesis Report, Delft University of Technology, Delft.*

[8] © CUR-PUBLICATIE 214, Geotextiele zandelementen, 2004, *Stichting CUR, Gouda.*

[9] © CUR-PUBLICATIE 168A, Oeverbeschermingsmaterialen, 1994, *Stichting CUR, Gouda.*

[10] EDWARD, P.J.K., TERAZAKI, M., YAMAGUCHI, M., The impact of tsunami in coastal areas: Coastal protection and disaster prevention measures; experiences from Japanese coasts, *Coastal Marine Sciences 30(2):414-424*, 2006.

[11] GEIST, L.E, (2001), Complex earthquake rupture and local tsunamis, *Journal of Geophysical Research, Vol. 107. No. B5, U.S. Geological Survey, Menlo Park, California, USA.*

[12] HARADA, K., KAWATA, Y. (2004) Study of the effect of coastal forest to tsunami reduction, Annuals of Disaster Prevention, *Research Institute of Kyoto Univ., No.47C, Kyoto.*

[13] HITACHI, S., KAWADA, M., TSURYA, H., (1994), Experimental studies on tsunami flow and armorblock stability for the design of a tsunami protection breakwater in Kamaischi Bay, *Hydro-Port 1994 Vol. I., Coastal Development Institute of Technology*, pages 765-783.

[14] HOFFMANS, G.J.C.M, VERHEIJ, H.J. (1997) Scour Manual, *Balkema, Rotterdam*.

[15] HORRILLO, J, KOWALIK, Z (2006), Wave dispersion study in the Indian Ocean Tsunami of December 26, 2004. *Science of Tsunami Hazards*, Vol. 25, No. 1, page 42.

[16] JICA STUDY TEAM, 2005, Study on the Urgent Rehabilitation and Reconstruction Plan for Banda Aceh City in the Republic of Indonesia. *Banda Aceh.*

[17] KAMEL, A.M., (1970), Laboratory study for design of tsunami barrier, Journal of the Water ways, *Harbours and Coastal Engineering Division, ASCE, Reston*, page 766-779.

[18] KATHIRESAN, K., RAJENDRAN, N., 2005. Coastal mangrove forests mitigated tsunami. *Estuarine, Coastal and Shelf Science 65*, 601-606.

[19] KATO, F., INAGAKI, S. AND FUKUHAMA, M. (2006) Wave Force on Coastal Dike due to Tsunami. World Scientific Publishing, *COASTAL ENGINEERING 2006; Proceedings of the 30th International Conference, San Diego, California, USA.*

Abstract available at http://www.pwri.go.jp/eng/ujnr/joint/37/paper/13kato.pdf

[20] KERR, A.M., BAIRD, H., CAMPBELL, S.J., 2006. Comments on "Coastal mangrove forests mitigated tsunami". *Estuarine, Coastal and Shelf Science 67*, 539-541.

[21] IDA, K. (1981), Tsunamis: their Science and Engineering, Ida, K., Iwasaki, T., *Terra Scientific Publishing Company, Tokyo.*

[22] IKENO, M., MORI, N. AND TANAKA, H.(2001), Experimental Study on Tsunami Force and Impulsive Force by a Drifter under Breaking Bore like Tsunamis, *Proceedings of Coastal Engineering,* JSCE, Vol. 48, 2001.

[23] IKENO, M., TANAKA, H.(2001), Experimental Study on Impulsive Force and Tsunami Running up to Land, *Proceedings of Coastal Engineering,* JSCE, Vol. 50, 2003.

[24] MANGKUSUBROTO, K.,et al, (2005), Rebuilding a better Aceh and Nias, *Report of a joint team of BRR and World Bank, Banda Aceh.*

[25] MATSUTOMI, H., et al. (2005), Aspects of Inundated Flow due to the 2004 Indian Ocean Tsunami, Coastal Engineering Journal, Vol. 48, No. 2 (2006) 167-195, *World Scientific Publishing Company, Tokyo.*

[26] NATAWIDJAJA, D.H, Neotectonics of the Sumatran Fault and Paleogeodesy of the Sumatran Subduction Zone, PhD thesis, *California Institute of Technology, Pasadena, California*, 2002. Available from http://etd.caltech.edu/etd/available/etd-05222003-155554/unrestricted/DHN_ Thesis.pdf

[27] PILARCZYK, K.W. (2003), Design of low-crested (submerged) structures –an overview –, *6th International Conference on Coastal and Port Engineering in Developing Countries, Colombo, Sri Lanka*.

[28] POWLEDGE, G.R., PRAVDIVETS, Y.P., (1994), Experiences with Embankment Dam Overtopping Protection, *Hydro Review*, February 1994, pages 1-6.

[29] RITSEMA, A.R. (1976), Tsunamis; alles verwoestende vloedgolven, *Natuur en techniek, jrg. 44*, *nr. 3,*1976, pp 164-179.

[30] SCHIERECK, G.J. (2001), Introduction to bed, bank and shoreline protection; engineering the interface of soil and water, *Delft University Press, Delft*

[31] SEA DEFENCE CONSORTIUM (Feb. 2007), Coastal Baseline Study Report, Vol II; Hydraulic Conditions, *SDC-R-60014.*

[32] SEA DEFENCE CONSORTIUM (Feb. 2007), Coastal Baseline Study Report, Vol III; Tsunami Modelling and Risk Assessment, *SDC-R-60014.*

[33] SEA DEFENCE CONSORTIUM (Feb. 2007), GEOTEKNIKA KONSULINDO, Draft report of geotechnical site investigation for Banda Aceh, Volume II, *SDC-RD-70016.*

[34] SPIELVOGEL, L.Q. (1976), Run-up of Single Waves on a Sloping Beach, in Tsunami Research, Heath, R.A., Cresswell, M.M., *Royal Society of New Zealand, Wellington*, pp 113-119.

[35] STEIN, S. OKAL, E.A. (January 2007), Ultralong Period Seismic Study of the December 2004 Indian Ocean Earthquake and Implications for Regional Tectonics and the Subduction Process, *Bulletin of the Seismological Society of America, Vol. 97*, No. 1A, pp S279-S295.

[36] STELLING, G.S. DUINMEIJER, S.P.A. (2003), A Staggered Conservative Scheme for every Froude Number in Rapidly Varied Shallow Water Flows, *International Journal for Numerical Methods in Fluids;* **43**:1329-1354.

[37] SYNOLAKIS, C.E. (1990), Tsunami Run-up on Steep Slopes: How Good Linear Theory Really Is, in Tsunami Hazard; a practical guide for tsunami hazard, Bernard, E.N., *Kluwer, Dordrecht*, pp 221-234.

[38] TANIMOTO, K (1981), On the Hydraulic Aspects of Tsunami Breakwaters in Japan, *Terra Scientific Publishing Company, Tokyo,*.

[39] TAW (1985), The use of asphalt in hydaulic engineering, Technical Advisory Committee on Waterdefences, *Rijkswaterstaat, The Hague.*

[40] TAW (2002), Technisch Adviescommissie voor Waterkeren, Technisch Rapport Asfalt voor Waterkeren, november 2002.

[41] THIO, H. K.,ICHINOSE, G., SOMERVILLE, P., (2005), Probabilistic Tsunami Hazard Analysis, *Risk Frontiers Quarterly Newsletter*, Vol. 5, Issue 1, July 2005.

[42] VERRUIJT, A. (1999) Grondmechanica, *Delft University Press, Delft*.

[43] VRIJLING, H. et al (1997), Probability in Civil Engineering; Part 1: The Theory of Probabilistic Design*, faculty of Civil Engineering Delft University of Technology, Delft*.

*[44]*WALTERS, R.A., (2005). A semi-implicit finite element model for non-hydrostatic (dispersive) surface waves, *International Journal for Numerical Methods in Fluids;* **49**: 721-737.

*[45]*WARD, N. (2000). Landslide tsunami, *Institute of Geophysics and Planetary Physics, University of California, Santa Cruz.*

*[46]*WARD, N. Tsunamis. *Institute of Tectonics, University of California, Santa Cruz.*
Article for publication in Encyclopedia of Physical Science and Technology, Academic Press. Available from http://www.es.ucsc.edu/~ward/papers/tsunami_ency.pdf

[47] WILKINSON, F. (2005), Coastal design and Tsunami Mitigation, *United Nations High Commissioner for Refugees,* ISBN 085 825 796 3

*[48]*YAMAMOTO, Y, et al (2005), Verification of the Destruction Mechanism of Structures in Sri Lanka and Thailand due to the Indian Ocean Tsunami, in *Coastal Engineering Journal, Vol. 48,* No. 2 (2006) 117-145, *World Scientific Publishing Company and Japan Society of Civil Engineers.*

Sites on World Wide Web

[49] http://www.eri.u-tokyo.ac.jp/

[50] http://www.ngdc.noaa.gov
Tsunami Event Database of the National Geophysical Data Centre

[51] http://www.waveofdestruction.org

[52] http://www.asiantsunamivideos.com

[53] http://www.nerc-bas.ac.uk/tsunami-risks

[54] http://www.geophys.washington.edu/tsunami/general/physics/characteristics.html

[55] http://www.wldelft.nl

[56] http://earthquake.usgs.gov/

[57] http://www.nae.edu

National Academy of Engineering. Article by Robert A. Dalrymple and David L. Kriebel, Lessons in Engineering from the Tsunami in Thailand.
[58] http://www.infoplease.com/ipa/A0107634.html
[59] http://www.worldbank.org
[60] http://www.earth.northwestern.edu/people/seth/research/sumatra2.html
[61] http://www.ew.govt.nz/enviroinfo/hazards/naturalhazards/coastal/tsunami.htm
[62] http://intern.forskning.no/arnfinn/tsunami/tsunami_english.swf
Nice simulation of plate tectonics (subduction) and relation with tsunami wave
[63] http://www.thaiappraisal.org/pdfNew/Monthly_Forum/MF31_Land%20Seminar-Mr.%20Uji%20Hino.pdf
Interesting slide-show with many pictures of tsunami protection measures in Japan
[64] www.icdp-online.org/.../hawaii/Ringof_Fire.gif
Website of the International Continental Scientific Drilling Program
[65] http://news.bbc.co.uk/1/shared/spl/hi/pop_ups/05/sci_nat_enl_1111709134/html/1.stm
[66] http://www.andaman.org/mapstsunami/tsunami.htm
Website with lot of information about earthquakes and tsunamis around the Andaman and Nicobar Islands, northwest of Sumatra.
[67] http://www.dcrc.tohoku.ac.jp/index.html
Disaster Control Research Center of Tohoku University, Japan
[68] http://www.noort-innovations.nl/